Lehrstuhl für Mensch-Maschine-Kommunikation
Technische Universität München

Anticipation Assistance For Drivers

Florian Ulrich Laquai

Vollständiger Abdruck der von der Fakultät für Elektrotechnik und Informationstechnik
der Technischen Universität München zur Erlangung des akademischen Grades eines

Doktor-Ingenieurs (Dr.-Ing.)

genehmigten Dissertation.

Vorsitzender:	Univ.-Prof. Dr.-Ing., Dr.-Ing. habil. Erwin Biebl
Prüfer der Dissertation:	1. Univ.-Prof. Dr.-Ing. habil. Gerhard Rigoll
	2. Univ.-Prof. Gudrun J. Klinker, Ph.D.

Meinem Großvater

Acknowledgments

Abstract

This work addresses several aspects related to the development of an anticipatory Advanced Driver Assistance Systems (ADAS). First relevant traffic situations are identified and the requirements related to timing and needed information are analyzed. This shows that the only technology that can fill the gap between long-range traffic information and short-range environment perception is Car2X Communication (C2XC). Together with cooperative perception it is possible to observe a large area and even capture vehicles which are not part of the C2XC network.

On this basis several variants of an anticipatory assistance system are developed which support drivers especially in longitudinal control of their vehicle. The Human Machine Interfaces (HMIs) can be divided into two classes: contact-analog Head-Up Display (HUD) concepts and Light Emitting Diode (LED) cluster based abstract displays. These systems are evaluated using non-interactive video experiments, an immersive stereoscopic driving simulator and a real vehicle. All variants proved that they induce an earlier and smoother speed reduction which leads to improved safety, fuel economy and traffic flow.

In order to have an adequate driving simulation environment available for anticipation-related experiments, an immersive stereoscopic simulator in a Cave Automatic Virtual Environment (CAVE) is developed. It serves as a basis for driving experiments in which also the car following behavior related to cars other than the direct leading car is recorded.

The data from these experiments serves for the development of a new Car Following Model (CFM) based on the widely used Intelligent Driver Model (IDM) by Kesting et al. (see [KTH10]). One variant of it extends the IDM with more human behavior such as reaction times and misjudgments related to obstacle distances and includes an implementation of the anticipatory assistance. The other version contains a larger extension with the development of the Behavior Map that enables the CFM to use multi-anticipation. This results in more realistic behavior in complex scenes as not only the direct leading vehicle is taken into account but all vehicles in a larger area around the ego vehicle. Traffic simulations with this CFM show that the positive effects of anticipation support can also be repeated in larger scenarios with varying penetration rates of the assistance system.

Zusammenfassung

Diese Arbeit beschäftigt sich mit verschiedenen Aspekten rund um die Entwicklung von vorausschauenden Fahrerassistenzsystemen. Zunächst werden relevante Verkehrssituationen identifiziert und die zeitlichen Anforderungen sowie die benötigten Daten analysiert. Dies zeigt, dass die Lücke zwischen langfristigen Verkehrsinformationen und kurzfristiger Umgebungserfassung nur durch den Einsatz von Car2X Communication (C2XC) gefüllt werden kann. Zusammen mit kooperativer Perzeption ist es möglich, ein großes Gebiet zu überwachen und sogar Fahrzeuge zu erfassen, die nicht Teil des C2XC - Netzwerks sind.

Auf dieser Basis werden mehrere Varianten von Systemen mit vorausschauender Assistenz entwickelt, die den Fahrer vor allem in der Längsführung unterstützen. Die entwickelten Systeme können in zwei Klassen unterteilt werden: kontaktanaloge HUD Anzeigen und auf LED Modulen basierende Anzeigen. Diese werden in nicht-interaktiven Videoexperimenten, einem immersiven stereoskopischen Fahrsimulator und einem Realfahrzeug entwickelt und evaluiert. Alle Varianten konnten eine frühere und gleichmäßigere Geschwindigkeitsreduktion herstellen, die zu erhöhter Sicherheit, niedrigerem Kraftstoffverbrauch und verbessertem Verkehrsfluss führt.

Um eine adäquate Fahrsimulation für Experimente im Bereich vorausschauender Assistenz zu haben, wird ein immersiver stereoskopischer Fahrsimulator für eine CAVE entwickelt. Er dient als Basis für Experimente, in denen das Folgeverhalten nicht nur zum direkten Vordermann sondern allen umgebenden Fahrzeugen analysiert werden kann.

Mit den Daten aus diesen Experimenten wird ein neues Fahrzeugfolgemodell auf der Basis des IDM von Kesting et al. (siehe [KTH10]) aufgebaut. Eine Variante erweitert das IDM um weitere menschliche Eigenschaften, wie beispielsweise mehrere Reaktionszeiten und Fehleinschätzungen von Hindernisabständen, und bindet die Funktion des vorausschauenden Assistenzsystems ein. Die andere Variante enthält eine größere Erweiterung mit der Entwicklung der Behavior Map, die Multi-Antizipation ermöglicht. Dies resultiert in realistischerem Verhalten vor allem in komplexeren Verkehrsszenarien, da nicht nur der direkte Vordermann, sondern alle Fahrzeuge in einem größeren Bereich um das Ego-Fahrzeug in die Geschwindigkeitswahl miteinbezogen werden. Verkehrssimulationen mit diesem Fahrzeugfolgemodell zeigen, dass die positiven Effekte der Antizipationsunterstützung auch in größeren Szenarien mit variierendem Ausstattungsgrad wiederholt werden können.

Contents

1

Introduction

Intelligent Transportation Systems (ITS) are expected to be the key for solving the already present or foreseeable traffic problems of modern cities. The long term goal is fully automated driving as already mentioned in [MIS02]. As technology evolves, future cars will have much more detailed information about their surroundings than today which enables developers to implement highly automated vehicles. In the next couple of years a system which autonomously controls the longitudinal and lateral car movement in everyday traffic is not expected to be available. So there still would have to be a human "driver" who monitors such systems which turns the human operator into a spectator instead of an actor as in the current situation. This can lead to fatigue and decreased situation awareness which in turn impairs the driver's performance to react on fault situations, which has already been observed in aviation (see [Bil91] and [WH92]).

Consequently a different solution must be found until an acceptable fault level can be assured. Such a system must keep the driver actively in the control loop (see also [EK95] regarding the "out-of-the-loop" phenomenon for highly automated tasks) while providing assistance in a way that lets him cope with situations that are currently not manageable or have room for improvements. A possible way to achieve this could be the extension of the driver's anticipation horizon so he can act in a better informed manner.

Anticipatory driving has a large potential to improve safety, fuel efficiency and traffic flow. The term "'anticipatory driving"' will be used equivalent to choosing the adequate speed for a traffic situation. Several studies have shown the correlation between speed and safety, among them the work of Wagenaar et al. [WSS90] who point out an 19.2% increase in fatalities and a 39.8% increase in serious injuries due to the raised speed limit from 55 mph to 65 mph in the USA. An Australian study (see Kloeden et al. in [Klo+97]) states that "In a 60 km/h speed limit area, the risk of involvement in a casualty crash doubles with each 5 km/h increase in traveling speed above 60 km/h".

Regarding fuel efficiency it can be stated that a lower speed can contribute over proportionally to fuel savings. This can be validated by state-of-the-art fuel consumption and emission models as described in [RAT04] and [RAT03]. Fuel consumption and the resulting emissions decrease not only linearly but with non-negligible quadratic influences of speed.

For the property "traffic flow" a simple answer cannot be given. As mentioned in [RF09], where a multi-agent simulation environment was used to assess changes in throughput due to the application of a brake warning system, overall throughput can be increased by reducing the possibility of jams. Also the well-known Nagel-Schreckenberg model (see
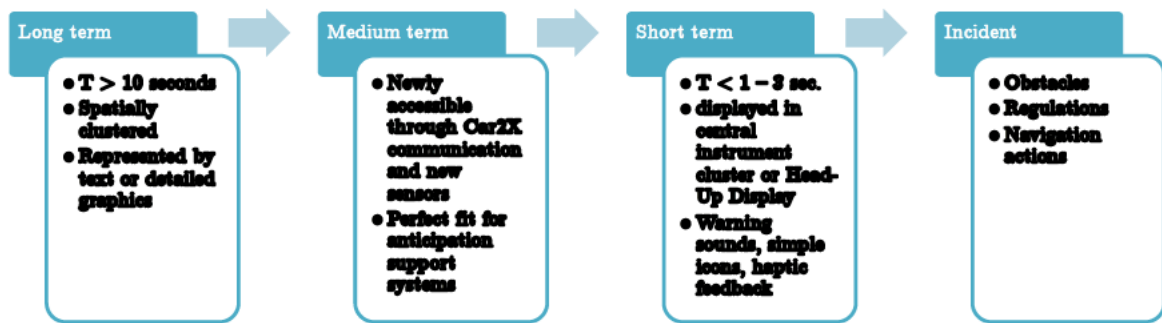
Figure 1.1: Distinguishable time frames ahead of the driver

[NS92]) can be used to mimic the formation of congestion waves in real traffic jams. It was shown that such waves originate from irregularities in the traffic flow such as sudden speed changes. In contrast (see [AST00]) increasing safety usually means increasing inter-vehicle distances and thus decreasing traffic density and throughput. These goals obviously cannot be unified and require a tradeoff.

Advanced Driver Assistance Systems (ADAS) have entered the market in recent years. Systems like Adaptive Cruise Control (ACC), Lane Departure Warning (LDW), Blind Spot Detection or Traffic Sign Recognition are becoming standard equipment for modern cars. Most recent advances cover systems for vehicular networks which are summarized under the term Car2X Communication (C2XC), see [CAR07]. This term includes the two subsets of Car2Infrastructure Communication and Car2Car Communication systems. The conglomerate of sensors readily available for current ADAS and the possibilities of the upcoming C2XC systems give access to a time frame ahead of the driver which is currently not covered in production systems. Such communication systems enable the use of foreign vehicles and the infrastructure as remote sensor systems. Systems like ACC or LDW can be counted to the short term assistance functions while navigation and Traffic Message Channel (TMC) information are part of the long term assistance or information systems. The proposed assistance functions for anticipatory driving would be an example for medium term assistance in figure 1.1. An overview regarding relevant sensors and communication systems is given in chapter 2.

Another way of classifying assistance functions and tasks is depicted in figure 1.2. Again the proposed anticipation support systems shall be located in the middle section "Guidance" as they do not involve highly automated or long term navigation tasks.

Based on the previous thoughts a system shall be developed which informs drivers about oncoming traffic situations and which induces earlier and smoother speed adaptations. The following questions related to different aspects of such an assistance system will be addressed:

- Which situations are relevant for anticipation support?

- What are the required actions to improve safety, fuel economy and overall traffic performance in these situations?

- When is the optimal time for assistance and which information is needed?
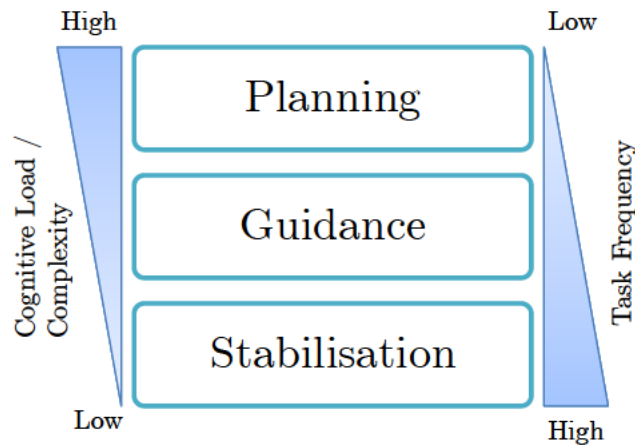
Figure 1.2: Task classification for different abstraction levels of vehicle control. The overview shows the relationships between cognitive load, complexity and frequency of tasks (adapted from [Rei95]).

- What is the influence on driving style in virtual and real environments?

- Will a stereoscopic driving simulator improve the conditions for anticipation-related experiments?

- Can the different behavior of assisted and unassisted drivers be modeled and applied in larger scenarios?

The structure of this document to answer these questions is as follows:

Traffic Situations and Relevant Data Sources (Chapter 2)   Here a set of traffic situations that are relevant for anticipatory assistance is identified. All of them force the driver to adapt his speed and have the potential of being recognized too late. Different settings are covered ranging from urban to rural and highway scenarios. For every situation it is analyzed how and with which constraints they could be detected by a vehicle. Relevant data sources are introduced and the basics about communication based sources are discussed.

Anticipation Support and User Interfaces (Chapter 3)   Based on the previous situation analysis several variants of Human Machine Interface (HMI) systems are developed that shall assist in longitudinal control. The timing algorithm originates from the work of Popiv et al. (see [Pop+10]) and is combined with all HMIs. It takes data from the ego vehicle and C2XC as an input for its deceleration strategy suggestions. All variants are evaluated in different driving simulator environments to support an iterative design process.

Real World Experiment (Chapter 4)   The most promising HMI variant is adapted to a real world scenario and integrated in a tractor truck. This step towards a more realistic environment serves as a valuable comparison possibility to the previous virtual experiments. After several data preparation steps the final results are presented.

Immersive Virtual Environment for Anticipation Experiments (Chapter 5)   Anticipation is closely related to a correct spatial perception of the environment. As the driving simulator used for the previous experiments has only limited capabilities of correct speed and distance presentation a new system is developed. It features a coverage of nearly the whole Field Of View (FOV), floor projection, head tracking and stereoscopic display technology. The results of an experiment related to speed and distance judgment are presented.

Traffic Simulations (Chapter 6)   To assess the impact of an assistance system on a larger scale it is necessary to conduct traffic simulations as a first step. The development process of a Car Following Model (CFM) is shown that is able to represent the behavior differences of assisted and unassisted drivers. Based on the data of a driving simulator experiment the Behavior Map (BM) is established to enable multi-anticipative behavior of the CFM. Traffic simulations serve both as a proof-of-concept of the BM and as a possibility to assess the impact of anticipatory assistance.

Discussion and Outlook (Chapter 7)   This chapter summarizes all outcomes and addresses the questions postulated before. Additionally several possible improvements are discussed together with further steps.

2

Traffic Situations and Relevant Data Sources

A prerequisite for developing and testing of anticipation support systems is the identification of relevant traffic situations. While anticipation support may have many faces and is not necessarily limited to dangerous situations, the situations described here all have in common that drivers need to lower their speed due to a static or moving obstacle on their way. In some of these situations it may happen that drivers cannot recognize them at all or in parts due to occlusions or because they are distracted. For both cases a system that provides knowledge about upcoming situations that require a speed reduction can be very valuable to prevent accidents, support a more ecological driving style and improve traffic throughput with a smoother driving style.

In order to achieve this goal a system must be aware of its environment, its position and the road network. While information about the road network and the route can already be provided by current navigation systems, the environment sensing is still a field of very active development. Many sensor technologies already exist for a number of assistance systems, but the fusion of all this information combined with information originating from a C2XC network still needs to be leveraged.

This chapter will first introduce a number of situations that could potentially be supported by an anticipatory ADAS. In later chapters a subset of these situations will be selected based on driver feedback which will then be implemented in an assistance system. Then several on-board and communication-based data sources will be discussed regarding their feasibility for such an assistance.

2.1 Situation Descriptions

As mentioned before the proposed assistance system shall support timely deceleration in many situations. Here the criteria for anticipation support shall be a longer time horizon (a few seconds up to 20 seconds) than is usually covered by the driver himself or current collision avoidance / mitigation systems. The situations can be grouped into several categories that will be defined in the upcoming paragraphs. Additionally it is determined for every situation how it could be detected as well as the maximum anticipation horizon. The properties about detection probability, accuracy etc. are based on a literature review.
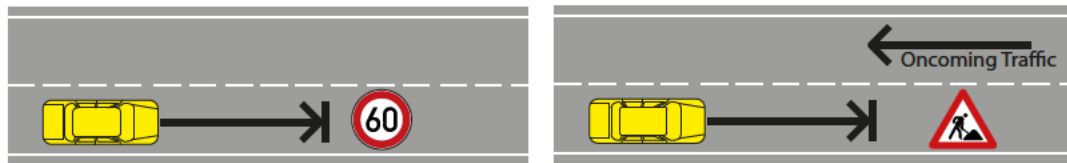
Figure 2.1: Sketch of a speed limit and a construction site situation. From an assistance point of view there is no significant difference whether this is located in an urban / rural road or a highway.

2.1.1 Speed Limitations and Construction Sites

Probably the most simple situation to detect and handle is a speed limit (see Fig. 2.1). It makes practically no difference whether it is located in an urban, rural or highway environment as it always has the same implications. Speed limits are no "physical" obstacles so no crash will happen in case the desired target speed is not met. This situation occurs very frequently so the potential is high that drivers get annoyed by the assistance and might turn it off if that is possible.

Table 2.1 shows the technical frame conditions for both the speed limit and construction site situation. Digital maps and camera-based sign recognition are already state-of-the-art, only C2XC is still not available. It is thinkable that especially variable speed limits are communicated with this data source which can be related to construction sites or traffic management systems. Here the maximum distance for anticipatory assistance is chosen to be 1 km to provide a reasonable time horizon. Regarding the recognition of the oncoming traffic the estimations in Tab. 2.2 are relevant.

2.1.2 Slower Leading Vehicles

In the situations shown in Fig. 2.2 the opposite lane could basically be used for overtaking in case of a slower leading vehicle. Several reasons can cause that this lane is not available. Examples are no-passing zones, oncoming traffic or a speed limit that would have to be exceeded for the maneuver. Table 2.2 shows the properties of the data sources which could

Object	Data Source	Ahead detection	Detection Probability	Accuracy	Update Rate
Fixed sign	Digital map	Always available	100%	Depends on map, typical <12 m	n.a.
Fixed / dyn. sign	C2XC	Distance: 1 km @100 km/h: 36 s	100%	Good GPS signal: 2 m	$\geq$ 1 Hz
Fixed / dyn. sign	Image recognition	Distance: 50 m @100 km/h: 1.8 s	$\approx$ 98% [EPR10]	Not determined	3 Hz

Table 2.1: Technical frame conditions for speed limit detection. The simplest approach is a limitation saved in a digital map, temporary limits can also be detected with cameras or be received by C2XC.
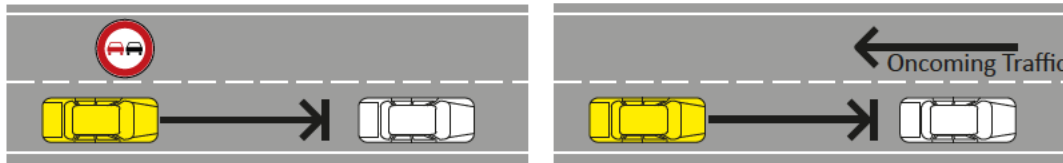
Figure 2.2: Sketches of two situations with slower leading vehicles and no overtaking possibility. In both cases drivers need to decelerate because they cannot overtake due to regulations or safety reasons.

potentially be used for the required information about involved objects. Especially data about oncoming traffic and the leading vehicles is essential as these objects are the most dynamic obstacles in the situation. While Radiowave Detection And Ranging (RADAR) can potentially be used for closer objects (usually up to 200m, see [HFL08]), C2XC could be very valuable for providing more long-term information.

In the traffic jam situation depicted in Fig. 2.3 the the cause for a required deceleration is not a blocked ego lane combined with a not available overtaking lane but a congested one-way road. This is usually found on larger interconnecting roads between cities or districts or on highways which are designed with separate lanes for each direction. Especially in the case of several lanes in one direction (but not limited to that) it is a challenge how to define the end of such a congestion which is required to have both relative speed and distance information.

This is one of the few dynamic situations for long-term anticipation that are already covered today by RDS-TMC. The information is broadcast along with the analog radio signal with comparably high latencies and low update rates. Most of the overall system

Object	Data Source	Ahead detection	Detection Probability	Accuracy	Update Rate
Leading vehicle	C2XC	Distance: 1 km @Δ v = 40 km/h: 90 s	100%	1 - 7 m	$\geq$ 1 Hz
Leading vehicle	Radar [HFL08]	20 m - 200 m (depends on road geometry)	>73%	Speed: 0.1 km/h Angle: 0.3°	$\geq$ 10 Hz
No-passing zones	Digital map	Always available	100%	Depends on map, typical < 12 m	n.a.
Speed regulation	Image rec. [EPR10] see speed limit	Distance: 50 m @100 km/h: 1.8 s	$\approx$ 98%	Not determined	3 Hz

Table 2.2: Technical frame conditions for the slower vehicle on ego lane situation detection. Depending on the situation variant it is necessary to know overtaking regulations or the properties of oncoming vehicles. In any case the properties of the leading car(s) must be available to determine the target speed.
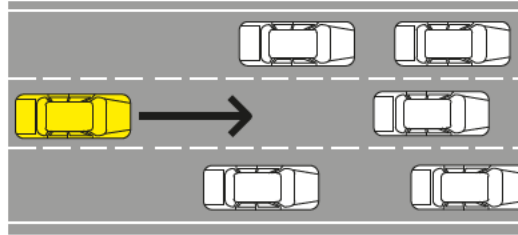
Figure 2.3: Sketch of a situation with slower leading vehicles or a highway jam. Here it is not possible to overtake slower leading vehicles. Due to the lack of oncoming traffic the situation analysis is more simple.

delay is attributed to the telematic chain that is involved in the process of detecting and forwarding an event. It can take several minutes until the information is then forwarded over the radio stations to the receivers in the cars. Systems that are based on the digital radio service Digital Audio Broadcast (DAB) such as mobile.info (see [mob07]) have better capabilities regarding positioning accuracy, update rate and delay than RDS based systems.

Also in this situation the use of C2XC could significantly improve several parameters of the telematic chain. With the positioning accuracy of a Global Positioning System (GPS) receiver each car can communicate its position to the surrounding vehicles or to a server based infrastructure that analyzes the traffic situation at a central point. Due to the fact that the whole chain of detection, classification and forwarding is automated, the time between the occurrence of an incident could be reduced significantly.

2.1.3 Lane Blocking in Urban Scenarios

In this situation the ego lane is either blocked by a different vehicle or regulated by a traffic light as seen in Fig. 2.4. A blocking vehicle could be a car maneuvering into a parking lot or a taxi waiting for a passenger. Traffic lights also block lanes temporarily, any

Object	Data Source	Ahead detection	Detection Probability	Accuracy	Update Rate
Leading vehicle	C2CC	Distance: 1 km @Δ v = 40 km/h: 90 s	100%	1 - 7 m	≥ 1 Hz
Leading vehicle	RDS-TMC mobile.info	Never - several hours	0-100%	RDS-TMC:0 - 1.41 km mobile.info: 11 m	TMC: > 12 s mobile.info: > 0.8 Hz, Lat. > 30 s
Leading vehicle	C2IC	Several km with RSUs	100%	Good GPS signal: 2 m	≥ 1 Hz, Lat. > 30 s

Table 2.3: Technical frame conditions for traffic jam situation detection. Currently only RDS-TMC is avalailable for jam information but has substantial drawbacks due to the detection scheme and related latencies.
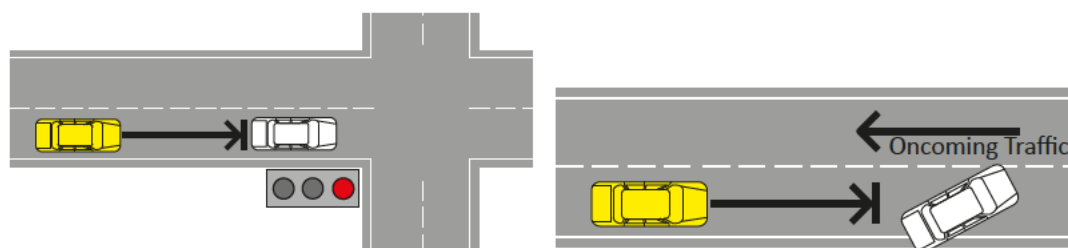
Figure 2.4: Sketches of two situations with blocked lanes in urban scenarios. In both cases drivers need to decelerate either because of a traffic light or a car meneuvering into a parking lot.

waiting cars in front of it only change the final stopping position of the ego vehicle. All these situations can be broadcast by the originating cars themselves or by a traffic light equipped with Car2Infrastructure Communication (C2IC) facilities (see Tab. 2.4). In the case of Car2Car Communication (C2CC) and C2IC an average maximum distance of 200 m is assumed if a direct connection between cars or the respective infrastructure is established. Additionally it is not always predictable for an assistance system which route is taken in urban scenarios and thus the selection of relevant obstacles increases significantly in complexity for larger anticipation horizons. Urban settings are also very challenging for RADAR sensors due to the complex geometric conditions which can limit the usable range of this sensor substantially.

2.2 Metrics for Anticipation Support

Different variants of an assistance system for anticipation support will be tested in the previously described situations. For the usability and acceptance of a system the subjective ratings of drivers are of high importance as they influence especially the long-term usage of

Object	Data Source	Ahead detection	Detection Probability	Accuracy	Update Rate
Standing / parking vehicle	C2CC	Distance: 200 m @Δ v = 50 km/h: 14 s	100%	1 - 7 m	≥ 1 Hz
Standing / parking vehicle	Radar	20 - 200 m (depends on road geometry)	> 73%	Speed: 0.1 km/h Angle: 0.3°	≥ 10 Hz
Traffic light	C2IC	Distance: 200 m @Δ v = 50 km/h: 14 s	100%	100%	unknown

Table 2.4: Technical frame conditions for blocked ego lane situation detection. Due to the geometrical properties of an urban scenario causing limitations in radio signal performance only short ranges can be covered. Ideally traffic lights should be equipped to function as a C2IC endpoint.

the assistance. Furthermore the objective effectiveness regarding safety and fuel efficiency must be assessed to evaluate the expected impact and differences between system variants. Regarding the objective effectiveness several metrics that will be used in experiments are explained in the following paragraphs.

Time To Collision The Time To Collision (TTC) parameter has proven to be a valuable indicator in safety analysis as proposed by Hayward in 1972 (see [Hay72]) who classifies it as "an adequate unit to rate the danger of almost any traffic event". It is defined as the "time that remains until a collision between two vehicles would have occurred if the collision course and speed difference are maintained". Equation 2.1 and figure 2.5 illustrate this definition, where $x_{i-1}(t)$ and $v_{i-1}(t)$ are the position and speed of the leading vehicle and $x_i(t)$ and $v_i(t)$ represent these values for the ego vehicle. The parameter L_{i-1} indicates the length of the preceding vehicle and the reference point is located at the middle of the front bumper.

$$TTC(t) = \frac{x_{i-1}(t) - x_i(t) - L_{i-1}}{v_i(t) - v_{i-1}(t)} \qquad (2.1)$$

Figure 2.5 shows the time-position relation for the TTC if it is defined for the conditions at the beginning of a braking maneuver. Here a leading vehicle starts braking and the driver of the ego vehicle tries to avoid a collision by also starting to brake after a reaction time. During the initial platoon the TTC is infinite and only gets a positive value if the preceding vehicle has a lower speed than the ego vehicle. In the case of departing vehicles the TTC has negative values indicating that there will be no collision. Low positive values are associated with high danger potential due to the short available time for a correcting driving maneuver to avoid a collision.
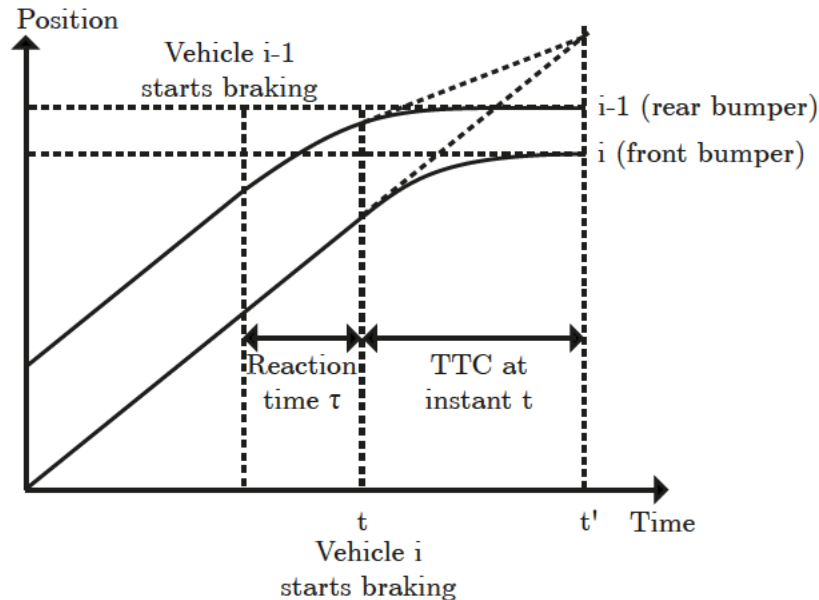
Figure 2.5: Illustration for the definition of Time-To-Collision (TTC). Here the TTC is defined for the conditions at the onset of braking of the ego vehicle (adapted from [MB01]).
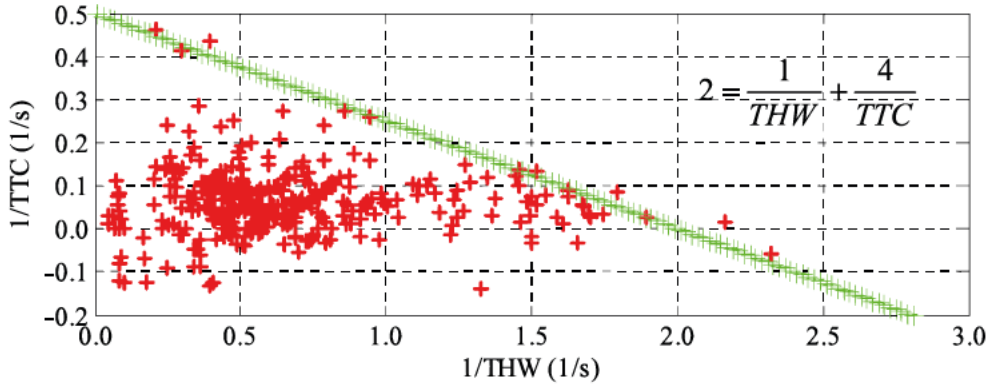
Figure 2.6: Results of the car following maneuvers in [Kon+08]. All drivers chose a risk level lower than 2 based on Eq. 2.3.

Time and Distance Headway The distance headway is defined as the distance between the rear bumper of the leading vehicle and the front bumper of the ego vehicle. With this definition it is already part of the TTC equation (numerator in Eq. 2.1) which shows that a high distance headway leads to a high TTC value and finally to a low danger potential within a situation. The main disadvantage of the distance headway metric is its independence of the ego speed leading to high variations of its value depending on the driving situation.

The Time Headway (THW) is defined as the time it takes for the ego vehicle to travel the distance headway with the current ego speed. Equation 2.2 shows that it is equal to the TTC with the only difference that the leading vehicle is assumed to be a static obstacle.

$$THW(t) = \frac{x_{i-1}(t) - x_i(t) - L_{i-1}}{v_i(t)} \tag{2.2}$$

Both metrics TTC and THW are limited to be reasonably applicable only in certain conditions. Kondoh et al. propose in [Kon+08] a combined metric called "Perceived Risk" that shall resemble the risk estimation of human drivers. The related equation 2.3 shows that both TTC and THW are used to produce a more universal metric.

$$\text{Risk Perception} = \frac{A}{THW} + \frac{B}{TTC} \tag{2.3}$$
$$\text{with} \quad A = 1 \quad \text{and} \quad B = 4$$

The term containing THW relates to the risk perceived in a static car following situation where the TTC becomes infinite and the containing term equals zero. In contrast the TTC term becomes relevant in dynamic situations. Fig. 2.6 shows the results of a driving simulator experiment with different car following situations. The red crosses denote the risk levels drivers accepted during these situations and the green line represents a risk level of 2 which is practically never exceeded.

Maximum Deceleration Sudden decelerations can have a number of negative consequences both on the ego vehicle and the following traffic. In the case of the ego vehicle they

can cause a rear end crash in the worst case, but also degrade energy efficiency in case of a hybrid or fully electrical vehicle. If the desired brake force is higher than can be achieved with recuperation, brake energy is lost due to additionally needed conventional braking. The crash scenario is also relevant for the following traffic, but also without a crash sudden braking can cause traffic jam waves upstream the movement direction as described by Horn in [Hor13]. As a consequence the maximum deceleration serves as a metric for both crash likelihood and the formation of traffic jams.

Fuel Consumption   Early anticipation could not only improve safety but also fuel efficiency by influencing the driving style. In experiments involving real vehicles the fuel consumption can be obtained directly from the on-board electronics. For virtual experiments it is necessary to use mathematical models such as the ones described in [KH04] to estimate this metric. As fuel consumption is closely related to the amount of emitted CO_2 this variable is of special interest these days.

2.3   On-board Sensor Systems

The following sections will give an overview on current and future data sources that are relevant for the proposed assistance function. First conventional sources which are readily available are discussed, then possibilities and properties of C2XC are analyzed.

On-board sensor systems are already widely used and have proved their reliability in a large number of systems. They all have in common that they are mounted on the ego vehicle and provide data at high update rates and low latency. Additionally the expected error types, rates and magnitudes are known as the sensors are integrated by the car manufacturer. This is important especially if the outputs of several sensor systems shall be fused into a global environment model.

2.3.1   Global Positioning System

The GPS uses an array of satellites to obtain the 3D position of a receiver (see also [Xu07] for a detailed description). This is possible if at least four satellites are "visible" from the receiver position and if the signal is not attenuated or distorted by buildings or other interfering objects. Even in a free field condition the positioning can have a non-negligible error that is usually modeled with an error vector as described in [FCP06]. Table 2.5 shows the stochastic parameters of such an error vector using a projection on the earth surface. Due to the comparably high computational effort needed to calculate the position from the satellite signals, consumer grade receivers achieve an update rate of only 1 Hz. Professional devices have update rates of up to 10Hz and in the case of Differential GPS the accuracy can be improved substantially using correction signals from reference stations with known positions.

Error Vector Mean length	Error Vector SD	Min. / Max.	Update Rate
18.1 m	16.7 m	0.1 m / 128.3 m	$\geq$ 1 Hz

Table 2.5: Typical characteristics of GPS positioning accuracy. The position error on the earth surface is modeled with an error vector of which length and angle are modeled separately (values from [FCP06]).

2.3.2 RADAR

RADAR sensors function by sending out electromagnetic waves at frequencies of several Gigahertz. By measuring the time-of-flight and angle of the echoed signal remote objects can be detected. Automotive RADARs can be divided in Short Range Radar (SRR) with a detection range of up to 30 m and Long Range Radar (LRR) with a practically usable range of up to 150 m (see [RN05]). Maximum range and accuracy can only be reached for objects with high percentages of metal content as they have the best reflection properties for the electromagnetic radiation used by RADAR. For pedestrians the working range can decrease from 200 m to 90 m as stated in [Tut08].

In the case of two RADAR equipped vehicles approaching each other a blinding effect can occur (see [Gam+07]) which can reduce the detection accuracy dramatically. This problem can be addressed with spread spectrum techniques and dedicated signal content, e.g. a chaotic signal. Typical specifications of LRR like operating range, FOV etc. are listed in table 2.6, whereas the detection probability depends on the distance to the interfering vehicle. Also the accuracy of the range and angular measurements are a function of the chosen RADAR system and the relative position of the measurement object.

2.3.3 Cameras

Sensors which use optical measurements have the advantage to be less susceptible to large variations in material composition of the measurement environment than RADAR sensors. Yet such sensors depend heavily on illumination properties which can be mitigated only to some extent by the use of light sources on the car. For the use case of anticipation assistance only cameras pointing towards the driving direction are relevant. Examples are cameras for Night Vision (NiVi) systems ([XLF05]), LDW([Pei+09]), Road Sign Recognition ([EPR10]) etc., see [HFL08]. A special property of NiVi cameras is the use of the infrared spectrum ($\lambda \in [780nm; 1000nm]$) which makes them susceptible for heat radiation from people, deer or other cars. The obtained pictures can be shown directly on a screen as a greyscale picture or be enhanced by additional markers around relevant objects on the road ahead as seen in [Bau+08]. In some systems an additional icon in the instrument cluster and / or a sound is generated to alert an inattentive driver. The other examples employ cameras for the visible

Range	Horizontal FOV	Detection prob. (Dist.)	Update Rate
0.5 - 250 m ($\Delta = \pm$ 1 m)	$\pm 30°$ ($\pm 4°$)	0.736 (140 m) - 0.999 (20 m)	30 Hz

Table 2.6: Typical characteristics of automotive Long Range Radar sensors, values from [RN05], [HFL08], [Gam+07] and [Sch05]

Range	Horizontal FOV	Detection prob.	Update Rate
300 m	± 36°	0.63	30 Hz

Table 2.7: Typical characteristics of automotive Night Vision sensors with pedestrian detection, values from [FLI08] and [KGV11]

spectrum ($\lambda \in [380\,\text{nm}; 780\,\text{nm}]$) to obtain a greyscale picture and therefore depend on environmental lighting and the headlights.

Current production systems are single camera setups while several developments have been made to employ stereo camera systems. The latter ones can be used to obtain depth information in addition to motion vector fields as described in [KL08] which leads to a much more detailed representation of the environment.

Light Detection And Ranging (LIDAR) sensors also belong to the group of optical sensors for ranges of up to 100 m. Unlike cameras they scan their working space in a manner similar to RADAR systems and thus provide angle and range information of reflection targets. The main difference to RADAR is the significantly larger FOV and a shorter usable range. Several attempts have been made (e.g. [LW09]) to implement a sensor information fusion of RADAR and LIDAR data for more reliable data. In summary the described sensors cover a range of approximately 200 m in front of the car with a minimal FOV of 30° and an update rate of 20 - 30 Hz. When we assume a static obstacle with optical detection properties we can detect it with a TTC of about 5.5 s.

The aforementioned onboard sensors can serve as a source for C2XC to provide information about the vehicle environment, in particular about surrounding non-connected vehicles. By patching together the provided environment information of all connected vehicles, a much more comprehensive environment model can be obtained than by using only the position information of a connected vehicle, see [RSK08].

2.4 Communication Based Sources

Besides the previously described on-board sensors there is a second class of data sources. These sources have either remote sensors as their input or semantically more complex information like traffic jam positions and types, road conditions or temporal usage restrictions provided by the police, traffic control centers, private companies or other institutions. They all have in common that their information is transmitted to the car via a wireless connection either from other cars (C2CC over a Vehicular Ad-hoc Network (VANET)) or from an infrastructure (C2IC with Road Side Unit (RSU)s or a Radio station network). Due to the nature of such communication based sources the transmitted data is always augmented with a spatial information as the position of the ego car cannot be taken as

Range	Horizontal FOV	Detection prob.	Update Rate
300 m	±22°	0.96	25 Hz

Table 2.8: Typical characteristics of automotive Front Camera sensors with vehicle detection, values from [ZBM06], [Lim+10] and [KGV11]

Range	Horizontal FOV	Vertical FOV	Update Rate
0.3 - 80 m, $\Delta = 0.2$ m	$\pm 80°$, $\Delta = 1°$	$3.2°$, $\Delta = 1°$	20 Hz

Table 2.9: Typical characteristics of an automotive LIDAR sensor, values from [LW09]

a reference. This process is called georeferencing and has an additional influence on the accuracy and in some cases the time delay for locating an event, see section 2.4.1.2.

2.4.1 Traffic Information Systems

Current implementations of traffic information systems use journalistic data from the police or other public forces, sensors on bridges, induction loops, Floating Car Data (FCD) and statistical analysis based on the former sources. This data is aggregated in traffic centers and is then provided to online services or broadcasted over radio station networks. The most traditional way of communicating this information are still announcements during the normal radio program. Online services convert it to a human readable augmented map, the radio broadcast via TMC or TMCpro is usually received by navigation systems for display and rerouting.
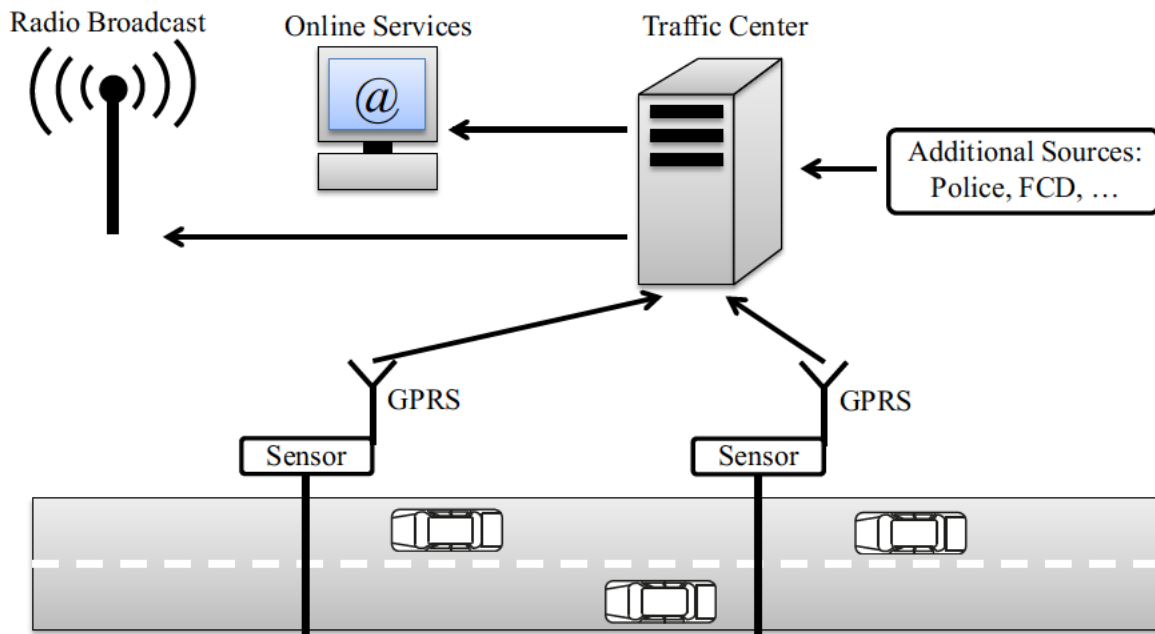
Figure 2.7: Telematic chain of current traffic information systems. Data is collected from fixed sensors, the police, FCD and other sources. The aggregated data is then distributed to online services and radio stations which broadcast it over Radio Data System (RDS)-TMC or DAB to receivers in navigation systems or on-board computers of cars.

2.4.1.1 Data sources

Data about the current traffic situation can be obtained in various ways as already seen in Fig. 2.7. The slowest and most inaccurate way are reports from the police or other public authorities. Fixed and mobile sensors are already an integral part of the telematic chain and serve also as basis for statistical analysis which also provides (synthetic) data.

Journalistic Data   This source is supplied by people participating in traffic who report their surrounding conditions to a central institution. They are either normal road users or action forces like police or firefighters. Private road users can report to radio stations or motor clubs running their own services. This is the least accurate and most delayed source among the traditional ones, Wischhof et al. state in [Wis+03] that delays of 20-50min are common.

Fixed Sensors   A network of video, RADAR and induction loop based sensors has been established along major routes. These can provide objective measurements regarding density, flow and speed at their place of installation. Such measures allow detailed implications about the current traffic state. Data from these sensors is always available and can be obtained with negligible delays.

Mobile Sensors   This relatively new source is fed by the current speed and position of cars floating with traffic. In the case of FCD such cars are equipped with telemetric units that gather this data from the car's bus systems and GPS sensor. It is then transmitted via the cell phone network to a traffic center. Another possibility is to use the GPS sensor of the cell phone or the positioning capabilities of a network cell itself to determine the movements of its carrier. That way network providers and even mobile device manufacturers also become a source for traffic centers.

Statistical Analysis   Based on the sources mentioned above and expert knowledge from previous days or years the traffic development over time can be extrapolated. This is not a source in the traditional sense as it provides entirely synthetic data, yet it is still a valuable tool.

2.4.1.2 Georeferencing Methods

Several ways of encoding geodata are currently used in traffic information systems like TMC, or TPEG Automotive Protocol (TAP) (according to [Frö07]). They all allow for a more or less accurate spatial referencing of traffic events and can be divided into direct, indirect and hybrid referencing methods.

Direct referencing uses absolute coordinates which allow the encoding of an arbitrary location. The most widely used system (e.g. for GPS) is the World Geodetic System 1984 (WGS84) which is based on a spherical coordinate system. In order to associate a WGS84 position to a certain road to evaluate whether an incident is on the future route the accuracy

of the on-board GPS system must be sufficient and the digital map material must be up to date.

Indirect referencing methods use higher level attributes which rely on the knowledge of the street network structure to address positions on it. The simplest variant are position names which have a similar structure like postal addresses. A main disadvantage of such addressing schemes is the need for a high number of characters to encode a position that makes it uninteresting for low-bandwidth applications. Another possibility is to use the link ID which is assigned to a node of a digital map or linear referencing using the relative position on a certain road segment. This system has the disadvantage that the map format is in most cases proprietary which leads to incompatibilities between different manufacturers.

The next example are pre-defined position codes that are assigned to important parts of the road network. Every relevant network part is assigned a unique number (ID) as it is done e.g. in the ALERT-C standard which is used for TMC. This requires large tables containing the mapping between a road network element and its ID but allows very efficient position encoding. A major drawback of this system is its inflexibility regarding street network changes and the lack of exact representation for arbitrary positions.

The last approach is called hybrid referencing as it uses a combination of the aforementioned techniques for a high robustness when using different digital maps and unavoidable positioning errors. In the ISO standard 17572-3:2008 1212 (see [ISO08]) the AGORA-C encoding algorithm is defined that uses both WGS84 encoded absolute positions along with additional environment data to identify a certain position even with sub-optimal GPS reception.

2.4.1.3 Traffic Message Channel

Currently the most widely used Traffic Information System is RDS-TMC which uses the ALERT-C protocol defined in ISO 14819-1:2013 (see [ISO13]). It uses the Radio Data System (RDS) channel of analog radio receivers to transmit the type of an incident, its position (encoded with location codes), affected road segments, the estimated duration and the proposed detour route. While the system already provides a great value for drivers, it still has some major drawbacks:

- Due to the low bandwidth of the RDS channel (60 Bit/s) it can take up to 30 min until all messages in the queue are received. This is especially a problem at the beginning of a trip when the initial route choice is made and potential incidents have not yet been received.

- The static definition of location codes allows only a very coarse position description of an incident. Often two neighboring locations are related to two consecutive on-ramps.

- Changes in the street network are usually only included by adding new location codes. This ensures compatibility with older receiving devices but also imposes an upper limit to the number of possible updates due to a fixed number of available location codes.

In Germany this system was introduced in 1997 to enable navigation systems to choose the optimal route under current traffic conditions.

2.4.1.4   TPEG Automotive Protocol

The TAP is an enhanced version of the initial Transport Protocol Experts Group (TPEG) standard. TPEG uses Intersection Location (ILOC) to encode positions (this includes a WGS84 coordinate and the names of three adjacent roads) which overcomes most problems when using different digital maps, but the re-recognition rate can sometimes still be as low as 60% (see [Ran06]). As a consequence the mobile.info consortium defined the TAP standard in [mob07] which uses a combination of TMC and AGORA-C georeferencing methods. If a TMC location code is available for an incident, this is used for positioning. Otherwise the redundant AGORA-C information is used which contains both WGS84 coordinates and geometric information about the surrounding street network comparable to the ILOC standard.

In contrast to RDS-TMC the TAP is not limited to a certain communication channel. Its binary or Extensible Markup Language (XML) encoded messages can be transmitted over DAB, Digital Video Broadcast (DVB) or the internet. Currently it is mainly used in combination with automated sensors and FCD which make it a very responsive service. It is used for the navigation systems of several major manufacturers for optimal routing decisions.

2.4.2   Car2X Communication

Besides the already existing communication based data sources a new class with the name Car2X Communication (C2XC) has been developed for several years now. It can be divided into two subclasses, Car2Infrastrucure Communication (C2IC) and Car2Car Communication (C2CC). In the case of C2IC all connected vehicles communicate with a centralized infrastructure while C2CC stands for an ad-hoc network between adjacent vehicles. Figure 2.8 shows how both topologies can be combined so that clusters of cars forming a VANET are connected via a RSU to a larger infrastructure. These networks serve both as a backbone for acquiring traffic data and to forward messages back to the vehicles. These messages can contain incident, weather and other information that is forwarded to the relevant receivers using broadcasting or geocasting (position selective delivery).

Message Propagation   It is essential to chose the appropriate message propagation scheme as Fig. 2.9 shows. Especially in dense traffic scenarios it can happen that schemes like Directional Flooding (see [Zan+08]) where every vehicle node repeats incoming messages cause a flooding of the network. The filtering process limits this issue by allowing propagation only in certain driving directions, but still it is possible to cause a serious impairment of network performance. With propagation schemes as proposed by Zang et al. in [Zan+08] where packets are transmitted in a modified single-hop manner this problem can be mitigated.

Another question especially for anticipatory assistance is the transmission quality at high distances. Figure 2.10 shows the reception probability between two network nodes for optimal conditions (see Xu et al. [XB06]). Using the IEEE 802.11p wireless standard the reception probability is still above 95% at a distance of 400m. Such conditions will probably occur very rarely and mostly in rural or highway settings. Urban environments
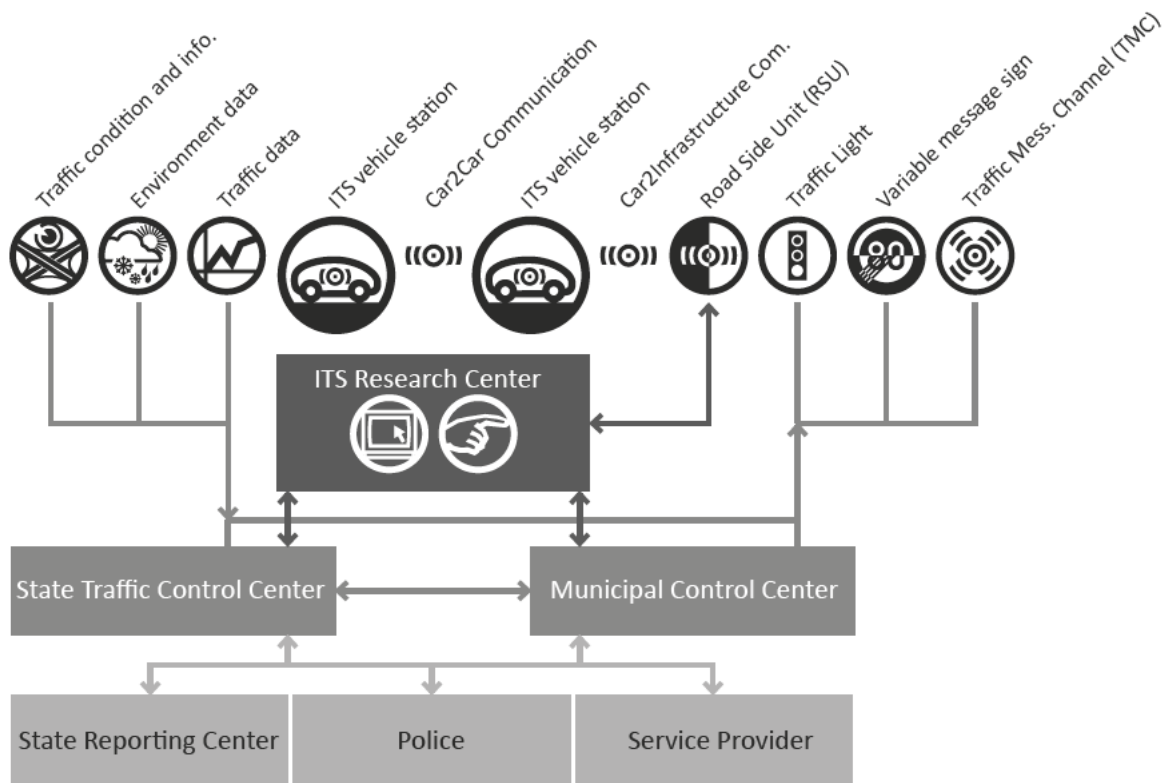
Figure 2.8: Example of an ITS infrastructure using Car2X Communication. A combination of C2CC and C2IC is used together with traffic centers and various sensor systems to build a modern ITS (based on [sim11]).
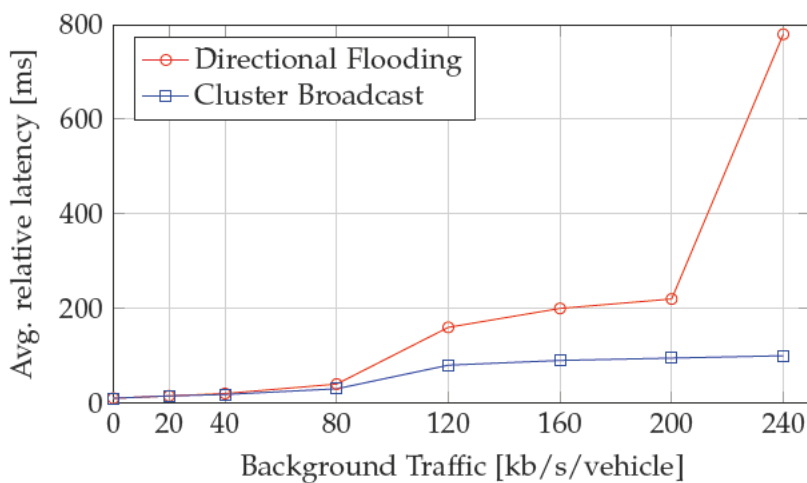
Figure 2.9: Packet latency in an IEEE 802.11p based Car2X network for varying background traffic. Depending on the broadcast mechanism the impact of background network traffic can vary widely (based on [Zan+08]).
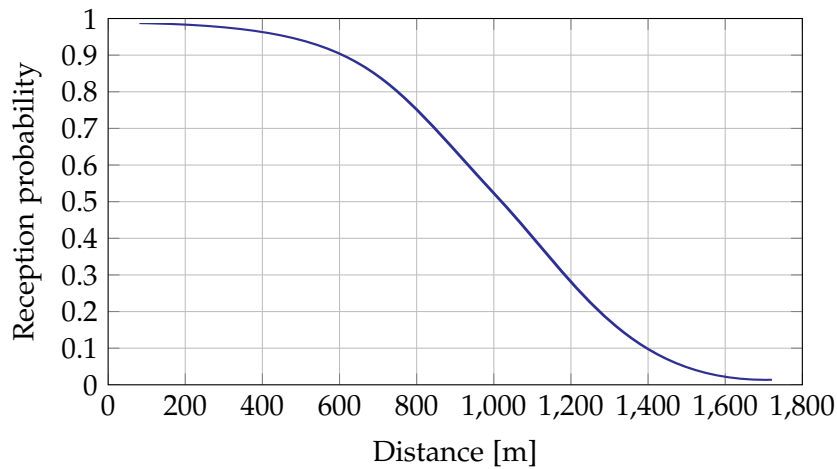
Figure 2.10: Reception probability in an IEEE 802.11p based Car2X network depending on the distance. The plot represents ideal conditions without interferences (based on [XB06]).

usually produce substantially more interferences through signal reflections or shielding effects especially in areas with high buildings.

Cooperative Perception   The success and reasonable benefit of using C2XC in real life depends heavily on the quality of the data base which is closely related to the penetration rate of equipped vehicles. It is not possible to give a general minimum penetration rate as it depends on the desired application. One possibility to obtain a more complete model of the traffic scene is the usage of the measurements from other vehicles besides the ones from the on-board sensors. This process is called "cooperative perception" because all cars in the network solve the perception problem in a cooperative way. Like that not only the data from the connected vehicles themselves can be used but also their measurements that cover vehicles without connection to the C2XC network.

A problem that arises from limited accuracies of the involved sensors systems (GPS for self-locating, RADAR, LIDAR or cameras for object detection and tracking etc.) are the different detections of the same object from the networked cars. Figure 2.11 shows the detections and how they can be associated to a single object as described by Rauch et al. in [Rau+13]. The next step is then to fuse these detections to obtain a unique tracking object. This fusion process must also take into account the detection quality of each connected sensor in order to minimize errors introduced by sub-optimal sensing conditions. Additionally tracking algorithms like Kalman filters can be applied to improve the final tracking result that is added to the cooperative environment model.

2.5   Summary of Prerequisites for Anticipatory Assistance

In this chapter a set of relevant traffic situations and their requirements for different sensor and communication technologies has been identified. These situations include complex scenarios in urban environments which are in some cases difficult to detect and analyze.

Figure 2.11: Matching the object detections of different vehicles for cooperative perception. During an overtaking maneuver each car tracks the others if possible and communicates the positions. Blue boxes represent locally perceived objects, transmitted objects are shown in red. The matching result is marked green (taken from Rauch et al. in [Rau+13]).

Sensor systems that are already in use today like RADAR or camera systems often suffer from the same problems like optical occlusions as a human driver.

In such cases communication based data sources that use C2XC have a clear advantage as they are not as strongly restricted to the geometrical properties of the environment as conventional sources. With either C2CC to build a VANET or C2IC for infrastructure communication such problems like large distance perception and the perception of obstructed obstacles become manageable. In the following chapters it is assumed that perfect C2XC is available in the form of precise vehicle or obstacle positions without transmission delays or other imperfections.

3

Anticipation Support and User Interfaces

After the relevant situations for anticipation support and potential data sources have been defined in the previous chapter, several HMI variants for an assistance system are developed. The underlying Business Logic (BL) is always the same and only a short overview will be given as it has already been developed by Popiv in [Pop12]. As especially this part of the proposed assistance system was developed in the Intelligent Support for Prospective Action (ISPA) project, the term "assistance" and ISPA are used as synonyms. It takes data from various data sources as input, determines the optimal deceleration strategy and provides this information to the HMI. This modular approach provides a simple way to exchange only the HMI for highest comparability.

The following sections cover the preliminary steps to develop both the assistance function and the basic HMI principles. Then the concepts of iconic interfaces displayed in the digital instrument cluster, more advanced interfaces for the Head-Up Display (HUD) and finally an abstract interface using Light Emitting Diode (LED) modules are explained along with results of user studies in the driving simulator.

3.1   Preliminary Steps

In chapter 2 several relevant situations for anticipation support were identified. The only on-board sensors that are relevant in these situations are the RADAR, LIDAR and cameras. Current long range RADAR sensors can cover distances up to ca. 200 m, depending heavily on the environment such as road geometry, buildings and so forth. Even on a rural road with a speed limit of 100 km/h and optimal sensor performance the covered time horizon is considerably less than 10 s. In order to provide assistance in a way so that drivers are informed about upcoming situations in time. Like that they are able to cope with the situation in a relaxed and confident way. This time horizon needs to be extended substantially with communication based sources as described in chapter 2. The different time horizons provided by the various sensor types are depicted in Fig. 3.1.

Earlier information especially with a time horizon of more than 10s is desirable as it can shift any driver action to an earlier time instant. Additionally it can be possible that the time taken for analyzing a situation could be shortened significantly if the available information is condensed in a way that allows faster decisions by the driver. These relationships are depicted in Fig. 3.2. Sommer found in driving simulator experiments (see [Som12]) that
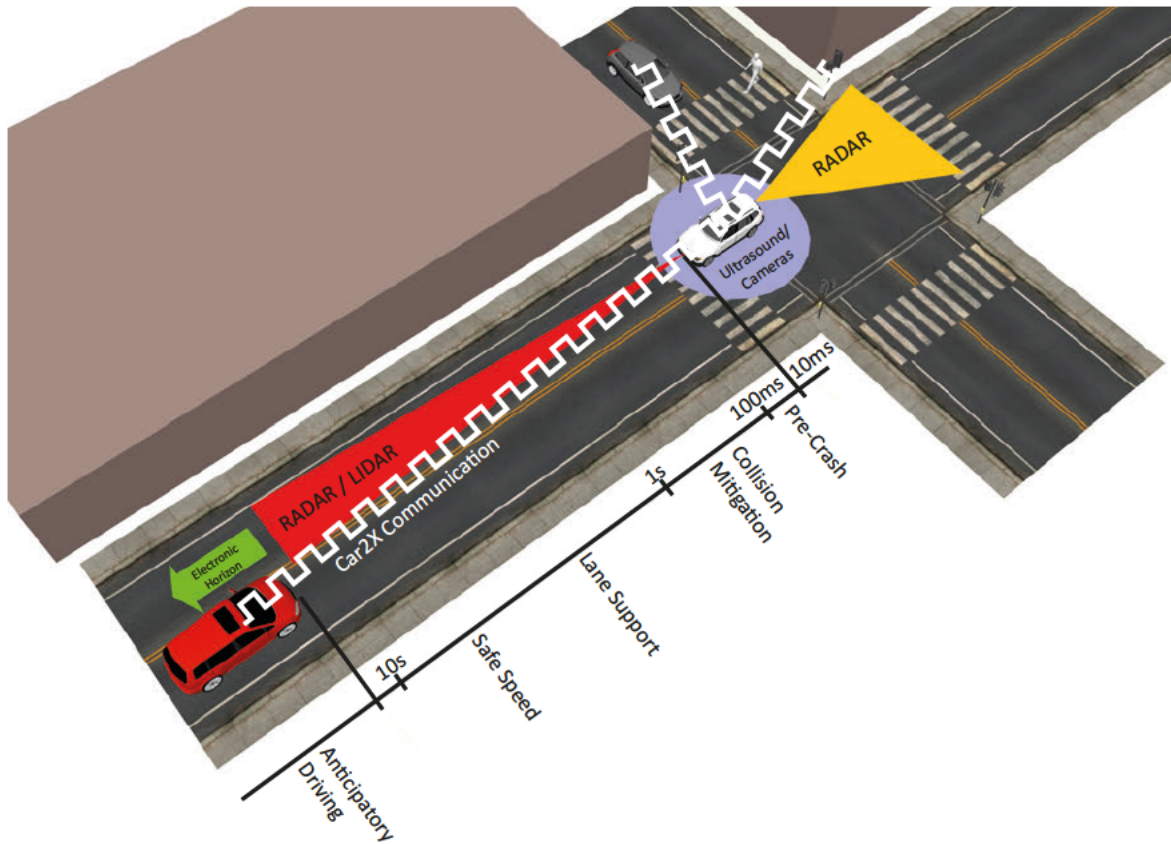
Figure 3.1: Time horizons for current and future driver assistance systems. Areas that are currently covered include the red and yellow triangle (RADAR and LIDAR) and the blue circle (ultrasound sensors and cameras). Communication based sensor information extends the electonic horizon to a very large area, represented by the green arrow. The white square wave represents Car2Car and Car2Infrastructure wireless connections.

the time at which a driver looks at visual cues for the upcoming situation varies widely (4 - 10s in the example of approaching a traffic light). She also found that the time interval between the first look at a cue until an observable action takes place also varies strongly, in the traffic light experiment the interval ranged from 3 s to 7 s. Also the type of situation has a strong influence on the time that the driver decides to let pass until he actively reacts on a situation. In the case of a jam the test persons reported to react "immediately" while some would react "in the last second" for a speed limit.

In [Ful84] Fuller states that the perceived level of risk originating from an aversive stimulus is very subjective. He also states that the actions that are taken are based on the anticipation of potential (and very individually assessed) risks connected to the upcoming situation. This variance in elapsed time from the perception of cues regarding the situation and an actual action is represented by the combination of the blocks "Recognition of driving situation" and "Decision" in Fig. 3.2 where a more timely and precise information can lead to more immediate and homogeneous actions among drivers.

Figure 3.2: Safety benefit from earlier driver actions rendered possible through anticipatory ADAS. Timely and detailed information enables a more precise and earlier decision on the needed actions and improves safety (based on [Pop12]).

Improved anticipation resulting in earlier and more precise driving actions can both lead to improved fuel consumption (see [Rei+98]) and a lower probability of encountering dangerous situations (see [WSS90] and [Klo+97]). Both properties are reported to be related to the chosen speed or speed profile in the mentioned publications. As a consequence a system supporting the driver with both assistance for his speed choice and further information about the upcoming situation could lead to an improvement in the aforementioned areas.

For the development of the assistance system the following questions need to be covered as stated by Schmidtke in [SB93]. The question about temporal aspects was formulated by Endsley in [End95] in the context of Situation Awareness (SA): "Situation awareness is the perception of the elements in the environment within a volume of time and space, the comprehension of their meaning, and the projection of their status in the near future". Consequently one can derive these aspects for developing an HMI for anticipation support (list based on [Pop12]):

- Content: which information should be provided?

- Form: how should it be communicated?

- Place: where should this information be presented?

- Time: When is the right time to provide it?

The answers to these questions can be divided into two groups: principles related to timing and activation of the assistance and ones that are related to the presentation of situation relevant information and maneuver recommendations. As already mentioned the BL implementing the timing and activation of the system has already been developed by Popiv in [Pop12] and is therefore not changed for the different experimental setups. The development of various HMI variants will be presented in more detail afterwards.

3.1.1 Business Logic

Based on the previous thoughts a system for anticipatory driving could provide assistance in choosing the right speed with the optimal way of deceleration along with an explanation why this is reasonable or necessary. The timing and activation behavior of the assistance system is controlled by a module determining the appropriate deceleration strategy. This
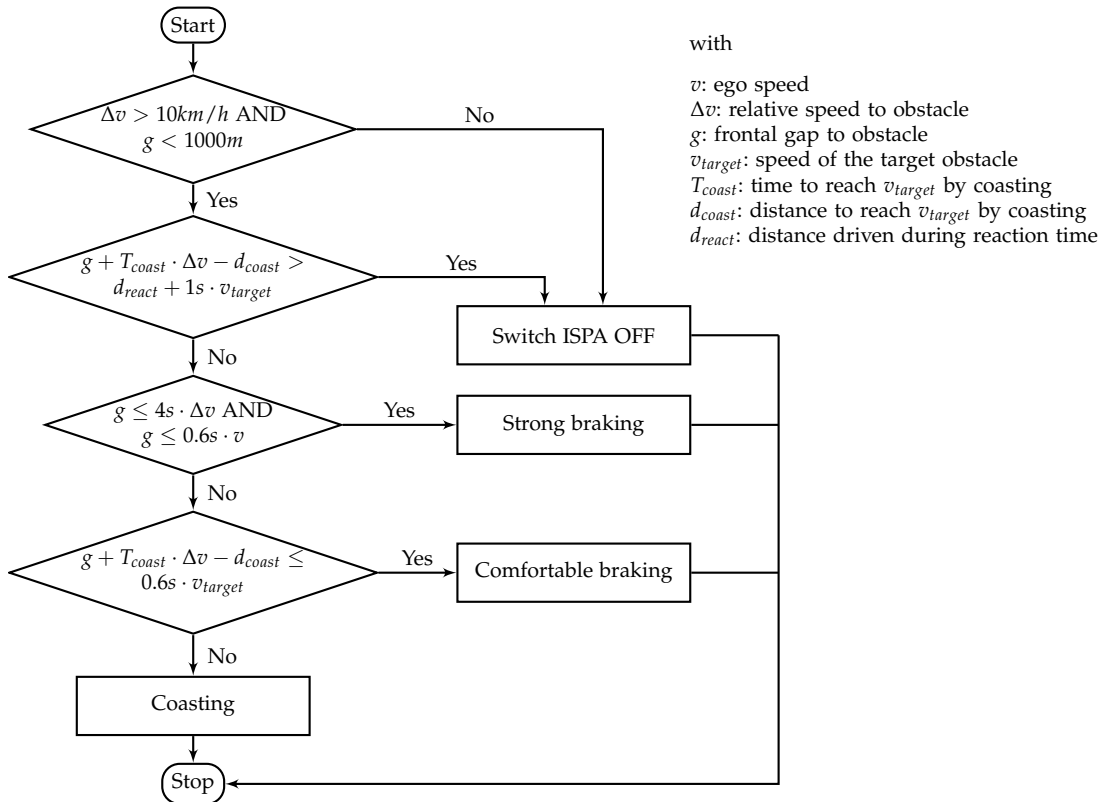
Figure 3.3: State diagram for ISPA timing and deceleration strategy selection. The proposed deceleration strategy is communicated to the HMI while additional information like the distance to the obstacle are directly provided by the sensors.

module obtains its information from the on-board sensors and communication based sources such as C2XC. In contrast to the sensor descriptions in chapter 2 the data used for the experiments is absolutely accurate. This means that there are no delays, no measurement noise and no false alarms or misses. The minimum set of required input data streams includes:

- Speed of the ego vehicle

- Speed development function during coasting (deceleration by engine drag torque)

- Speed, distance, type and position of obstacles on the ego lane

3.1.2 Interface Conception

The following paragraphs give some practical examples and implications of these principles and how they can be applied for the assistance systems to be developed. These guidelines have been assembled by Popiv in [Pop12] and are based on the work of Endsley in [EBJ03].

Comprehension- and projection-oriented presentation An assistance system should present information at a high abstraction level rather than provide cues that can easily be perceived by the driver himself. Such low level cues must be integrated into a larger context by the driver which requires a higher amount of working memory than information at the level a driver uses to decide further actions. An example for such a high level information could be "you must stop before passing the intersection" instead of providing easily available information like "you are on the secondary road". The first information allows for anticipatory driving while the second version only gives details about the current situation.

This principle is closely related to the three levels of cognitive processes: skill-, rule- and knowledge based processes. Vicente and Rasmussen state in [VR92] that the goal of ecological interface design is "to design interfaces that do not force cognitive control to a higher level than the demands of the task require, but that also provide the support for all three levels". As a consequence the interface should offer all information that is required by the knowledge-based process and still facilitate the two lower levels of cognition. Like that the user can identify potential malfunctions of the system and also does not need to rely on only one type of information.

Goal-oriented presentation Assistance outputs shall be co-located with a specific goal and also provide answers for the major decisions related to a certain goal. This is important for the transition between goal-driven and data-driven approaches. It should be possible to survey the current and future state of a system or the situation at the same time.

Continuous presentation For global Situation Awareness (SA) the operator must be able to obtain information about all of his goals at all times. In situations where a goal is more important to the user the related information must be more detailed. The system state and eventual changes must be transparent to the user while they should not be annoying due to their permanent presence (see also [Nor02]).

Salient presentation of important cues System outputs related to key features of the assistance function must be identified and designed to be salient in the HMI. Especially outputs related to prototypical situations must be targeted in order to ease the goal switching process in critical situations. This can be particularly helpful in mobilizing appropriate mental models.

Extraneous information exclusion Any extraneous information that is not relevant to both a particular situation and the needs of a general SA should not be present in an HMI. The resulting clutter reduction facilitates the concentration of the user to the relevant cues especially in critical situations.

Parallel processing support Multi-modal interaction should be possible especially in data rich environments. According to Reif (see [Rei10] pp. 122-123) the most relevant sensory channels in the automotive domain are the visual, auditory and haptic channel. Although these channels have different information rate capacities and delays (see [Joh94]

and [Sch00]), their combination can yield a quicker and more complete SA formation and resulting actions (see also Fig. 3.2).

Facilitation of the most beneficial action For skill-based behavior an interface can use signals that become connected to certain actions after a learning phase. Examples of such signals are color changes, audio events or haptic feedback.

Temporal aspects These aspects include not only the question when the assistance shall be activated but also how the interface can reveal temporal relations in the upcoming situation. Based on the work of Cook et al. (see [CNM07]) the following points should be considered:

- Reaction time: in the time gap between the perception of a stimulus and an observable action several cognitive processes take place. These include the comprehension of the stimulus, the anticipation of the outcome of an action and the final decision from several possibilities to fit the current situation.

- Temporal constraints: the reaction time can be limited to a certain maximum in a specific situation. This must be addressed by the HMI in a way that the effort to interpret its output is adequate to meet this constraint.

- Movements and long lasting actions: movements and coordination tasks take a certain time. This must be considered especially in dynamic environments that complicate the execution of e.g. manual tasks.

- Temporal perception: the HMI design must facilitate the understanding of temporal relations in the current and future situations. This is of special importance for anticipatory assistance.

The issues "reaction time" and "movements" need to be considered for the activation time of the assistance as can already be seen in Fig. 3.3 depicting the Business Logic (BL) of the system. Regarding the other aspects "temporal constraints" and "temporal perception", these have an influence on the content of the User Interface.

Summary of requirements The ideal HMI which uses all of these principles would present the information in a comprehension- and projection-oriented way and would be continuously available. Events that the system has been explicitly designed for are communicated with salient cues while leaving out any extraneous information. The multi-modal interface should reveal appropriate actions for the current situation and provide cues for temporal relations in the scene to allow extrapolation by the user. Also the time needed to derive a decision from the perceived situational cues needs to be considered and eventually be adjusted to the selected level of cognitive abstraction. Additionally the interface shall provide cues that the user can link to certain actions to facilitate quick skill-based reactions.

In the following sections several variants of HMI implementations which are based on the above principles will be developed. Depending on the implementation different

Figure 3.4: Initial HMI variants for the anticipatory ADAS: Iconic (left) and Bird's Eye Perspective (right). Both images show the output for exactly the same situation but with very different graphical implementations.

principles are more emphasized than others in order to explore the boundaries of sensible feature combinations.

3.2 Iconic User Interfaces

Many HMI implementations in the car such as turn-by-turn navigation systems use icons due to their simplicity and language-independent nature. The icons are either binary switched on and off or are enhanced with simple animations. This shall be the basis for the first design iteration of an HMI for the proposed assistance system. For a comparison an interface developed by Duschl in [Dus+10] is also presented and both systems are evaluated in a driving simulator study.

3.2.1 Animations with explicit action requests

The first version of an HMI for the anticipatory ADAS is based on simple animated icons. It comprises a standardized traffic sign symbol that represents the upcoming situation and an action recommendation implemented with animated pedal symbols, see Fig. 3.4 on the left. All icons are arranged between the instrument gauges for Rotations Per Minute (RPM) and speed which is both a conservative choice yet the most prominent position available with a standard dashboard design.

3.2.1.1 Design Principles

In the example shown in Fig. 3.4 the system informs the driver about a traffic jam with the corresponding official sign. All traffic signs were modified in a way that their usually colored borders are shown in gray scale to emphasize that this is not an information about a current regulation but a future situation. The pedals represent the accelerator and brake pedals of an automatic gear shift car. If the BL suggests coasting, the accelerator pedal is marked orange (otherwise it is white) and animated to resemble a releasing motion. In case the BL suggests comfortable or strong braking, the brake pedal is animated to show a pressing motion and is marked orange. If no information is to be communicated to the user all icons are removed from the display.

Regarding the design principles formulated above, the system fulfills the point "comprehension- and projection-oriented presentation" in a way that an abstract yet commonly used

sign informs about the upcoming situation. Additionally the low-level cues regarding the pedals are given so different abstraction levels are covered. The co-location of the icons and the current speed covers the principle of goal-oriented presentation. During the suggested deceleration the icons stay visible for a continuous presentation and provide a salient cue by appearing at the beginning of a detected situation. Extraneous information is left out due to the minimalistic approach. Here only the visual channel is used for the initial design, but the onset of the assistance could be emphasized e.g. with a gong sound which would also tackle the principle of using low level signals. The reduction to simple icons limits the possibilities for the presentation of temporal relations in the future situation and therefore is not covered in this implementation.

The second HMI variant in Fig. 3.4 was developed by Duschl in [Dus+10] and is introduced for a comparison between a very simple and comparably complex interface design. It shows a simplified view of the traffic situation in a range of up to 1000m ahead of the ego vehicle. By using the metaphor of a bird eye perspective already proposed by Nestler et al. in [Nes+09] the driver's point of view is shifted to a position above his own vehicle. Also in reality this would allow him to survey a larger area around and especially in front of him which improves the possibilities for enhanced anticipation.

Different than the iconic variant it always displays a minimum amount of graphical elements which are the symbol representing the ego vehicle and the road representation. The suggested deceleration strategy is encoded by the color of the ego vehicle by using green for coasting, orange for comfortable braking and red for strong braking. Also the size of the symbol increases in steps with a higher deceleration suggestion. While the ego vehicle is always positioned at the same place, the relative motion of the other vehicles is shown on the virtual road that also roughly depicts the shape of the road. Additionally a standard traffic sign is shown next to the road representing the upcoming situation.

This design also covers different abstraction levels which are demanded by the "comprehension- and projection-oriented presentation" principle. It both presents high-level cues by visualizing the traffic situation ahead and low-level ones with the deceleration suggestion encoded with the ego vehicle. For the goal-oriented presentation the HMI is also located close to the speed gauge and a minimum set of graphical elements is always shown for continuous presentation. The onset of a situation is made salient by initially placing an oversized version of the traffic sign in the middle of the visualization which is then moved with an animation to its final position and scale. Again this HMI uses only the visual channel but could be enhanced with the auditory channel in the same way as the iconic interface. The bird eye view allows for a simple recognition of basic temporal relations in the scene while leaving out unnecessary details such as vehicle type etc.

3.2.1.2 User Study

Both HMI variants shall now be tested in a fixed-base driving simulator together with the baseline condition without any assistance. The simulator is based on a BMW 6 series convertible car and uses three monoscopic projection screens to achieve a 180° horizontal FOV. The 26 participants (17 male, 9 female) with an average age of 34 years have mileages of less than 10000 km per year (seven drivers), 10000 - 20000 km per year (eleven drivers) or more than 20000 km per year (eight drivers).

Study structure   The sequence of tasks that had to be accomplished by the test drivers included an introductory drive, a first-contact situation and three drives with different assistance configurations:

- Introductory drive (20min): Drivers shall become familiar with the driving simulator. This also serves as a possibility to reduce the effects of Simulator Adaptation Syndrome (SAS) for the following tasks to obtain unbiased results. Especially some of the older drivers experienced nausea already in this phase and quit the experiment.

- First-contact situation (3 situations, 5min per system): This task serves to evaluate the HMIs whether they can be understood intuitively without any previous knowledge. By alternating the first system to be used learning effects are minimized for this section and the presented situations were not used in the following experiment parts. After the driving task users had to report orally what their understanding of the system is. After that the different HMI variants are explained to the drivers.

- Main experiment (11 situations, 20 min per system): These test drives are used to obtain objective data from the simulator and subjective data with the help of questionnaires. Three conditions are tested: no assistance (baseline), Bird's Eye Perspective and the Iconic HMI. Each variant is driven with the same test track but in varying orders of situations to minimize learning effects. After each 20 min drive a questionnaire about the current configuration must be filled out by the participants.

- Final questionnaire: In this step final comments can be made for both HMI variants. Additionally they can be compared and a final general preference can be given.

With this structure it is possible to obtain subjective ratings regarding intuitive understanding of the system, relative ratings between the variants and objective measures related to safety and foresighted driving. The situation "Static traffic jam" on a highway shall be investigated in more detail (see Fig. 3.5) as it will be used for most subsequent experiments.

Results   First the subjective results shall be investigated starting with the questions related to likability, feeling of safety, understandability and the level of support for adapting to the situation. Fig. 3.6 shows the results for both systems and reveals that the Bird's Eye Perspective gets overall better ratings. In the case of likability the difference is statistically significant ($p = 0.003$ using a Wilcoxon matched pairs signed ranks test) as well as the understandability ($p = 0.002$). The two other questions show no significant difference with a 5% error threshold.

Regarding the overall wish for such an assistance system the result is very positive with the interquartile range between the two highest rankings, see Fig. 3.7 for details. When participants had to decide which HMI variant they would choose if the assistance system was an integral part of their car the Bird's Eye Perspective was again ranked higher (median 1) than the Iconic HMI (median -1 with larger interquartile range).

The participants also had the chance to give general feedback with free text fields. This is especially valuable for later versions of the tested HMI variants and gives an insight into the reasons why a certain variant worked better or not. In the case of the Bird's Eye

Figure 3.5: View of the situation "Static traffic jam" on a highway. Trees along the road combined with a long-drawn curve make it impossible to see the rear end of the traffic jam in time.

Perspective it was mentioned 11 times that it is clearly understandable and the visualization of distance to the obstacle and oncoming traffic are rated positively. Six participants wanted to have even more information in the HMI and the color scheme was overall mentioned seven times to be not understandable or that it should be improved (see Tab. 3.1 and Tab. 3.2). The color scheme was mentioned several times to be sub-optimal, especially for the ego car. Participants mentioned that the green color of the ego car icon suggests that everything is in order and it is even possible to accelerate similar to a green traffic
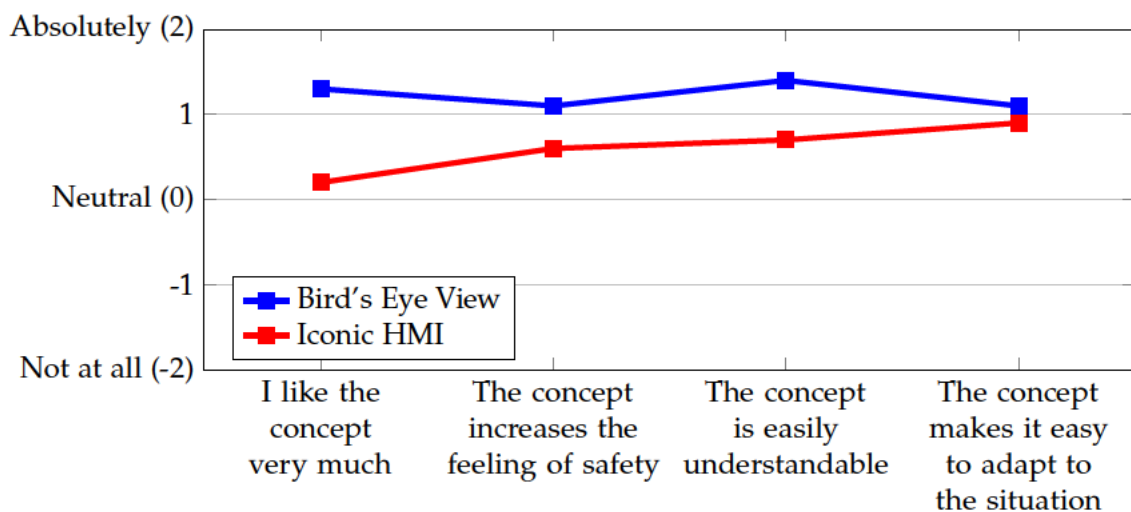
Figure 3.6: Results of likability measures of the first HMI prototypes for the anticipatory ADAS. Generally the mean values of the Bird's Eye Perspective are ranked higher than the Iconic HMI. Only the first and second question show a significant difference at the 5% level.
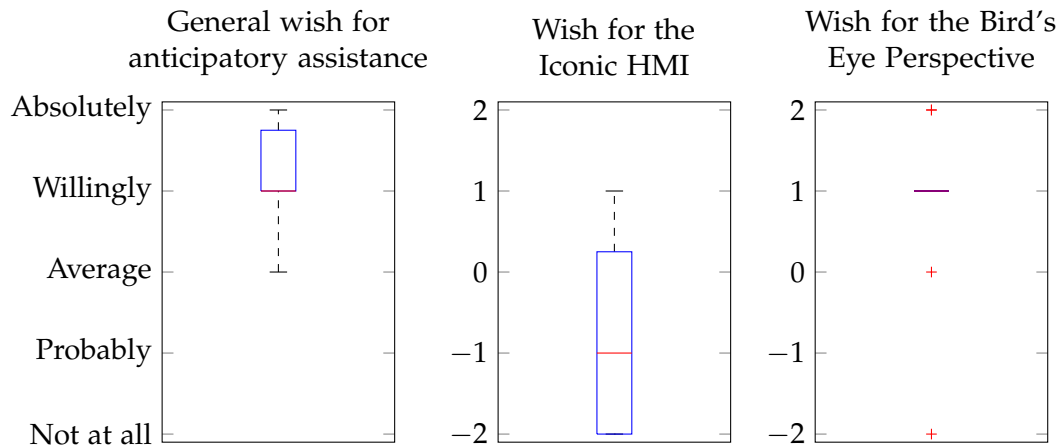
Figure 3.7: Results of the general wish for an anticipatory ADAS and separate results for the Bird's Eye Perspective and the Iconic HMI. The results for the distinct HMI versions are only for the case if a car is already equipped with the system and the HMI can be chosen freely.

light. This property should be adjusted in future versions of the HMI. The facts that no elements of the HMI were rated to be unnecessary, only a low number of references to missing information (explicit distance information was mentioned three times) and the overall very positive rating of the concept show that it is already at a very mature state.

On the other hand the Iconic HMI seems to have several issues that need improvement. Especially the visualization of the pedals was mentioned ten times to require improvements (see Tab. 3.3) and seven times to be not understandable or unnecessary (see Tab. 3.4). Also it was not clear to three participants why the traffic signs were shown in a modified version. Similar to the other HMI an explicit distance information was missing for the participants. The simple design was mentioned five times to be positive. While three participants liked the explicit action recommendation encoded with the pedal animation, this metaphor seems to be very problematic due to the numerous negative statements about it.

The plots in Fig. 3.8 show the helpfulness of both HMI variants in the different situation types. For all situations the Bird's Eye Perspective is rated higher while both systems have a comparable relative rating of the situations. The situations with the highest ratings are "Traffic jam", "Stagnant traffic" and "Construction site" which all belong to areas outside of

Positive Properties (count)	Improvable Prop. (count)
Easily and clearly understandable (11x)	Additional information (6x)
Distance visualization (7x)	Color scheme (3x)
Oncoming traffic visualization (5x)	
Ego lane indication	

Table 3.1: Positive and improvable properties of the initial Bird's Eye Perspective version. Generally the higher level of detail is appreciated while some participants would like to have even more information.

Missing (count)	Unnecessary (count)	Not understandable (count)
Distance information (3x)	none	Color scheme (4x) Meaning of leading vehicle arrangement (3x)

Table 3.2: Missing, unnecessary and poorly understandable properties of the initial Bird's Eye Perspective version. Although the visualization supports rough distance estimations this can still be improved. The visualization of a future situation was not always clear using the Bird's Eye metaphor.

urban roads. In later experiments the focus will lie on these situations because they are most relevant for the system. Drivers stated that the other situations occur too frequently and would cause considerable annoyance by the system and could possibly lead to a deactivation of it.

The objective results from the driving behavior show that both variants convince the driver to decelerate earlier and over a longer period of time. From the data in Tab. 3.5, which represents the approach of a static traffic jam on a highway, we can see that the coasting phase in the baseline case begins at 494 m in average and has a large Standard Deviation (SD). The latter indicates that drivers without assistance perceive and react on a situation very individually. For the assisted cases deceleration begins at more than 900 m before the jam with less than ca. 80 m SD indicating an equalization of driver behavior and a significantly longer distance and time to adapt their speed. The maximum deceleration during the approach is also decreased in the assisted cases with a statistically significant difference between both variants and the baseline. With at least 2 m/s^2 less deceleration with assistance means a safety improvement especially for the interaction with following drivers.

Drivers approached the situation with a speed of approximately 150 km/h which would lead to a coasting distance of more than 1.5 km. Because the assistance system starts to inform the driver from a maximum distance of 1 km, it is always activated from this distance on. During the baseline experiments four accidents occurred which all had a TTC value of ca. 5 s (4.3 s, 4.2 s, 5.5 s and 4.6 s) when they first saw the jam. Van der Horst states in [Hor90] that 5 s are a TTC value for critical situations which matches with the observed accidents.

Positive Properties (count)	Improvable Prop. (count)
Simple design (5x) Color scheme (3x) Explicit action recommendations (3x)	Pedal visualization and animation (10x) Meaning of signs not clear (5x)

Table 3.3: Positive and improvable properties of the initial Iconic HMI version. Especially the animated pedals and the traffic signs are must be improved, the simple design and the clear action recommendations are rated positively.

Missing (count)	Unnecessary (count)	Not understandable (count)
Distance information (6x)	Pedals (7x)	Pedals (7x)
Situation and track visualization (4x)	Pedal animation (5x)	Modified traffic signs (3x)

Table 3.4: Missing, unnecessary and poorly understandable properties of the initial Iconic HMI version. Again the pedal visualization seems to be unwanted or not understood, distance information is missing.
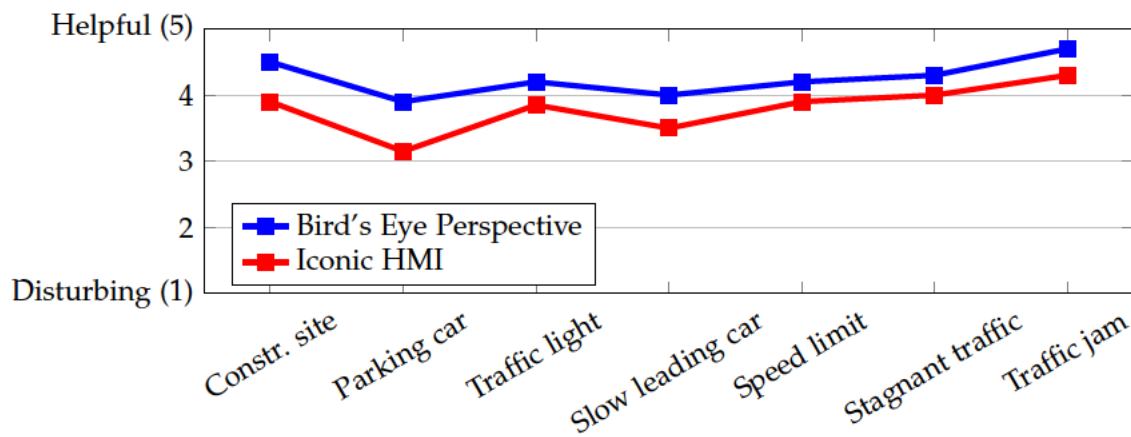
Figure 3.8: Rating of the helpfulness of anticipatory ADAS in different traffic situations. Generally the Bird's Eye Perspective is rated higher, the relative rating of the situations is valuable for the situation selection in future experiments.

Variant	Opt. Brake Dist./TTC	Coasting Dist./TTC	Brake Dist./TTC	Maximum Deceleration
Baseline	1000 m 24.3 ± 5.0 s	494 ± 259 m 14.8 ± 6.4 s	225 ± 50 m 6.4 ± 1.7 s	8.4 ± 2.2 m/s^2
Iconic HMI	1000 m 21.2 ± 2.9 s	907 ± 83 m 20.5 ± 4.1s	571 ± 239 m 13.3 ± 5.2 s	6.4 ± 2.0 m/s^2
Bird's Eye Persp.	1000 m 22.7 ± 3.9 s	932 ± 42 m 22.3± 4.3 s	620± 246 m 15.2 ± 5.2 s	6.0 ± 2.2 m/s^2

Table 3.5: Distances, TTC values and maximum decelerations with their SD for different phases of a traffic jam approach using different HMI variants. Both the coasting and the braking phase start earlier with the Bird's Eye Perspective than with the Iconic HMI while coasting starts considerably later in the baseline case.

Variant	Fuel Consumption (Mean/SD)	Travel Time (Mean/SD)
Baseline	100% ± 9%	100% ± 9.3%
Iconic HMI	95.6% ± 11%	102% ± 9.7%
Bird's Eye View	96 ± 12%	102.4% ± 14.6%

Table 3.6: Influence of anticipatory ADAS on fuel consumption and travel time. The baseline values are normalized to represent 100% for easier comparison.

The driving style also has a significant influence on the fuel consumption. If only the consumption during a deceleration phase is regarded, savings of up to 50% are possible. However, these phases account for only a small fraction of the overall travel time which reduces the impact. Tab. 3.6 shows the fuel saving potential for the whole test drive of 20 minutes with statistically significant savings of ca. 4% in both variants related to the baseline.

In terms of travel time the assistance increases it due to the lower average speed during deceleration phases. When experiencing high time pressure drivers might be tempted to ignore the assistance or to turn it off. But the objective measures show that the increase in travel time is only ca. 2% in average which can be neglected in most cases.

Discussion and Conclusion   The initial versions of both HMI variants proved that the anticipatory ADAS animates drivers to decelerate earlier. This shows that the time horizon for foresighted driving is extended which improves especially safety measures like TTC and maximum deceleration. Longer deceleration phases cause a lower fuel consumption with a difference of ca. 4% related to the baseline experiment. The overall travel time for a 20 minutes drive increased by ca. 2% which is negligible in related to the improved safety measures.

At this point two very different HMI variants have been presented which both had the desired impact on driver behavior. The relatively complex Bird's Eye Perspective provides a detailed view of the traffic scene ahead while the Iconic HMI is very minimalistic on the one hand and perceived to be patronizing on the other hand. The main changes that need to be made for the Iconic HMI is a replacement for the very explicit action recommendations with the pedal animations with a different element, the use of standard traffic signs and the introduction of a detailed distance indicator.

In the following sections it will be investigated if it is possible to use even more simplified outputs to inform the driver about the proposed deceleration. This could replace the pedal visualization while still using the traffic signs to give feedback about the reason for the deceleration. Additionally it shall be investigated how psycho-optical effects could be used to induce an unconscious speed reduction.

3.2.2   Informative Icons as Component for other HMIs

The Iconic HMI that was used in the previous experiment will now be adapted according to driver feedback. This means that the animated pedals are removed and the gray borders of
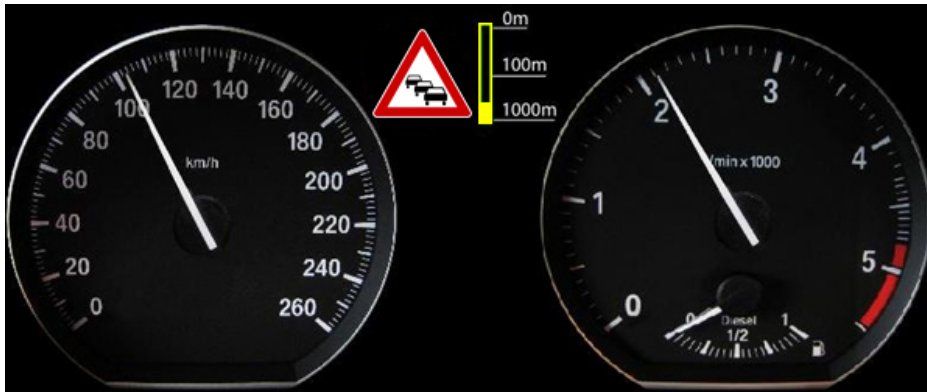
Figure 3.9: Improved version of the Iconic HMI. It will be used as a recurring element in further HMI variants to inform about the upcoming situation and the distance to it.

the traffic signs are replaced by their original color. A distance indicator bar is introduced with a logarithmic scale to cover larger distances as well as smaller ones with adequate accuracy. Fig. 3.9 shows the result with the described elements placed in the instrument cluster between the speed and RPM gauges.

Design Principles Similar to the original Iconic HMI the traffic signs are only visible during an active action recommendation to create a salient cue when the system changes its state. The scale of the distance bar is always visible to make the state switching not too prominent. Because the action recommendation with the pedals was removed, the color scheme of the distance indicator bar shall serve as a minimal version of it. The scheme is taken from the ego vehicle in the Bird's Eye Perspective but with the adaption that coasting is not encoded with green but with yellow color.

Due to its simple nature and small screen area footprint it can easily be combined with other elements to form a new HMI. It provides the information about the obstacle type and the distance as well as a rudimentary action recommendation encoded with the color scheme. Another possibility that arises from the modular screen design is to distribute the Iconic HMI and the action recommendation / driver activation elements over several screens. Like that the explanation for the activation can be moved to a less prominent place while the action recommendations reside at an easily visible position.

The following section will present several possibilities how this HMI element can be combined with elements in the HUD, haptic feedback and various LED arrangements. All of them share the intention to provide very low level and thus easily interpretable cues instead of the very detailed information provided by the Bird's Eye Perspective.

3.3 Abstract Interfaces in the Head-Up Display

HUD systems were originally introduced into military aircraft to support pilots (see Fig. 3.10). The idea was then adopted for passenger cars either with a transparent projection screen (Peugeot, Fig. 3.10 center) or a virtual projected image (BMW, Fig. 3.10 right). In the

Figure 3.10: Implementations of Head-Up displays. First applications were military aircraft (left), later the technology was adopted for cars (center and right picture).

case of a virtual image the geometrical properties have several advantages compared to the projection screen variant. Besides less required eye movement away from the horizontal gaze direction and only minimal effort for accommodation switching between the road and the virtual image plane the position of it allows an overlay of virtual elements similar to the Augmented Reality (AR) paradigm.

The HUD is very well suited to present low-level cues that can be perceived from the parafoveal and peripheral FOV. In contrast to the displays in the instrument cluster and the dashboard (also called Head-Down Display (HDD)) which require an eye movement away from the horizontal line of gaze of $\alpha_{HDD} \approx 17°$, the HUD only requires a movement of $\alpha_{HUD} \approx 4°$ (see also Fig. 3.11). Another advantage is the lower effort for accommodation caused by the high distance of $d_{HUD} \approx 2.2$ m to the virtual image. The standard size for the projected virtual image of the BMW HUD is 222.4 x 85.4 mm (see [Mil10]) which is sufficient for 2D elements with a fixed position. If graphical elements should appear to be part of the outside world (contact-analogue HUD graphics) the required image size is usually considerably larger. For this reason a new setup is required to achieve such an image for driving simulator experiments.

3.3.1 Hardware Design

The projected HUD as it is used by e.g. BMW has a light source and a display module that produce the image (see Fig. 3.12). To increase the length of the optical path without increasing the package volume of the HUD module, two mirrors are used: a folding mirror and a concave mirror. The concave mirror is also used to compensate the optical distortions caused by the windscreen shape. Also the windscreen needs a special structure to compensate the double reflections at both of its outer surfaces. To do this a wedged layer of plastic is inserted into the glass screen to combine both reflections.

The basic principle used in the combiner HUD of mirroring a projected image with a screen can also be used in a different geometric arrangement for a driving simulator. One possibility depicted in Fig. 3.13 is to use a standard video projector together with a rear projection foil. The projector is mounted above the car and the frame with the foil stands on the roof at the upper edge of the windscreen. An acrylic glass combiner screen mounted near the bottom edge of the windscreen (taking the function of the windscreen of the built-in HUD) mirrors the image on the projection foil towards the driver and lets the light of the main projection screen for the driving scene pass. The mirrored (virtual)
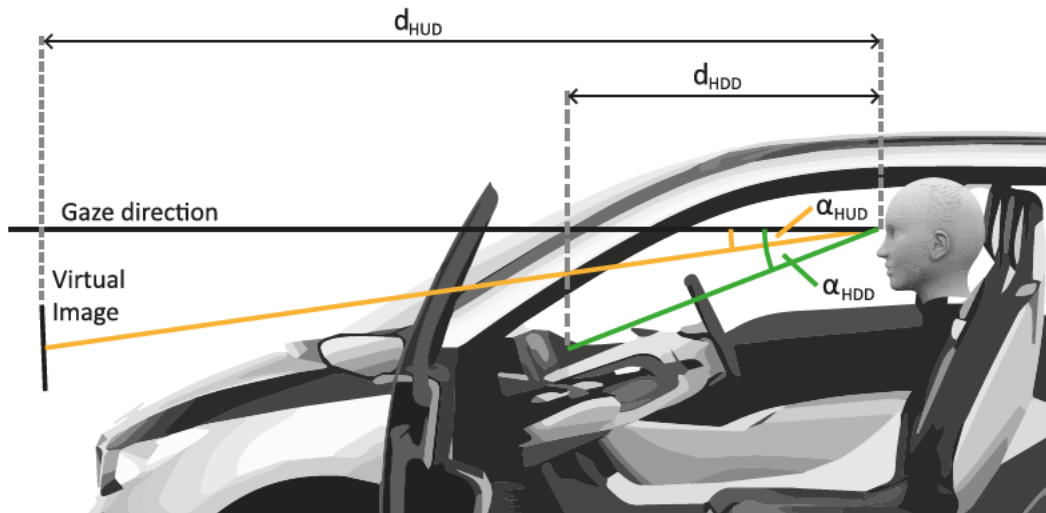
Figure 3.11: Geometrical layout of the Head-Up Display and the Instrument Cluster. The virtual image plane of the HUD is located at a distance of $d_{HUD} \approx 2.2$ m, the instrument Cluster (HDD) at $d_{HDD} \approx 0.5$ - 0.8 m. The viewing angle of the HUD is $\alpha_{HUD} \approx 4°$, the angle of the HDD is $\alpha_{HDD} \approx 17°$.

HUD image seems to be positioned in front of the engine hood at the same position as the built-in HUD image. Like that a virtual image having the size of the rear projection screen can be produced with off-the-shelf components. The display content can be generated with standard computing hardware.

Generally it would also be possible to display the content of the large HUD to be a part of the driving scene projection. But this would have several shortcomings:
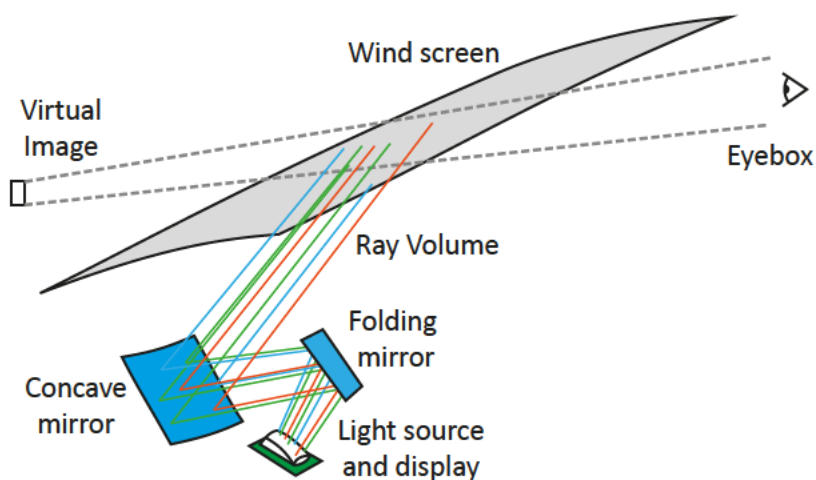
Figure 3.12: Basic optical principle of a combiner based Head-Up Display. A light source and a display module produce the image which is then mirrored at the windscreen. This results in a limited space for head positions (the eyebox) in which the virtual image is visible.
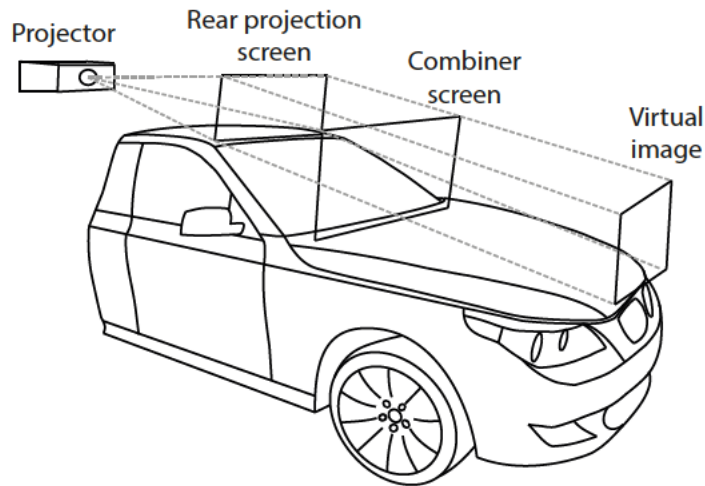
Figure 3.13: Hardware mockup for a large Head-Up Display. A projector generates a picture on a rear projection screen which defines the size of the virtual image. The combiner screen made of acrylic glass acts as a semi-transparent mirror for the driver and makes the virtual image appear in front of the car.

- All Business Logic and graphic rendering components of an assistance system would have to be included in the driving simulator. Using separate Hardware allows a more flexible software design and supports the reuse of a system with different simulator platforms.

- The actual distance of the virtual image is comparable to a real car and requires at least a minimal change in accommodation from the driver.

- A higher resolution for the HUD can be achieved than is possible with the scene projection. Even with a 4k projector (resolution 4096 x 2304) the resolution of a middle-class projector for the HUD usually cannot be outperformed.

A very valuable property of the presented design especially for research purposes is its scalability. By using a larger rear projection foil and combiner screen and a higher distance between the projector and the foil theoretically any size of the virtual image can be produced. This mockup can now be used for the driving simulator experiments to evaluate different HMI variants for the HUD.

3.3.2 Virtual Road Markings

The idea behind virtual road markings emerged from the application of real road markings to reduce speed at potentially hazardous road segments. One of the first studies regarding the effectiveness of such markings has been conducted by Denton in [Den80]. For the experiment a pattern of 90 yellow transverse bars spanning over the whole lane width was installed upstream a roundabout. The bars had a width of 0.6 m and a progressively decreasing distance from initially 6 m to finally 3 m. In the twelve months before the installation 14 crashes were recorded while there were only two during the 16 months

Day Time:	7-9 am	2-4 pm	6-8 pm	Mean
Before	59.1 km/h	57.8 km/h	54.9 km/h	57.0 km/h
After	42.2 km/h	45.2 km/h	44.7 km/h	44.1 km/h
% change	-28.6%	-21.7%	-18.5%	-22.6%

Table 3.7: Speed reduction by transversal bars upstream a roundabout. The installation proved to be effective by reducing the speed up to 28.6% (data from [Den80]).

after installation. For the data in Tab. 3.7 measurements have been recorded three weeks before and after the installation. The results show a reduction between ca. 18% and 28% depending on the time of day. This could indicate that the degree of susceptibility varies with the driving forces behind a trip.

Drakopoulos showed in [Dra03] that markings with groups of 10 chevrons similar to the ones depicted in 3.15 are very effective for speed reduction. He installed 16 sets of 10 chevrons on a length of 186m upstream a highway ramp. This resulted in an average speed reduction at detector B (sample size 25000 vehicles) which was positioned 12 m after the chevron pattern of 23.4% (24.5 km/h), see Tab. 3.8. Detector A was located 597 m upstream the first chevron set, detectors C and D were installed on a comparison ramp with similar geometry. The study yielded statistically significant changes due to the large sample size with promising results for speed reduction.

In a different study conducted by Meyer (see [Mey01]) transversal bars were installed to lower the speed in a work zone. He installed several detectors along the prepared area and one at the beginning of the installation as a reference. Fig. 3.14 shows that the speeds relative to the first detector are lower, but not to the extent observed by Denton. One interesting fact is that the overall speed decrease is higher for the upper 5% and 15% of the speed range. Although the speed differences are statistically significant, their magnitude is comparably small which Meyer attributes to a sub-optimal bar design and layout.

3.3.2.1 Graphical Implementations for Anticipatory ADAS

The studies presented in the previous section showed that road markings with bars or chevrons can have a considerable effect on the speed choice. Examples of successful experiments are depicted in Fig. 3.15. While these markings are installed statically on the road surface, a large HUD as shown previously could serve as a display to generate a

Detector:	A	B	C	D
Before	96.6 km/h	103.4 km/h	80.5 km/h	74.1 km/h
After	91.8 km/h	78.9 km/h	78.9 km/h	77.3 km/h
% change	-5.0%	-23.4%	-2.0%	+4.3%

Table 3.8: Speed reduction by chevrons upstream a highway ramp. The installation proved to be effective by reducing the speed up to 23.4% (data from [Dra03]).
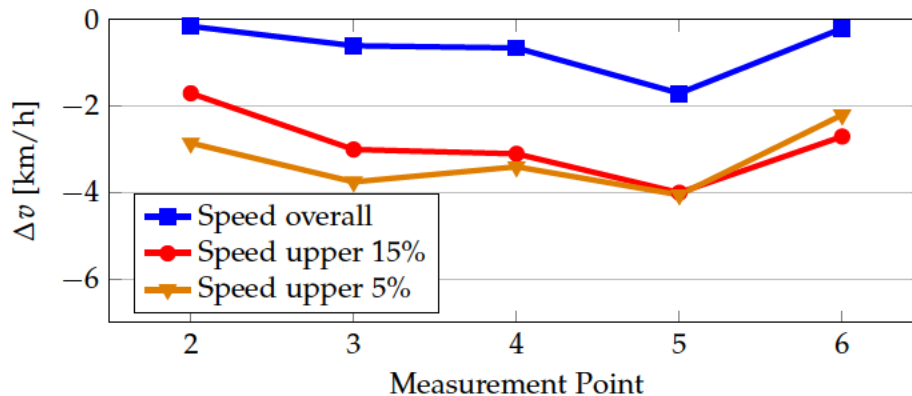
Figure 3.14: Speed development with transversal speed bars in a work zone. For the first four measurement points the pattern had increasing bar density. When the density stayed uniform (last measurement points) speed increased again. The effect is stronger for faster drivers (upper percentiles), data from [Mey01].

contact analogue version of such markings. Like that it would be possible to "take along" the markings which are then controlled by the BL of the anticipatory ADAS. As mentioned before it is necessary to provide also the reason and distance information related to an activation of the system, so the Iconic HMI developed previously will be combined with the virtual road markings.

Different than the real markings which can be seen on the whole visible length of the road ahead, the virtual version can only be used for a part of the road close to the ego vehicle. The reasons for this are mainly technical as even the large HUD does usually not cover the required FOV for such an implementation. Also it would be necessary to have very accurate 3D digital maps and the precise ego position available to render the markings at the right position especially for larger distances. Rendering the virtual content only in close vicinity minimizes the problem so the road geometry and ego position do not have to be taken into account at all. A tradeoff for this could be the usage of the steering wheel angle to adjust the geometry of the markings, but this has not been done in this work.

The perceived movement speed of the markings is not equal to the speed of the ego vehicle but dependent on the recommended deceleration strategy. This results in an actually lower speed than the road movement which reduces the optical flow and consequently the potential distraction in the peripheral FOV. Another benefit of the lower speed is that a single bar is longer visible even in the narrow area covered by the HUD.

Transversal Markings Several variants of the real world markings shown in Fig. 3.15 have been adopted for the HUD. There are two versions of chevron patters, one pointing away of the driver similar to the real chevrons and one pointing towards the driver to amplify the effect of an arrow shape pointing against the driving direction (see Fig. 3.16 left and middle image). Another version are the bars spanning from both edges of the ego lane (see Fig. 3.16 right) of which two variants exist with different bar lengths. In order to
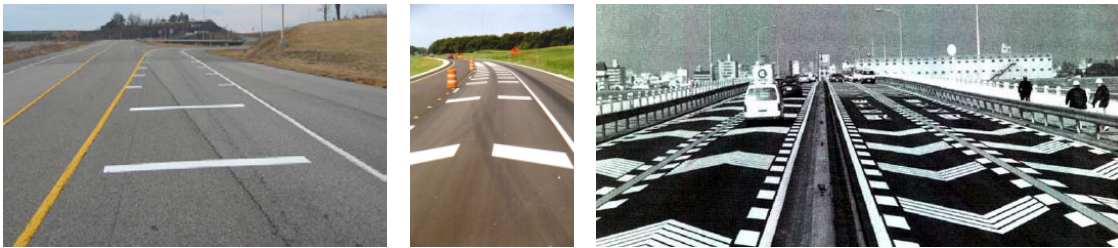
Figure 3.15: Pavement markings for speed manipulation. The left and middle markings were developed by Katz in [Kat07] and are installed in the USA, the chevrons in the right image served as basis for the work of Drakopoulos in [Dra03] and are installed in Japan.

test the influence of the HUD size a test run was made with the chevrons pointing towards the driver which were displayed in the standard HUD of the driving simulator mockup.

In a preliminary driving experiment these versions have been tested regarding their subjective properties. The experiment was conducted with 15 participants (11 male, 4 female, average age 22.73 years) who accomplished a test track with the "traffic jam on a highway" situation. After the experiment they filled out a questionnaire including the distraction, subjective influence on speed and subjectively perceived workload (see also Eilers et al in [ENH86]).

Figure 3.17 shows that the two version of the transversal bars were rated to be the least distracting visualizations. The chevron versions were rated to be distracting by ca. one third of the participants, even the one displayed in the small HUD. Regarding the subjective speed influence ratings (see Fig. 3.18) the strongest influence was attributed to the chevrons pointing towards the driver in the large HUD. This is followed by the chevrons pointing away from the driver, then the long bars and the small HUD variant. The lowest influence rating was given to the short bars. Based on the distraction rating and the subjective speed influence the chevron variant pointing towards the driver in the large HUD shows the best combination.

The data in Fig. 3.19 is based on a one dimensional rating scale. It ranges from 0 corresponding with "not demanding" to 110 corresponding to "extremely demanding" and was developed by Eilers et al. in [ENH86]. The relative ratings of the variants show roughly the opposite tendency than the distraction rating. Both bar versions have an equally low

Figure 3.16: Virtual road markings in the large Head-Up Display. Different chevron shapes (pointing towards or away from the driver) and transversal bars with different lengths were evaluated in a preliminary experiment (scene and HUD content digitally mixed for illustration purposes).
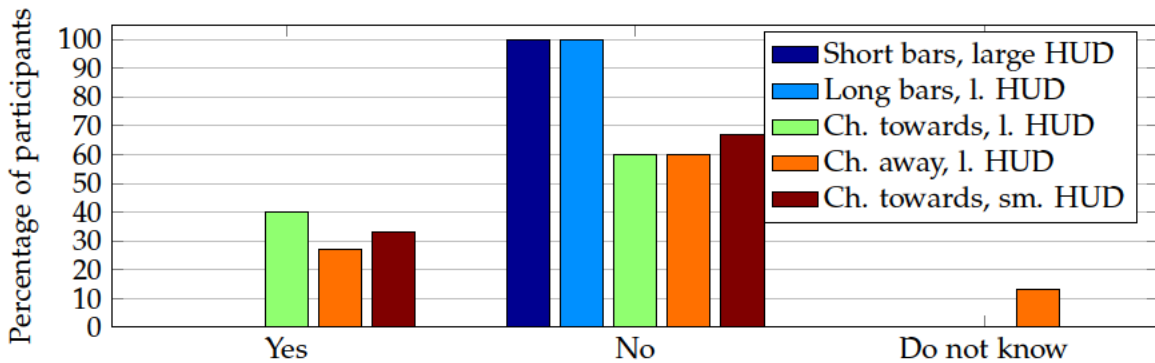
Figure 3.17: Distraction caused by different transversal bar visualizations in the HUD. The bars spanning from the lane edges have the lowest distraction potential, followed by the chevron variant in the small HUD.

rating while the highest rating is given to the chevrons in the small HUD. This effect has probably its origin in the fact that the small HUD has a comparably low resolution and graphics quality but still draws some attention. When drivers try to observe the content of the display this can only be done with a certain amount of attention.

Overall the best ratings were given to the chevrons pointing towards the driver. If they shall be combined with the Iconic HMI developed before the icons can only be positioned above the chevron area which is very close to the parafoveal FOV. This has been reported to be distracting by participants of a video-based study. A tradeoff between the optimal subjective ratings and the icon position is the visualization using transversal bars. This allows the icons to be positioned lower in the display area which causes less distraction. The result is shown in Fig. 3.20 which also contains the red dot used for the Peripheral Detection Task (PDT) which was developed by Martens et al. in [MW01].

Another effect that can be achieved with the bars spanning from the lane edges is a change in perceived lane width. Martens et al. show in [MCK97] that several studies found a positive relation between lane width and speed. One study showed that every
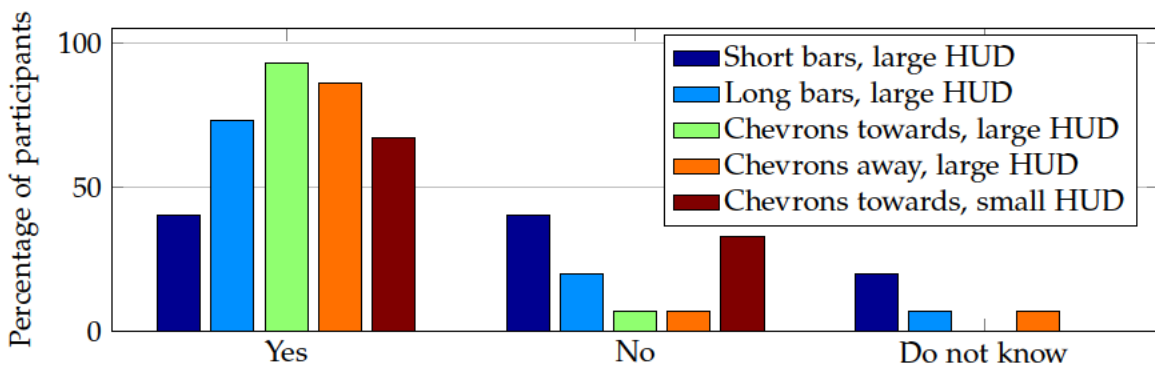
Figure 3.18: Subjective speed influence caused by different transversal bar visualizations in the HUD. The highest perceived influence is caused by the chevron variants in the large HUD.
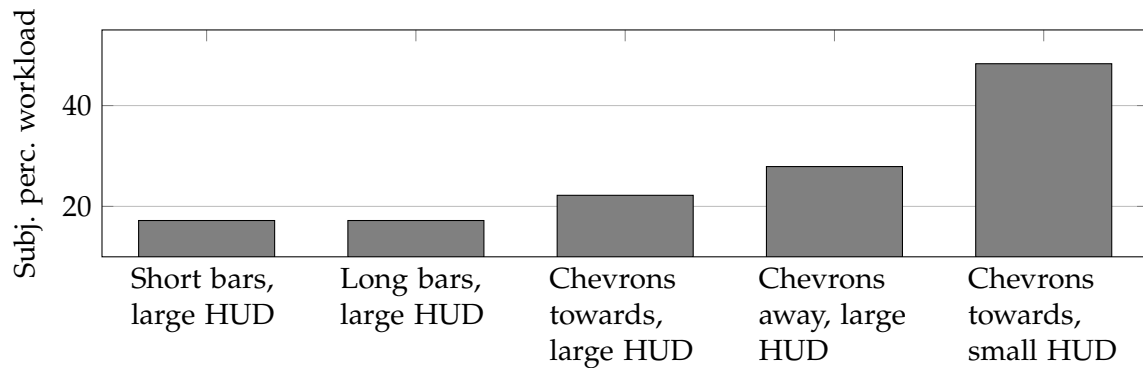
Figure 3.19: Subjectively perceived workload caused by different transversal bar visualizations in the HUD. The lowest values are assigned to the bar versions while the small HUD imposes high subjective workload (see [ENH86] for description of workload scale).

meter of decreased lane width decreases the driven speed by 5.7 km/h. This effect is also implemented by displaying longer bars for a higher recommended speed reduction. The bars from both sides never touch so there is always some area left on the bottom end of the HUD to display the Iconic HMI components.

Rumble Strips The basic function of the rumble strips is equal to the horizontal bars but extends them with haptic feedback in the driver seat. This is based on the concept of real rumble strips (see Fig. 3.22) which use small elevations on the road surface. These elevations cause car body vibrations and as a result a broader range of sensory channels
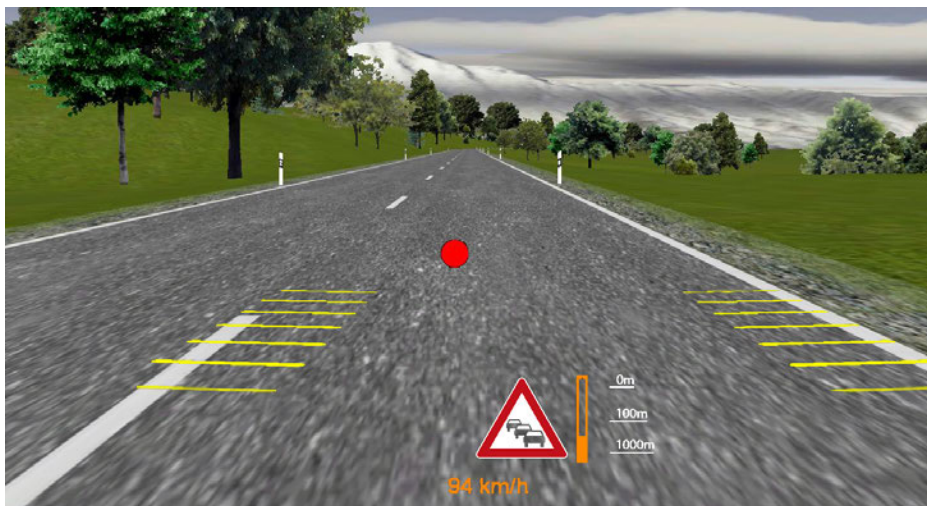
Figure 3.20: Picture of the transversal markings produced by the contact analogue Head-Up Display. The space between the markings is used for the Iconic HMI elements to inform the driver about the reason for the assistance activation. The red dot is part of the PDT (scene and HUD content digitally mixed).
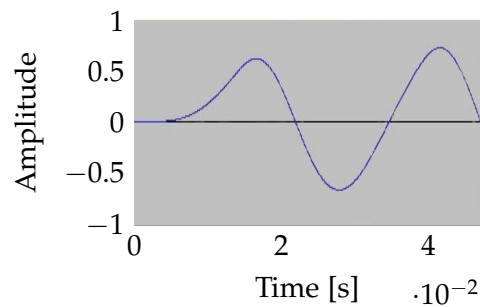
Figure 3.21: Plot of the audio signal for the rumble strips. This signal is played for every strip passing under the ego vehicle.

is activated. Like that the probability increases that a driver recognizes the strips even if he is not actively looking at them. In the driving simulator this is realized by installing an electroacoustic transducer causing structure-borne noise in the back rest of the driver seat. This transducer is coupled to the audio output of the computer generating the driving simulator sound via an active lowpass filter. Every time a rumble strip passes under the ego vehicle the waveform depicted in Fig. 3.21 is sent to the transducer.

Figure 3.22 right shows the implementation in the HUD in combination with the Iconic HMI. Different than in the transversal bars version the strips are closed like real rumble strips (the gap in the picture in Fig. 3.22 exists due to the lack of readily available fitting rumble strip elements). As a consequence the Iconic HMI elements must be placed above the strip visualization.

Vertical Bars The vertical bars are inspired by two different ideas in the work of Manser et al. (see [MH06]) and Anhäuser (see [Anh04]). Speed can be influenced with bar patterns

Figure 3.22: Picture of real rumble strips for speed reduction (left) and the implementation in the HUD (right). Several sets of rumble strips were installed upstream a construction site with small but statistically significant speed reductions (see [Mil+05]). Every time a virtual strip passes "under" the ego vehicle a rumble sound is produced by the subwoofer in the driver seat creating vibrations for haptic feedback (scene and HUD content digitally mixed).
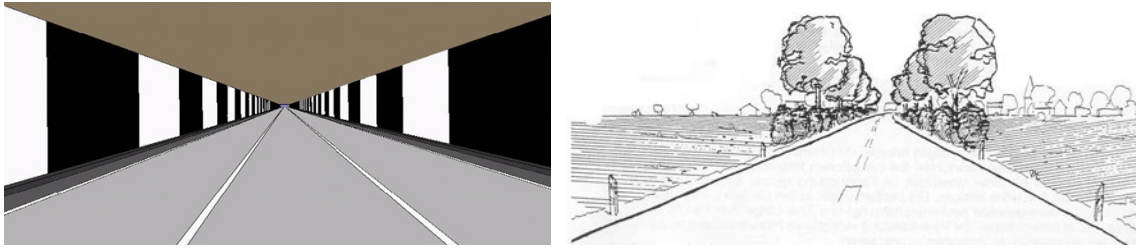
Figure 3.23: Bar markings on tunnel walls and plantation of trees for speed manipulation. The findings by Manser et al in [MH06] show that with markings on tunnel walls both accelerations and decelerations can be induced. Anhäuser states in [Anh04] that tree plantation can alter the speed perception.

aligned vertically at the edges of the road as shown in Fig. 3.23. In a simulator study where drivers had no tachometer available it was shown that increasingly narrow black and white bars induce a speed reduction. The opposite effect could also be achieved with increasingly wider bars.

Anhäuser proposes a different approach by making roads appear more narrow and by accentuating the road shape with vegetation, especially large trees. Such vegetation is known to the driver as natural barrier and if located at the edges of a lane they facilitate the recognition of the road geometry due to the larger FOV covered than only with the flat road surface.

The implementation in the HUD is shown in Fig. 3.24 together with the elements of the Iconic HMI. Similar to the rumble strips and the transversal bars the bar density is controlled by the proposed deceleration strategy. The density changes by a factor of 2 between deceleration levels, using a higher density for stronger decelerations.

Figure 3.24: Picture of the vertical bars produced by the contact analogue Head-Up Display. The bars can be used to alter the speed perception and also the perceived width of the road causing a speed adaption (scene and HUD content digitally mixed).
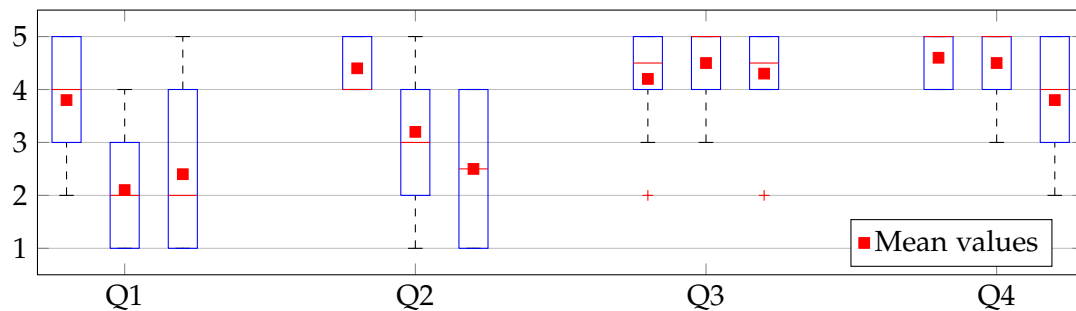
Figure 3.25: Subjective ratings in the pre-evaluation of the transversal bars, rumble strips and vertical bars. The plots represent the results of every system in this order for the four questions (5 = absolutely agree, 1 = absolutely disagree).

Preliminary Evaluation   A small test was conducted to assess the general subjective impression about every HMI variant. Ten participants used the systems in varying orders to minimize learning and order effects. After each test drive they completed a short questionnaire about the following questions:

- General positive and negative aspects and comments

- (Q1) Would you use the system in your own car?

- (Q2) Do you find the visualization optically appealing?

- (Q3) Did you understand the visualization intuitively?

- (Q4) Did the system help you with anticipatory driving?

The last four questions had to be rated on a scale from 1 (absolutely disagree) to 5 (absolutely agree). Figure 3.25 shows the aggregated results of all variants. The left bar in a group refers to the transversal bars, the center one to the rumble strips and the right one to the vertical bars. Generally the transversal bars were rated best with all ratings positioned in the highest interval except question Q1. Then follows the rumble strip variant with questions Q3 and Q4 nearly equally rated, only the usage in the own car was not desired by drivers. The vertical bars had overall the lowest ratings with wide interquartile ranges indicating low consistency between drivers.

The free answers about the prototype systems showed for the transversal bar version that the distance information, contact analogue bars, color scheme and unobstructed view of the scene were rated positively. Still the meaning of the bars was not clear to some drivers and some proposed to turn off the bar animation earlier. For the rumble strips the distance information and the sound pulses in the driver seat were rated positively, but the latter latter were also mentioned on the negative side. A suggestion of the participants was to use the sound only for higher deceleration levels due to their very alarming nature. The vertical bars seemed to be the most problematic variant which is shown in the ratings of Fig. 3.25 and also the free answers. The distance information and the basic optical appearance were again seen positive. In contrast the size of the bars, the substantial obstruction of the driving scene and the resulting driver distraction were judged very negatively.

3.3.2.2 Evaluation of the Transversal Bars and Rumble Strips

Due to the low ratings and the limited time duration for an evaluation per participant the HMI version using vertical bars will not be included in the following evaluation. The transversal bars will be used in the experiment without modification, the rumble strips are modified based on the driver feedback to use the seat vibration only for the deceleration strategies with active braking. If the system proposes the coasting strategy only the optical system is triggered.

Peripheral Detection Task The PDT was originally developed by Martens et al. in [MW01] as a way to measure workload. They argue "that the functional visual field decreases with increasing workload". In most implementations a dot appears at one of several possible fixed positions on a horizontal line, here five positions were chosen evenly distributed over the road width below the horizon (see also Fig. 3.20). This happens every 3 - 6 s with a rectangular probability distribution with a maximum display duration of 2 s. As soon as the driver recognizes the dot he shall press one of the two possible buttons on the steering wheel close to each hand as an acknowledgment. If this does not happen within the 2 s time interval, the dot is marked as "missed". Victor et al. states in [VEH08] that the dot position has only a marginal influence and that the measures "reaction time" and "detection rate" are well suited indicators for cognitive workload. In the following experiments these parameters are saved for every dot appearance:

- Consecutive dot numbering

- Reaction time with millisecond resolution (marked as miss if higher than 2 s)

- Number for identifying the current driving situation

- Dot position

The dots are implemented as part of the HUD visualization and the system is coupled to the steering wheel buttons via a Controller Area Network (CAN) interface.

Experiment Design The evaluation can be separated into three major parts derived from the assistance configurations: baseline, transversal bars and rumble strips. If a system for anticipation support is tested, an essential property of the evaluation must be that upcoming situations cannot be foreseen due to a similar constellation in a previous evaluation part. This contradicts with the wish of the engineer executing the experiment to require only a minimum amount of test persons for time and organizational reasons. A tradeoff to accomplish both goals to a large extent is to use small modular parts for the test track design which can be alternated for every participant. These modular parts are:

- Short introductory drive on a rural road (Intro)

- Blocked ego lane with oncoming traffic on a straight road (Blocked Straight)

- Blocked ego lane with oncoming traffic on in a curve (Blocked Curve)

Track 1-4	Track 5-8	Track 9-12	Track 13-16
Intro	Intro	Intro	Intro
Blocked Straight	Blocked Curve	Highway 1-4	Highway 1-4
Limit 70/50	Limit 70/50	Intro	Intro
Blocked Curve	Blocked Straight	Blocked Straight	Blocked Curve
Highway 1-4	Highway 1-4	Limit 70/50	Limit 70/50
		Blocked Curve	Blocked Straight
Highway 1	Highway 2	Highway 3	Highway 4
On-Ramp	On-Ramp	On-Ramp	On-Ramp
Limit 120/100	Limit 120/100	Stop&Go	Jam
Stop&Go	Jam	Jam	Stop&Go
Jam	Stop&Go	Limit 120/100	Limit 120/100
Exit Ramp	Exit Ramp	Exit Ramp	Exit Ramp

Table 3.9: Composition of the 16 test tracks for the driving simulator experiments. The four basic tracks are extended by the variation of the highway parts Highway 1 - Highway 4.

- Consecutive speed limits: First 70 km/h, then 50 km/h (Limit 70/50)

- Highway on-ramp (On-Ramp)

- Consecutive speed limits: First 120 km/h, then 100 km/h (Limit 120/100)

- Approaching a static traffic jam (Jam)

- Approaching slow-moving stop-and-go traffic (Stop & Go)

- Highway exit ramp (Exit Ramp)

Still it is not possible to permute these parts freely as it would not lead to a reasonable track layout. This means that the track segments especially for the highway must be grouped as shown in Tab. 3.9.

Such a track design ensures a minimum of order effects. Due to the limited set of track modules an assistance configuration combined with a certain track layout is tested by only a single driver. This means that a comparably high number of participants is needed, here it was chosen to use 15 per assistance configuration resulting in overall 45 participants.

For a detailed evaluation of both HMI variants several objective and subjective metrics are recorded. The subjective metrics are obtained with questionnaires while the objective ones are derived from the PDT and the vehicle dynimcs data. The following evaluation procedure has been chosen:

- Questionnaire with demographic data (age, gender, mileage etc.)

- Introductory drive to acclimatize with the driving simulator

- Test drive with either no assistance (baseline), transversal bars or rumble strips
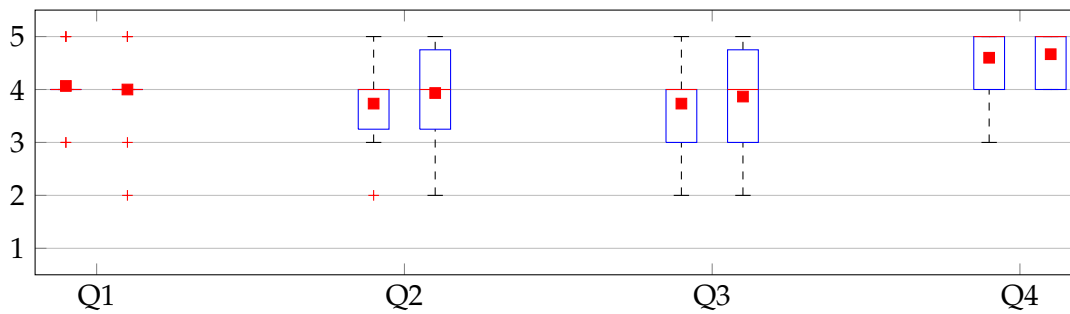
Figure 3.26: Subjective ratings in the main evaluation of the transversal bars (left boxes) and rumble strips (right boxes). The plots represent the results of both systems in this order for the four questions
(5 = absolutely agree, 1 = absolutely disagree).

- Questionnaire with open questions and semantic differential

The mockup depicted in Fig. 3.13 served as driving simulator, the HUD visualizations were developed using Adobe Action Script 3.

Results Overall 45 persons participated in the experiments (41 male, 4 female, avg. age 22.5 years) with 15 drivers for each variant. First the subjective ratings shall be investigated. Similar to the pre-evaluation the participants had to rate the same questions Q1 - Q4 for which the results are depicted in Fig. 3.26. While the transversal bars were degraded slightly, the rumble strips increased their ratings especially in the first two questions about the usage in the own car and the optical appearance. Although no change was made to the visualization of the rumble strips the perception was increased probably due to the less patronizing nature through less usage of the driver seat vibration.

A more detailed subjective rating is generated by the semantic differential shown in Fig. 3.27. The word pairs had a different alignment in the questionnaire to force the participants to give a more reflected rating than just selecting positive or negative values. This has been changed in the visualization for simpler comparability of both HMI versions. The two most negative ratings for the rumble strips judged them to be "obtrusive" and "patronizing", the latter also being the worst rating for the transversal bars. For the rumble strips this is probably due to the usage of the seat vibration as this system output can hardly be ignored and consequently has a high potential for annoyance. If the mean values of the semantic differential ratings are calculated (0.74 for the transversal bars, 0.77 for the rumble strips) the rumble strips even get a sightly better rating, but with no statistical significance.

The speed profiles of the three configurations (see Fig. 3.28) depict the intended effects for both HMI variants. All plots are normalized to begin at the first assistance output (in the baseline case the first theoretical output) and shifted to have the same starting speed for better comparability. All plots are averaged values of all participants as the single graphs would not allow a reasonable comparison due to the different starting speed in the situation depending on the previous track module.

The baseline graph shows that the unassisted drivers keep their initial speed for a longer time and then need to apply a stronger deceleration to achieve the desired final speed.
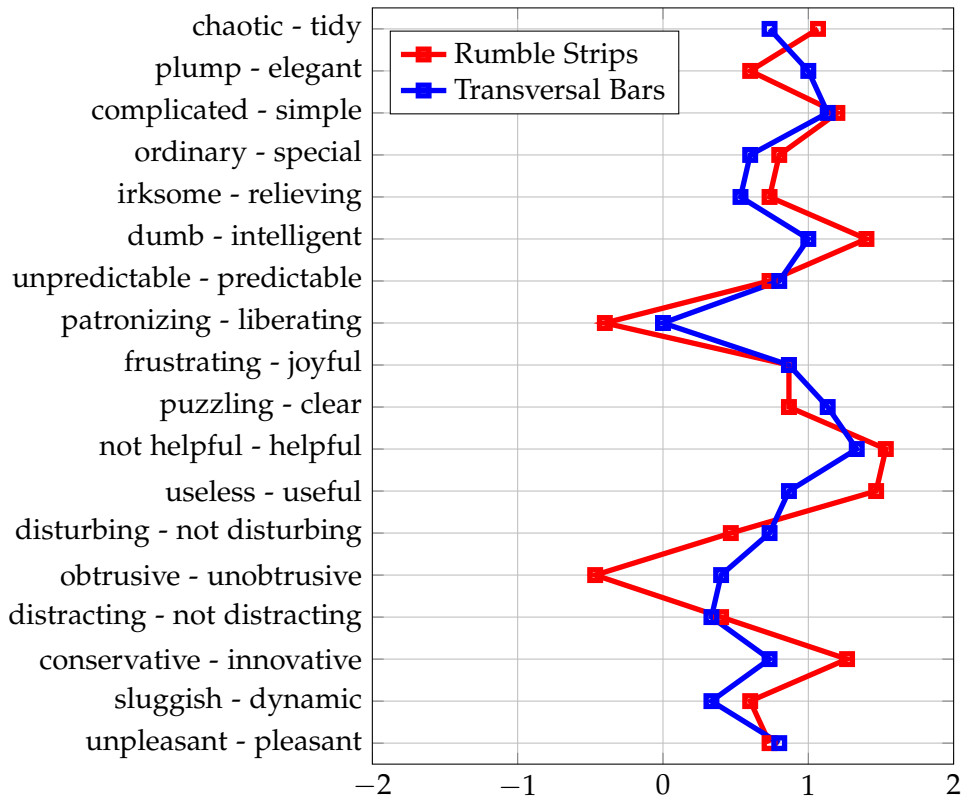
Figure 3.27: Semantic differential of the transversal bars and rumble strips in the main evaluation. The word pairs were normalized so that the positive adjectives are on the positive scale for easier comparability.

In this situation the final speed is not zero as the cars in the jam move very slowly. For both assisted cases drivers start decelerating earlier and in a smoother way (see maximum deceleration values in Tab. 3.10 and Tab. 3.11). At the maximum position of the baseline plot the transversal bar variant has a 18 km/h lower speed and the rumble strips variant a 27 km/h lower speed. While the speed profile of the transversal bars still retains the basic shape of the baseline, the rumble strips show a close to linear speed reduction. Due to the lower average speeds in the assisted cases (see Tab. 3.10 and Tab. 3.11) it takes drivers longer to reach their target speed. For the transversal bars it takes 2.4 s longer to reach the minimum speed of the baseline, for the rumble strips it takes even 17.5 s.

It was also analyzed how much active braking was applied by the drivers by calculating the integral of the brake pedal positions. In both assisted cases there is a statistically significant difference compared to the baseline (see Tab. 3.10 and Tab. 3.11). The reaction time in these tables is defined as the time between the first assistance output and a driver reaction characterized by a following deceleration of at least 0.01 m/s^2. With the transversal bars drivers decelerated significantly earlier by 3.1 s and with the rumble strips by 5.2 s.

These metrics reveal that the rumble strips showed an objectively better performance on the speed selection than the transversal bars. On the other side the subjective feedback
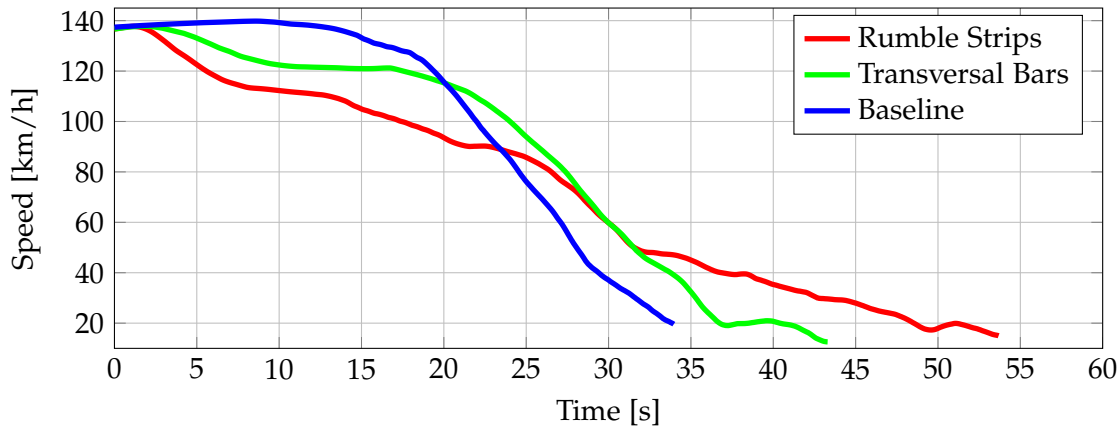
Figure 3.28: Speed profiles of the baseline, transversal bars and rumble strips configuration. The plots are shifted to have the same starting speeds for better comparability. Every plot shows the average speed profile for each assistance configuration.

shows that the rumble strips have a higher potential for annoyance which is probably closely related to the objective results. The more drivers are influenced by an assistance system the higher is the chance that it will not be accepted in the long term.

For the PDT data in Fig. 3.29 only the time intervals are analyzed with activated assistance. If the data from the whole experiments was taken into account, the impact of the different assistance variants would not be as clearly visible. The analysis of the PDT results shows that while in the baseline condition nearly all dots are recognized, the assisted drivers missed several points, in the case of the rumble strips even statistically significant compared to the baseline. The reaction time for the dot acknowledgment also increased in the assisted cases, again the effect was strongest for the rumble strip variant. Both variants show a statistically significant increase in reaction time.

3.3.3 Discussion

Several versions of abstract HMI systems for the HUD have been developed which all had a positive effect on the driving style. This included earlier and smoother deceleration, lower average speed during deceleration and improved anticipation. The acceptance of drivers

Metric	Δ Avg. (Ass. - Base.)	Significance	p
Average speed	-18.6802 km/h	$\checkmark$	0.010122
Brake integral	-169.3301	$\checkmark$	0.046487
Max. deceleration	1.4563 m/s^2	X	0.12486
Reaction time	-3.108 s	X	0.067873

Table 3.10: Comparison of vehicle dynamics and derived metrics for the transversal bars. Here the situation "Highway Jam" was analyzed.

Metric	Δ Avg. (Ass. - Base.)	Significance	p
Average speed	-22.7629 km/h	√	0.011401
Brake integral	-182.0305	√	0.027925
Max. deceleration	1.9779 m/s^2	√	0.038088
Reaction time	-5.1907 s	√	0.011392

Table 3.11: Comparison of vehicle dynamics and derived metrics for the rumble strips. Here the situation "Highway Jam" was analyzed.

varied strongly with the implementations. Especially systems with output that drivers could not easily ignore (such as the original rumble strip version) had low acceptance ratings which could even lead to a deactivation of the system.

Currently the visualizations occupied large areas of the HUD. If other HMI elements shall be included belonging to different assistance and information systems, the layouts would have to be reconsidered. Still the basic concept of using very simple optical and acoustical cues to inform about a proposed deceleration combined with simple icons to explain the reason proved to be feasible.

3.4 Abstract Interfaces with LEDs

Large HUD systems as proposed in the previous section have the main disadvantage of being currently not available due to technical and economical issues. Another possibility to create a simple, large-scale output device that could be implemented with reasonable effort in the near future would be the usage of RGB-LED modules. Display elements based on this technology become more and more common in end-user applications such as TV sets, interior lighting and large display walls. This makes full-color LEDs (RGB-LEDs) readily available at a reasonable price.

Several research efforts have investigated potential use cases, one of them is an extension for a NiVi system as proposed by Weigel et al. in [Wei+09], see Fig. 3.30. The image stream
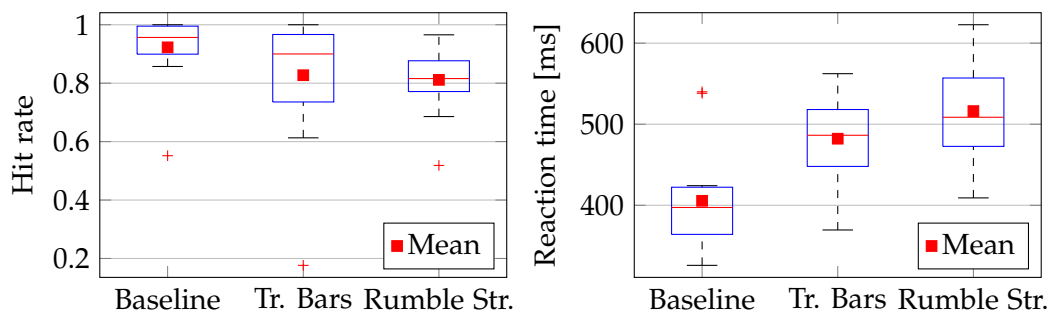

Figure 3.29: Results of the Peripheral Detection Task for the abstract HUD visualizations. The hit rate represents the percentage of dots recognized within 2 s, the reaction time is defined as the interval between the dot display and the button press by the driver.

Figure 3.30: LED modules for augmenting a Night Vision system. Left: The system displays a simple icon using the LED matrix in the actual line of sight between the driver's head and the obstacle recognized by the NiVi system (image from [Wei+09]). Right: LED line activating a group of LEDs in the line of sight towards the obstacle (image from [Mah+07]).

from an infrared camera is analyzed to obtain the presence and position of potential obstacles such as deer or people on the road. This information is the fed into a controller that generates simple icons with an LED matrix representing the type of obstacle. The specialty of this setup is that it implements a contact-analog HUD with very simple elements by displaying the icon in the line of sight towards the real obstacle position. In conventional NiVi systems which simply display an enhanced version of the camera image, drivers need to orientate twice: first the obstacle position must be recognized in the display, then the corresponding position must be determined in the real world. As this requires substantial mental effort this process requires some time.

The system tested by Mahlke et al. in [Mah+07] works in a very similar way but uses only a simple line array of LEDs. Figure 3.30 shows the setup in a test vehicle. Their results show that the recognition rate of an obstacle did not increase with the assistance systems (baseline: 58.2%, far infrared display: 56.9%, LED: 57.7%). Still the performance could be increased especially with the LED system which had a recognition time of 5.2 s compared to 9.5 s for the worst camera display. Additionally the LED system required the lowest percentage of fixation time with 6% while the worst conventional display based system required 38% for monitoring the display.

All these findings show that a very simple visual display system can significantly improve driver performance and often outperform a more complex visualization. Such simple displays also have the advantage that as soon as the driver has learned the functionality and built up a considerable level of trust it can even be enough that the mere detection of a system output causes a higher level of alertness or the preparation of a braking maneuver. This can be the critical reaction that decides whether an accident occurs or not.

In a comparable way to these examples an LED array could also be used to enhance the presented anticipatory driver assistance system. The first steps are to develop suitable hardware modules that can be coupled to the Business Logic with the help of a software component controlling the LEDs.
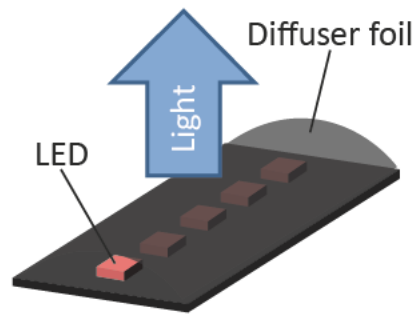
Figure 3.31: Mechanical and optical design of the prototype LED module. The implementation uses a diffuser foil to attenuate the individual LED spots and a more even brightness distribution.

3.4.1 System Design

The development of the LED system took place in two stages. With the first very simple mockup the basic feasibility of such a system is tested. The feedback from a video experiment in a driving simulator environment is used to create an improved version of both the hardware and the visualization.

3.4.1.1 Prototype with diffuser foil and single-color capability

The first prototype implementation of a LED module is based on readily available RGB-LED stripes with all diodes of the same color connected in parallel. Two modules were made containing five LEDs each, both modules were controlled by the same driver electronics. As shown in Fig. 3.31 left the light is radiated through a diffuser foil. Previous tests with drivers with direct LED lighting showed that the individual light sources are too accentuated especially in darker environments such as a driving simulator. Even lowest light intensities were perceived to be disturbing. The diffuser foil both attenuates the primary light source and creates a more even light distribution.

The first prototype with the simpler LED module is depicted in Fig. 3.32. The two modules are mounted left and right of the steering wheel, the Iconic HMI elements are again positioned in the instrument cluster between the RPM and the speed gauge. A software component is needed to interpret the deceleration suggestion by the Business Logic of the assistance system which are then converted to control commands for the LED driver electronics. This component assigns the same colors to the LEDs that are shown by the distance bar:

- Coasting (motor drag torque): yellow (255, 255, 0)

- Light braking (-0.2 g): orange (255, 140, 0)

- Strong braking (-0.4 g): red (255, 0, 0)

If no deceleration is needed the LEDs are turned off, between different states colors are changed smoothly with a linear transition of 1s duration.

Figure 3.32: First LED prototype in combination with instrument cluster visualization. The instrument cluster shows the Iconic HMI, the LED modules are installed left and right of the steering wheel.

Combination with the Iconic HMI   It is essential to combine these very abstract display elements with more detailed information provided by the Iconic HMI. Figure 3.32 shows that this is done similarly to the initial experiments with these graphical elements. The combination allows an experienced user to perceive the activation of the LED modules from his peripheral FOV to know that a deceleration is necessary. Especially for early usage and if the driver suspects a malfunction of the system the elements in the instrument cluster are important cues to validate the assistance function.

This prototype setup was tested with a video experiment in the driving simulator. Previously recorded driving scenes from the environment simulation were played back together with the according assistance outputs. After experiencing several situations with the assistance they were asked for general feedback about potential improvements of the system and further experiments. The main points for criticism were the high brightness of the individual LEDs, the quick and not smooth enough color transitions and the non-interactive evaluation.

3.4.1.2   Large LED Arrays

A more advanced version of an LED module has been developed in conjunction with Wierer (see [Wie10]) and Chowanetz (see [Cho11] and [LCR11]) with the goal of a more precise lighting control and a substantially improved illumination uniformity. As shown in Fig. 3.33 the LEDs radiate into the edge of an acrylic sheet. The sheet has a white coating on the side pointing away from the driver and on the upper edge. An additional black coating was applied over the white coating in order to block any light that could either be seen from outside the car or be visible to the driver as a mirror image in the windscreen. The only possibility for the light to leave the sheet is the side pointing to the driver. Due to internal reflections in the sheet the illumination caused by a single LED is distributed very evenly. Still the illuminated area of the sheet is small enough to distinguish the lighting of each single LED.

This has become important as the new LED driver hardware allows individual control of all color channels of each LED. Each of the maximum 18 modules in a system contains nine RGB-LEDs which leads to 486 channels that need to be addressed. To achieve this the
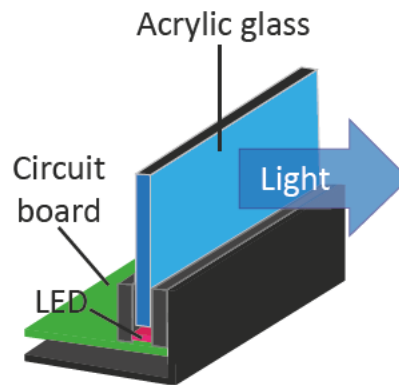
Figure 3.33: Mechanical and optical design of the improved LED module. The LEDs radiate their light into the edge of an acrylic sheet with white coating for smooth illumination.

Digital Multiplex (DMX) standard (see [Deu00]) has been chosen for the bus communication as it is widely used for professional lighting equipment. It allows to control 512 channels with a resolution of 256 bit over a simple three-wire connection. Each LED module has a connection on both ends so the signal wiring can be done very efficiently with a very short wire between two adjacent modules. The connection to a standard PC is established with a Universal Serial Bus (USB) to DMX interface which is controlled by a stand-alone program. This program forwards the LED intensity data it receives over a Transmission Control Protocol / Internet Protocol (TCP/IP) network connection from the BL. The luminous intensities of the individual color channels per LED are 600mcd for the red channel, 1400mcd for the green channel and 400mcd for the blue channel.

Color Calibration The selected LEDs do not have the same primary colors than most monitors which offer a sRGB calibration. Figure 3.34 shows in the xy-plane that the covered area of the CIE gamut is different for sRGB and the LEDs. If the desired colors for the LED display are chosen on a computer screen they usually will not match the color perception for the modules if the same RGB-values are sent to the driver electronics.

Therefore, a user study was conducted with the setup shown in Fig. 3.34 on the right. It consists of a calibrated sRGB monitor in front of which one of the modules is positioned. The monitor shows a Graphical User Interface (GUI) with a reference color and slider elements to control the color displayed by the module. The monitor and the module are positioned in a way so the user can observe them side by side. After the study it should be possible to obtain the color values for the LEDs with equation 3.1 containing c_{LED} and c_{sRGB} as the respective color vectors and M as the 3x3 transformation matrix between the two color spaces.

$$c_{LED} = M \cdot c_{sRGB} \tag{3.1}$$

To obtain the values of M it is necessary to have several color pairs that can be used for a Least Squares Algorithm. The 20 participants had to match five colors (red, green, blue, orange, yellow) with slight variations for each participant. These variations provide a better coverage of the whole color space and like that 100 unique color pairs could be
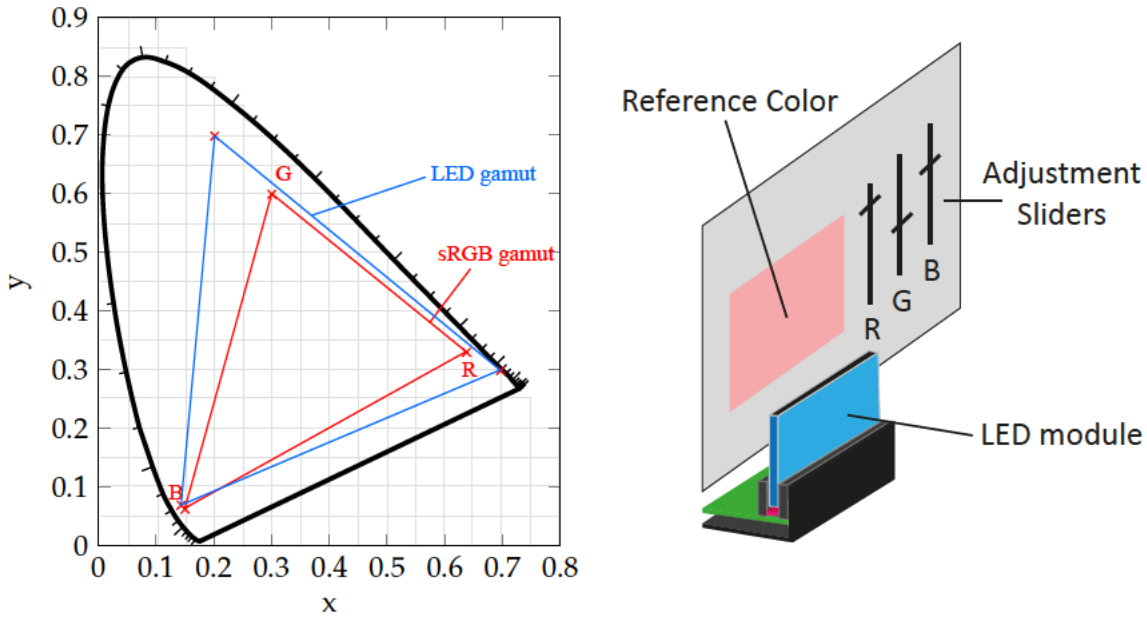
Figure 3.34: Comparison of the sRGB and the RGB-LED gamut in xy color coordinates and calibration setup. Due to the different coverages of the CIE - gamut a color calibration is necessary. The setup on the right is used for a user study to obtain the color calibration.

recorded. Due to the substantially higher brightness of the LEDs compared to the monitor it was sometimes very challenging for participants to adjust the color independently from the brightness. This led to variations in the gray value (equal to brightness) and so the user-defined colors were normalized to have the same gray values as the corresponding reference color. The result of the Least Squares optimization based on these gray value - normalized vectors with a residual of 0.13 is the content of matrix M_{norm} in Eq. 3.2.

$$M_{norm} = \begin{bmatrix} 1.173 & -0.123 & -0.152 \\ -0.171 & 1.246 & -0.33 \\ -0.179 & -0.187 & 1.345 \end{bmatrix} \tag{3.2}$$

In some cases it can happen that the transformation yields a result with one or more values being out of the possible range of [0,255]. An example for this is a $c_{sRGB} = (255, 0, 0)^T$ which would lead to $c_{LED} = (299, -44, -46)^T$. In such cases the values are clamped to the closest end of the value range to obtain a valid color vector.

Combination with the Iconic HMI   As with the previous implementation the Iconic HMI is used to provide more detailed information about the type and distance of the upcoming traffic situation. Different than in the prototype version these elements are displayed in the HUD and the LED modules will be placed on the engine hood. So both the LEDs and the additional information are closer to the primary FOV which should further improve the possibility to perceive the system output without being forced to look away from the road too much.

Array for
„Dynamic Guiding Points"

Array for
„Static Guiding Point"
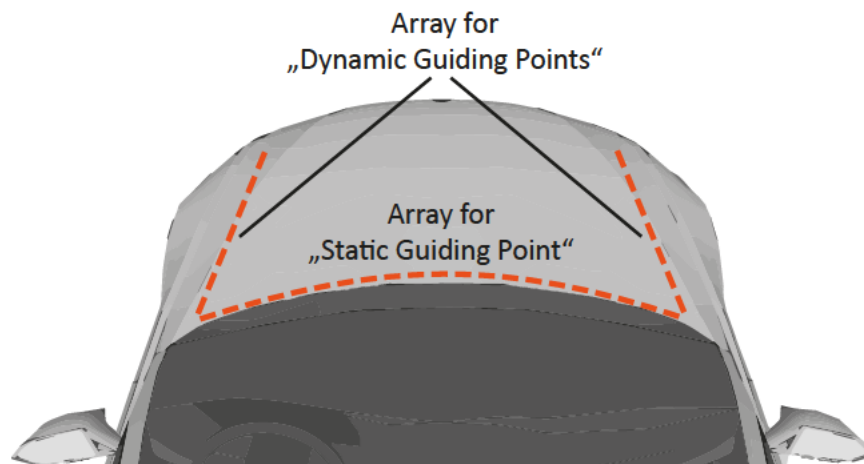
Figure 3.35: Top view of the two LED arrangements on the engine hood. Due to the shape of the hood and the asymmetric driver position it is not possible to achieve a symmetrical arrangement when viewed from the driver's point of view.

Through the modular design it is possible to arrange the LEDs in many ways. The first variant is the "Static Guiding Point" for which the modules are aligned along the lower edge of the windscreen (see Fig. 3.35) comparable to the implementations shown in Fig. 3.30. The main difference is that the modules are placed outside the windscreen so the effort for accommodation is slightly reduced and no reflections in the windscreen distract the driver. With the possibility of controlling every single LED more sophisticated visualizations can be implemented then with the first module versions.

The Static Guiding Point can encode the proposed deceleration and the distance. This is achieved by using the same color scheme as with the prototype variant, but this time with calibrated colors. The distance is encoded with the number of illuminated LEDs, starting with three LEDs in the center of the array. This corresponds to an obstacle distance of 1000 m (the maximum activation distance for the anticipatory ADAS). During an approach the number of LEDs increases smoothly by interpolating the brightness of the outer LEDs with the neighboring ones. At a distance of 5 m all LEDs are lit which leads to a larger illuminated area for smaller headways that are potentially more dangerous. In the case of a driver not reacting to the system the LED array is turning increasingly red with a growing illuminated area.

For the other variant "Dynamic Guiding Points" the modules are aligned in two rows approximately along the driving direction when viewed from the driver position (see Fig. 3.35). These two arrays display moving light dots similar to the application in tunnels proposed by Zlocki et al. in [Zlo10]. They showed that drivers can be influenced in their speed choice by moving lights on tunnel walls (see Fig. 3.36). Zlocki et al. argue that drivers tried to move along with the lights which were intended to produce more homogeneous traffic for higher throughput.

Now it shall by possible to "take along" the moving lights with the car and use the effect to influence the driver's speed choice. This is achieved by displaying three light dots on each LED line that move towards the driver. When a deceleration is proposed the three
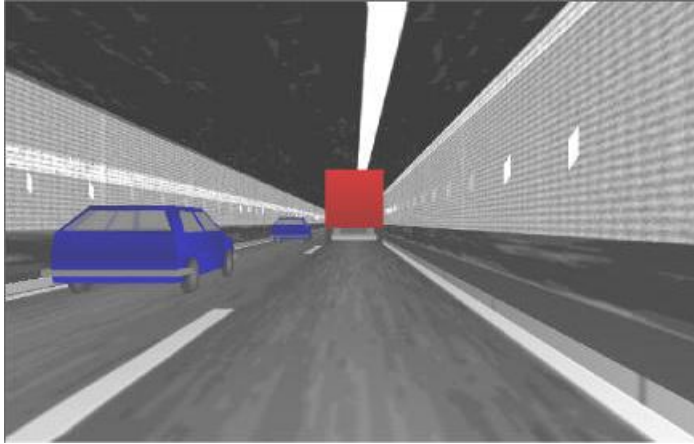
Figure 3.36: Influencing the speed choice of drivers in tunnels. Zlocki et al. show in [Zlo10] that drivers can be influenced in their speed choice by moving lights on tunnel walls.

dots increase their brightness from zero to the final value in a smooth way while standing still. As soon as the final brightness is reached the movement begins following Eq. 3.3 with f being the update rate of the animation.

$$v_{dot} = \frac{v_{ego} - v_{target}}{km/h} \cdot 1.78cm \cdot 0.04 \cdot f \qquad \text{with} \quad f = 25Hz \qquad (3.3)$$

This shows that the speed of the light dots depends on the relative speed related to the target speed which resembles the behavior of the moving lights on the tunnel walls. Higher relative speeds lead to faster moving dots, during an approach they move towards the driver. When the dot speed reaches 0 they fade back to black.

Preliminary User Study Before the main user study can take place, a number of 14 participants (11 male, 3 female, avg. age 26.9 years) rated the first implementations of the large LED arrays and the prototype with two LED strips. For this purpose they made a short introductory drive without assistance to get used to the simulator. After that they drove on a different test track with assistance, but without being instructed about the function behind it. Then they were asked about their understanding of the system (their mental model) and they had to rate all variants with the same questions Q1-Q4 as in the large HUD experiments:

- (Q1) Would you use the system in your own car?

- (Q2) Do you find the visualization optically appealing?

- (Q3) Did you understand the visualization intuitively?

- (Q4) Did the system help you with anticipatory driving?

Also they had to give general feedback about the evaluated systems for issues that are not covered by the other questions. Finally they were asked to adjust the brightness of both

Variant	Minimum	Maximum	Mean	Median
Static Guiding Point	0.05	0.5	0.16	0.1
Dyn. Guiding Point	0.05	1	0.45	0.4

Table 3.12: Brightness settings obtained in a user study for the large LED arrays. The mean and median values of the Dynamic Guiding Points are both higher which is probably due to the fact that they cover a smaller FOV.

large LED variants to a reasonable level as this was one of the major problems with the earlier implementations. For this task they could change the brightness interactively in a range of 5% to 100% of the possible brightness of the LEDs. The results of this task are shown in Tab. 3.12 and indicate that only very low brightness values are necessary in a relatively dark environment such as the driving simulator. This is especially important as the brightness would have to be increased substantially to make the array illumination still visible in daylight.

Figure 3.37 shows the driver view of both large LED arrays. This is a picture from the preliminary experiment where the arrays for the Dynamic Guiding Points were still constructed out of individual LED modules. Participants mentioned several times that the movement of the dots is very uneven which was mainly caused by the discontinuous dot movement between the modules due to the split acrylic sheets. Consequently the construction was updated so the four modules of each strip shared a common sheet which improved the optical quality significantly.

The result of questions Q1-Q4 in the questionnaire are depicted in Fig. 3.38. It shows that both variants based on the new LED modules get better ratings which are except for Q1 in the positive half of the scale. Also the results of the semantic differential in Fig. 3.39 indicate that the new implementations improved the subjective performance related to the prototype version. While the prototype has many ratings on the negative half of the

Figure 3.37: Driver view of the two LED arrangements on the engine hood. For demonstration purposes all LEDs of both HMI variants are illuminated.
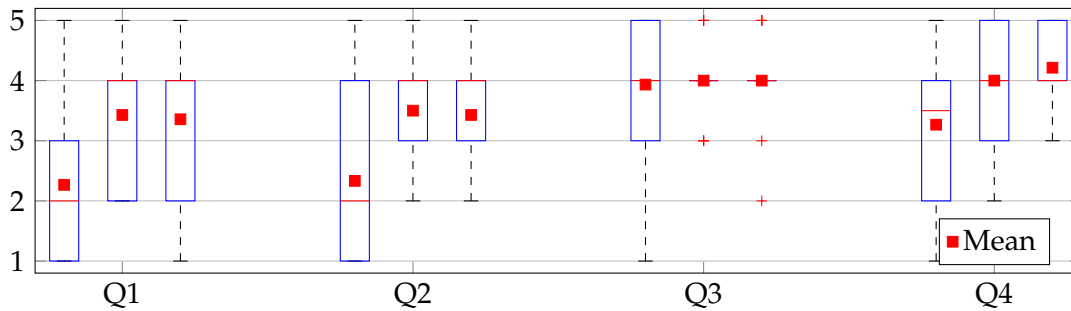
Figure 3.38: Subjective ratings for the LED prototype, the Static Guiding Point and the Dynamic Guiding Points in the preliminary evaluation. The plots represent the results of every system in this order for the four questions (5 = absolutely agree, 1 = absolutely disagree).

scale, the only word pair with a distinct negative rating for both new variants is "obtrusive - unobtrusive".

3.4.2 Main User Study

In the final user study for the LED based HMI variants only the newer ones "Static Guiding Point" and "Dynamic Guiding Points" will be included due to their superior rating in the previous experiment. As already mentioned the hardware setup for the Dynamic Guiding Points was changed so that each line consisting of four modules shared a common acrylic sheet for improved optical appearance. Also the median brightness values assessed previously are used for this experiment. All color transition times were set to 2 s to address the related issues mentioned by drivers before.

The structure of the study is identical to the one used for the HUD variants which is a between-subject-design. Every participant tests only one variant resulting in overall 45 drivers if 15 drivers are used for both variants and the baseline. Also the track configuration defined in Tab. 3.9 is identical to the HUD experiment in order to present an individual test course for every driver. The evaluation procedure for all drivers is arranged as follows:

- Determination of demographic data (age, gender, mileage etc.)

- Introductory drive to get used to the driving simulator physics

- Drive on the test course with or without assistance

- Only assisted drivers: Completion of questionnaire regarding subjective ratings

During the actual test drive the PDT is presented in the HUD to assess the cognitive workload by analyzing the percentage of acknowledged dots and the reaction time after their presentation.

Results The subjective results for questions Q1-Q4 did not change noteworthy, only the ratings of the Static Guiding Point were improved in average by 0.2. Regarding the semantic differential ratings the Static Guiding Point was rated to be more "dynamic", less "obtrusive"
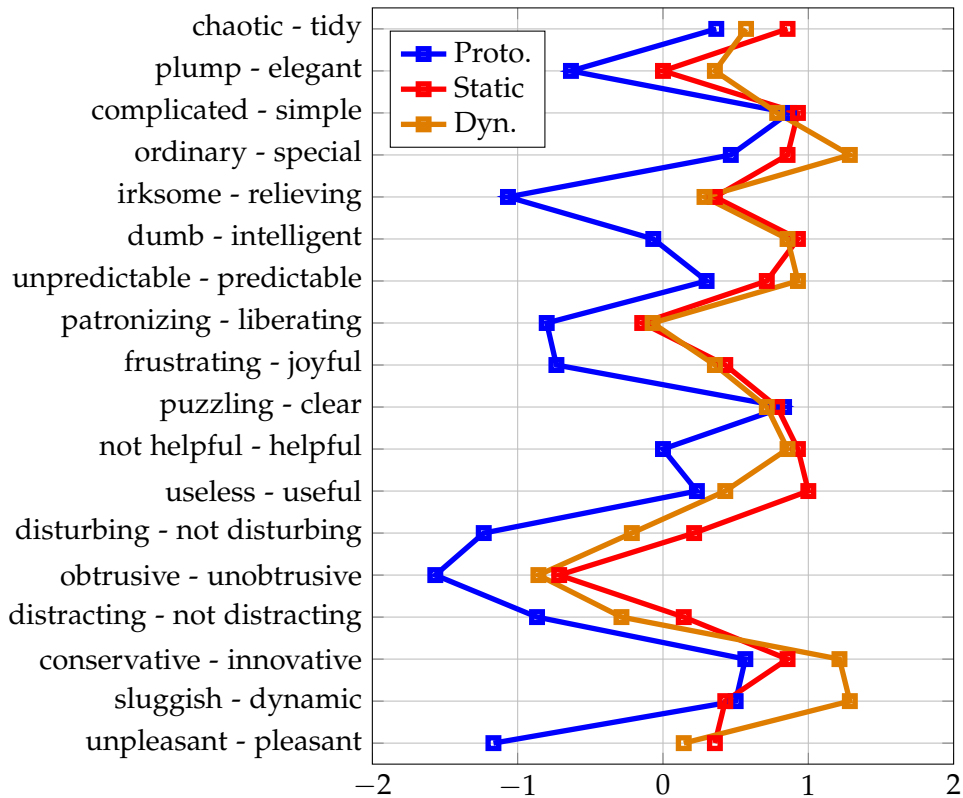
Figure 3.39: Semantic differential of the LED prototype, the Static Guiding Point and the Dynamic Guiding Points. The word pairs were normalized so that the positive adjectives are on the positive scale for easier comparability.

and more "clear" than in the preliminary evaluation. This was probably mainly due to the fact that the brightness was adjusted as this was the only objective change in the system. The Dynamic Guiding point was rated to be less "dynamic", less "disturbing", more "useful" and more "relieving" than in the previous implementation. Again this is partly attributed to the adjusted brightness, but the main effect is probably due to the common acrylic sheet for each LED strip. In any case these results should be seen as more reliable due to the higher number of participants.

For the objective measures it can be seen in Fig. 3.40 that both LED systems show the desired effect of an earlier and more constant deceleration. The speed difference between the maximum speed of the baseline at the corresponding time instant for the Static Guiding Point is 25.3 km/h and 27.1 km/h for the Dynamic Guiding Point respectively. If we compare the speeds at a time of 20 s after the assistance activation, the baseline drivers for both the HUD and LED variants have an average speed of ca. 120 km/h. For the HUD variants the speed using the Transversal Bars was also ca. 120 km/h, using the Rumble Strips it was ca. 90 km/h. The LED variants achieved an even higher decrease in the same situation, resulting in a speed of ca. 90 km/h for the Static Guiding Point and ca. 80 km/h for the Dynamic Guiding Points.
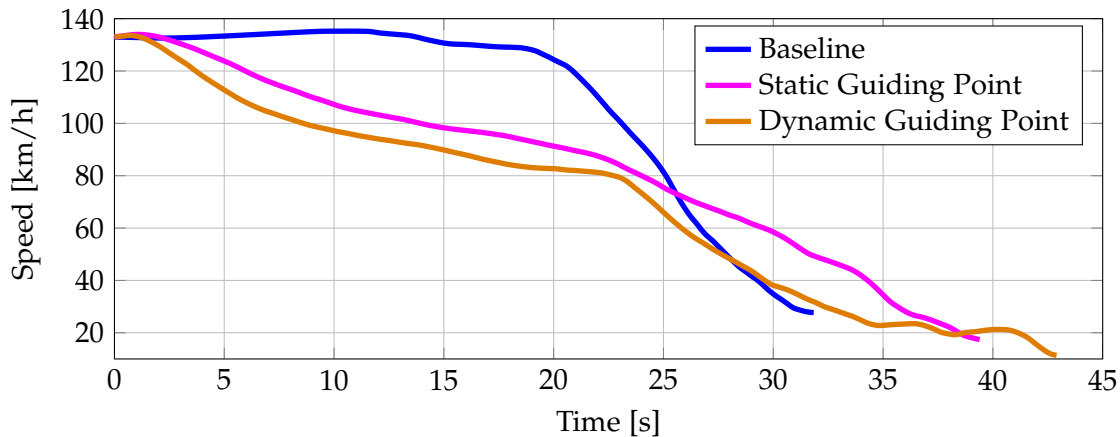
**Figure 3.40:** Speed profiles of the baseline, Static Guiding Point and the Dynamic Guiding Points configuration. The plots are shifted to have the same starting speeds for better comparability. Every plot shows the average speed profile for each assistance configuration.

The safety metrics in Tab. 3.13 and Tab. 3.14 also indicate a better performance of the LED variants. While the average speed difference for the HUD systems were -18.7 km/h and -22.7 km/h, the same metrics with the LEDs have values of -25.2 km/h and -27.5 km/h. In contrast the maximum decelerations were higher and the reaction time was also higher. This shows that the LEDs were more effective at lowering the speed while drivers took more time to react on it and they did this with stronger decelerations.

The last investigated metric is the PDT of which the numbers are shown in Fig. 3.41. As in the previous experiment the hit rate decreases and the reaction time increases for the assisted cases. The hit rate values are nearly identical for the baseline cases but the LED variants have a significantly higher value of ca. 0.9 than the Rumble Strips. Interestingly the shift of ca. 100ms in reaction time is comparable in both experiments, but the baselines differ by ca. 200 ms even for the same track and simulator setup.

3.4.3 Discussion

In this section several HMI variants on the basis of LED modules have been developed and evaluated. The goal was to create interfaces that are exceptionally simple to comprehend

Metric	Δ Avg. (Ass. - Base.)	Significance	p
Average speed	-25.1658 km/h	√	0.012822
Brake integral	-221.8307	√	0.0061898
Max. deceleration	2.265 m/s^2	√	0.0079403
Reaction time	-5.5333 s	X	0.38075

Table 3.13: Comparison of vehicle dynamics and derived metrics for the Static Guiding Point. Here the situation "Highway Jam" was analyzed.

Metric	Δ Avg. (Ass. - Base.)	Significance	p
Average speed	-27.5334 km/h	√	0.011401
Brake integral	-121.3838	X	0.15846
Max. deceleration	2.32 m/s^2	√	0.00049369
Reaction time	-7.088 s	X	0.24104

Table 3.14: Comparison of vehicle dynamics and derived metrics for the Dynamic Guiding Points. Here the situation "Highway Jam" was analyzed.

through the fact that the activation of the assistance and consequently the need for a deceleration can be perceived without explicitly looking at them. This has been achieved by arranging LED modules on the dashboard or the engine hood which encode the proposed deceleration strategy with the same colors as the distance indicator bar in the Iconic HMI. While the first prototype suffered low acceptance ratings due to the direct lighting and too quick color changes, the following versions could minimize these issues and provided additionally distance or relative speed information.

The large LED array would also have the advantage of providing a display for other assistance systems besides the anticipation support. As mentioned in the introduction comparable systems have been used to improve NiVi systems by indicating the correct direction of an obstacle from the driver's point of view. It would also be thinkable to combine the display with navigation information to give rough direction information or to combine it with a Lane Departure Warning system replacing the LEDs in the mirrors.

For the following experiments the Static Guiding Point variant will be used with slight modifications if needed as it produced high impact on driving speed combined with high acceptance. By the use of readily available hardware components that could be included in current designs comparably easy, this system is close to a potential implementation in a real world application. It can be installed without substantial effort in driving simulator mockups and even a tractor vehicle that is normally used for large trucks.
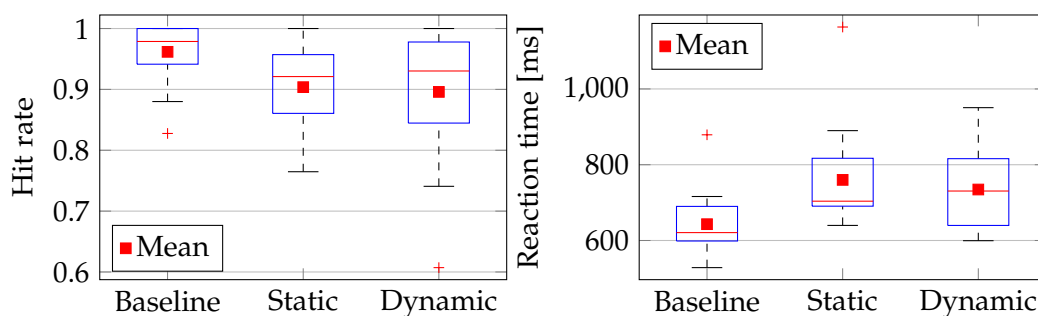

Figure 3.41: Results of the Peripheral Detection Task for the LED based visualizations. The hit rate represents the percentage of dots recognized within 2s, the reaction time is defined as the interval between the dot display and the button press by the driver.

4

Real World Experimental Evaluation

The next approach to investigate the effects of an anticipation support system shall be a real world experiment. Up to this point an assistance function was combined with several HMI variants and tested in different environments in a driving simulator.

All of these experiments aimed at gaining a sufficiently usable and effective system that supports drivers in anticipating upcoming situations and unobtrusively influences them to decelerate earlier and smoother. Using such a system in a real vehicle opens new evaluation possibilities and allows for obtaining close to realistic driver behavior patterns.

4.1 Motivation

A real world experiment provides many aspects that a simulator experiment can never achieve or only with a substantial technological effort. In [WLH12] de Winter et al postulate that despite the difficulties including measurement accuracy, limited repeatability and increased physical danger it is still feasible to conduct such experiments. The most noticeable advantages are the increased physical, perceptual and behavioral fidelity originating from the physical setup. Also it is more valid to transfer the obtained results to real world situations especially as there has been only limited research regarding the transfer of driving simulator experiments to real driver behavior (see also [WLH12]). Finally there are no problems at all regarding simulator sickness which also shall be attributed to the realistic environment.

The initial opportunity to conduct this experiment was provided by the ERES department of MAN Truck and Bus in Munich. MAN develops and produces various kinds of utility vehicles and provided a traction truck of type TGX 18.480. An essential prerequisite for this experiment was also the availability of the BMW test course in Aschheim near Munich. It provides a track which is built similar to a German Autobahn with a length of ca. 8 km and a drawn out curve which is not entirely visible.

Given those circumstances and the previously mentioned differences originating from the experiment type it was decided to conduct an experiment in a comparable manner as it was done in section 3.4 (see also [LCR11] and [LDZ13]). In addition to those differences the application of a utility vehicle also causes a much lower maximum speed of $89\frac{km}{h}$ as well as strongly different deceleration capabilities and an elevated point of view. Also the lighting conditions are vastly different from the simulator environment which needed to be

relatively dark due to the projector based image generation. The most mentionable reasons for reimplementing such an experiment with a real vehicle are

- Integration of the system in a utility vehicle

- Use of a real vehicle for higher immersion

- Inclusion of professional drivers

- Realistic physical vehicle behavior and collision potential

- Different environment light conditions

Compared to a real driving situation the main difference that remains is the lack of foreign vehicles in the situations and the limitation on static obstacles. The latter is a result of the non existent C2XC infrastructure in the test vehicle as well as the test course.

To assess the effectiveness and usability of the system objectively and subjectively the following measures are recorded for the last 1000 m before the obstacles:

- Average speed

- Maximum deceleration

- Time loss due to earlier deceleration

- Time gain regarding anticipation

A questionnaire serves to obtain answers to the following subjective questions:

- How intuitive is the system without introduction?

- Does it fulfill the intention of improved anticipation?

- Is it optically appealing?

- How do malfunctions affect the system perception?

- Which properties are ranked positively and which negatively?

Examples for relevant real situations that could be covered with the test course layout would be a static traffic jam or an obstacle on the current lane without the possibility to overtake. The latter situation can occur with a construction site on the ego lane and oncoming traffic on a two lane road as depicted in Fig. 4.2. Both examples have static objects which easily can be represented by a barrier as it is shown in Fig. 4.1. The picture also gives an impression of the curve in which the obstacles are placed. Due to the vegetation and buildings inside the curve the relatively low obstacles can be seen only very shortly before a potential collision.

Figure 4.1: Barrier representing an obstacle on the ego lane

4.2 Setup and Preparation

As mentioned before a system variant comparable to the experiment described in section 3.4 is used for this setup. Figure 4.3 depicts the data sources, the control block and the output devices of the proposed system. A real test vehicle has several differences from a driving simulator mockup that need to be taken into account in order to have a stable test setup. Those differences include a more rigid fixture of the LED modules on the dashboard, less accurate measuring devices like the GPS receiver and not directly available data such as the current track position.

4.2.1 Experiment System

A notebook computer provided by MAN is used to interface the vehicle CAN bus of which the data is forwarded by a TCP/IP connection to the central control software named "WarnMe". The CAN bus provides the following parameters:

- Vehicle speed

- Accelerator pedal position
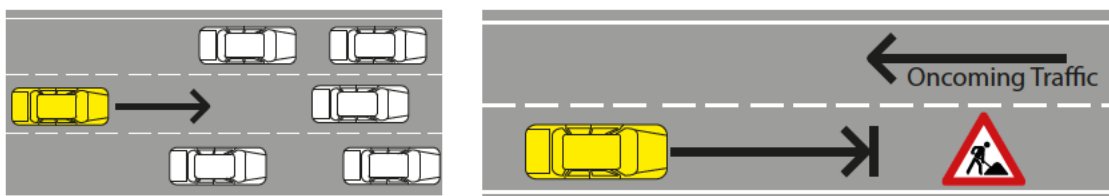
Figure 4.2: Potential situations for the real world experiment
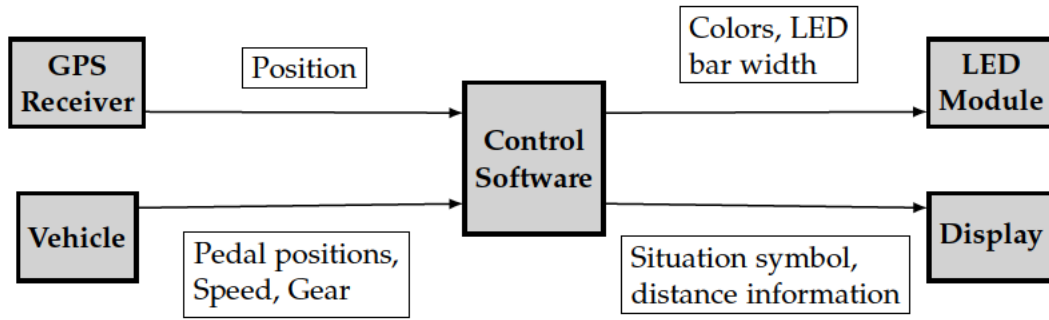
Figure 4.3: System diagram for the assistance system of the real world experiment. The control software is also used as an HMI for the investigator and data logging.

- Brake peal position

- Selected gear

The control software acquires the GPS position and speed from a consumer GPS receiver that works with an update rate of 1 Hz. Part of this software is again the state machine which implements the ISPA functionality described in previous chapters. Based on the mentioned data sources and the knowledge of the obstacle positions and the speed curves for coasting the ISPA system can generate the deceleration strategy proposal for the driver. The speed curves are obtained on the MAN test course by accelerating to the maximum speed of 89 km/h, shifting to the desired gear and stepping off the gas pedal. This procedure is repeated for every gear of the upper four main gears. For an easier calculation of the estimated deceleration distances in the ISPA system the curves were described using a linear fitting procedure. For the parameters a and v_0 in the equation $v(t) = a \cdot t + v_0$ the values can be taken from the regression coefficients in Tab. 4.1.

Gear	a in m/s^2	v_0
5	-0,570432	12,207668
6	-0,559708	19,310903
7	-0,561095	24,359081
8	-0,447859	26,933176

Table 4.1: Parameters of the linear approximation of the speed curves caused by motor torque

The HMI which was used in the related driving simulator experiment consisted of the LED array with nine modules and a section of the HUD containing a symbol representing the upcoming situation and the distance. As HUDs are not readily available for utility vehicles and prototyping such a system would be far too costly, an alternative to this display must be found. In this setup the solution is a standard Liquid Chrystal Display (LCD) which is mounted in the instrument cluster between the speed and the RPM gauge as Fig. 4.5 shows. The LCD is mounted in a way so the gauges besides it and the original display containing the gear information are still completely visible. For the LED modules

Speed curve for coasting and its linear fit
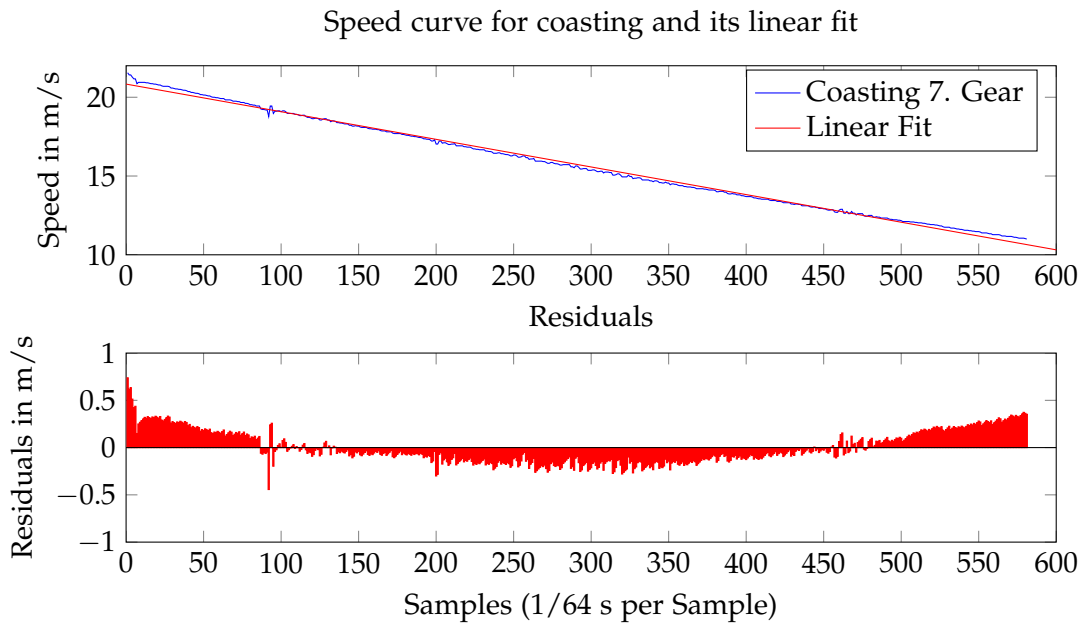
Figure 4.4: Linear regression of the deceleration speed development caused by motor torque

the highest brightness value is chosen as the experiments are conducted during daylight. Also the LED array needs to be adapted to the different spatial circumstances meaning that the modules are placed inside the cockpit and only three of them are used. The modules are mounted on a wooden panel to adapt the shape of the dashboard. Participants from the driving simulator experiment noted that the light ribbon should start growing directly in front of the driver and not in the middle of the dashboard as it was done in the simulator.

4.2.2 Test Course

The test course is located along the shoreline of a lake north of Munich, the selected track is marked in orange in Fig. 4.6. All minimum requirements for the experiment are met by the track layout, including two long straights to reach the maximum speed and a not entirely visible curve in the east of the course which allows for positioning the obstacles at different positions. The curve in the west is fully visible and thus a "virtual" obstacle is placed there to create a false alarm. Additionally the marked track is built similar to a German Autobahn so there are enough lanes all the time to circumnavigate the obstacles in the worst case. With a length of approximately 7.5 km the time intervals between assistance activations are long enough to avoid an unrealistic activation frequency. Figure 4.7 shows the positions of the three real obstacles in the east curve. They are arranged in a way so one obstacle cannot be seen from another one's position. This shall make it harder for the participants to foresee whether an obstacle is present in a certain round or not. Additionally the barriers are hidden behind bushes or crash barriers when they are not needed for a certain round. This task is accomplished by a helper person who is in contact with the investigator over a voice radio system.

Figure 4.5: Picture of the LED modules and the instrument cluster display. The auxiliary display is small enough to maintain a free sight on the built-in instrument gauges.

In order to calculate the correct distance to the obstacles along the track which is also used later to derive the track position a GPS track needs to be recorded. This is done by driving along the course with a low speed of ca. $20\frac{km}{h}$ on the right most lane. The first measure ensures that enough data points are recorded due to the low update rate of 1 Hz. Additionally driving on the outer lane causes that the recorded positions of the reference track are as distant as possible on the parallel track segments with opposite driving directions. This shall prevent that an ego vehicle position is mapped to the opposite
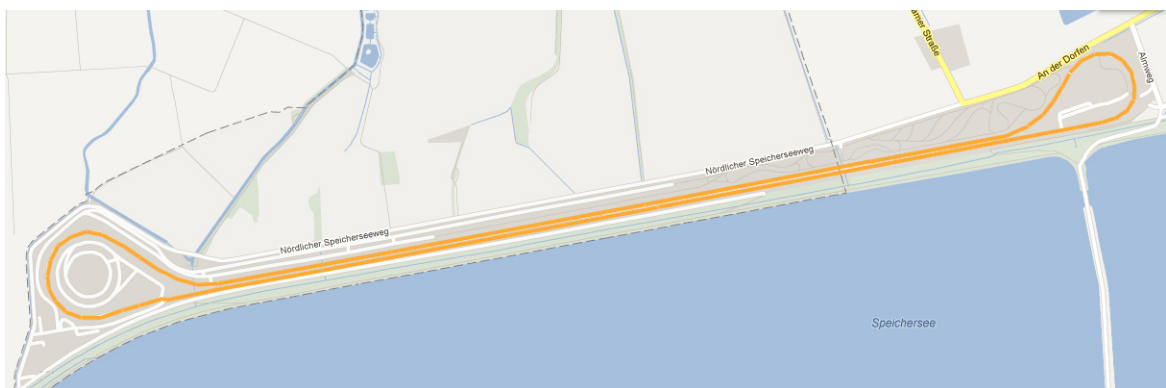

Figure 4.6: Map of the test course for the real world experiment. The assignment of the correct track position is especially error prone on the long parallel parts of the track due to their proximity. The curve in the east is not entirely visible.

Figure 4.7: Positions of the obstacles in the real world experiment. A helper moved the obstacles away from the track when they were not needed so drivers cannot learn their positions.

driving direction due to adverse directions of the measurement error of the reference track and the current measurement during an experiment. Another measure to optimize the reference track is to leave out erroneous measurements. These include measurements with the exact same position as the previous one or with a distance between data points larger than 20 m. During the experiment the closest point on the reference track to the current position is determined. As the positions of the obstacles on the reference track are also known, the correct distance along the track can be determined.

4.3   Experiment Execution

The experiment took place on two days because of a maximum number of 6 participants per day. As the number of easily available participants was limited to 12 persons the time frame was defined by these circumstances. All of them held at least an internal driving permit for the MAN facilities (3 participants) or a regular driving license (9 participants) for this kind of utility vehicle. The average age was 34.9 years, two drivers had an annual mileage of less than 5000 km, three had 15000 - 20000 km and the rest had more than 20000 km.

In the first group every participant drove 9 rounds using the assistance. The reference group drove on the second day without assistance output. The whole system ran in the background in order to record the potential output. It is desirable to obtain an assessment of the system also from this group and therefore a 10th round had to be accomplished by the participants. In this round obstacle T2 was placed on the track and the drivers were introduced to the system in the same way as the assisted drivers after the first contact situation. The goal behind the allocation of the obstacles to the rounds was to give the drivers the possibility to familiarize with the vehicle and the track. Also it should not be foreseeable in which round and on which position the obstacles are positioned. At the beginning of each trial the following tasks were conducted:

Round	1	2	3	4	5	6	7	8	9	10
Obstacle	x	T2	x	T1/T4 (FA)	x	x	T3	x	T2 (Miss)	T2

Table 4.2: Obstacle distribution for each round in the real world experiment. Target T4 is a false alarm (FA), the last occurrence of target T2 is a malfunction / miss.

- Take seat in the vehicle, fill out demographic data

- Briefing about the vehicle, NO explanation of the assistance system, information that there can be obstacles on the course, which can be run over if necessary. Instruction that the middle lane must be used so there is at least one more lane on each side to circumnavigate potential obstacles.

- Start data logging

- Drive one round to become familiar with the setting, then the first obstacle is placed in the non visible curve

- Drive the next round with assistance experiencing the obstacle situation

- Stop and fill out the next part of the questionnaire

- Introduction to the assistance system

- The rest of the trial follows Table 4.2

The first round for the group of assisted drivers was intended to create a first contact situation. Due to the fact that no prior information about the assistance function and the intention behind the experiment was given, this could reveal problems regarding intuitive understanding and other principal weaknesses. For the reference group the same sequence of rounds was used, the only differences were that there was no stop after the second round for the questionnaire and the accomplishment of an additional 10th round.

4.4 Experiment Analysis

After the experiment the log files and questionnaires are analyzed. Before the actual analysis can take place the different update rates of the recorded data sources need to be adjusted. Also the questionnaires are converted into a digital representation for easier handling. These steps and their outcomes are explained in the following sections.

4.4.1 Data Preparation

During the driving time of each participant the logging process runs permanently. As a result the data sets of each participant need to be divided into single rounds which are limited by the beginning and the end of the reference GPS track. Several of the following analyses are based on the track position which means that the data sets need to be extended

with an unambiguous position reference based on the obstacle distances. Basically the track position could be reconstructed completely from the obstacle distances and the GPS speed measurement. But this approach would be suboptimal because of the previously mentioned erroneous position measurements and the low update rate. This is why a much more accurate approach is chosen where only the first position measurement inside the reference track is determined and the position is derived from the internal tachometer signal of the vehicle.

Another issue that needs to be addressed are the different sampling rates of the utilized data sources. There is one common log file which is updated with the internal processing rate of the control software which is set to 64 Hz. Sources with a lower update rate are sampled in a "sample and hold" manner meaning that the current value is used until a new datum is received from a source. The different sampling rates are:

- GPS receiver: 1Hz

- Vehicle CAN bus: ca. 20 Hz

- Control software / data logging: 64 Hz

That way the original sampling times are lost and need to be reconstructed by finding the points in a signal with the help of value changes. This is especially important when a signal shall be smoothed with more sophisticated filter algorithms than low pass filters. When the old sampling times are found the original signal with a lower sampling rate can be reconstructed and fed into a filter. This filter was implemented with the Matlab function "Smooth" using the filter algorithm "rloess" which applies a weighted local regression with a second order polynomial. Such filters are especially useful in this application as they are robust against outliers that exist for only one or two samples like in the GPS measurements. After the filtering the signal is upsampled again using Spline interpolation to a rate of 64 Hz which is then used throughout the analysis.

In the previous section it was mentioned that the reference track was recorded in a way that erroneous position assignments do not occur during the experiment. But still this happened several times as depicted with the red curve in Fig. 4.9 and led to wrong distance calculations. This had no effect during the experiment as it only occured at distances larger than 1000 m in which the assistance system is not activated. For the data analysis the GPS distance measurement at 1000 m is taken as the reference and then the rest of the signal is being reconstructed in both directions using the vehicle tachometer. Also for this reconstructed signal the resampling process described in the previous paragraph is being applied. After these preparation steps the analysis itself can be conducted as described in the following paragraphs.

4.4.2 Vehicle Dynamics

As it was mentioned before obstacles were placed on the course in the rounds 2, 4, 7 and 9 for both participant groups. Only the reference group had to drive a 10th round to obtain a subjective system assessment and additional vehicle dynamics data. Due to the fact that the ISPA system ran in the background also for the reference group, it is possible to determine

Downsampling, smoothing and upsampling
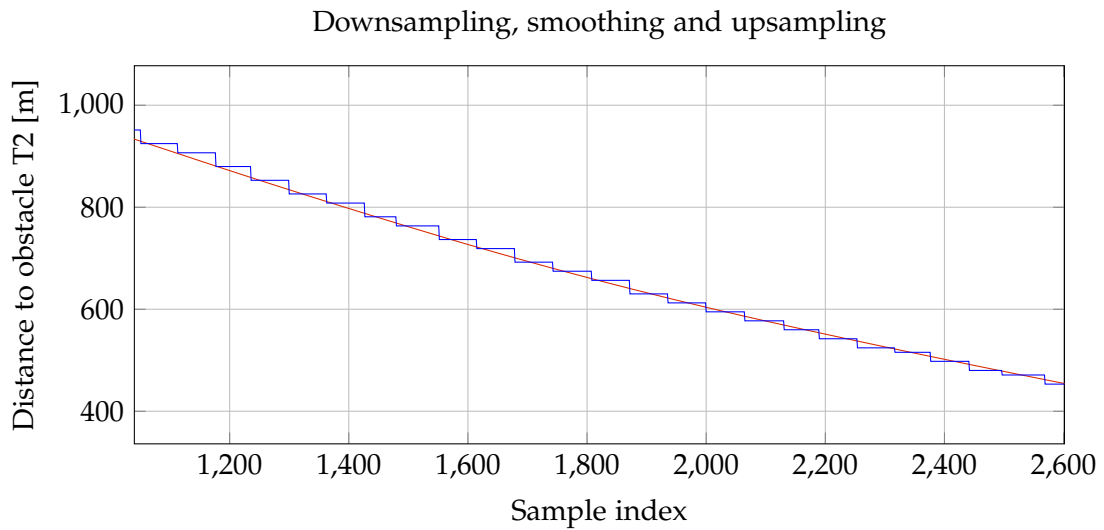
Figure 4.8: Resampling and filtering of raw input data, for example the obstacle distance derived from GPS measurements

a hypothetical reaction time as if the HMI would have been activated. This allows to derive a time advantage in terms of potentially earlier anticipation.

For all rounds containing an obstacle the following metrics are analysed on the last 1000 m before the respective obstacle:

- Speed development relative to track position

- Average speed until standstill

Repair and resampling of the obstacle distance
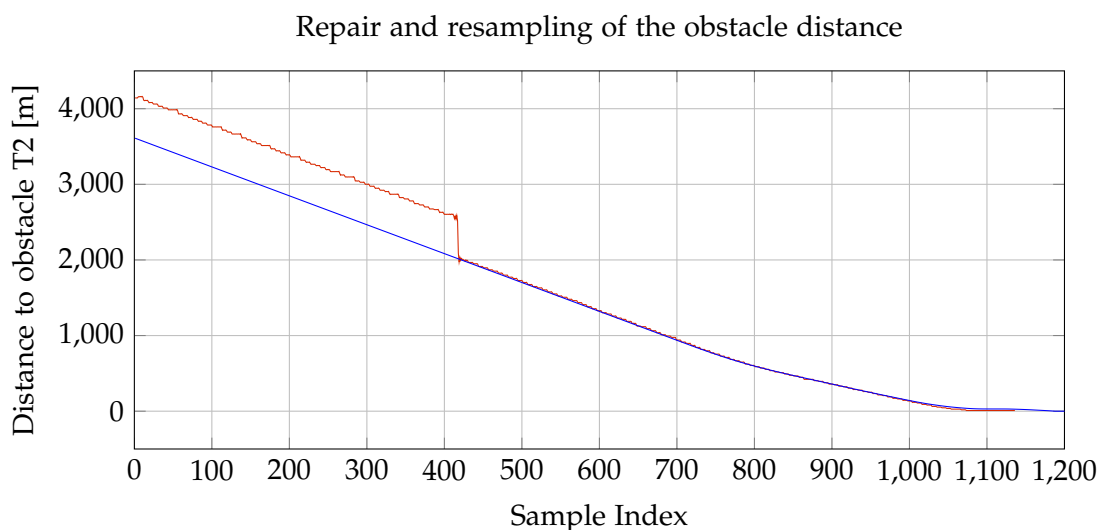
Figure 4.9: Erroneous GPS measurements: reconstruction of obstacle distances starting at 1000 m in both directions using the vehicle tachometer

- Start speed

- Integral of brake pedal position

- Travel time until standstill

- Maximum deceleration

- Reaction time to HMI output

The speed signal is taken from the vehicle tachometer via the CAN bus because of its higher accuracy and update rate than the GPS speed signal. It can be used to plot the speed development of all drivers to obtain a general overview of the different deceleration strategies of assisted and baseline drivers. This can in turn provide an insight to potential security improvements originating from lower speeds and steadier deceleration. Lower speed implies less kinetic energy stored in collision partners which in turn means less severe accidents. Steadier speed decrease results in a security improvement for the following cars because this behavior causes a lower trigger potential for traffic jam waves that could in turn result in collisions (see also [NS92]).

For the average speed, the integral of the brake pedal and the travel time the standstill in front of the obstacle is the end of the analysis interval. The maximum deceleration is derived from the vehicle tachometer signal because there is no simple access to on board sensor data available.

In this experiment the "reaction time" is defined as the time elapsed from the first assistance output until the driver reacts with a deceleration of minimum 0.64 m/s^2. This time interval is also calculated for the reference group to provide a baseline for this metric.

From all data sets speed curves as shown in Fig. 4.10 are plotted. Additionally all metrics described in the list above are also calculated from the data sets and entered in a table like Table 4.3. For all of those metrics a Mann-Whitney U Test is conducted (see [MW47]) to derive a statement whether a metric is statistically different between the two participant groups.

The first round to be analyzed is round 4 with obstacle T1 as it shows the intended effects in a very distinct way. Figure 4.10 contains the speed plots of both the assisted and the reference drivers. It can be noticed that both groups enter the situation with practically the same speed distribution (see also Table 4.3) which means that the initial conditions are comparable from the vehicle dynamics perspective. While the reference group keeps its initial speed of ca. 23 - 25 m/s until 400 m before the obstacle, the assisted group decelerates to a speed interval of 16 - 22 m/s at the same track position. When the obstacle becomes visible about 100 m in front of it, the assisted group has already decreased its speed much more which means that less deceleration is needed after this point. This is also represented by the significantly lower maximum deceleration with a difference of 1.3403 m/s^2 (see Table 4.3).

As a consequence the initial speed is reduced in a smoother manner and over a longer distance which is also reflected in the lower average speed by -4.0929 m/s. Both results underline the potential to increase overall safety and decrease the probability of the generation of a traffic jam wave. The integrals of the brake pedal positions do not differ significantly, but there is a substantial increase of travel time of more than 11 s on the last 1000 m.

Baseline Round 4 Target 1

Assisted Round 4 Target 1
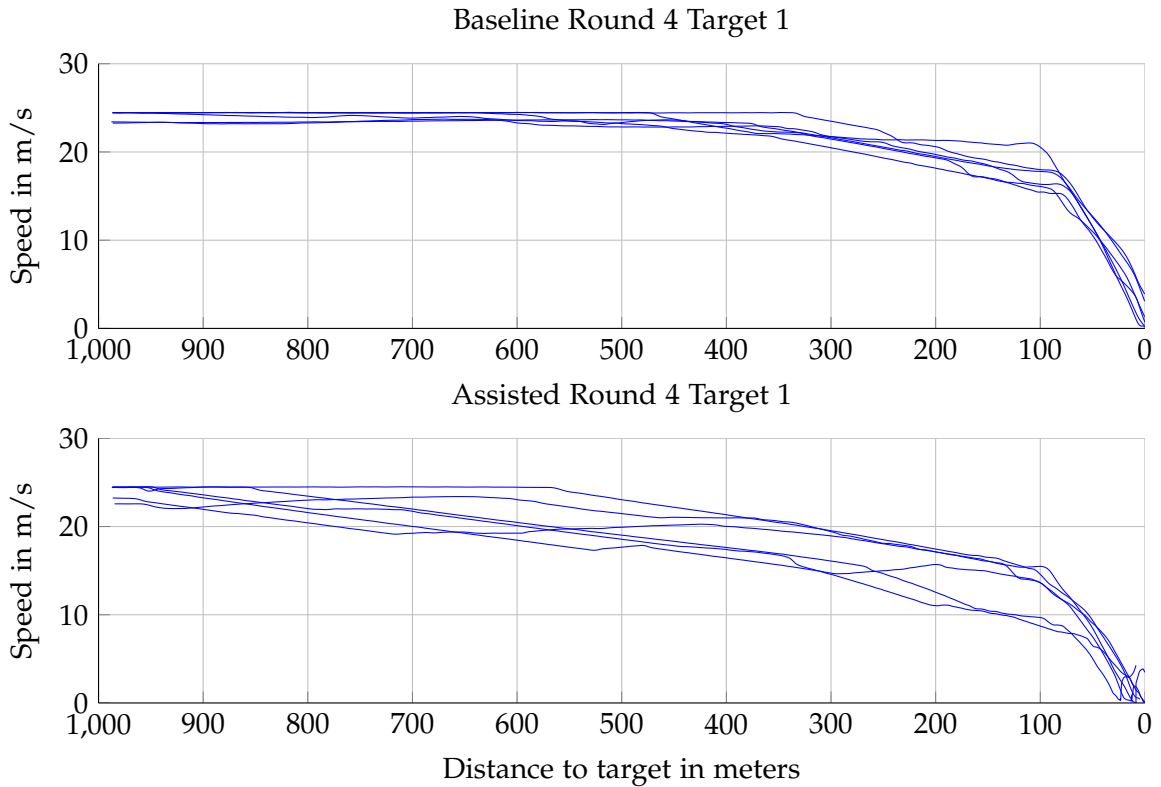
Figure 4.10: Speed development in round 4 for obstacle T1

Also the by more than 20 s decreased reaction time suggests that the assisted drivers are informed about the upcoming situation significantly earlier which again leads to a safety improvement.

Metric	Δ Avg. (Ass. - Base.)	Significance	p
Average speed	-4.0929 m/s	√	0.0095238
Start speed	-0.14758 m/s	X	0.58874
Brake integral	-199.2	X	0.91429
Travel time	11.6276 s	√	0.0095238
Max. deceleration	1.3403 m/s^2	√	0.0095238
Reaction time	-20.526 s	√	0.0021645

Table 4.3: Comparison of vehicle dynamics and derived metrics for round 4, obstacle T1

A more detailed analysis of the chosen metrics shows Fig. 4.11 with several box plots. It also reveals that the interquartile ranges of the brake integrals and the start speed overlap to a large extent which suggests very similar distributions. The narrow interquartile range for the reaction time of the assisted drivers shows that nearly all of them were close to the ideal deceleration start time from a vehicle dynamics view. In contrast the distribution is

much wider for the reference drivers showing that the chosen start time for deceleration is very individual without assistance.
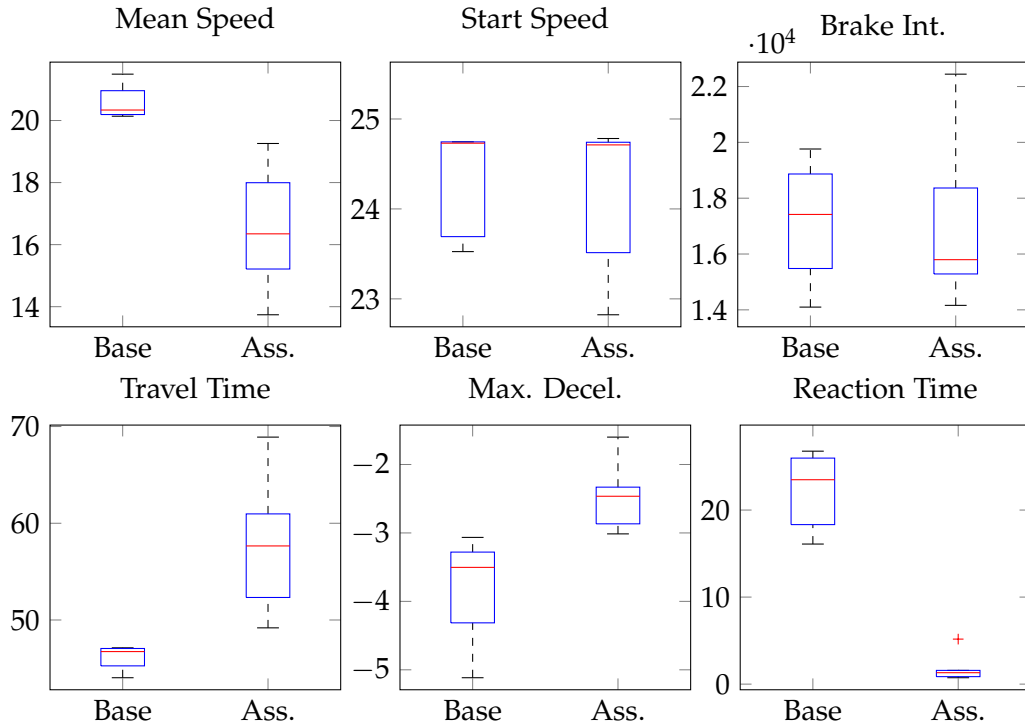
Figure 4.11: Metrics in round 4 for obstacle T1

A different constellation can be found for obstacle T3 which is placed after the exit of the large left hand curve in the east as shown in Fig. 4.7. It can be observed that both participant groups first decelerate because of the curve and then accelerate again when they can see the the beginning of the straight. Similar to the previously described round the start speeds are not significantly different which points out that there are comparable initial conditions. At a distance of 500 m before the obstacle the assisted group has a ca. 5 m/s lower speed distribution and at a distance of 200 m it is even ca. 10 m/s lower except for one outlier.

Also in this round the average speed is significantly lower but with a smaller difference of -3.9032 m/s. The travel time difference is higher for this obstacle while the derived reaction time is on the one hand much lower than in the previous discussion and on the other hand not significantly different between the groups. This very different outcome is produced by the way how this time interval is calculated. Because the threshold for the speed difference as a trigger is exceeded quickly due to the course shape, this value is exceptionally low in that round. For comparability between the rounds this trigger condition is used in the same way. Again the maximum deceleration value is significantly different, this time with an amount of 1.5275 m/s^2. It can be seen in Fig. 4.13 that the overall tendencies are comparable to the fourth round. A small difference can be noted regarding the brake integrals. The interquartile ranges have only minimal overlap and the
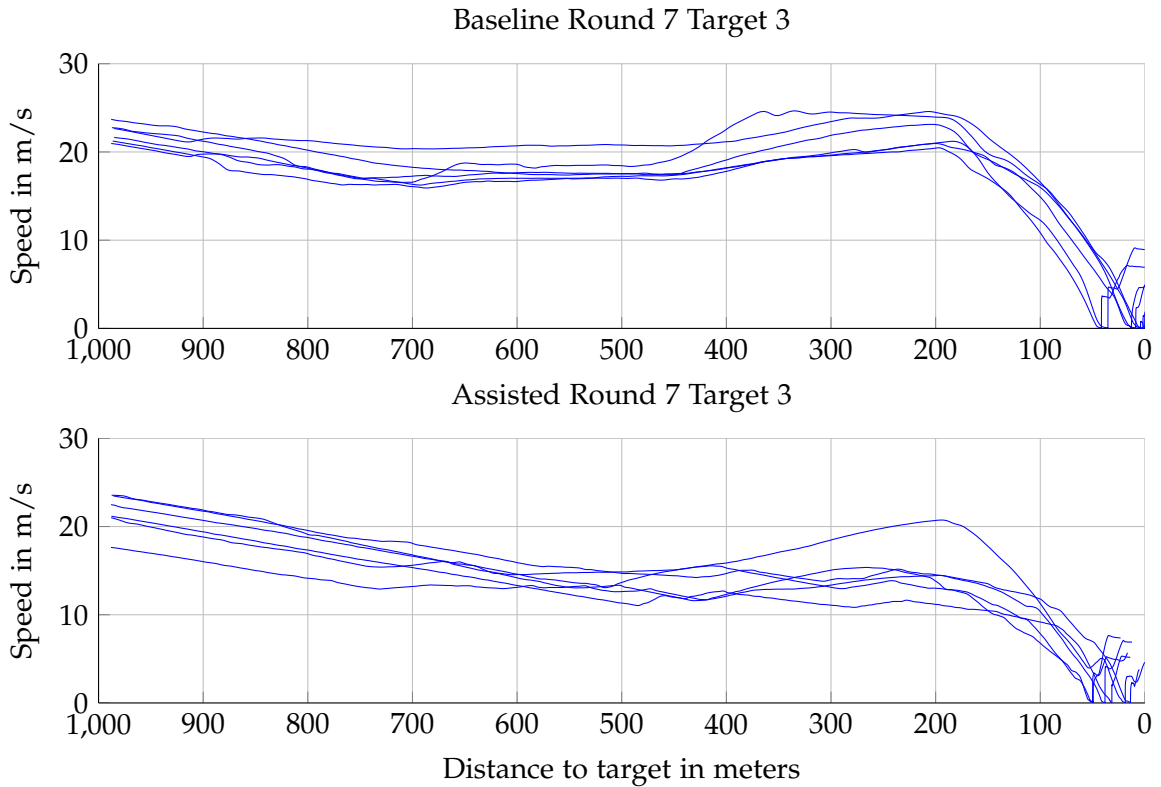
Figure 4.12: Speed development in round 7 for obstacle T3

medians differ by a larger amount which suggests that the assisted drivers utilized the brake by trend less.

Obstacle T2 was used in round two and nine and the tenth round of the reference group. Here the tenth round shall be discussed as two of the assisted drivers passed by the obstacle in round 2 at high speed without stopping. The ninth round showed no significant differences between the groups which is a positive result in this case because a malfunction implemented as "Miss" intentionally occured in this round. Consequently the assisted drivers had no advantage over the reference drivers which is reflected in the metrics. The

Metric	Δ Avg. (Ass. - Base.)	Significance	p
Average speed	-3.9032 m/s	√	0.0021645
Start speed	-0.63056 m/s	X	0.69913
Brake integral	-3375.6	X	0.30952
Travel time	15.737 s	√	0.0021645
Max. deceleration	1.5275 m/s^2	√	0.0021645
Reaction time	0.4974 s	X	0.58874

Table 4.4: Comparison of vehicle dynamics and derived metrics for round 7, obstacle T3
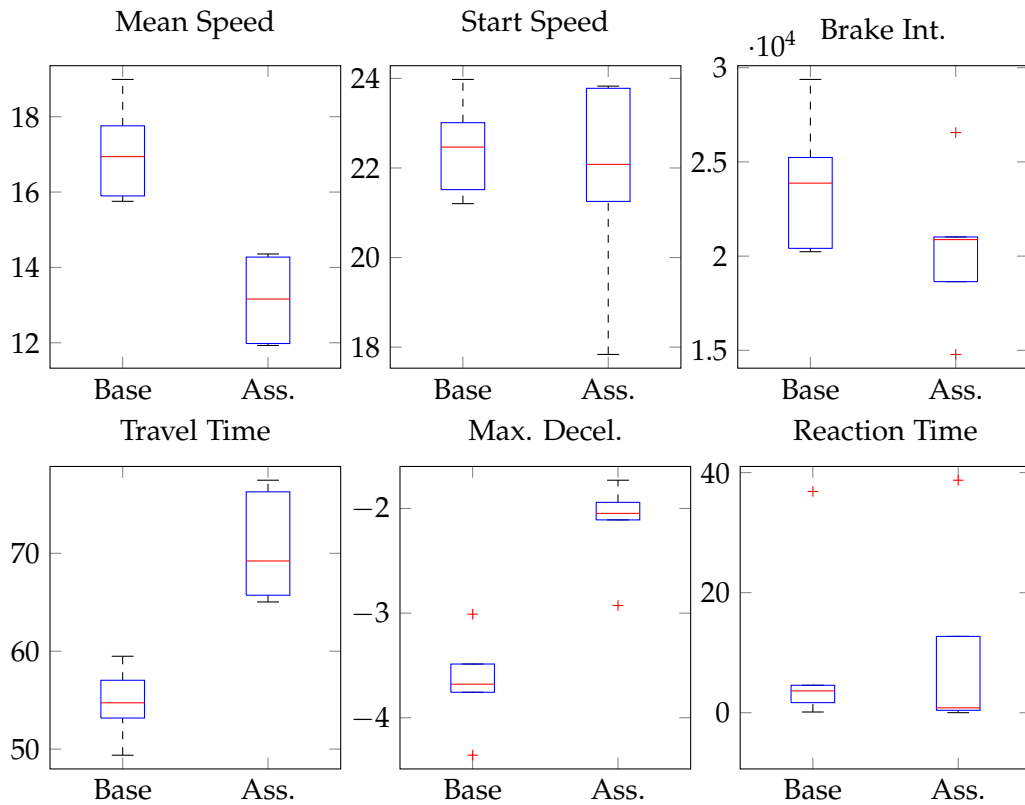
Figure 4.13: Metrics in round 7 for obstacle T3

tenth round allowed for a comparison within the same group. In this case the 9th round of the reference group is taken as the baseline because of the short time span between the trials as compared to the second round. Similar to the previously discussed rounds the speed distribution within one group is shifted lower, for example at the 300 m mark the reference group has a speed of 17 - 20 m/s while the assisted group drives at 10 - 17 m/s. As can be seen in Tab. 4.5 the differences in the average speed distributions exceed slightly the significance level. All other metrics except the start speed show a significant difference, this time even for the brake integral. The results for this last trial round are also interesting

Metric	Δ Avg. (Ass. - Base.)	Significance	p
Average speed	-3.348 m/s	X	0.055556
Start speed	-4.4159 m/s	X	0.13203
Brake integral	-6459.84	√	0.0079365
Travel time	13.8375 s	√	0.031746
Max. deceleration	1.6953 m/s^2	√	0.0079365
Reaction time	-7.5156 s	√	0.004329

Table 4.5: Comparison of vehicle dynamics and derived metrics for round 10, obstacle T2
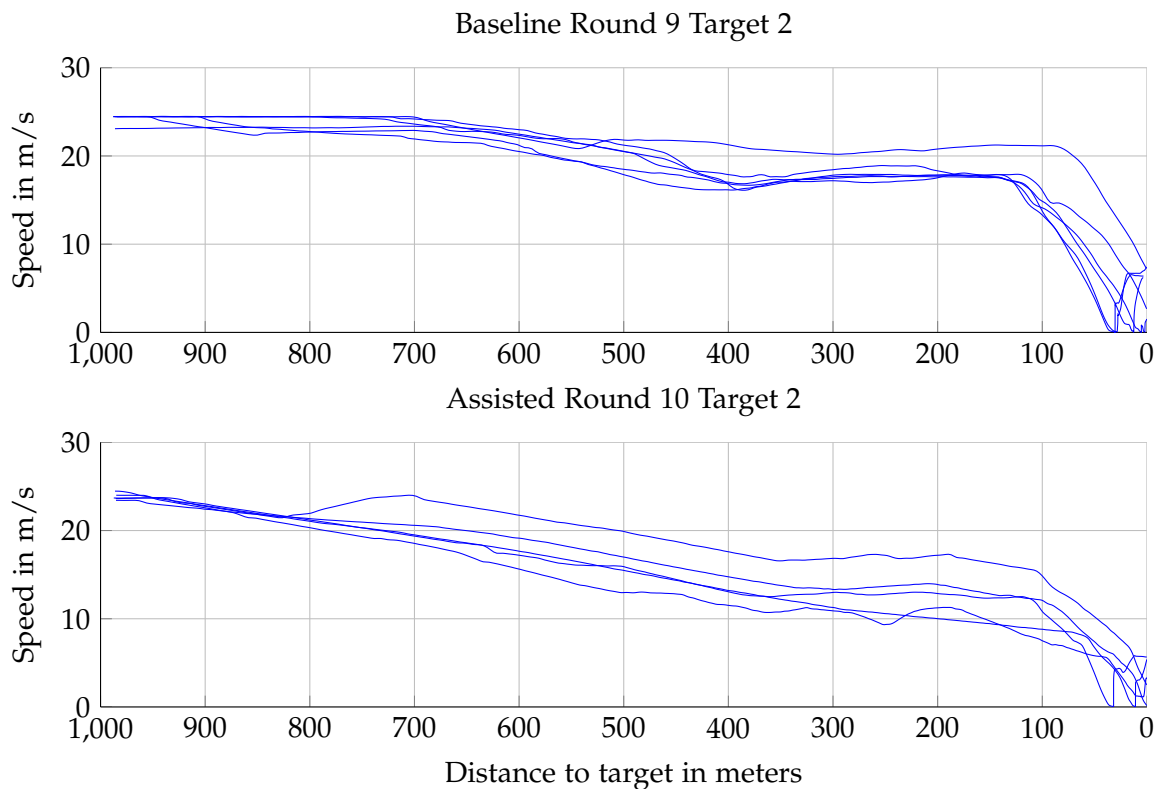
Figure 4.14: Speed development in round 10 for obstacle T2

from the perspective that the drivers experienced the obstacles before several times without assistance. This happened within a relatively short time span of ca. one hour so it can be assumed that they developed a higher alertness than can be expected in every day use. Still the assistance provides a measurable information advantage and safety gain which is a very positive result.

4.4.3 Questionnaire

The questionnaire consists of two nearly identical parts. Each contains statements with a ranking on a linear scale, word pairs forming a semantic differential and finally open questions. Also demographic data must be entered by the participants at the beginning of the form and the second part contains the additional question whether they would use the system in their vehicle. Only the assisted group fills out the first part of the questionnaire, which is done directly after the first contact situation with the system. The second part is used by both groups because the reference group also gets an explanation of the system and experiences it in one round.

Overall the system gets a positive rating as can be derived from the boxplots in Fig. 4.16. There are slight differences between the first contact rating and the final rating. Regarding the optical quality the assessment is improved by one unit after the experiment. The ratings
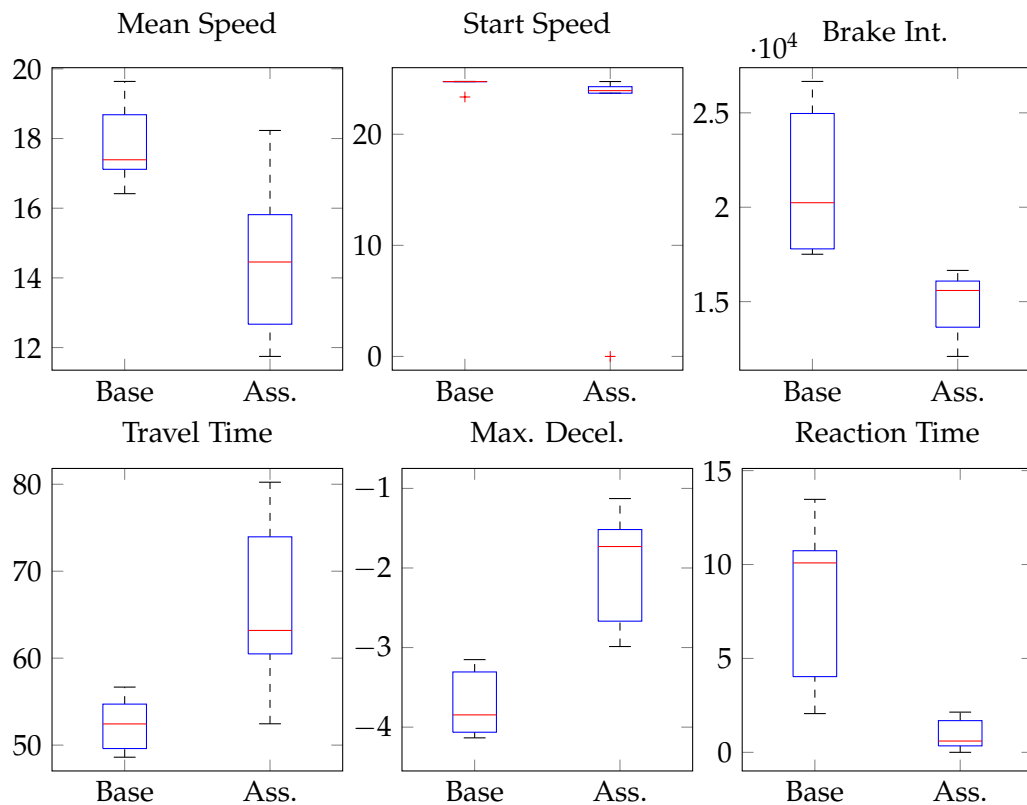
Figure 4.15: Metrics in round 10 for obstacle T2

for the support of anticipatory driving and the usage in the own vehicle are located in the highest intervals.

The results of the semantic differential in the two parts is depicted in Fig. 4.17. Again it must be noted that question 1.4 was only answered by the assisted drivers while question 2.5 was answered by both groups. For easier interpretation of the plots the wordpairs are aligned so that the positive words refer to the right side of the figure. This is intentionally not the case in the questionnaire so the participants need to reflect their rating more instead of choosing a constant rating for all word pairs. In general a more positive rating can be seen in the figure although it is not statistically significant if analyzed over all pairs. The largest improvements occur for the pairs "plump - elegant", "ordinary - special", "conservative - innovative" and "sluggish - dynamic".

In the last section of each part several open questions have to be answered by the participants. Questions 1.5 and 2.6 asked for prominent positive features which produced among others the following answers:

- Very simple, easily understandable presentation

- Anticipation even though the obstacle could not be seen because of the curve ⇒ superior to human performance

- Color change of the LED display

Do you find the display optically appealing?

Did you understand the system intuitively?

Did the system support you in anticipatory driving?

Would you use the system in your vehicle?
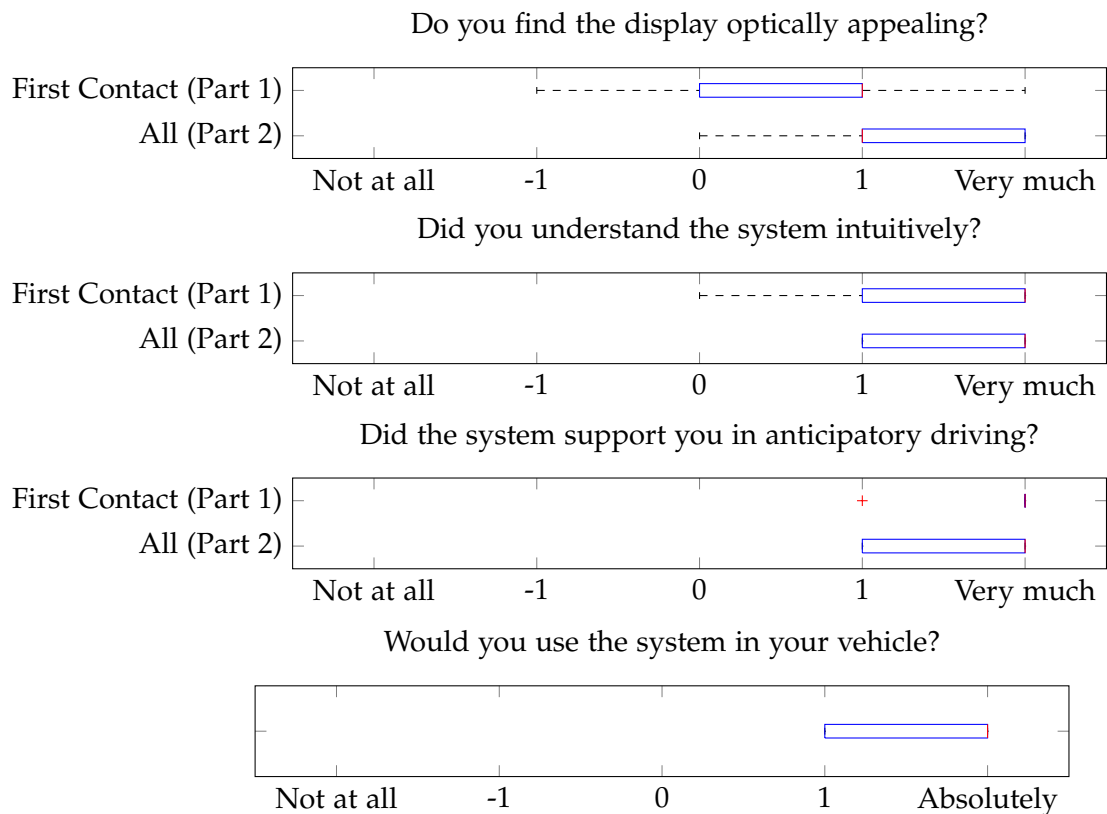
Figure 4.16: Questions 1.1 - 1.3 (after first contact) and 2.1 - 2.4 (after driving part)

- Acoustic hint (guides attention to the display)

- Obstacle distance information

- Simple display in the field of view with illuminated bar, precise information in the instrument cluster, color and stepping of the LED bar

- Convenient in the field of view

- Early warning

In both cases (directly after the first contact and after repeated use of the system) drivers assess the improved anticipation, the distance information and the colored LED output to be especially positive and reasonable. Also the unobtrusive output and the information distribution over the display and the LED bar are rated to be beneficial.

The prominent negative features have to be pointed out in questions 1.6 and 2.7 where the participants mentioned among others the following ones:

- Two systems with equal meaning

- Spatial encoding of the sound at first use
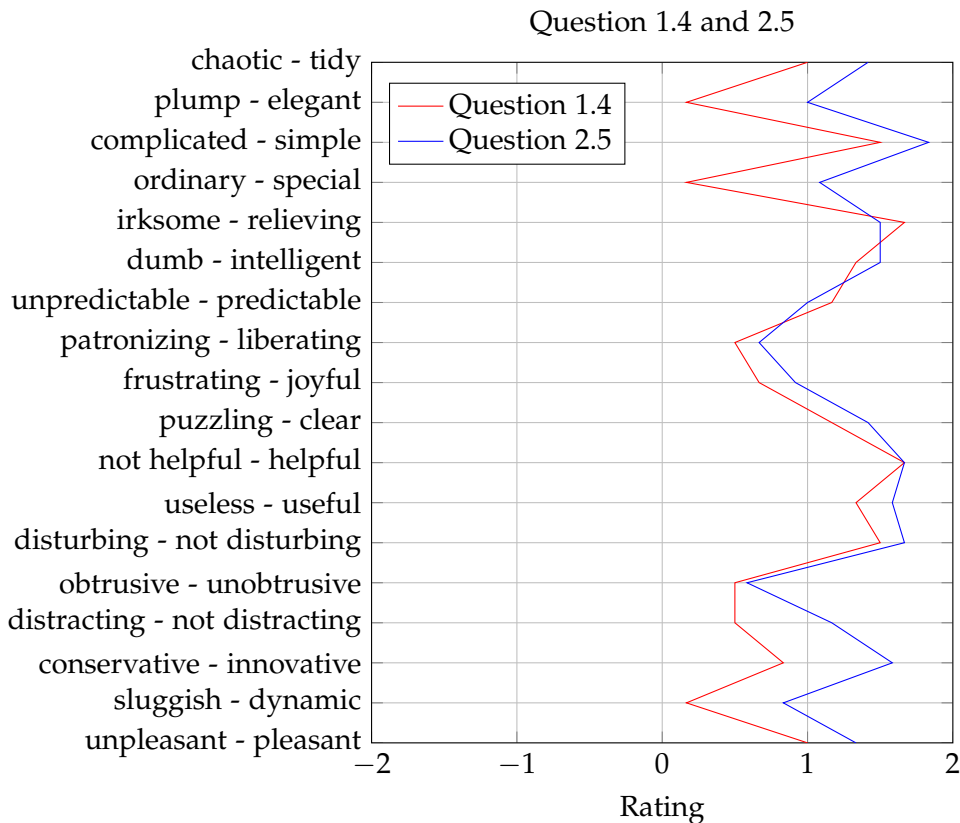
Figure 4.17: Comparison of the normalized word pairs from the real world experiment questionnaire. Both ratings are overall positive while the one at the end of the experiment (question 2.5) is slightly better.

- I perceived the warning to be too early

- Position of the display

- The early warning made me feel like an obstacle when stepping off the gas pedal

- LED bar badly visible in sunlight

In both questions regarding negative aspects the most prominent ones are the early warning and the unobtrusiveness of the LED system. If these statements are combined with the positive statements regarding the LED system, they are judged to be generally sensible but should be visible more easily. The fact that the early warning is mentioned in both the positive and negative feature group in comparable numbers can be interpreted that the activation time is already sensible in most situations. But this conclusion should not be overrated due to the small number of participants.

4.5 Conclusions

In this chapter an experiment was presented in which the ISPA system was integrated in a tractor truck. The main motivation for this experiment was the possibility to test the system in a real vehicle on a test track with professional drivers. As a side effect the drivers took the experiment more serious. This can be attributed to the more realistic environment and the results can be transferred to a real traffic situation with much higher confidence than results from a driving simulator (see also [WLH12]).

Both the subjective ratings and the objective metrics show that the system is also effective in a realistic driving environment. The overall outcome is comparable to the previously described driving simulator experiments which in turn shows that this preliminary work produced valuable input to the system variant used here. It was possible to inform drivers substantially earlier about obstacles on the course than would have been possible with their own senses. The result was in most cases a significantly lower average speed and maximum deceleration on the last 1000 m. This safety improvement is opposed by an increased travel time which adds only marginally to the overall travel time of a common work day.

5

Immersive Virtual Environment for Anticipation Experiments

All driving simulations which have been used so far had a common setup: an instrumented passenger car mockup stands in front of a projection screen on which the simulated scenario is displayed. For an experience as realistic as possible the car physics is modeled with high detail, an audio simulation provides the usual sounds in a car and screens in the dashboard show the common instruments like Speedometer, RPM gauge etc. This environment suited well for the development of an assistance system and testing its usability, acceptance and effectiveness.

The ISPA system is intended to provide an aid for improved anticipation of the upcoming traffic constellation. Here anticipation is especially related to the recognition of potential obstacles, the prediction of their movements and possible implications for the driver. For such spatial and temporal anticipation it is important that the driver is able to perceive the environment with high detail and if possible with a 3D impression as natural as possible. This goal is motivated by the fact that drivers draw 90% of their information from vision (see [Tay82]).

A display system that is aimed at exactly those requirements is the Cave Automatic Virtual Environment (CAVE). It was first built and documented by Carolina Cruz-Neira et al. in [CSD93] where it is described as "useful tool for scientific visualization". The naming is also a reference to Plato's "The Simile of the Cave" (see [PlaBC]) where he discusses inferring reality from the shadows (projections) on the cave wall. In a CAVE the user is situated inside an array of projection walls (in some implementations also the floor and ceiling) which provide a stereoscopic image based on the user's head position. The result is a space in which a person can move freely and which acts like a window to a virtual world that ideally appears to be real to the user. This effect is called "immersion" and its degree depends on the sensory perception quality provided by the system.

This chapter describes how the benefits of a CAVE system can be combined with a driving simulation in order to foster the spatial perception of test drivers. Several studies and surveys like [Win+07] have tested the feasibility of a stereoscopic presentation of the scene and its implications on spatial perception, Simulator Adaptation Syndrome (SAS), hardware requirements etc. While some authors state that such a setup provides positive effects regarding 3D perception only in a small radius of up to 20m (see [SS91]), Piao and McDonald (see [PM03]) investigated that inter-vehicle distance ranges from 7m at 10km/h

to 30m at 120km/h. As a result it depends on the actual driving speed whether drivers can track surrounding vehicles with stereo vision or not.

Mollenhauer argues in [Mol04] that drivers switch between a near and far point with a frequency of ca. 1Hz and in doing so the near point is covered by the area with effective 3D vision. Bauer et al. state that stereopsis is beneficial especially in dynamic situations which would also be a positive factor for a stereoscopic presentation (see [Bau+01]).

While these statements stand in favor of using stereoscopic display systems, there are also reasons against it. Very obvious ones are the increased hardware requirements leading to higher costs and the higher complexity of the setups (both hardware and software). Other problems arise from the different depth cues present in a CAVE where especially the accomodation does not match the other depth cues. If the projectors in such a system are misaligned leading to a distorted stereo presentation, performance can be decreased as explained by Pfautz in [Pfa01].

Even if there are some reasons pointing against the use of a stereoscopic setup, several authors suggest an improved task performance and immersion. As the disadvantages originate more from a practical side, it is still assessed to be a feasible step for a research setup.

In the following sections the mechanisms of human visual perception of 3D space are investigated, then the general requirements for a driving simulation are established. After that the hardware and software setup will be described and the whole system finally evaluated in a user study.

5.1 Human Depth Perception in a CAVE

The perception of depth is usually attributed to stereo vision, but this is only an incomplete description as humans use several cues to extract depth information from the two images of each eye. In [CSD93] Cruz-Neira mentions the cues listed in Tab. 5.1. Commonly used desktop setups for viewing three dimensional scenes cover the points 1, 2, 7 and 8 in Tab. 5.1. This can be improved by stereoscopic display systems and head tracking to also include numbers 3, 4 and 5. No display system to this point has reproduced correct accommodation which still leads to irritations for users especially for close objects. In a setting where the virtual object is 50cm away from the viewers head position while the relevant projection wall is at a distance of 2m, it was observed in previous experiments in the CAVE that correct vision is hard to achieve for subjects.

In contrast to a desktop application where the rendering engine assumes a fixed head position in front of the screen perpendicular to the screen center, this is usually not the case in a CAVE setup. The desktop scenario uses the theory of a camera projection similar to the physical setup of a photo camera. This means that the rendered image content is determined by the focal length, position and rotation of the virtual camera. The focal length in conjunction with the size of the virtual image plane define the FOV. As common screen dimensions are usually not equal in width and height, two different FOV angles can be defined with equation 5.1.

$$\alpha = 2 \cdot \arctan\left(\frac{d}{2f}\right) \tag{5.1}$$

Nr.	Cue	Description
1	Occlusion	Surfaces hidden by obstructing objects / parts
2	Perspective projection	Geometric distortions through projection (vanishing points, converging parallel lines etc.)
3	Binocular Disparity	Differences between left and right image due to different viewing position and angle
4	Motion Parallax	Relative motion of foreground and background elements during viewer movement
5	Convergence	Lines of eye gaze intersect at the focused object distance
6	Accommodation	Eye focus distance controlled by the ciliary muscle to derive a sharp picture of the desired object
7	Atmosphere	Distance fog and decreasing contrast for distant objects
8	Lighting and shadows	Relative brightness due to surface position and rotation, shadow directions etc.

Table 5.1: List of cues in human three dimensional space perception

where α : angle coverage / Field Of View
d : image plane dimension
f : focal length

Here it is assumed that the angle α e.g. in the horizontal direction is equally distributed for the left and right image part. As Fig. 5.1 shows this is not true any more for a display system like the CAVE. If we draw a line through the viewers head position perpendicular to a projection screen, usually both the horizontal and vertical FOV angles are not distributed
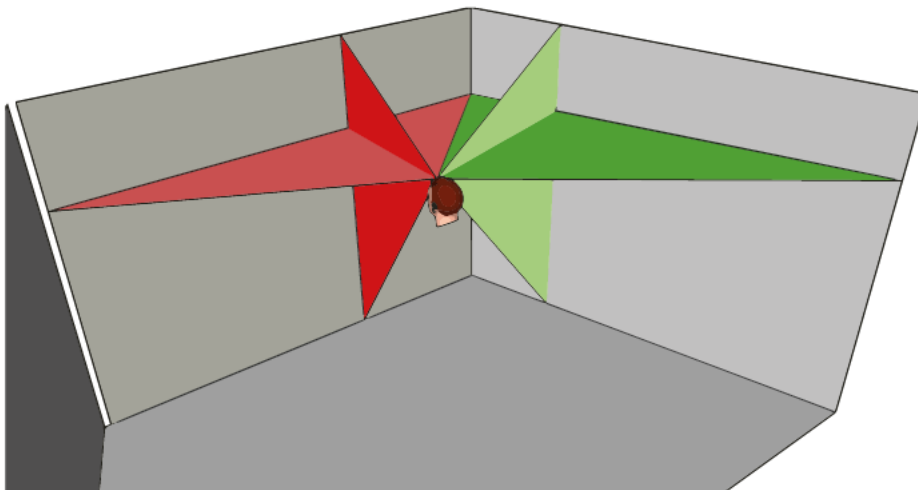

Figure 5.1: Asymmetric Field Of View for the CAVE walls, projection center is usually not perpendicular to the center of the image plane.
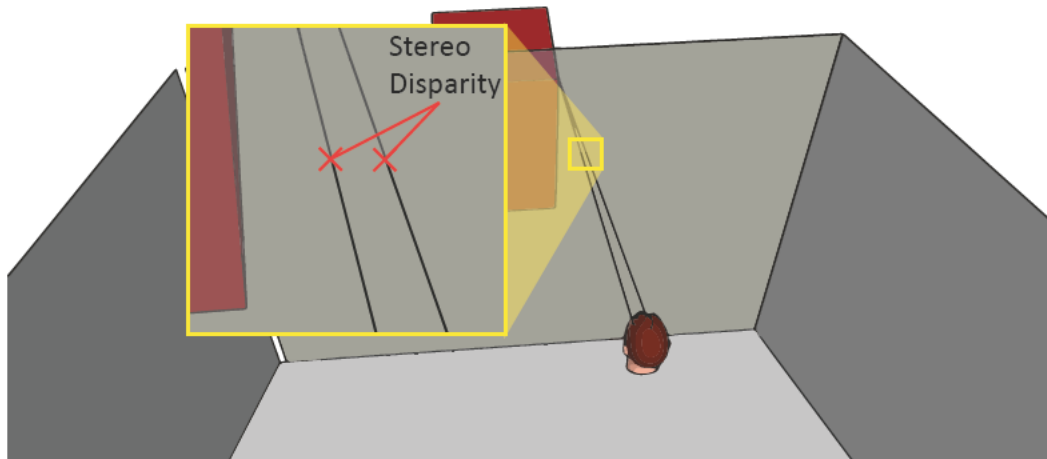
Figure 5.2: Stereo vision in a CAVE based on the Window Projection Paradigm

equally to the left/right and upper/lower screen portions. This implies that Eq. 5.1 cannot be used any more.

Instead the Window Projection Paradigm can be used as suggested by Cruz-Neira in [CSD93]. Figure 5.2 shows that each projection wall can be interpreted like a viewing window to the virtual scene. If we take a corner of a virtual red cube and draw the lines of sight from each eye of the viewer, these lines intersect the wall at different points. This leads to stereo disparity in the rendered images for both eyes (see detail in 5.2) which in turn causes the depth cues discussed before.

To present different pictures for each eye on the same display surface several technologies are available which can be separated in two groups: active and passive stereo. Systems that belong to the active stereo category use shutter glasses that have Liquid Crystal layers on the glasses worn by the user. Additionally they contain an electronic unit that obtains a synchronization signal from the projectors and switches the according glass transparent or opaque. This must happen at a high switching frequency (usually 120 Hz) to avoid flicker and resulting eye fatigue. As the projectors display the two images sequentially, the effective frame rate is only half of the switching rate.

Passive stereo systems have the advantage that they do not have to be synchronized between the projectors and the glasses and need no time sequential switching which decreases the effective frame rate. They can be implemented with light polarizing filters that are either orthogonally mounted for linear polarization or have opposite rotation direction in the case of circular polarized filters. Here it is especially important that the screen medium does not affect the polarization which limits the possible choices for the surface materials.

A very old way to passively separate the pictures of both eyes is the anaglyph technique. It uses two color filters which act basically like an optical high-pass or low-pass filter and thus distort the original color space heavily. The human visual system mixes the two colors which results in a grey or brown image. Based on the same idea but with the ability to overcome the color issues is the system developed by Infitec (see Fig. 5.3). As described by Jorke et al. in [JSF09] the system uses very narrow band-pass interference filters that
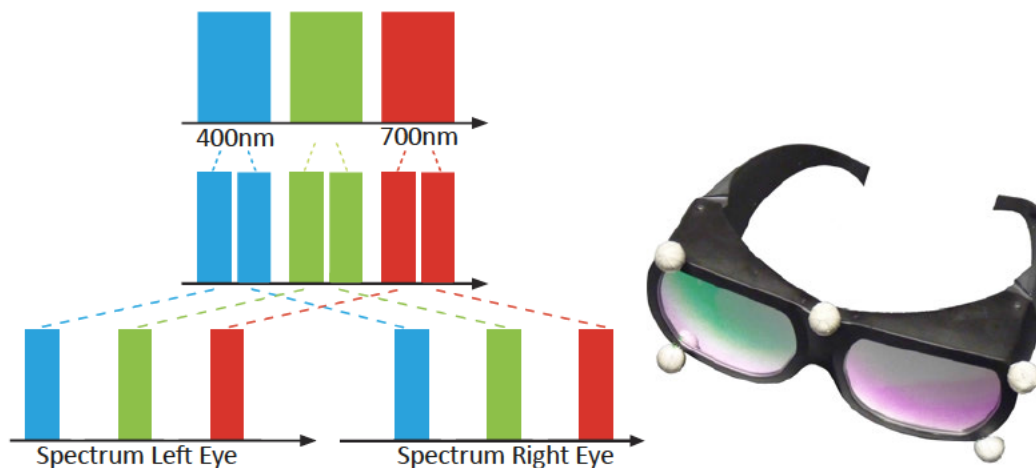
Figure 5.3: Infitec filter system: interference filters both in the projectors and the 3D glasses enable the separation of the left and right eye pictures (left image based on [Maß12]). The 3D glasses are equipped with reflective tracking targets.

cover several intervals of the visual spectrum. The center frequencies are shifted between the eyes (see also Fig, 5.3) so the images still contain information from several parts of the spectrum while creating a separation of both pictures. The advantages of the system are the maintenance of the original frame rate, no synchronization requirement, color correctness, high light efficiency and the versatility regarding projector technology and screen material.

The last essential component of an interactive 3D system is the tracking system that provides the position and rotation of the user's head. In order to provide a seamless presentation of the virtual world distributed over all four screens (three walls and the floor) the head tracking information must be updated in real time to calculate all eight views (four screens, two views per screen). The term "real time" means that both the update rate and the delay between tracking and rendering must be below a certain threshold. Both the tracking and the rendering pipeline run at an update rate of 60 Hz (time period $0.01\overline{6}$ s. The delay is somewhat less stable as it depends on tracking and rendering frame rate, network delay and sometimes filter algorithms. Adelstein performed experiments regarding head tracking latency (see [ALE03]) where he observed a Just Noticeable Difference (JND) in latency of 13.6 ± 0.6 ms and a Point of Subjective Equality (PSE) of 58.8 ± 2.6 ms. The latency interval defined by the JND is defined between the 50% and the 75% detection probability while the PSE value is located in the center of the JND interval. This means that a latency of 52ms can be detected by subjects with a probability of 50%. A system using head tracking should therefore stay below this time delay, DiZio et al. propose a maximum delay of 40 ms in [DL97] to prevent SAS.

5.2 Hardware Setup

In the previous section it was already motivated why a stereoscopic presentation might be beneficial for experiments in the context of an anticipation supporting system. The system
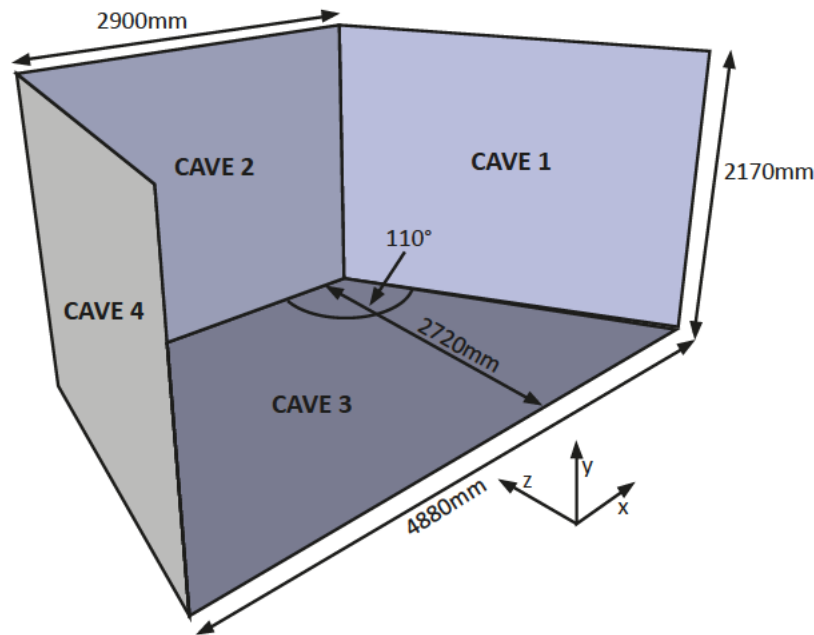
Figure 5.4: Wall dimensions of the CAVE. Each wall is rear projected, the floor is used in front projection mode. The tracking cameras are mounted on the top edge of the walls.

that is used for the following experiments is the CAVE installation as depicted in Fig. 5.4. It is a stereo projection system with Infitec filters (wavelength multiplex, see above) consisting of four sides: three walls and the floor. All walls are used with rear projection while the floor has front projection. Rear projection is beneficial especially for the walls as it avoids that the user casts a shadow on the screen he is potentially looking at. The floor projection does not suffer from this issue as users usually face towards the middle wall and their shadow is cast behind them with a very small profile causing only low impairments.

Many CAVE installations use a rectangular setup while this construction has 110° angle between the walls. This provides a larger working area and is advantageous if larger car mockups are placed inside it as depicted in Fig. 5.5. The red dots in this figure originate from the infrared flashing system built into the tracking cameras. A synchronization cable connects all cameras to ensure a controlled image capture which is essential for tracking. The circles and line markings on each screen are used to calibrate the projector positions in order to match the image for the left and right eye on every screen and also the alignment between the screens.

The car mockup is based on a 1998 Audi TT Coupé of which the cockpit for both the driver and front passenger are still included. The original steering wheel is attached to a Logitech G25 Force Feedback wheel, the original pedals were also adapted to the gaming wheel electronics. Like that it is easily possible to access the steering angle, pedal positions and also to apply force feedback with standard software interfaces over an USB connection. Also the buttons on the steering wheel and the direction-indicator control can be accessed with the help of an IO Warrior USB interface produced by Code Mercenaries.
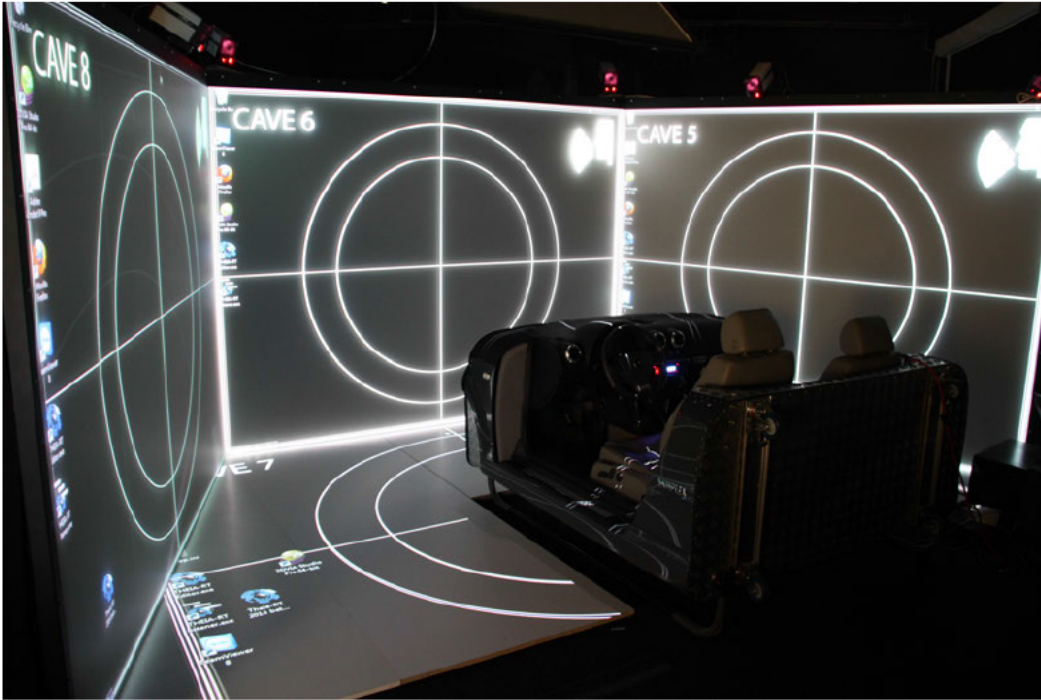
Figure 5.5: Car mockup the CAVE. Missing physical parts of the car are added virtually by the driving simulation. These parts would otherwise obstruct the line of sight of the tracking cameras and make head tracking practically impossible.
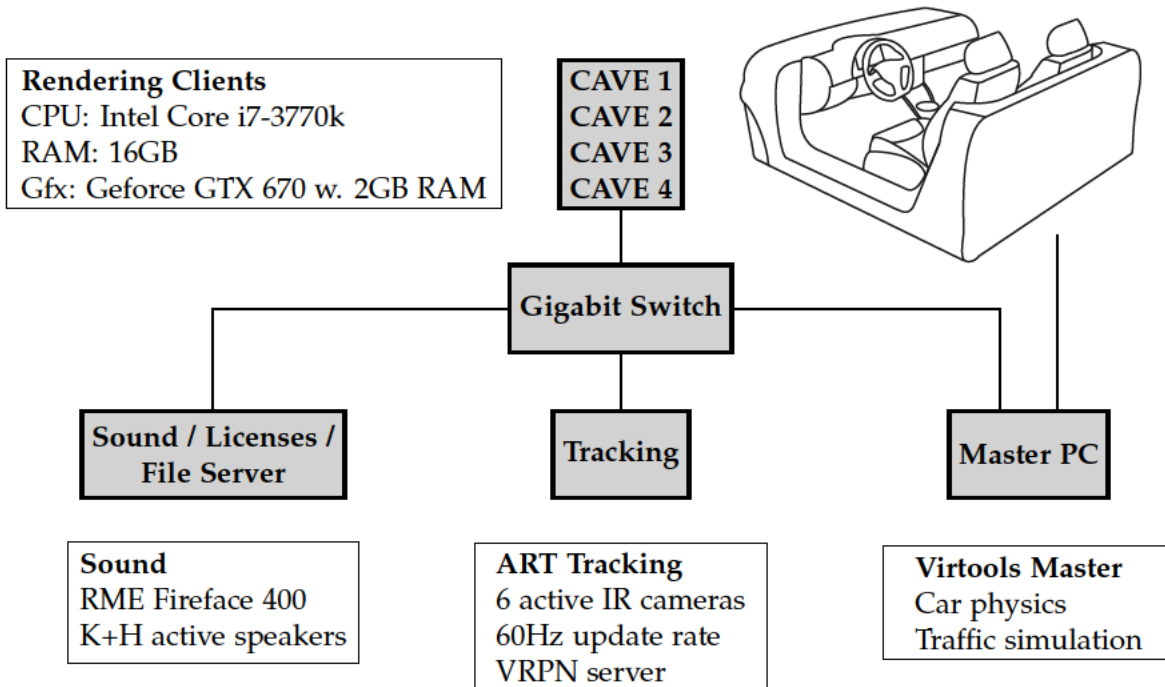

Figure 5.6: Hardware architecture of the CAVE driving simulator. All communication and synchronization is done using Gigabit Ethernet connections.

Figure 5.6 shows the overall hardware architecture of the CAVE driving simulator. The central elements are the Master PC and the four rendering clients "CAVE 1" to "CAVE 4". Each of the rendering clients is connected to one projector pair (left and right eye) of one wall and produces the stereoscopic image with the side-by-side technique. This means that the two projectors are configured like two displays creating an extended desktop while projecting on the same screen surface. Head tracking is implemented with the ART tracking system by mounting tracking targets on the 3D glasses (see Fig. 5.3). The tracking information is calculated by the ART software "DTrack" which provides its output to a Virtual Reality Peripheral Network (VRPN) server (see also [Tay+01]).

The car mockup is attached to the Master PC with a USB connection which transmits the steering and pedal positions as well as the steering wheel buttons. If required an additional computer can be added to the network to render the content of the digital instrument cluster mounted in the mockup. All shared configuration and asset files are stored on a file server which is also used for sound generation. Therefore it is attached to a RME Fireface 400 professional audio interface that provides high quality and low latency sound output.

5.3 Driving Simulator Software Architecture

Based on the described hardware setup and the theoretical motivations for a stereoscopic driving simulator in a CAVE the following sections will describe the overall software architecture. The system shall be based on the Virtools development framework and be as modular and extendable as possible. Additionally existing software packages (both internally developed and commercially available) shall be reused in order to follow existing standards and benefit from the robustness of proven tools.

5.3.1 Requirements for the Simulation

Setting up the driving simulation for a given experiment is a complex task which depends heavily on the chosen simulator design. Two phases must be distinguished in this case: the offline preparation of the scenario and the online behavior of the simulator. For the preparation phase it is desired that scenarios consisting of the static 3D environment and the dynamic components like other cars can be defined quickly but still with the possibility of detailed parametrization. The online behavior on the other hand must be reproducible but also be interactive if required by the experiment design. Also the perceived simulation quality comprising visual detail, frame rate etc. must satisfy certain conditions.

Several requirements for the final framework can be established based on the knowledge gained from previous developments and the use of commercial software packages such as Silab (see [Krü+05]). The following points shall be accomplished in the long term:

- Independence of specific hardware configurations:
  It shall be possible to run the simulator with minimal changes as well on other systems like a desktop PC with a standard screen or Head-Mounted Display (HMD), with a different car mockup and only one projection screen, with or without head tracking

- Modular design for extendability and exchangeability:
  If possible the simulator shall be distributed over several stand-alone applications

that can be distributed over several computers. Also software modules shall be exchangeable like the ego car model, car physics, extensions for assistance system prototypes etc.

- Realistic behavior of external traffic:
  The other vehicles in the simulation should move realistically regarding car following, lane changing, right of way, route choice etc. Also they shall interact with the ego vehicle.

- Efficient and realistic scenario design tools:
  In order to create also larger environments without having to place every single object by hand an automated generator is desired. Also the road networks should have a realistic layout to create a convincing environment and realistic results.

- Realistic sound:
  Sounds provide several important cues to the driver regarding driven speed, road type, engine RPM and play an important rule on the level of immersion (see also [BG03])

- High frame rate and low latency for minimal SAS:
  Very dynamic tasks like driving demand a high optical fidelity including frame rates of minimum 60Hz as described by Hubbold et al. in [Hub+95] and low latency (less than 40ms) as proposed by DiZio in [DL97].

- Flexible data logging and interchange with other software modules:
  Saving experimental data during an experiment is essential and therefore must be provided by the simulator. Technically related to this function is the possibility of transferring simulation data in real time to external programs like assistance systems.

The following sections describe how these requirements have been met and to which extent it could be done within the scope of this thesis.

5.3.2   The Development Environment

Creating interactive applications for a PC cluster environment running a CAVE is different from a standard desktop application in several ways. Most obvious is the lack of common interaction methods like keyboard, mouse or touch pad. Also the presentation of a 3D environment is not common in the desktop world except for game scenarios. Finally the problem of state synchronization between the participating PC clients is usually not present to this extent. This ranges from the frame-wise synchronization of all clients related to 3D rendering to the position of moving objects in the scene and input from the user. These tasks should be abstracted from the application developer to enable an efficient development cycle.

The framework chosen here is Virtools from Dassault Systèmes as it provides different ways and abstraction levels for developing applications for an immersive environment. The most high level approach is graphical programming based on Virtools Building Block (BB) networks as seen in Fig. 5.7 in the bottom screen portion. Every BB has one or more
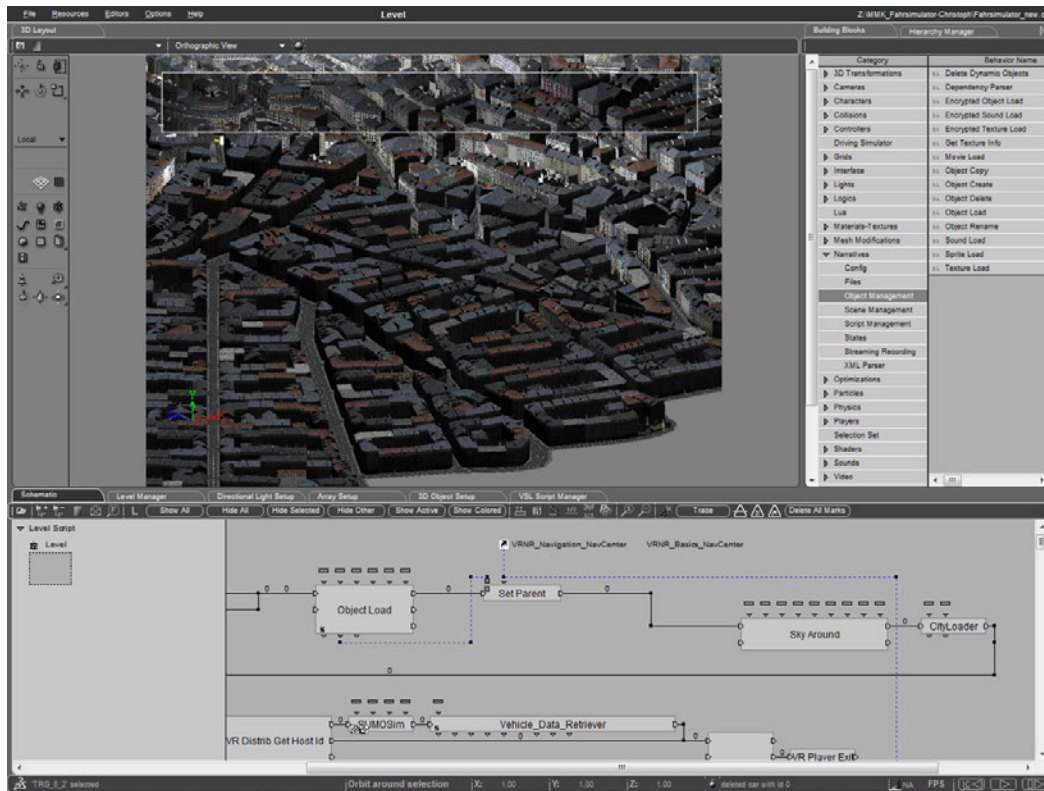
Figure 5.7: Screenshot of the Virtools Development Environment. Key elements are the 3D preview in the upper left area, the asset browser and Hierarchy Manager in the upper right area and the Schematic Editor in the lower screen portion.

activation inputs on its left edge, at least one activation output on its right edge and an arbitrary number of parameter inputs and outputs on the top and bottom edges. The connection of activation inputs and outputs determines the order in which Building Blocks are executed while the parameter connections determine the data flow between the blocks.

A Building Block can either be provided with Virtools or be programmed with the Virtools Scripting Language (VSL) or C++. VSL is a scripting language with a syntax comparable to C++ and can be developed directly within the Virtools development environment. This makes it valuable for rapid prototyping in cases where the BB approach would produce too large or ineffective schematics. The drawbacks compared to a native C++ implementation are the lower execution speed and limited possibilities due to the restriction to the VSL- Application Programming Interface (API). A C++ extension can use any feature that is available to the C++ language ranging from simple TCP socket servers to complete physics engines such as nVidia PhysX.

Virtools defines an application as a "composition" of abstract entities like 3D objects, data and behaviors which can manipulate the other two types. Behaviors can be a single BB or larger schematics consisting of several Building Blocks. Virtools offers only a very limited number of included primitive geometric objects such as spheres, boxes etc. As a
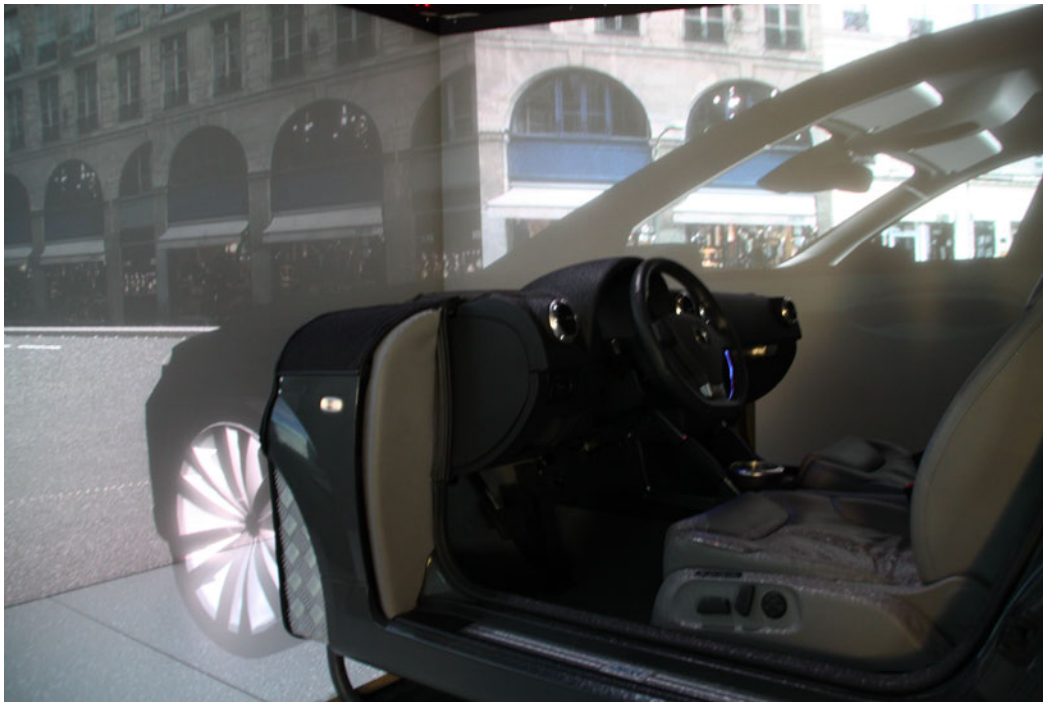
Figure 5.8: Combination of real and virtual elements of the driving simulator mockup. All directly reachable parts for the driving part are represented by a physical mockup while elements like front wheels, ceiling etc. are added virtually.

result it must always either be combined with a Digital Content Creation (DCC) software or create its own objects at runtime.

An essential feature of this framework is also the physics engine provided with it. It is based on the Havok engine which is usually included in game engines. The physics engine provides several Building Blocks that enable the simulation of vehicle physics. It requires the steering and pedal positions as input in conjunction with the road geometry and an extensive set of parameters that define the physical parameters of the car such as dimensions, mass, center of mass, wheel damping etc. For the driving simulator it is used in a way that the car physics is only calculated on the master PC which is connected to the car mockup. The movements of the car representation are then used to move the 3D model of the ego car and also the representation of the CAVE in the virtual world. That way test drivers can move through the virtual world similarly to a real car and also step out of the mockup and walk around the car and explore the close vicinity (limited by the dimensions of the CAVE) of it as depicted in Fig. 5.8.

5.3.3 Integration of Driving and Traffic Simulation

Another goal that was previously defined is the integration of a realistic simulation for the behavior of other cars in the environment. Implementing a high-performance and exhaustive traffic simulation from scratch was not a feasible option for this project. In order to have full access to the traffic simulation for further enhancements the open source

simulator Simulation of Urban Mobility (SUMO) developed by the German Aerospace Center DLR was chosen (see also [Kra+12]). It is a microscopic traffic simulator that is used widely in academia and has gained a considerable set of features over the years. There are import filters for a large variety of different street network definition standards and especially data from Open Street Map (www.openstreetmap.org) which provides free map data including the road geometry. Another valuable property of SUMO is the abstraction of Car Following Models which can easily be interchanged.

Time synchronization of driving and traffic simulation SUMO is originally an offline simulation meaning that it is usually not calculating traffic movements in real time. If the provided set of configuration files defines a simple network, the simulation runs considerably faster that real time, but can also be slower than real time for large scenarios. Because the driving simulator works with real time conditions by definition (the user can only interact in real time) it is necessary to couple both simulations. In this case Virtools defines the simulation speed as it runs in real time.

It provides the Traffic Control Interface (TraCI) connection for interacting with the simulation at runtime which is essential if the two simulations shall be coupled regarding their time base. When SUMO is configured to use the TraCI connection it opens a TCP socket server and waits for an incoming connection after all configuration files have been loaded. Then the process starts as depicted in Fig. 5.9 where Virtools is started after SUMO is already waiting. When the user plays the composition the SUMO Simulation Manager is started and the simulation time counter starts running causing t_{virtools} to start at 0 s. After an unknown time amount t_{offset} the Manager connects to SUMO, issues the first data subscriptions and initiates a simulation step.

Subscriptions are a concept in SUMO to streamline the communication over TraCI. This is done by defining a subscription of certain parameters for all desired vehicles and a defined time interval. When a simulation step is triggered by Virtools the acknowledgment from SUMO contains the data for all subscriptions. This way the needed data does not need to be requested for every time step causing a significant communication overhead.

The traffic simulation uses a fixed time step size which is also the time resolution for simulation step triggered by Virtools. In contrast the length of a frame is basically determined by the desired frame rate but can also quickly increase in case of a performance bottleneck. This implies a variable and non-predictable frame duration which needs to be taken into account for the synchronization. So the SUMO Manager takes the last frame duration of Virtools and triggers a simulation step of this length in the traffic simulation. This way a delay for the time synchronization of one Virtools frame is introduced which can be neglected for high frame rates.

In SUMO the time step size should be chosen smaller than the expected frame duration in Virtools, but even then the desired step length can never be met exactly. As a consequence the driving simulator must always request the actual simulation time in the traffic simulation and initiate a simulation step only if the Virtools simulation time is more than one SUMO time step size ahead. This synchronization technique is self regulating, but only if it is ensured that SUMO is able to calculate the scenario in real time or faster. Otherwise it
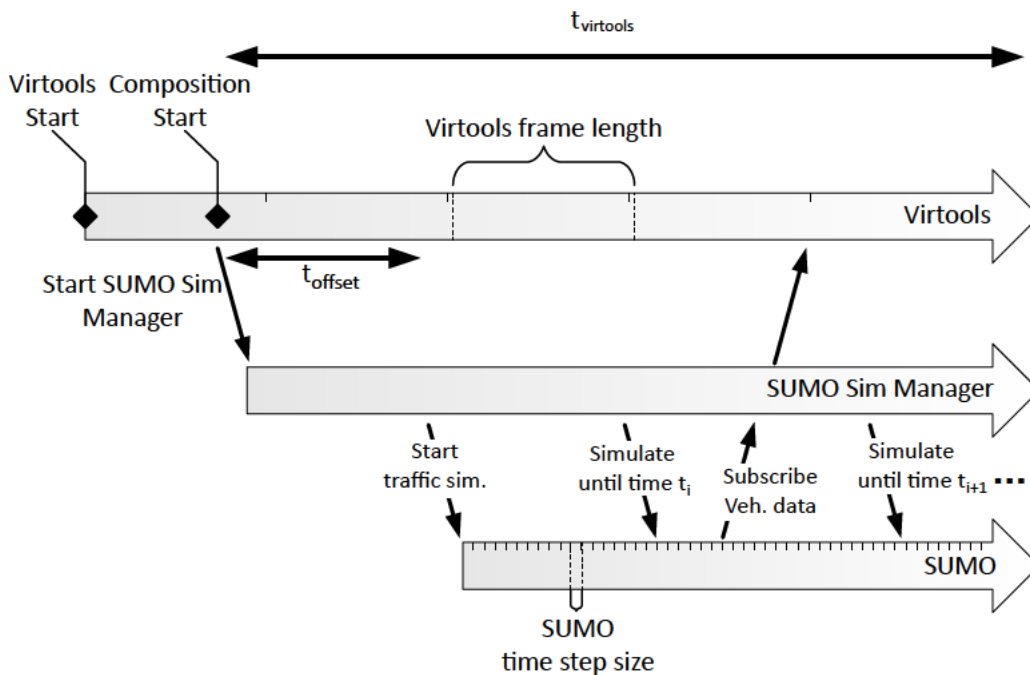
Figure 5.9: Synchronization scheme between Virtools and SUMO. Virtools acts as the master controlling real time conditions to which the number of simulation steps in SUMO is synchronized.

could happen that it never "catches up" causing the two applications to run increasingly asynchronous.

Data buffering in the SUMO Sim Manager   By default only a very limited set of parameters like speed, position etc. are subscribed from SUMO to move vehicles correctly. The Manager therefore acts as a buffer if several Building Blocks request the same data set which is then directly provided by it. Otherwise every request by a BB would in turn cause a request towards SUMO which can be a performance bottleneck especially with a high number of vehicles (more than 50). If parameters like fuel consumption, emissions etc. are needed these subscriptions are added dynamically. Such requests can originate from Building Blocks implementing an assistance function or simply the "Data Logger" (see Fig. 5.10) to record experimental data.

Movement distribution in the cluster   Now that the information about traffic movement is available in real time in Virtools, this must be used to move 3D representations of the vehicles according to it. These 3D objects must be loaded and instantiated at runtime because it potentially cannot be determined beforehand which vehicle types will be present at which quantities. Usually this is not a problem on a single machine setup because Virtools offers the possibility to load assets at runtime. But the cluster distribution mechanism only
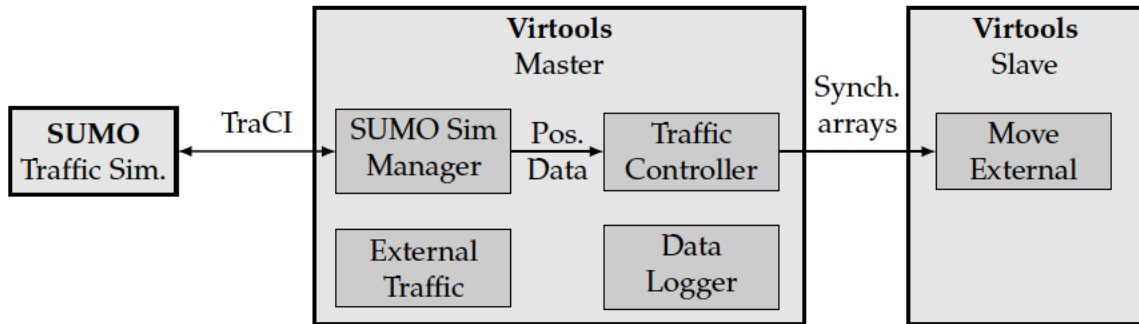
Figure 5.10: Architecture for synchronizing the traffic movement in a cluster environment. Only the master communicates directly with SUMO, the slaves only follow the position changes and creation/deletion of vehicles controlled by shared arrays.

works reliably in case of objects already existing from the beginning of the execution of a composition.

This is caused by the fact that the distribution mechanism uses the automatically generated object IDs to identify the objects. In the very likely case that the composition on the master contains a different number of 3D objects than the clients, these IDs will be different between the hosts. A solution to this is the usage of several array objects already present at design time of which the synchronized content controls the traffic. The following synchronized arrays are used:

- List of objects to be added to the scene:
  All vehicles that shall be added to the scene in the next frame are listed here. It contains an ID generated by the Master and the vehicle type.

- List of objects to be deleted:
  Vehicles which shall be removed from the scene in the next frame. Only the previously assigned ID is necessary.

- Positions and rotations of all vehicles:
  Here all the movements of the SUMO vehicles are synchronized. The array contains the ID, position and rotation of each vehicle to be moved.

Additionally each host uses a local array to store the relationship between the local ID of a 3D object and the ID used by the Master for synchronization. To optimize the computational effort for creating a new car instance the object is not loaded from an external file at runtime but each host creates one instance of each vehicle type at the beginning of the simulation and hides these prototype objects. If a new instance is needed a copy of the prototype object is created with a unique ID which is stored together with the related global ID in the local array. This approach is more efficient because the process of loading a file, parsing and building a 3D object is not necessary. The pre-loading is managed by the "External Traffic" BB in Fig. 5.10 while transferring the movement data from the Manager to the synchronization arrays is done by the "Traffic Controller" block.

The last step for a distributed traffic visualization is the animation of the virtual car models. SUMO only provides the position and rotation of the car, where the position can

change discontinuously because SUMO makes discrete switches when changing lanes. If the test drivers in the simulator are close to the virtual traffic (e.g. waiting at a traffic light) they can closely examine the movements of the other cars. So it is necessary that the car position and rotation are interpolated linearly (due to performance reasons), wheel rotations are calculated based on the movement and the steering angle of the front wheels is adjusted. In the case of a lane change an interpolation is calculated based on a sine wave and a duration of two seconds.

Representation of the ego vehicle in the traffic simulation   With the architecture presented above the ego car and the simulated traffic from SUMO can already coexist in the same 3D environment so the test drivers can react to the other vehicles. For a realistic interaction (and not just reaction of the human driver) the loop must be closed and the ego vehicle must also be represented in SUMO as proposed by Punzo et al. in [PC11].

To achieve this a Building Block which is handling the ego vehicle issues a command via TraCI to add a new vehicle to the SUMO simulation. Then the new vehicle can be moved to arbitrary points on the road network, the only limitation is that the desired position is on the route that is assigned to the vehicle. The main issue related to this approach is that SUMO does not use Cartesian coordinates for positioning a vehicle but a combination of edge, lane and distance from the beginning of the edge.

For this reason the Virtools Building Block must do this conversion for which it needs the geometry of the used road network. This means that the network must also be loaded by Virtools at the beginning of the simulation. During the simulation the 3D position of the ego vehicle must be mapped to the closest position on the SUMO network. This is done for every frame and can be accelerated by using an appropriate network representation and the knowledge of the previous lane. Like that the starting point for the search algorithm can be selected advantageous for a quick result.

The proposed approach has been tested thoroughly and produced the desired result of the other vehicles reacting to the ego car. A possible performance improvement could be a reduced communication overhead by transmitting the speed so messages only occur for e.g. lane or speed changes.

5.3.4   Scene Generation with the CityEngine

One of the declared requirements for the driving simulator is an efficient way to generate the 3D environment. This must be possible in an at least partially automated way while allowing the definition of details if desired. Also there is a firm prerequisite that the generation process of the 3D content can be aligned to the scenario definition in the traffic simulation. The CityEngine by ESRI (see [PM01]) provides all this functionality although it was originally designed to be used by Geographic Information System (GIS) experts and city planners. It offers the possibility to import the current structure of a city or district and supports a meaningful projection of the development in the future. Recent developments also made it interesting for game developers or movie makers to use it for city and landscape generation at larger scales.
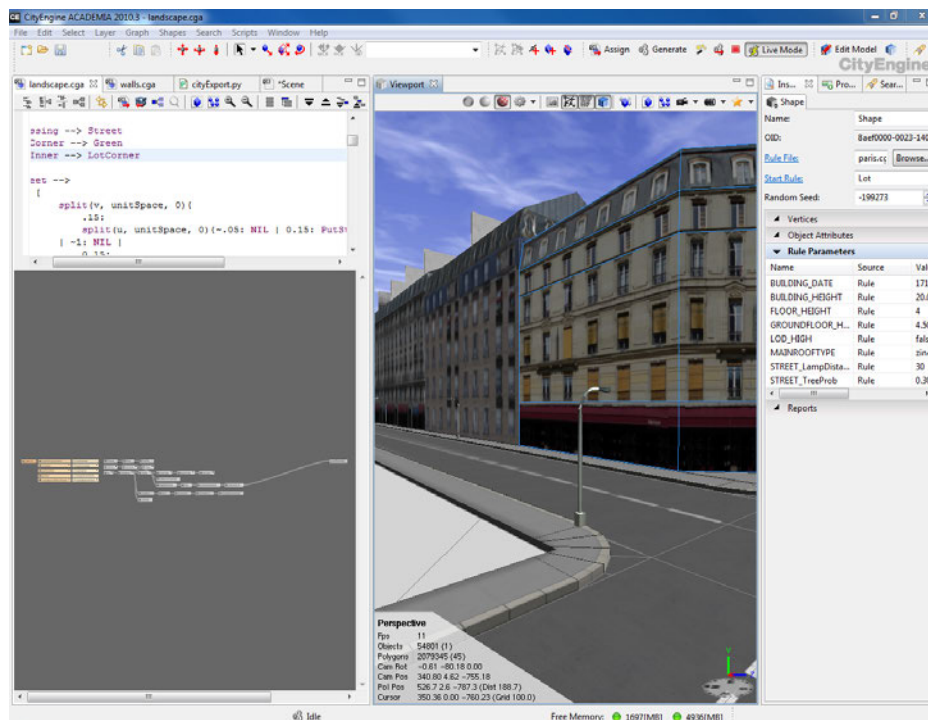
Figure 5.11: Screenshot of the procedural landscape generator CityEngine. The top left area shows the text based rule file editor, below is the graphical version. The center area shows a 3D preview, in the right column all parameters are displayed.

Process of geometry generation   Its specialty is the procedural generation of 3D geometry, especially architecture. This process starts from a street network which can gradually grow with the city and continues by adding buildings in the lots that are defined by the street pattern. After that the actual 3D models can be generated based on further rules for 3D modeling. The number of lanes is for example set automatically based on the area type but can also be adjusted later by the user. The same applies to the buildings where the basic building type is determined by the position in the city. The ground plan is determined by the lot which is aligned to the streets and the final shape is derived by gradually refining the geometry starting from the bounding geometry.

Both the street network and the building geometry are based on Lindenmayer - systems (see [Lin68]) which were originally developed to describe the fractal growth of plants. The same theory can be applied for various applications and is widely used in the CityEngine. The main difference here is a modification that allows the definition of local constraints and global goals in order to control the behavior e.g. at the shore of a lake or the influence of a city's height profile.

Also there is always a certain random factor included which means that some details of a building might change if it is generated again. But even then the ground plan and the basic building type will stay the same. Besides modeling cities it is possible to define arbitrary landscapes as long as they can be defined with a rule set for the CityEngine.
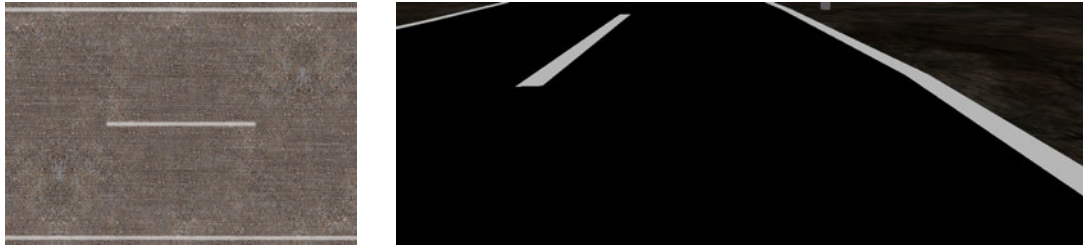
Figure 5.12: Examples of road surface textures with high (left image) and low (right image) contrast. The image on the right is an example of the previous driving simulator of the Institute for Human-Machine-Communication. In the new version speed perception is improved to generate more realistic experimental results.

Street network improvement and export When the 3D model of a street is generated 2D textures are used to define the appearance of the road surface. Because the CityEngine is intended to be used by architects or comparable professions who mostly inspect the scenery from a larger distance, the textures shipped with the software usually have a low resolution. This is an advantage when the scene shall be rendered where short computation times are desired. In contrast to this a driver in the simulator can step out of his virtual vehicle and inspect his surroundings and views the road surface from a distance of usually less than 2m. For this case and even more important for a correct speed perception textures with higher resolutions must be applied. Blakemore et al. suggest in [BS00] that the perceived speed directly correlates with the contrast of the road surface. An example of a texture with very high contrast and resolution is depicted in Fig. 5.12 on the left. In this fashion several sets of textures have been assembled to represent new, used and damaged asphalt as well as cobblestone road.

After the whole scene is generated it can be exported to several file formats that are frequently used in 3D modeling programs. During this export it is possible to define a Python script that is executed after the saving process. This script reads the basic geometry information of the street network consisting only of nodes and connecting edges to write it to a XML file that can be read by the SUMO toolchain. In addition to the node positions and the connection definitions the number and width of lanes belonging to an edge are saved in the file. This is important especially for rendering the SUMO controlled traffic so the vehicles are positioned on the correct lane.

5.3.5 Audio Simulation

The last essential component for the driving simulator and especially the achieved immersion and correct speed perception is the sound simulation inside the car cabin. Several sound sources contribute to the acoustical scene as described by Becker-Schweitzer in [Bec08]. As shown in Fig. 5.13 three dominant sources can be identified: the sound generated by the tires, the engine (both air and car body transmission) and the head wind producing sound dependent on the aerodynamic properties of the car. These sources can be generated separately and then mixed in real time by the audio engine.
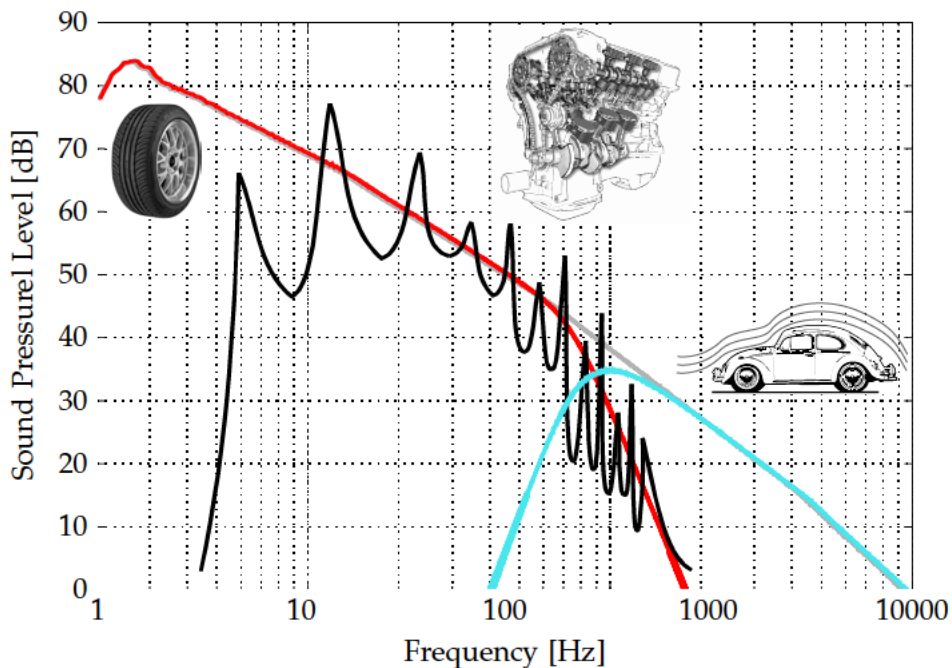
Figure 5.13: Dominant sound sources perceived by the driver. As shown the wheel sound (red plot), engine sound / vibrations (black plot) and the aerodynamic sound components (blue plot) add to the overall impression (based on [Bec08]).

There are several ways to generate these sound sources like physical modeling (see [DKP01]), sample based generation (see [Bri96]) or spectral analysis and synthesis (see [TVK98]). While the approach of physical modeling is a very generic way of sound generation, the application of a driving simulator usually does not require such high versatility. A hybrid approach with offline sample generation based on physical modeling is followed by the St. Petersburg based company Sonory [Son13].

The very basic structure of spectral analysis and synthesis is depicted in Fig. 5.14. In a first step recordings from real engines or physical modeling processes are analyzed using Short Term Fourier Transformation (STFT). This method takes overlapping time windows with a length that is short enough to treat the audio signal as stationary signal within the window (see [TVK98]). To minimize the artifacts caused by windowing (which is equal to a convolution of the windowed signal with a rectangle function with the size of the window) different windowing functions can be applied. A tradeoff must be made between the width of the main lobe of a frequency component representing the achievable frequency resolution and the attenuation of the side lobes caused by windowing.

After that the windowed signal is used as the input of a Fast Fourier Transformation (FFT) turning the time-domain signal into a frequency-domain representation which can then be saved in a database, see also Fig. 5.14 top row. In order to simplify the re-synthesis only dominant parts of the signal can be chosen to generate a time-domain signal again. This can be done by peak picking as described by McAuley et al. in [MQ86] or by a mixed approach of deterministic and stochastic signals as done by Verma et al. in [VLM97]. Then a
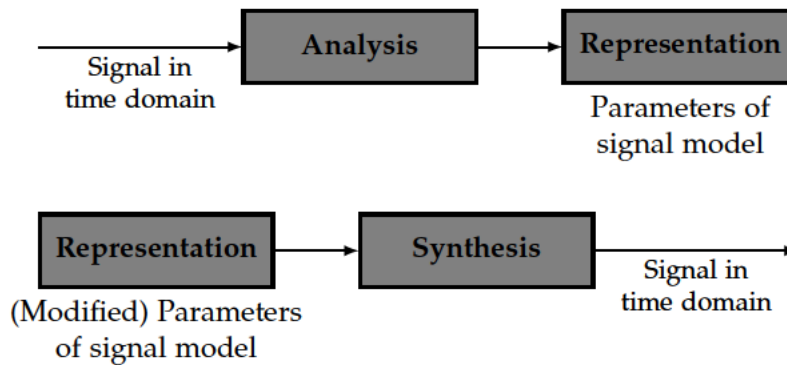
Figure 5.14: Analysis, representation and synthesis of an audio signal. Real sound samples are analyzed and the extracted parameters stored in a database. For a real time application the relevant parameter sets need to be selected and applied for sound re-synthesis.

synthesized signal can be reproduced with the inverse process at runtime based on the data annotated with additional information about the corresponding driving scene or vehicle state.

The sample based approach is known for several years now as also mentioned in [Bri96]. It was used in Samplers for music production first and was then adapted for extension cards of Personal Computers due to its simple implementation compared to the potential tonal qualities. The key features are a reproduction of periodic waveforms, the application of time-domain envelope filters and pitch shifting through variable playback speed. Similar to the spectral modeling technique input recordings from either physical modeling or real sound sources need to be available. These need to be prepared in a way so they can be looped at playback without any artifacts caused by an inappropriate selection of loop points. This can lead to effects like high frequency clicks caused by an unsteady value jump from the end to the beginning of a sample. Also if the length of a sample does not match the perceived dominant frequency unwanted low frequency components can be introduced by the looping process which are not present in the original signal.

Once a wavetable consisting e.g. of the individual samples of a note played on a musical instrument is constructed it also may be necessary to switch between different styles of the note. Examples for this are the sound difference occurring from the onset of a sound ("attack") or the dynamics of playing ("velocity") which requires several wavetables. Each of them is played back via a envelope scaler similar to a variable gain amplifier as seen in Fig. 5.15. The envelope in turn is controlled by timers or other parameters which can be the motor load in the case of engine sounds. Then the weighted outputs of all wavetables are summed which generates the final waveform. The different sound sources and their modeling approach will be described in the following paragraphs.

Engine Sound   The engine sound is a complex conglomerate of tonal, stochastic and transient components that also vary depending on the motor speed, torque load and several other parameters. As the wavetable approach is both simple and able to capture even complex sounds as long as they are repetitive, it was chosen for this sound source. The
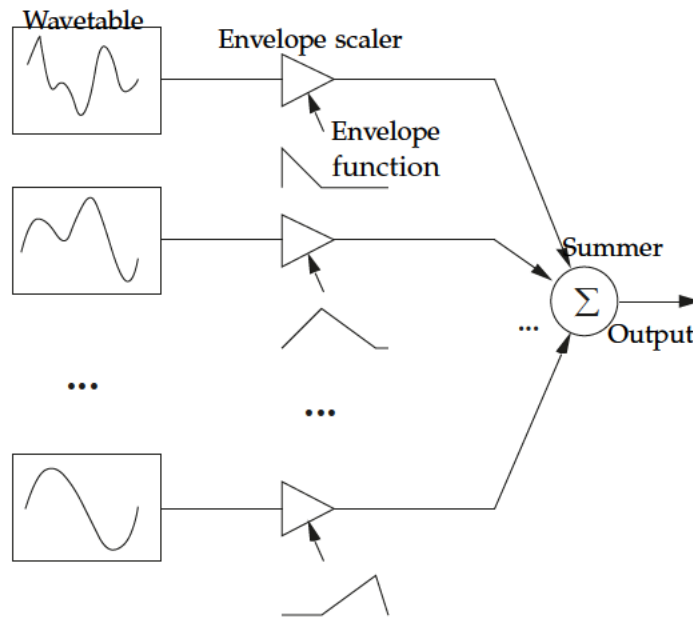
Figure 5.15: Mixing several wavetable sources with envelope functions. This can be used for varying sound properties of the same basic sound, e.g. attack and decay sounds of a musical instrument (based on [Bri96]).

dependency of the spectral components on the RPM of the engine is plotted in Fig. 5.16 representing the STFT of an engine ramp up. Diagonal lines represent motor orders which are multiples of the RPM value and therefore linearly dependent on it. As the coloring of each motor order changes over time this means that the spectral composition changes and ultimately the perceived sound. This also means that it is not feasible to record the engine sound at a single speed and pitch shift the sample over the whole required RPM range.

Similarly the frequency components also change depending on the engine load, see Fig. 5.17. This effect can be experienced when a driver quickly changes the accelerator pedal position and the engine speed follows only with some delay due to the mechanically coupled vehicle inertia.

The two parameters RPM and load have the strongest influence on the perceived engine sound and shall be the input parameters for the engine sound simulation. In the sample based approach presented here these parameters must be used to determine the sample to be used. One problem arises from the fact that the original sounds have been recorded with a continuously increasing motor speed at distinct load levels. In order to generate the sound of a constant motor speed for an unknown time interval it is not possible to directly take the samples from the original recording. Instead a gradual pitch shifting must be applied to compensate the increasing RPM number so the linear change is converted into a stepwise change as shown in Fig. 5.18. Here the whole recording was divided into 15 segments determining the preliminary loop points.

When the audio segments are played back by the audio engine of the driving simulator they should overlap to a certain extent to minimize audible artifacts originating from
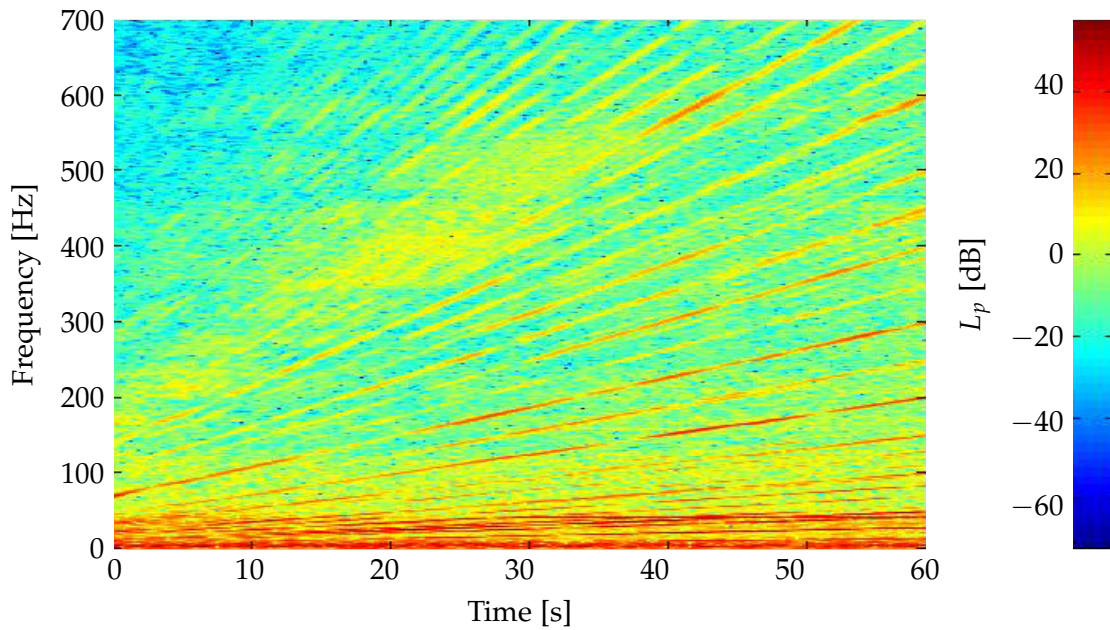
Figure 5.16: Varying spectral components during engine RPM ramp up. While engine order frequencies increase according to the RPM, their levels vary over the RPM range (based on [Sch08]).
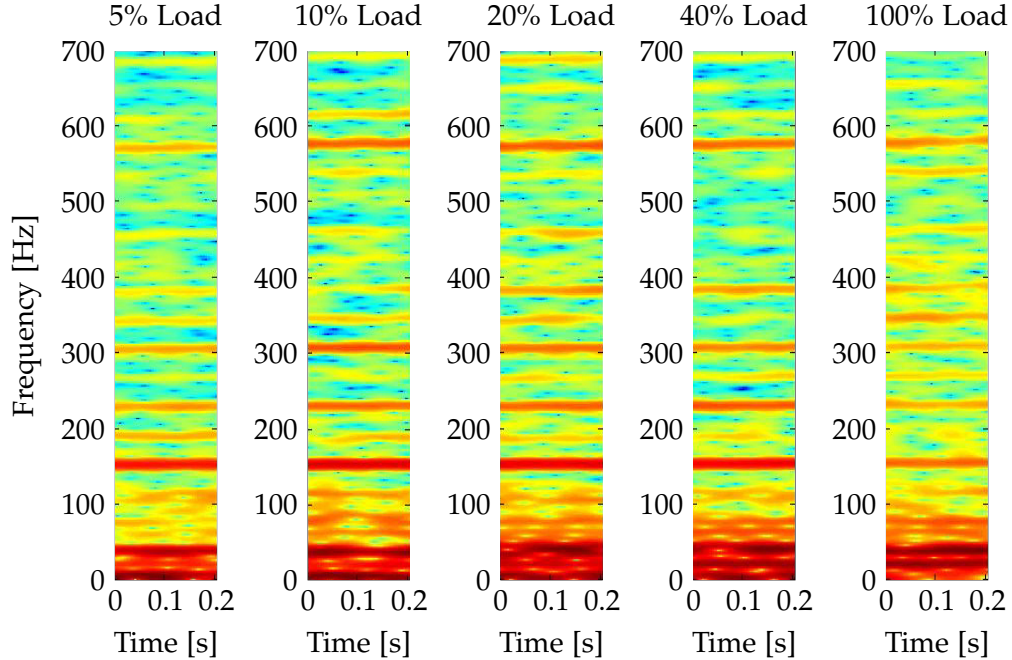

Figure 5.17: Varying spectral components depending on the engine load. The engine speed is always 3000 s^{-1} for all plots (based on [Sch08]).

107
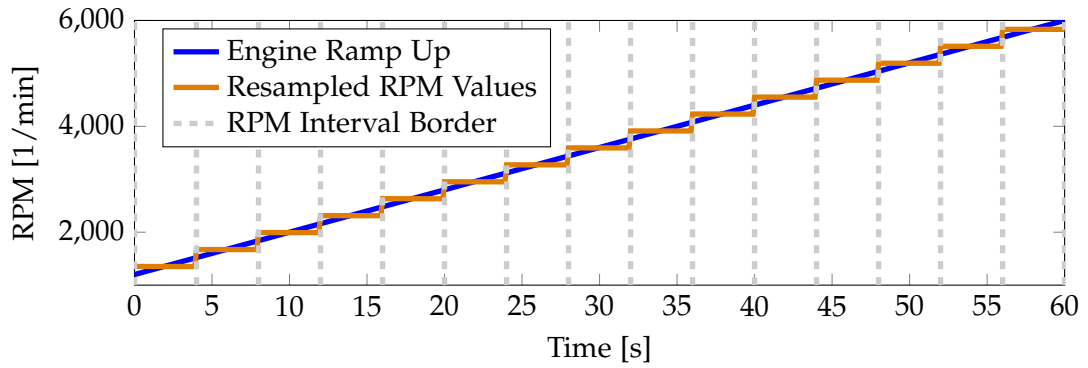
Figure 5.18: Engine RPM ramp up and resampling scheme for sound generation. The available RPM range is divided into intervals of equal length and the sound data is being resampled to a constant RPM value derived from the middle of each interval.

switching between two segments. Here the overlap was chosen to be 50% (25% at each end) and cross-fading is applied in this region by the audio engine. Consequently the previous loop points are divided into two new point shifted in opposite directions from the original one.

It was already mentioned that the loop points must be carefully chosen in order to prevent the generation of sound artifacts due to the looping technique. One prerequisite for a loop point is to chose a zero crossing. The next one is a comparable slope, at least the sign of the slope must be identical. Like that several candidates for loop points can be determined and the following procedures will choose one of them. In the current implementation all 15 segments have approximately the same length which can cause looping artifacts with mainly low frequency components if the number of engine rotations is not integer. To accomplish this it is necessary to analyze the waveform in order to reconstruct the border and position of full rotations. This can be achieved with the autocorrelation function $\Phi(t)$ in Eq. 5.2 which reveals periodic components (self similarity) in a time-domain signal $x(t)$.

$$\Phi(t) = \int_{-\infty}^{\infty} x(\tau) \cdot x(t + \tau) d\tau \tag{5.2}$$

Then the length of a recurring waveform (e.g. from a complete engine revolution) can be determined by the distance of two local maxima. The distance of two loop points should then be an integer multiple of the maximum distance.

When the exact positions of the loop points are determined the segments can be pitch shifted relative to the center of the segment. Now it is possible to loop the segment with constant engine speed and not noticeable sound character changes if the segments are short enough. The sound engine FMOD (see [FIR13]) used for this implementation can then apply real time pitch shifting to produce the related sound for any required RPM value.

As mentioned before the second input parameter for the segment selection is the engine load. This value can either be obtained directly by the vehicle physics simulation or be estimated with the accelerator pedal position and the RPM value. If the load value is not

available the equation 5.3 can be used for an estimation.

$$\text{Load} = \frac{\text{Acc} \cdot (\text{RPM}_{max} - \text{RPM}_{min}) - \text{RPM}_{cur}}{\text{RPM}_{max} - \text{RPM}_{min}} \tag{5.3}$$

Here Acc represents the accelerator pedal position normalized to a range of [0...1], RPM_{max} is the maximum RPM of the engine, RPM_{min} the idle RPM value and RPM_{cur} the current one. The idea is to make a linear assignment of a RPM value to a certain accelerator pedal position and derive the load from the difference to the current RPM. The load value is then limited to a range of [-1...1], where a positive value represents an acceleration torque.

Similar to the segments representing different RPM ranges the load can also be segmented in several levels. The resulting minimum of two load levels already yields usable results, sound banks with five levels provide a decent quality. Again there is no hard switching between the levels but the sounds are blended by cross-fading in the same way as for the RPM segments. All in all there are 75 different sound samples in the case of 15 RPM segments and 5 load levels.

Tire Sound   While the sound produced by the engine is usually recorded in a laboratory environment allowing precise load and RPM control, the sound of the tires rolling over different road surfaces needs to be recorded in the field. For this task a passenger vehicle is instrumented with an On Board Diagnosis (OBD) interface to record the precise speed values in real time. Additionally a large-diaphragm microphone captured the interior noise of the vehicle. In this setup there will inevitably also be engine and wind noises which must be minimized. To achieve this the car is accelerated to the highest possible / allowed speed and the neutral gear is selected during the experiment to minimize the noise generated by the engine. Then the vehicle decelerates by various friction sources such as tire friction or aerodynamic drag. Some of these parameters depend on the speed in a non-linear way such as the aerodynamic drag as defined in Eq. 5.4.

$$F_d = c_d \cdot A \cdot \frac{1}{2}\rho v^2 \tag{5.4}$$

with c_d : drag coefficient A : cross-sectional area

ρ : fluid density v : speed

Lewis proposes a logarithmic dependency of external wind noise on speed in [Lew73]. As the engine noise is increasingly damped (equal annoyance of engine and wind noise at 100 mph $\approx$ 161 km/h in 1983, but only 60 mph $\approx$ 97 km/h in 1992 as stated by Hucho et al. in [HS93]) the wind contribution increases its ratio. Because wind noise can be generated by a filtered noise source in real time and tire sound recordings have a limited upper speed limit these sources are modeled independently.

Different than with the controlled linear RPM ramp-up it is important to have the current speed value available for the whole sound recording. A single notebook PC records the OBD data and the sound simultaneously to minimize the time delay between the two data sets. As the speed is updated less frequently than the sound it needs to be upsampled and interpolated linearly. The following procedure is similar to the one applied for the engine noise. The only differences are the nonlinear pitch shifting based on the recorded
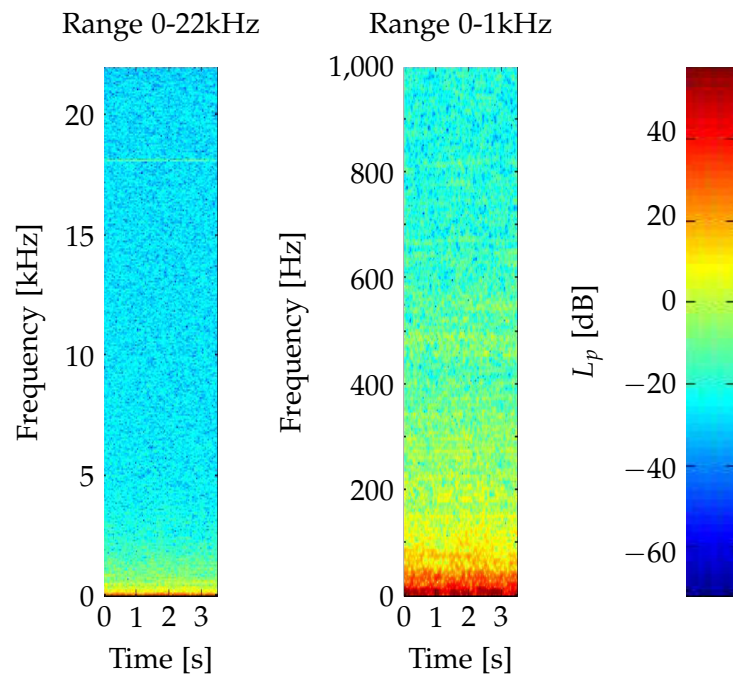
Figure 5.19: Spectrum of wind noise inside the car cabin. The left plot shows the range of 0 - 22 kHz, the right one 0 - 1 kHz representing a similar spectrum to a lowpass filtered white noise.

speed values and that there is no comparable element to the different load levels. As a result the tire sound simulation only depends on the speed and the chosen road surface.

Here the surface types new, old and damaged asphalt as well as cobblestone were implemented. The information about the current surface type must be provided by the 3D engine which can derive this information from the street network definition.

Wind Noise The contribution of the wind noise to the overall soundscape is modeled in a different way than the previous sound sources which were based on pre-recorded samples. Figure 5.19 shows the spectrogram for a range of 0 - 22 kHz on the left and a detailed view for 0 - 1 kHz in the right side. This shows that there are no distinct amplitude peaks and especially above 2 kHz the levels are evenly distributed. For a realtime sound simulation it is desirable to use sources that are by definition continuous to avoid problems arising from looping and sample switching.

In order to generate the wind noise a Digital Signal Processor (DSP) is used in the FMOD engine (see [FIR13]) to generate white noise. This signal is then fed into a variable lowpass filter and the final signal gain is also dynamically assigned. Contrary to the proposal of Lewis in [Lew73] of a logarithmic relation between speed and external wind noise, the law for aerodynamic drag (see Eq. 5.4) suggests a quadratic relation which has shown convincing results in the driving simulator. The constant Vol_0 defines a fixed coefficient to

control the relative level of the different sound sources.

$$Vol = Vol_0 \cdot \left(\frac{Speed}{200} \right)^2 \qquad Vol \in [0...1] \tag{5.5}$$

$$f_{cut} = 800 + Vol \cdot 100 \tag{5.6}$$

The parameter f_{cut} determines the cutoff frequency of the first-order Butterworth lowpass filter of the noise generator. Like that the wind noise contains more high frequencies at higher speeds, for a Vol_0 of 0.3 the f_{cut} ranges from 800 Hz to 830 Hz with a speed range of 0 - 200 km/h.

5.4 Evaluation of Spatial Perception

After the driving simulator is established it can be used for further experiments in the area of anticipatory driver assistance. Referring to the initial goal this immersive and most notably stereoscopic simulator is intended to produce a high Sense Of Presence (SOP) which includes the ability to anticipate events in a virtual environment (see also the questionnaire by Witmer et al. in [WS98]). The intention of improving the SOP and providing high quality spatial cues for natural anticipation shall now be evaluated in a driving simulator experiment. In this experiment drivers shall follow another car at a certain distance, keep a certain speed and judge their own performance in these tasks.

5.4.1 Experiment Design

The experiment shall investigate the influence of a stereoscopic presentation of the driving scene on the perception of distances and ego speed. To achieve this the test drivers must accomplish the following tasks with and without stereoscopy (here the Interpupillary Distance (IPD) is set to zero):

- Follow for 650 m with a distance of 70 m (track segment 1)

- Drive for 600 m with a speed of 50 km/h (track segment 2)

- Drive for 500 m with a speed of 30 km/h (track segment 3)

- Follow for 900 m with a distance of 20 m (track segment 4)

Before the actual tasks started every driver makes a short test drive with stereoscopy to acclimate to the simulator setting and to determine whether he is prone to SAS. This is the only time when the test drivers can compare their actual speed as shown by the tachometer in the virtual instrument cluster with their own speed perception. In all other cases the tachometer and RPM needles are turned off so this can only be derived by the environment perception and the sound simulation.

Figure 5.20 depicts the network topology as it was used in SUMO to program the behavior of the leading vehicle. It follows the route marked red which has only few connections to adjacent roads in order to force the routing algorithm to stay on the desired
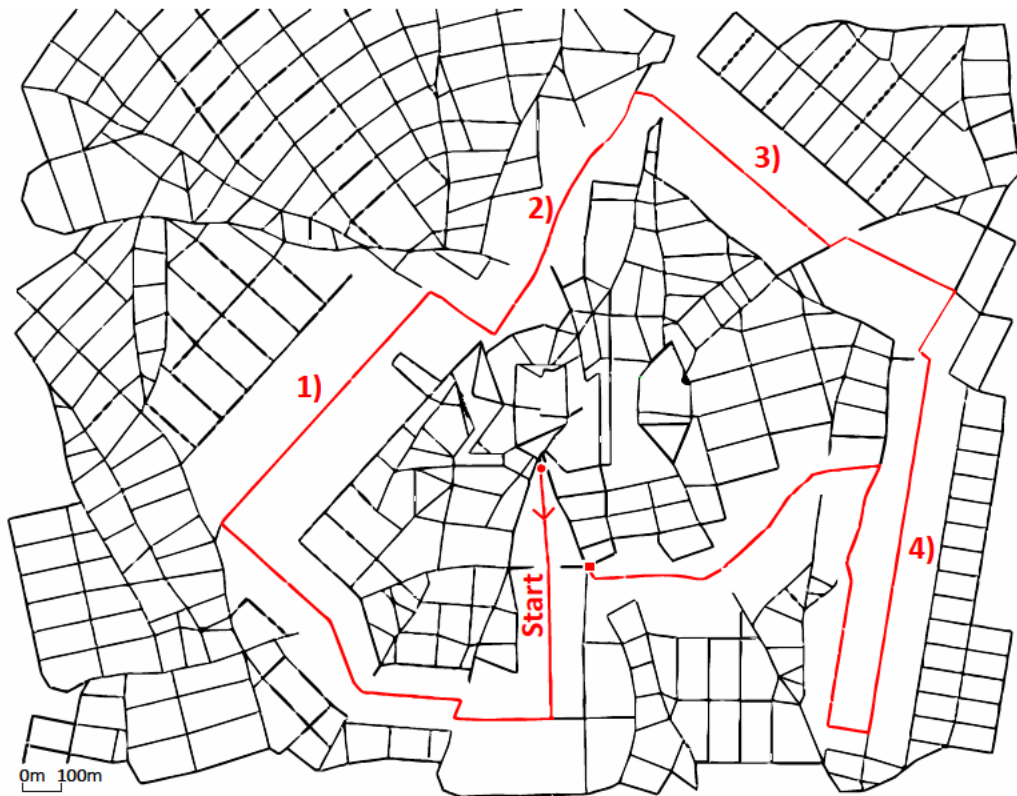
Figure 5.20: Street network used for the SUMO controlled vehicle in the distance and ego speed evaluation. The red line shows the route for the leading vehicle which is divided into four segments with different tasks assigned.

track. The network model used in the CityEngine has more crossings and connections with the surrounding network for a more realistic road geometry.

The order in which the stereoscopic and monoscopic tasks had to be accomplished is alternated for every test driver to minimize the impact of learning effects. During the experiment all tasks are communicated to the driver with an iconic representation in the digital instrument cluster. This is implemented using standard traffic symbols that are accompanied by a gong sound to make sure that they are registered by the driver. That way every participant drives the track twice and answers a questionnaire containing the following points after both stereo configurations:

- How realistic was the simulation in general?   Not at all $\longleftrightarrow$ Perfect

- How would you judge the estimation of speed?   Very simple $\longleftrightarrow$ Very difficult

- How would you judge the estimation of distance?   Very simple $\longleftrightarrow$ Very difficult

- Did you experience vertigo?   Not at all $\longleftrightarrow$ Very much

The rating for each question is made on a five position scale which allows a neutral choice. Additionally the drivers had the opportunity to give feedback about positive and negative aspects of the simulation run.
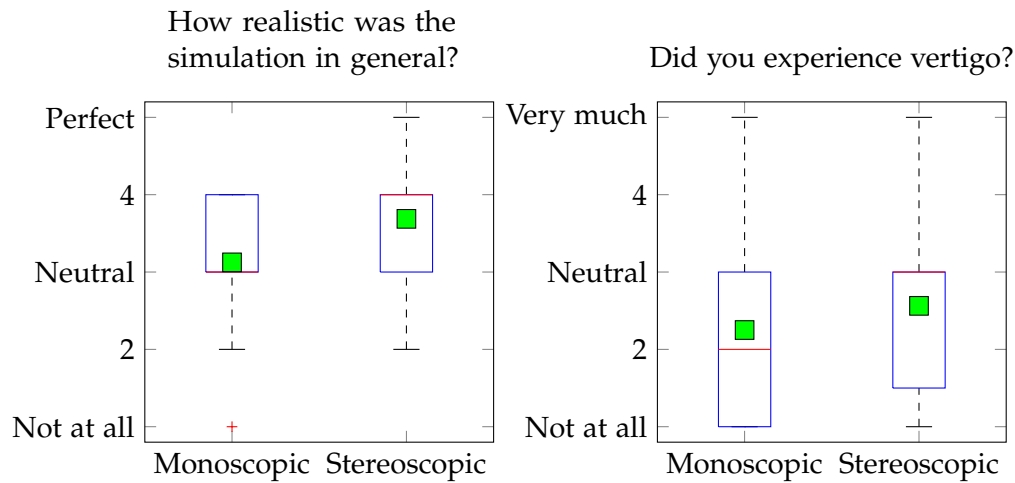
Figure 5.21: Results of the driving simulator evaluation: Realistic presentation and SAS. The red lines represent the median, the green squares the mean values.

5.4.2 Results and Discussion

The evaluation was conducted with 18 test persons (16 male, 2 female) of which two could not finish the experiment completely due to the SAS and were left out of the analysis. The average age was 25.7 years, 60% stated to drive less than 10000 km per year.

Questionnaire Figure 5.21 shows the results of question 1 and 4 which deal with the overall impression of the simulator. For both the question about realistic presentation and SAS (the wording "vertigo" was chosen for simpler understanding by the test persons) the interquartile ranges overlap widely. Although the median values (the red lines) differ in both cases by 1, the mean values (green squares) are closer to each other and the Mann-Whitney U Test (see [MW47]) showed a rejection of the Null hypothesis at a level of p = 0.054 for the question about realistic presentation and p = 0.423 for the experienced SAS. Still the mean values show a tendency in both cases suggesting that the simulation is more realistic with stereoscopic presentation but also the likelihood of the SAS is higher.

Comparable results can be seen in Fig. 5.22 for the ease of judging speed or distance. The interquartile ranges overlap to a large extent, the medians are nearly equal for the speed case and equal in the distance case. For both questions the Mann-Whitney U Test shows no statistically significant difference (p = 0.135 for the speed, p = 0.400 for the distance estimation). Again the mean values have a positive tendency for the stereoscopic configuration for both measures.

Driving Behavior Analysis The analysis of driver behavior is controlled by trigger elements positioned on the virtual road. As shown in Fig. 5.23 drivers needed a certain settling time to adapt to the new task which is represented by the large speed overshoot at the 5 s position. To compensate this the first and last quarter of the measurement range are neglected so the derived metrics are not disturbed by such effects. In the figure the red line
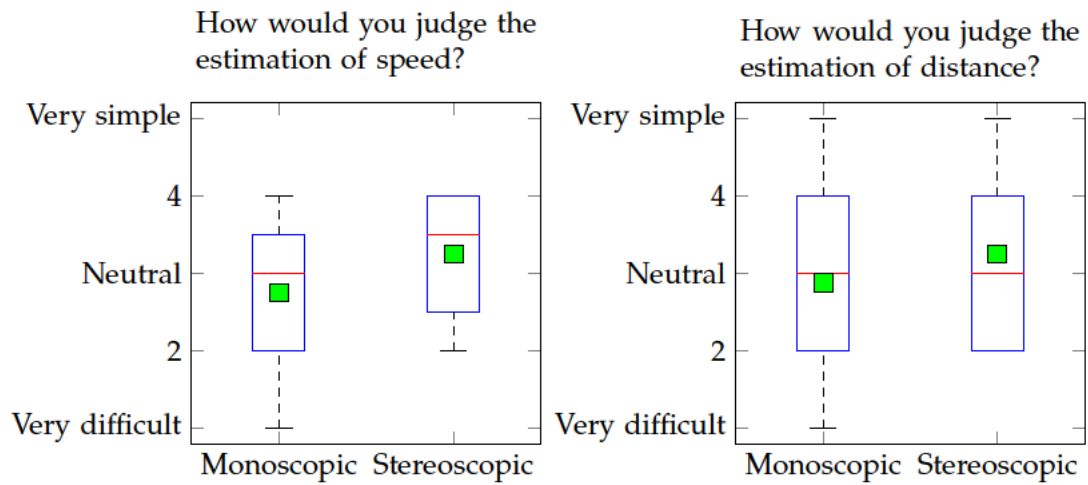
Figure 5.22: Results of the driving simulator evaluation: Ease of speed and distance judgment. The red lines represent the median, the green squares the mean values.

represents the targeted speed of 50 km/h while the green one at ca. 71.6 km/h indicates the mean speed driven in the trimmed measurement range.

For each driver the average speed and distance to the leading vehicle is calculated for the center 50% of the measurement range. Then the target value of the respective track segment is subtracted and the resulting deviation from the intended value is used to produce the box plots in Fig. 5.24 and Fig. 5.25. As the plots for the distance estimation in Fig. 5.24 show the interquartile ranges overlap to a large extent. The Mann-Whitney U Test for the 70 m distance task shows no significant difference ($p = 0.337$) as well as for the 20 m distance task with $p = 0.418$. For both distances the interquartile range of the monoscopic
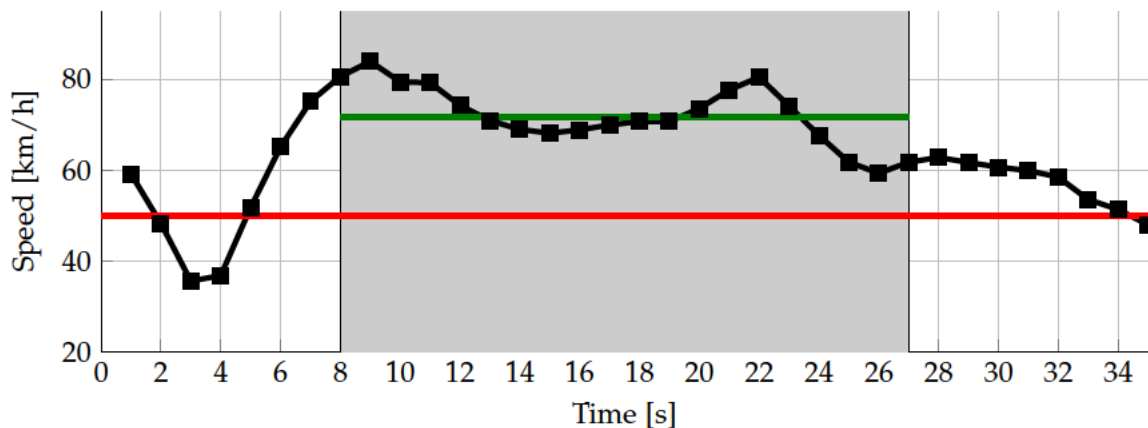
Figure 5.23: Example result of the speed judgment experiment in the stereoscopic driving simulator. The red line indicates the proposed speed, the green line the average within the measurement range, the black line the actual speed and the gray rectangle the center 50% representing the measurement range.

Metric	Distance 70 m (2D/3D)	Distance 20 m (2D/3D)
Mean error	47.52 m / 22.03 m	22.83 m / 21.29 m
Standard dev.	67.19 m / 33.90 m	32.89 m / 17.73 m
Rel. mean error	67.9% / 31.5%	114% / 106%
Median error	29.46 m / 16.48 m	13.87 m / 18.97 m

Table 5.2: Metrics for distance estimation in the driving simulator experiment

task is larger and the mean value (green squares) is higher by tendency as well as the absolute error. In the majority the test drivers underestimated the distances causing them to actually choose higher distances. Notably the maximum values and the outliers showed only approximately half of the error in the stereoscopic case.

Still the mean error is considerably higher than in a real setting as evaluated by Taieb-Maimon et al. in [TS01]. They measured a distance estimation error of ca. 2.77 m at a speed of 50 km/h which linearly increases with speed.

For the speed estimation experiments the relative errors are much lower than for distance estimation, see Tab. 5.2 and Tab. 5.3 for comparison. In the 50 km/h segment the relative errors in both the monoscopic and the stereoscopic case are ca. 20% and in the 30 km/h segment ca. 30%. The absolute errors are always in a range of ca. 6 - 10 km/h, see Tab. 5.3. Regarding the box plot in Fig. 5.25 the interquartile ranges overlap almost completely suggesting no statistically significant difference between the variants. This is confirmed by the Mann-Whitney U Test with p = 0.836 for the 50 km/h segment and p = 0.585 for the 30 km/h segment. Both the median and mean values have a tendency to be higher in the stereoscopic case, but this is no reliable effect due to the low H_0 rejection probability and the small sample size.

If we compare especially the ego speed judgments with results obtained by Evans in [Eva70] the estimation errors are in a close proximity with real driving. Evans chose a different approach by having a driver set a certain speed in a real vehicle while the test person shall judge the speed without being able to look at the tachometer. In order to compare the results we must add the mean error in the driving simulator experiment to the intended speed which then results in the actually driven speed. So in the 50 km/h trial the driven speed in the stereoscopic case would be 60.04 km/h while it is perceived like 50 km/h by the test drivers. The driven speed of 60.04 km/h equals 37.32 mph and the standard deviation of 11.09 km/h is equal to 6.89 mph which is between values found by Evans for the measurement speeds of 35 mph and 40 mph.

For the 30 km/h trial (which equals 18.65 mph) the standard deviation was 6.61 km/h in the stereoscopic case (equals 4.11 mph) which is even lower than the value in Evans' evaluations (6.9 mph). These results combined with the tendency of a lower standard deviation in the stereoscopic case show that at least for the speed judgment the simulator produces comparable results to a real world experiment. The low performance for distance judgment could be improved by introducing more visual cues like trees (the experiment took place in a city environment), humans and other objects of known size. In the current configuration the simulator can lead to results that show at least relative validity, with
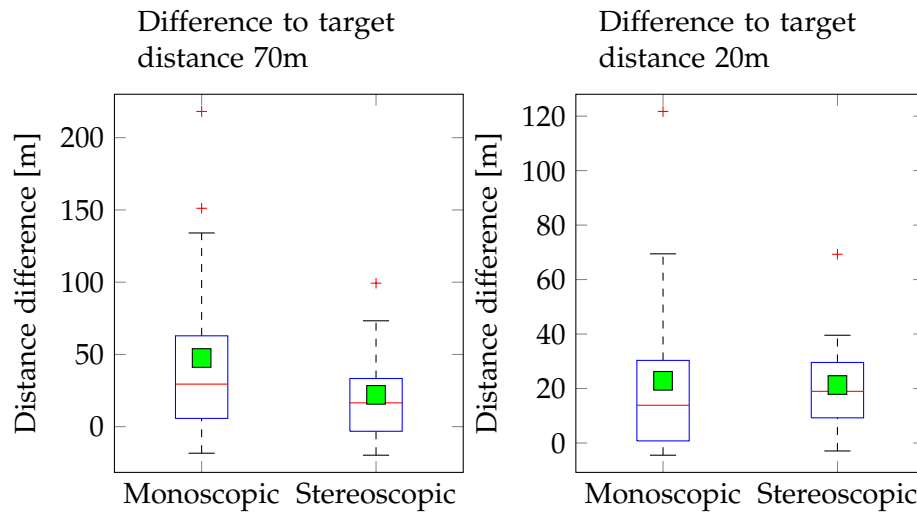
Figure 5.24: Results of the distance estimation in the stereoscopic driving simulator. The plots show the estimation error for the monoscopic and the stereoscopic case. The red lines represent the median, the green squares the mean values.

enhancements regarding the distance estimation with the mentioned measures it could even reach validity for real applications. Besides this it also provides the facilities to generate realistic scenarios based on actual road networks with a high level of detail regarding the 3D modeling. Foreign vehicles are controlled by a proven traffic simulator with the ability to exchange behavior models in a very modular way. Finally the vehicle's interior sound is generated based on realistic samples which improves the quality of speed judgment and the level of immersion. An extension for the sound simulation could be the acoustic representation of surrounding cars to improve the environment perception.

The simulator environment has at this stage the maturity to conduct actual driving simulator studies for evaluating assistance systems. Also it can serve as a basis to collect behavior data that can later be used in driver models to resemble the behavior of assisted and non-assisted drivers.

Metric	Speed 50 km/h (2D/3D)	Speed 30 km/h (2D/3D)
Mean error	9.07 km/h / 10.04 km/h	8.95 km/h / 10.15 km/h
Standard dev.	11.37 km/h / 11.09 km/h	8.06 km/h / 6.61 km/h
Rel. mean error	18.1% / 20.1%	29.8% / 33.8%
Median error	6.61 km/h / 8.46 km/h	7.19 km/h / 10.21 km/h

Table 5.3: Metrics for speed estimation in the driving simulator experiment
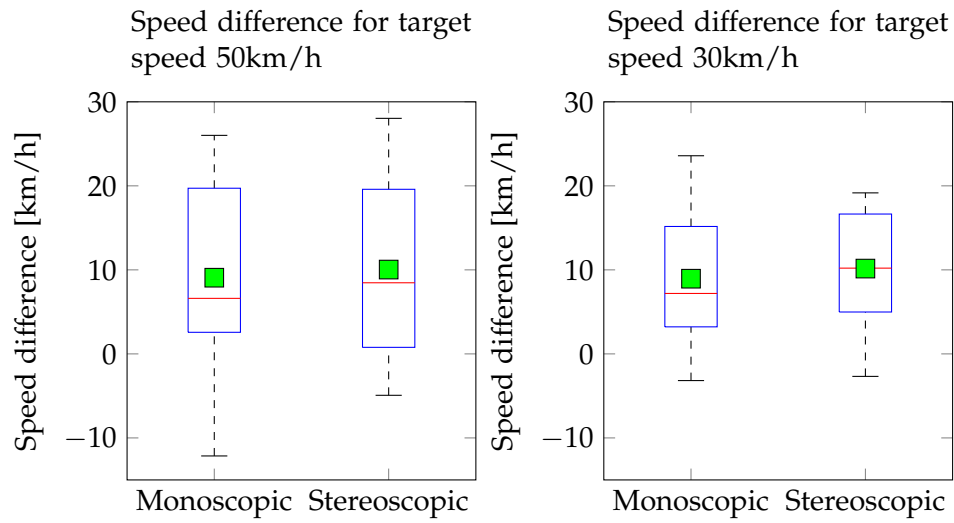
Figure 5.25: Results of the speed estimation in the stereoscopic driving simulator. The plots show the estimation error for the monoscopic and the stereoscopic case. The red lines represent the median, the green squares the mean values.

6

Traffic Simulations

Up to this point all experiments were carried out with a single test person experiencing a certain scenario in a driving simulator. Some of these experiments took up to three hours per person and consequently required a substantial amount of time to be invested. In addition it is also not possible to assess the impact of an assistance system on a larger scale, especially at varying rates of equipped vehicles. If such a question shall be answered, one approach is to connect several identical driving simulators as proposed by Maag et al. in [Maa+12] to have all human test persons drive in the same scenario at the same time. In most cases such experiment setups are limited to a number of simultaneous drivers of less than 10 test persons. While this is already an improvement over single driver setups, the number is still too low for experiments with a target of 100 vehicles or more.
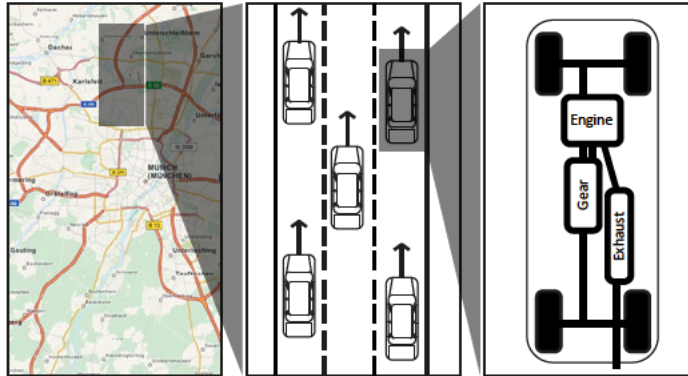
Figure 6.1: Classification of traffic simulations (left to right): macroscopic simulation (network level), microscopic simulation (vehicle level) and submicroscopic simulation (component / driver level)

This option is both not economically feasible and still very time consuming and so a traffic simulation can be a valuable solution to this problem. As also described by Krajzewicz et al. in [KHW02], traffic simulations can be divided into macroscopic, microscopic and submicroscopic simulations depending on the level of detail. Macroscopic simulations model traffic as a continuous flow in a network, similar to liquids running in a pipe network. This allows for the coverage of large areas in which not a single vehicle is of interest but e.g. the identification of potential bottlenecks. In microscopic simulations vehicles are

used as an entity which provides a much more detailed insight on the individual behavior. The SUMO project can be counted to this type of traffic simulations and will be used for experiments later on. Due to the Open Source nature of the program it can also be extended to fulfill the requirements for a submicroscopic simulation like PELOPS (see [Brö10]) which will also be used for experiments. PELOPS also models subsystems of a vehicle like the engine, tires, etc. but also driver perception and reactions on assistance systems. It can be desirable to have very detailed models in order to adapt them in a sophisticated way to the parameters of a simulated scenario. But this usually comes at the cost of computation time which is then the counterpart in the tradeoff especially for real time applications.

Following the above explanations of different simulation types, a microscopic or submicroscopic simuation is needed for assessing the impact of an assistance system. A possible procedure for this could be the recording of driver behavior for different participant groups in a driving simulator. From the resulting data driver models can be parametrized which are able to resemble the different behavior patterns. The main weakness of this approach is its dependency on reliable models resembling the behaviors of assisted and non-assisted drivers as also proposed by Lüßmann et al. in [LS12].

6.1 Lane Change and Car Following Models

Driver behavior models usually contain two sub models that control the final driving actions: a Lane Change Model (LCM) and a Car Following Model (CFM). As suggested by their names the LCM controls lateral vehicle steering while the CFM is responsible for longitudinal control. The basic theory behind the two model types and how they interact shall be described in the following paragraphs.

6.1.1 Lane Change Models

On a road with several lanes the driver needs to decide whether to stay on the current lane or not. Also when he enters a major road from a minor one he needs to assess if it is possible to enter the major road without provoking a dangerous situation for him or other vehicles. This behavior has implications on travel time and fuel consumption for himself as well as the other drivers if they are influenced by his maneuvers. Based on [TK10], the following criteria are usually used:

- Safety Criterion
  A different driver should not be forced to conduct a critical braking maneuver due to one's lane change decision. For a LCM a deceleration threshold must be defined that can be expected of other drivers.

- Incentive Criterion
  The driver will take the actions by which he gains maximum individual advantage. Still the laws of traffic like driving on the rightmost lane or forbidden right hand overtaking must be obeyed. In order to prevent frequent lane changes caused by marginal individual advantages, a threshold must be introduced for the minimum required

advantage. This is also a point where personality (aggressiveness or politeness) can have an influence on the function that determines the potential advantage.

For the above mentioned criteria it can be necessary that the CFM provides an interface to assess the potential speed on a neighboring lane for this situation. If the currently driven speed is below the desired speed and the difference is lower for an adjacent lane, a lane change can be beneficial if all traffic rules can be fulfilled.

6.1.2 Car Following Models

As the ISPA system shall mainly influence the longitudinal control of the vehicle, the focus in the following sections lies on the development of a CFM while the corresponding LCM of a simulation shall stay untouched. Complex behavior models as used in Pelops (see [Brö10]) like the Wiedemann model (see [Wie74]) often use a higher level state machine to determine the basic behavior based on the environment. To give a rough overview, several models known from the literature which are also implemented in PELOPS or SUMO shall be discussed here. All presented models are space continuous and either inherently time discrete or can be converted to time discrete versions.

6.1.2.1 Wiedemann Model

The Wiedemann model (see [Wie74]) tries to provide a very detailed description of driver behavior for which it needs a comparatively high number of parameters. It models four different states which are determined by the parameters Δv as the relative speed and Δx as the relative distance. These two parameters are only determined for the directly preceding vehicle.

Figure 6.2 shows an example trajectory of the ego vehicle approaching a slower preceding vehicle. If it is assumed that the acceleration of both cars equals zero at the beginning, the ego vehicle approaches at constant speed until the distance Δx (not including vehicle lengths) falls below the perception distance. Then it slows down until the distance is small enough to come to the state of "unconscious behavior" where the driver's actions are governed by subconscious actions of a simple car following behavior until external effects force him to a different state. The figure defines several thresholds:

- SDV: Threshold for the perception of speed differences

- SDX: Distance threshold above which the driver is not influenced by a preceding car anymore

- CLDV: Threshold between conscious and unconscious reaction to the predecessor (approach)

- OPDV: Threshold between conscious and unconscious reaction to the predecessor (departure)

- BX Maximum reaction threshold for negative relative speed

- AX Overall distance at standstill: predecessor length + safety distance s_0
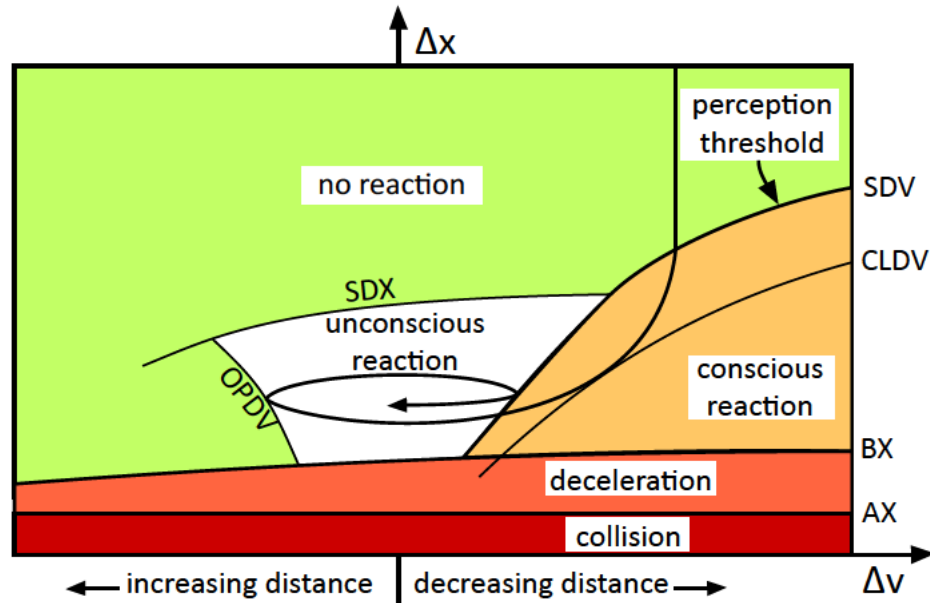
Figure 6.2: States of the Wiedemann model (adapted from [Wie74]) defined by the relative velocity Δv and relative distance Δx between the ego vehicle and the preceding vehicle

Based on these thresholds four distinguishable states can be defined:

- No Reaction
  The driver does not need to react on different vehicles as they are out of the driver's perception area. The desired velocity has been reached or it is being targeted. Oscillations around the desired speed as can be observed in reality are not modeled as the model is intended for use in dense traffic scenarios.

- Unconscious Reaction
  The driver does not consciously perceive a change in the distance to the preceding vehicle. Still he reacts to the driving style of the other vehicle by preparing a braking maneuver and stepping off the accelerator pedal. No active braking takes place.

- Conscious Reaction

  – Nonhazardous Situation
    The driver recognizes a change in the distance to the preceding vehicle and actively brakes. The equation describing this is:

$$\dot{v}_n = \frac{-0.5 \cdot (\Delta v)^2}{(\Delta s - s_0)} + \dot{v}_{n-1} \tag{6.1}$$

with $\dot{v}$: Acceleration output

      $\square_n$: Index of n-th vehicle

    $\square_{n-1}$: Index for the preceding vehicle of the n-th vehicle

       s_0 : Safety distance (including vehicle lengths)

Δs : Inter vehicle distance (including vehicle lengths)

Δv : Speed difference

- Hazardous Situation
  If the driver enters a hazardous situation unexpectedly, the remaining time for a braking maneuver is potentially short. In this case the speed reduction must be higher the closer the obstacle is and the higher the speed difference is. Consequently an additional term is used to restore the minimum distance which shows the following equation:

$$\dot{v}_n = \frac{-0.5 \cdot (\Delta v)^2}{(\Delta s - s_0)} + \dot{v}_{n-1} + B_{min} \cdot \frac{(s_{hazard} - \Delta s)}{s_{hazard} - s_0} \tag{6.2}$$

with $\quad B_{min}$: Linear factor for maximum deceleration

s_{hazard} : Threshold for hazardous braking maneuver

- Crash
  A crash occurs when the distance Δx becomes smaller than the length of the preceding vehicle. For this model the crashed vehicles are not removed from the simulation.

6.1.2.2 Krauß Model

In contrast to the previously described Wiedemann model, Krauß developed a CFM (see [Kra98]) with substantially less parameters and lower computational demand. It is the standard model used in the traffic simulator SUMO and the intentions behind it are stated here:

> "Our main interest will be focused on the qualitative macroscopic
> properties of the model proposed here, because one cannot really expect
> to be able to capture the microscopic details of vehicle motion correctly
> with a model of this simple structure." (from [Kra98])

The model features a limitation for acceleration and deceleration and calculates a safe speed to guarantee a collision free behavior. Adapted from [Kra98], the following equations define the basic behavior:

$$v_{n,\text{safe}}(t) = v_{n-1}(t) + \frac{g_n(t) - g_{n,\text{des}}(t)}{\tau_b + \tau} \tag{6.3}$$

$$v_{n,\text{des}}(t) = min[v_{n,max}, v_n(t) + a_n(v) \cdot \Delta t, v_{n,\text{safe}}(t)] \tag{6.4}$$

$$v_n(t + \Delta t) = max[0, v_{n,\text{des}}(t) - \eta] \tag{6.5}$$

$$x_n(t + \Delta t) = x_n(t) + v_n \cdot \Delta t \tag{6.6}$$

$$\tau_b = \frac{(v_n + v_{n-1})/2}{b} \tag{6.7}$$

with $\quad \Box_n$: Index of n-th vehicle

$\Box_{n-1}$: Index for the preceding vehicle of the n-th vehicle

Δt : Time step length with $\Delta t \leq \tau$

τ : Driver reaction time

$g(t)$: Current gap to predecessor

$g_{des}(t)$: Desired gap to predecessor

η : Random perturbation for suboptimal driving ($\eta > 0$)

a, b : Typical acceleration and deceleration bounds: $-b \leq \dfrac{dv}{dt} \leq a$ with $a, b > 0$

This set of model equations shows a version of it which is already adapted for time discrete applications, while it would also be possible to use it in a time continuous way.

6.1.2.3 Kerner Model

The model proposed by Kerner et al. in [Ker04] introduces three traffic states: Free Flow (F), Synchronized Flow (S) and Wide Moving Jam (J). In contrast to the previously described models it is a Cellular Automata (CA) model (KKW model by Kerner, Klenov and Wolf), but uses a very small cell size of only 0.5m. As a consequence its output provides a more realistic behavior for detailed analysis than most other CA models. The two traffic states "F" and "S" can be represented on the flow-density plane (see Fig. 6.3). If projected to the gap-speed plane, the synchronized flow state is represented by the shaded area in Fig. 6.3 right. In this case the model decelerates if the current gap g to the preceding vehicle is smaller than the safety gap g_{safe} and accelerates if g is higher than the synchronization gap G.
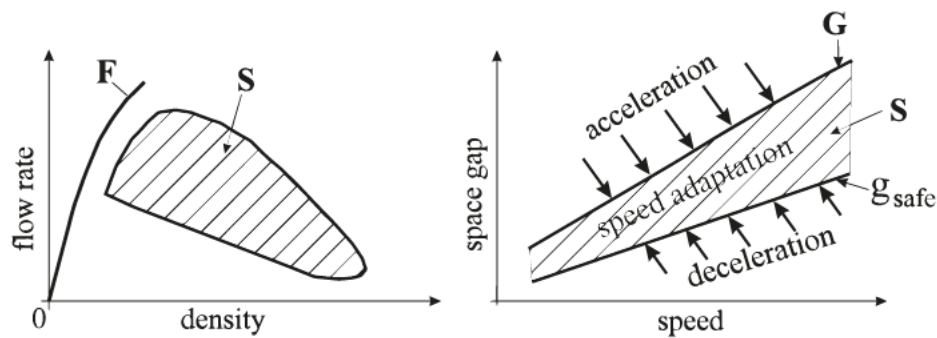
Figure 6.3: State diagram for the CA Model by Kerner et al. Left: Representation of Free Flow (F) and Synchronized Flow (S) in the flow-density plane. Right: Representation of Synchronized Flow in the gap-speed plane.

6.1.2.4 Intelligent Driver Model

The Intelligent Driver Model (IDM) is a very simple yet complete model which is by design crash free. Treiber and Kesting (see [TK10]) postulate the following rules that should apply in general for a plausible car following behavior:

- Acceleration to the desired velocity v_0 if no other interference from other vehicles applies and obstacles are sufficiently far away (v_l: Velocity of leading vehicle, g: netto distance to leading vehicle, a_{mic}: acceleration function):

$$\frac{\partial a_{\mathrm{mic}}(g, v, v_l)}{\partial v} < 0, \qquad \lim_{g \to \infty} a_{\mathrm{mic}}(g, v_0, v_l) = 0 \quad \text{for all } v_l \tag{6.8}$$

- In synchronized traffic and equal conditions the acceleration should decrease (and the braking deceleration increase) with a decreasing gap to the leading vehicle:

$$\frac{\partial a_{\mathrm{mic}}(g, v, v_l)}{\partial g} \geq 0, \qquad \lim_{g \to \infty} \frac{\partial a_{\mathrm{mic}}(g, v, v_l)}{\partial g} = 0 \quad \text{for all } v_l \tag{6.9}$$

The equality sign in the left inequation is valid if all vehicles are distant enough that they do not influence driving behavior.

- For dynamic approaches with equal conditions the acceleration shall be lower (the deceleration shall be higher) the higher the approach rate is respectively the higher the speed of the leader is:

$$\frac{\partial \tilde{a}_{\mathrm{mic}}(g, v, v_l)}{\partial \Delta v} \leq 0 \quad \text{or} \quad \frac{\partial a_{\mathrm{mic}}(g, v, v_l)}{\partial v_l} \geq 0, \quad \lim_{g \to \infty} \frac{\partial a_{\mathrm{mic}}(g, v, v_l)}{\partial v_l} = 0 \tag{6.10}$$

Again the equality sign applies in the case of no interferences.

- In a queue a certain minimum distance g_0 to the leading vehicle shall be kept

$$a_{\mathrm{mic}}(g, 0, v_l) = 0 \qquad \text{for all } v_l \geq 0, g \leq g_0 \tag{6.11}$$

The IDM is based on general understandings of traffic and uses parameters that can be derived from real world traffic measurements or known car design parameters. As stated in [THH00] and [TK10], the following principles (so-called *First Principles*) are met:

- The acceleration follows the common plausibility rules stated in equations 6.8, 6.9, 6.10 and 6.11

- The equilibrium gap g^* during car following shall not fall below certain safety gap which is defined by the minimum distance g_0 and the time headway T by $g^* = g_0 + v \cdot T$

- The approach of slower or standing vehicles or obstacles happens in a collision-avoiding intelligent braking strategy:

  - If the situation is "under control" a smooth braking maneuver is used by gradually applying a comfortable deceleration which is smoothly removed shortly before the standstill

  - If the situation is critical a stronger deceleration than the comfort deceleration is being applied to bring the situation back under control. If possible the comfort deceleration is applied for the rest of the maneuver.

- During car following and approaching there shall be smooth transitions. The parameter *Jerk J* as the derivative of the acceleration should therefore be not infinite (comfortable values are $|J| \leq 1.5 m/s^3$). This demands an acceleration function $a_{\text{mic}}(g, v, v_l)$ and $\tilde{a}_{\text{mic}}(g, v, \Delta v)$ which is continuously derivable by all variables.

- The model should be as simple as possible and have easily interpretable parameters. If possible every parameter should reflect only one aspect of driver behavior and contain plausible values.

Based on the above principles the IDM model equations are formulated as follows:

$$\dot{v}_n = a_n \left[1 - \left(\frac{v_n}{v_{n,0}} \right)^\delta - \left(\frac{g_n^*(v_n, \Delta v_n)}{g_n} \right) \right] \tag{6.12}$$

with $\square_n$: Index of n-th vehicle

$\square_{n-1}$: Index for the preceding vehicle of the n-th vehicle

$$g_n^*(v_n, \Delta v_n) = g_{n,0} + \max \left(0, v_n T + \frac{v_n \cdot \Delta v_n}{2\sqrt{a_n b_n}} \right) \tag{6.13}$$

$\Delta v_n = v_{n-1} - v_n$

g_n : current gap to leading vehicle

g_n^* : desired gap to leading vehicle

$g_{n,0}$: minimum gap to leading vehicle

$v_{n,0}$: desired velocity of n-th vehicle

a_n : maximum acceleration of n-th vehicle

b_n : comfortable deceleration of n-th vehicle

The term for g_n^* contains a static portion $g_{n,0} + v_n T$ as well as a dynamic portion defined by $v_n \cdot \Delta v_n / (2\sqrt{a_n b_n})$ which is responsible for the intelligent braking strategy defined in the First Principles.

As stated in the last principle, the parameters shall be described with the help of three standard situations as also described in [TK10]: (i) During *Acceleration* on a free road the maximum acceleration a_n is used. It gradually reduces to zero in a way defined by δ when the desired velocity $v_{n,0}$ is reached. (ii) The situation *Car Following* is governed by the time headway T plus the minimum gap $g_{n,0}$ for stagnant traffic. (iii) For the *Approach* towards slower or standing vehicles the actual deceleration value is below the comfortable deceleration b_n. The transitions between the described situations happen in a smooth way.

In the second principle an "intelligent braking strategy" is proposed for the system. The model equation 6.13 implements this behavior and shall be discussed in more detail here. It was already mentioned above that the term $v_n \cdot \Delta v_n / (2\sqrt{a_n b_n})$ is responsible for the dynamic approach behavior. Due to the required smooth transitions the static term $g_{n,0} + v_n T$ is also always present, so to inspect the braking strategy isolated the static term is set to zero. Also the acceleration term for free driving $a_{n,F}(v_n) = a_n[1 - (v_n/v_{n,0})^\delta]$ shall be neglected. An example for such a situation could be the approach towards a traffic light or a standing vehicle, so this also simplifies the equation by setting $\Delta v_n = v_n$. The resulting

acceleration for the IDM is then:

$$\dot{v}_n = -a_n \left(\frac{g_n^*}{g_n} \right)^2 = -\frac{a_n \cdot v_n^2 (\Delta v_n)^2}{4 a_n b_n g_n^2} = -\left(\frac{v_n^2}{2 g_n} \right)^2 \frac{1}{b_n} \tag{6.14}$$

If the *kinematic deceleration* is defined by

$$b_{n,\text{kin}} = \frac{v_n^2}{2 g_n} \tag{6.15}$$

where the braking distance equals the current gap, the IDM acceleration in this special case is reduced to

$$\dot{v}_n = -\frac{b_{n,\text{kin}}^2}{b_n} \tag{6.16}$$

The kinematic deceleration $b_{n,\text{kin}}$ is then the minimum deceleration needed to avoid a collision. The self regulating nature of the IDM can be derived from these statements:

- A critical situation is characterized by larger values for the kinematic deceleration than the comfort deceleration

- In this case a stronger deceleration is applied than the kinematic deceleration: $|\dot{v}_n| = b_{n,\text{kin}}^2 / b_n > b_{n,\text{kin}}$. Like that the kinematic deceleration is gradually reduced to the comfort deceleration, the situation gets "under control" again.

- If the situation is uncritical and braking is not necessary ($b_{n,\text{kin}} < b_n$), then the current deceleration $b_{n,\text{kin}}^2 / b < b_{n,\text{kin}}$ is even lower. $b_{n,\text{kin}}$ consequently increases towards the comfort deceleration.

Parameter	Typ. value Highway	Typ. value City
Desired speed v_0	120 km/h	54 *km/h*
Time Headway T	1.0 s	1.0 *s*
Minimum Gap g_0	2 m	2 *m*
Acceleration exponent δ	4	4
Acceleration a	1.0 m/s²	1.0 m/s²
Deceleration b	1.5 m/s²	1.5 m/s²

Table 6.1: Typical parameter values for the IDM as defined in [TK10].

The IDM equations proposed up to this point have the disadvantage, that the cars at the tail of a queue possibly never reach their desired speed. Because of that they increase their gap size gradually. The reason for this is that the decelerating influence of the leader vehicle does not drop to zero if the desired gap $g^*(v, 0) = g_0 + vT$ is exceeded. A modification which does not affect the other model properties notably is to distinguish two cases with the variable z:

$$\dot{v} = \begin{cases} a_n (1 - z_n^2) & \text{if } z_n = \frac{g_n^*}{g_n} \geq 1, \\ a_{n,F} \left(1 - z_n^{\frac{2 a_n}{a_{n,F}}} \right) & \text{else} \end{cases} \tag{6.17}$$

$$\text{with } a_{n,F}(v) = \lim_{g_n \to \infty} a_{n,\text{IDM}}(g_n, v_n, \Delta v_n) = a_n \left[1 - \left(\frac{v_n}{v_{n,0}} \right)^{\delta} \right] \tag{6.18}$$

This modified version of the model works with the same parameter set and has except for the following behavior close to the desired velocity the same dynamical properties.

Every parameter controls a distinct property of driver behavior. Different speed limits and their implications on the driven speed can be directly controlled with the parameter v_0 for the desired velocity. This does not change the overall characteristics of a driver-vehicle unit but adapts it to the external restrictions. The IDM does not model human reaction time in any way and consequently behaves more like an ACC system than a human driver. Still the model can be extended to reflect distance estimation errors, reaction times and even multiple leading cars.

6.2 Deceleration model for static objects

The following sections describe the steps that lead from an initially very static model to a more versatile approach that can be combined with virtually any existing CFM. The first approach models the typical speed development when approaching a static obstacle with and without the ISPA assistance system. To obtain a more general model the IDM is combined with the first static model and finally the next evolutionary step produces the BM which incorporates natural driver behavior in a very unique way.

In a first step the general nature of the deceleration phase when approaching an obstacle shall be investigated. For this purpose the speed data from a driving simulator experiment conducted in [Cho11] with 30 participants (15 drivers with and 15 drivers without assistance) will be analyzed (see also experiment description in [LCR11]). From each data set the interval from the first (theoretical) ISPA output until its last output to the driver is extracted as shown in Fig. 6.4. The term "theoretical" means that the ISPA system was also active for the baseline (non assisted) drivers and its output was recorded, but the corresponding HMI was not active. All drivers experienced the same situation which was a static traffic jam behind a long drawn curve on a three lane highway. As described in the previous chapters the LED based HMI using the Static Guiding Point was installed in the simulator.

A general relationship that can be observed is that a higher staring speed leads to earlier and stronger deceleration. Additionally some drivers perform the deceleration in steps and some decrease their speed to much so they start accelerating again. The first step towards mimicking this behavior is to model the basic speed development when approaching a static obstacle like the rear end of a static traffic jam.

6.2.1 Model Generation

The proposed model creates a speed development consisting of a linear part that keeps the original speed and a deceleration part with the shape of an exponential curve as depicted in Fig. 6.5. For the moment the model only depends on the initial speed at assistance activation and neglects parameters such as obstacle distance. It is not a conventional CFM and consequently it does not update its behavior every simulation step by analyzing the
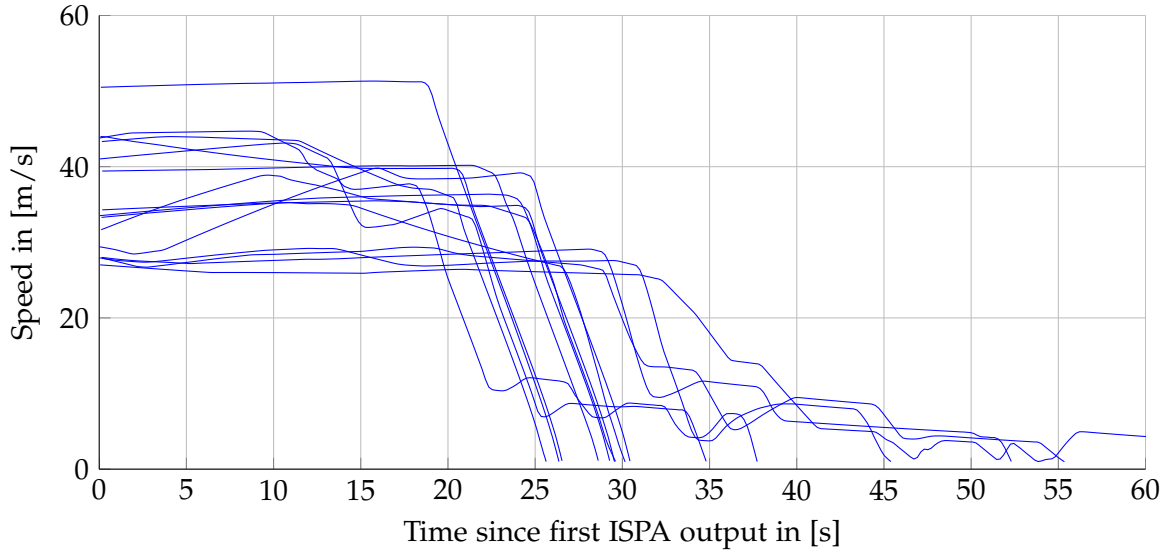
Figure 6.4: Speed curves of the baseline drivers. Some of them perform a stepwise deceleration as marked in the figure.

ego vehicle environment. Because the shape of the model curve does not take into account the stepwise deceleration of some drivers, the end point of the analyzed time interval of each driver is shifted towards the standstill or the first step during the deceleration. The following properties shall finally be addressed by the model:

- Dependency only on the initial speed at assistance activation

- Varying time until deceleration is started

- Varying shapes of the speed curves during deceleration

The corner time t_{lin} depending on the start speed v_0 is modeled as follows:

$$t_{\text{lin}} = p_1 \cdot v_0^{p_2} \tag{6.19}$$
$$\text{with} \qquad p_1 = 915.12 \qquad p_2 = -1.0359$$

Two participants from the baseline group were left out of the analysis because of their very different behavior from the other drivers. For the others the individual corner time t_{lin} was determined by searching for the first acceleration value lower than -0.4 m/s^2. These time values were then used to determine the two design parameters p_1 and p_2 by applying a Least - Squares curve fitting algorithm.

The exponential part of the model curve follows equation 6.20. A trend which can be observed in the raw curves from Fig. 6.4 is that the shape of the deceleration part changes according to the linear speed which is determined by the corner value of the input curves (see also [Ton10]).

$$v = v_0 \cdot e^{\frac{-(t-t_{\text{lin}})^2}{2\sigma}} \tag{6.20}$$
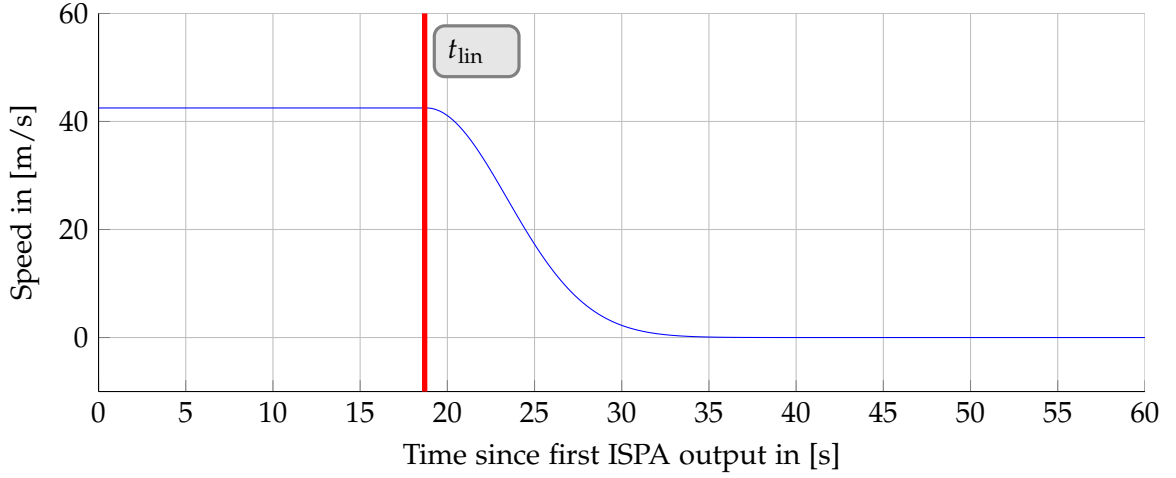
Figure 6.5: Basic shape of the deceleration model. The time t_{lin} marks the transition from the linear part to the exponential part.

$$\sigma = p_3 \cdot v_0^2 + p_4 \cdot v_0 + p_5$$

In order to model this relationship the value of the parameters p_3, p_4 and p_5 depend on the corner speed which is shown in Fig. 6.6 with the solid lines. Again it is necessary to determine a function that fits the relationship between the parameters and the linear speed. Also in this case the best option was found to be an exponential function as defined in Eq. 6.21. As with the other parameters the values of p_6 - p_9 were determined with a Least - Squares algorithm which produced the dashed lines in Fig. 6.6. The values of p_6 - p_9 for the respective p_3 - p_5 are listed in Tab. 6.2.

$$p = p_6 \cdot e^{p_7 \cdot (v_0 - p_8)} + p_9 \tag{6.21}$$

Parameter	p_6	p_7	p_8	p_9
p_3	-0.5361	-0.0801	29.61	-0.2431
p_4	16.1202	0.0041	27.5055	-9.9736
p_5	0.085	-1.3028	27.251	500.00

Table 6.2: Parameters p_6 - p_9 which determine the functions of p_3 - p_5 depending on the linear speed of the model.

Up to this point the initial goals have been met and so the resulting model curves for different starting speeds can be plotted like in Fig. 6.7. As mentioned before some of the drivers performed a stepwise deceleration which cannot be explained with the road geometry or the behavior of the surrounding vehicles. An explanation for this behavior could be that drivers decelerated too much at the beginning and re-estimated the situation from time to time. During this phase they stopped decelerating and continued after they re-estimated the distance to the preceding vehicle.
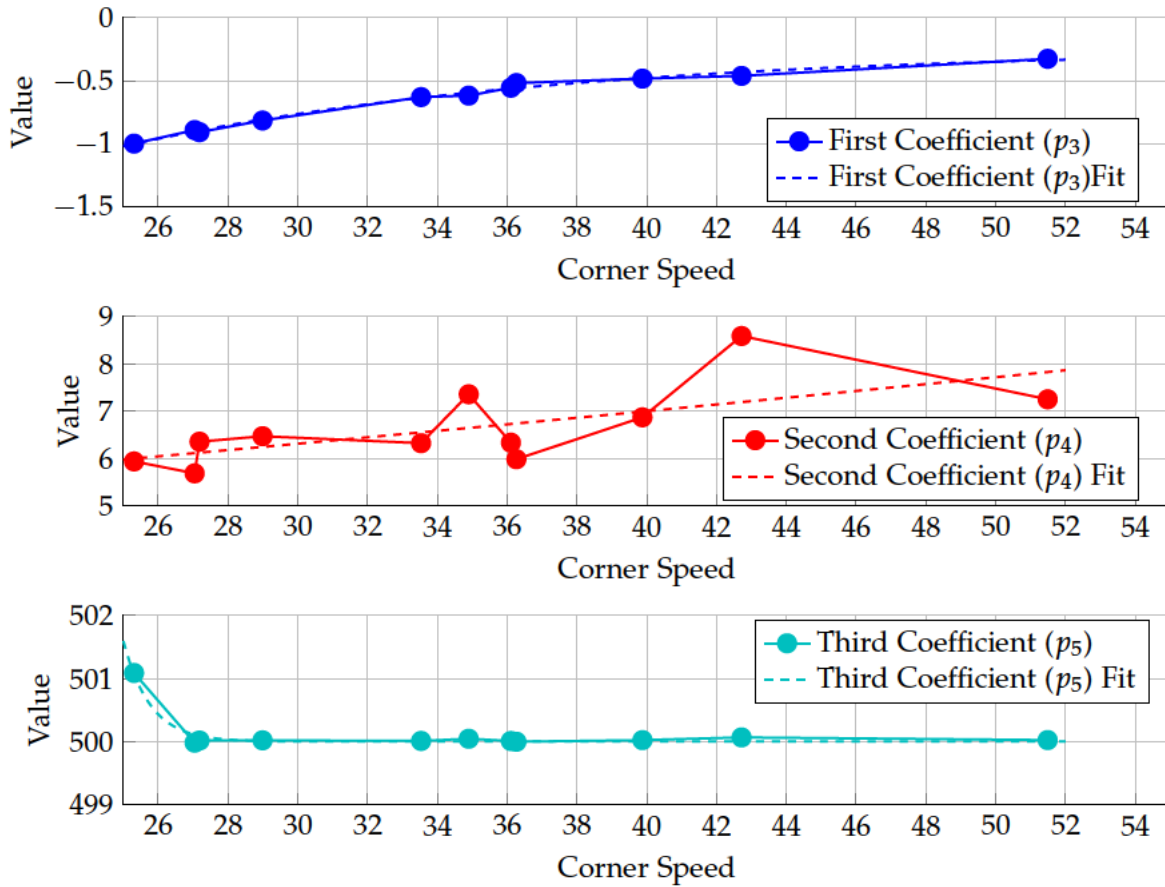
Figure 6.6: Results of the Least - Squares curve fitting for the exponential part of the deceleration model. Each data point represents the parameter value for the respective linear speed

This behavior shall now be incorporated into the model with the introduction of a distance estimation error as proposed by e.g. Daum et al. in [DH09]. It is used in such a way that the expected distance is compared to the actual distance for every simulation step. If the difference exceeds the tolerance defined by the right curve in Fig. 6.8, a new speed curve is generated and the deceleration process starts over. This happens until the actual distance falls below 50m where it is assumed that drivers use their usual car following behavior and are not influenced by the ISPA system any more if eye contact is given.

In order to test the proposed model and validate the behavior especially regarding the stepwise deceleration and stability in larger scenarios, the next step is to implement it in a traffic simulation.

6.2.2 Software architecture

The model described in the previous section shall now be implemented for the submicroscopic traffic simulator PELOPS. It uses the behavior model suggested by Wiedemann in [Wie74] which has several high level states as shown in Fig. 6.2.
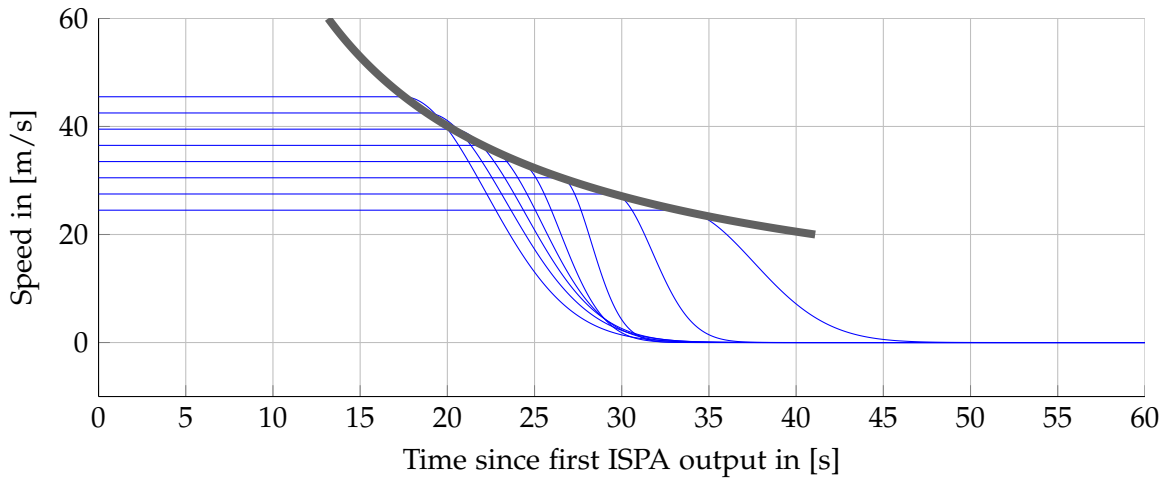
Figure 6.7: Family of functions with only the starting speed as input parameter. The gray line indicates the model function for the corner times.

In order to alter the behavior of certain vehicles in a simulation, an interface as described in [BC02] must be available. As the proposed model shall not be implemented in hardware as a Electronic Control Unit (ECU), a software module is used in a Software-in-the-loop (SIL) manner to access a vehicle. This means that an independent functional module or simulation is synchronized to the process loop of a host application which is PELOPS in our case. Therefore it is important that the time step size is fixed. If no real time simulation is required, all participating programs wait for each other's completion which allows for computationally costly implementations. PELOPS offers an interface to the Matlab extension Simulink as the block diagram in Fig. 6.9 shows.
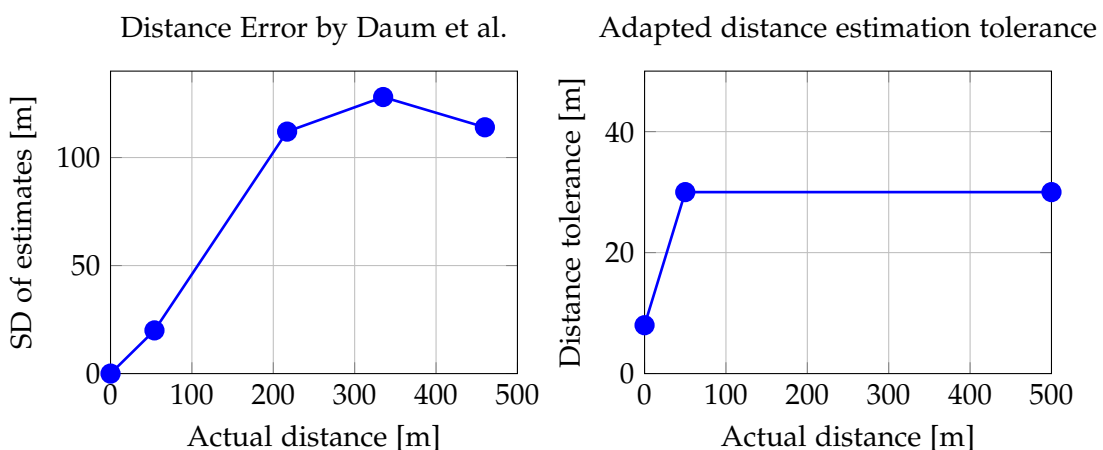
Figure 6.8: Distance estimation error determined by Daum et al. in [DH09] (left) and adapted distance tolerance curve as used in the model (right).
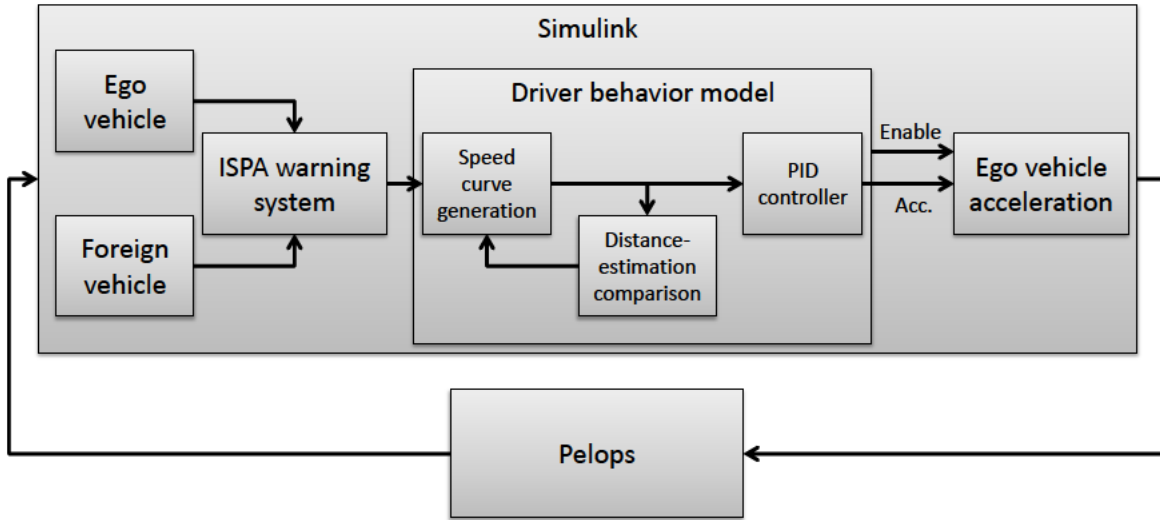
Figure 6.9: Co-Simulation with Simulink and Pelops in a Software-in-the-loop topology.

On the Simulink side the interface offers several blocks which provide output from the PELOPS simulation including e.g. speed from the ego car, distance to neighboring vehicles and other data. Also there are blocks for data input back to PELOPS, most notably the acceleration and a related enable switch. The previously described deceleration model provides its output as a vehicle velocity which implies that it needs to be converted to the acceleration required by the Simulink interface. As it is not clear from the documentation whether the acceleration is directly applied to the final speed or if it controls the accelerator pedal, a control loop needs to be constructed. This shall ensure that the desired speed is followed as closely as possible. A general purpose controller like a PID (Proportional, Integral, Derivative) controller (see [Min22]) as shown in Fig. 6.10 can be used to form a closed loop over the whole Simulink structure (see also Fig. 6.9). The PID controller can be
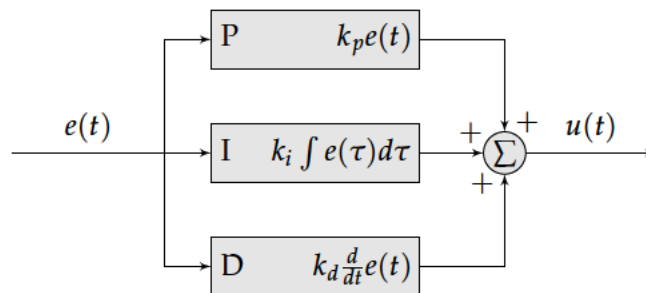
Figure 6.10: PID controller as used in the static Car Following Model in PELOPS

parametrized with the values k_p, k_i and k_d, the resulting analytical expression is Eq. 6.22.

$$u(t) = k_p \cdot e(t) + k_i \cdot \int_0^t e(\tau)d\tau + k_d \cdot \frac{d}{dt}e(t) \tag{6.22}$$

$$\text{with} \quad k_p = 20 \quad k_i = 0.3 \quad k_d = 0.6$$

133
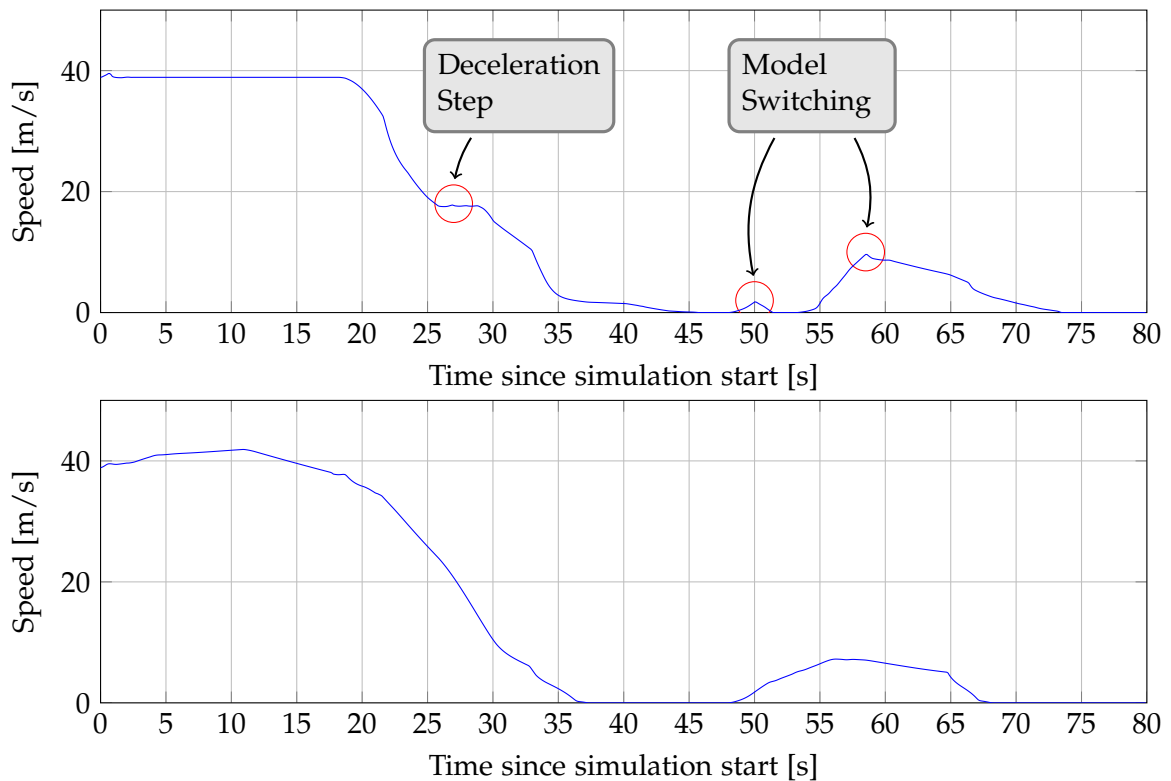
Figure 6.11: Speed plot from a PELOPS simulation run with ISPA assistance. The upper plot shows a stepwise deceleration and spikes due to switching between the PELOPS driver model and the described deceleration curve. The lower plot corresponds to the same situation with a real driver. Data collected in [Ton10].

Also the Business Logic of the ISPA assistance system needs to be implemented. The necessary information is provided at run time through the SIL interface in Simulink. At this stage no distinction is made between the different deceleration suggestions, the subsequent speed curve generation is equally executed for all outputs.

6.2.3 Traffic simulation with multiple vehicles

In the next step the model shall be tested in a larger scenario with several interacting vehicles. The intention behind this experiment is to obtain a first insight about the overall behavior of the system and the suitability of the chosen combination of the PELOPS Wiedemann model and the static deceleration model.

For this purpose a scenario was developed in PELOPS containing 20 vehicles in the test group (see Fig. 6.12) approaching a static traffic jam with 140 km/h $\approx$ 38.9 m/s from a distance of 1000 m. Similar to the experiments with real drivers the location is a three lane highway with the only difference that there is no bend like in the driving simulator. This has no effect on the simulation as sight occlusions are not calculated. Different equipment percentages shall be tested at the 0%, 5%, 10%, 20%, 50%, 70% and 100% levels starting at

the front of the test group. The assignment of ISPA equipped and baseline vehicles is fixed and consequently only seven simulation runs (one for each configuration) are conducted.

During the simulation several metrics are being recorded besides the speed:

- Acceleration to obtain maximum deceleration

- Fuel consumption

- Crash events

These metrics shall then serve for a comparison of the different configurations described above. An analysis of them follows in the next section.
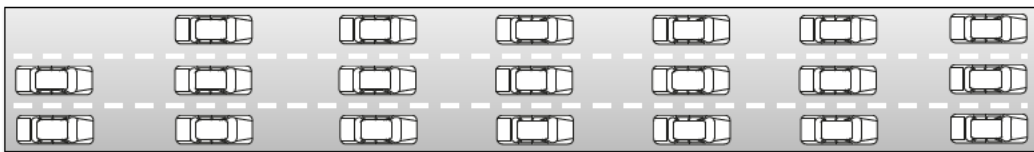
Figure 6.12: Vehicle positions in the test group of 20 cars, the front of the group is located at the right border of the figure. For 5% equipment percentage the lower car in the rightmost column is chosen.

6.2.4 Experiment Results

After running the described scenario configurations, the first outcome to mention is that not a single crash occurred. Given that the ISPA system is intended to improve safety, this result shows that the model produces at least no unwanted behaviors. It also must be noted that the experiment design with a very low number of simulation runs cannot serve as a reliable proof for this conclusion.

The two other analyzed metrics "acceleration" and "fuel consumption" show an unexpected tendency as depicted in Fig. 6.13. While the assistance should lead to a smoother deceleration and thus to lower maximum decelerations, this metric increases with a growing number of equipped vehicles. An explanation for this outcome are the switching events between the driver models. It can be observed in Fig. 6.11 that model switching leads to spikes in the speed graph which leads to high positive or negative acceleration values. The reason for this is that the original PELOPS model and the deceleration model always run in parallel and produce different acceleration outputs due to their very different structure. Because the SIL interface in Simulink does not offer the information about the output of the other model, only a hard switch can be implemented between the two values.

The fuel consumption shows overall an expected result. With an increasing equipment percentage the average consumption of the test group decreases. This relationship is both nonlinear and of very low magnitude, the highest decrease equals 2.4% of the initial value. Also for this metric the problematic construction of model switching could add to the marginal effect.

Overall the main problem of the design described above is the switching between two very different car following models. Additionally the proposed static model has no linkage

to the LCM due to the limited access through the SIL interfaces. The consequence is then to use a general purpose CFM which is coupled to the ISPA output and the resulting actions at a higher level. This approach shall support a more generic use of the resulting model and an overall more realistic behavior.
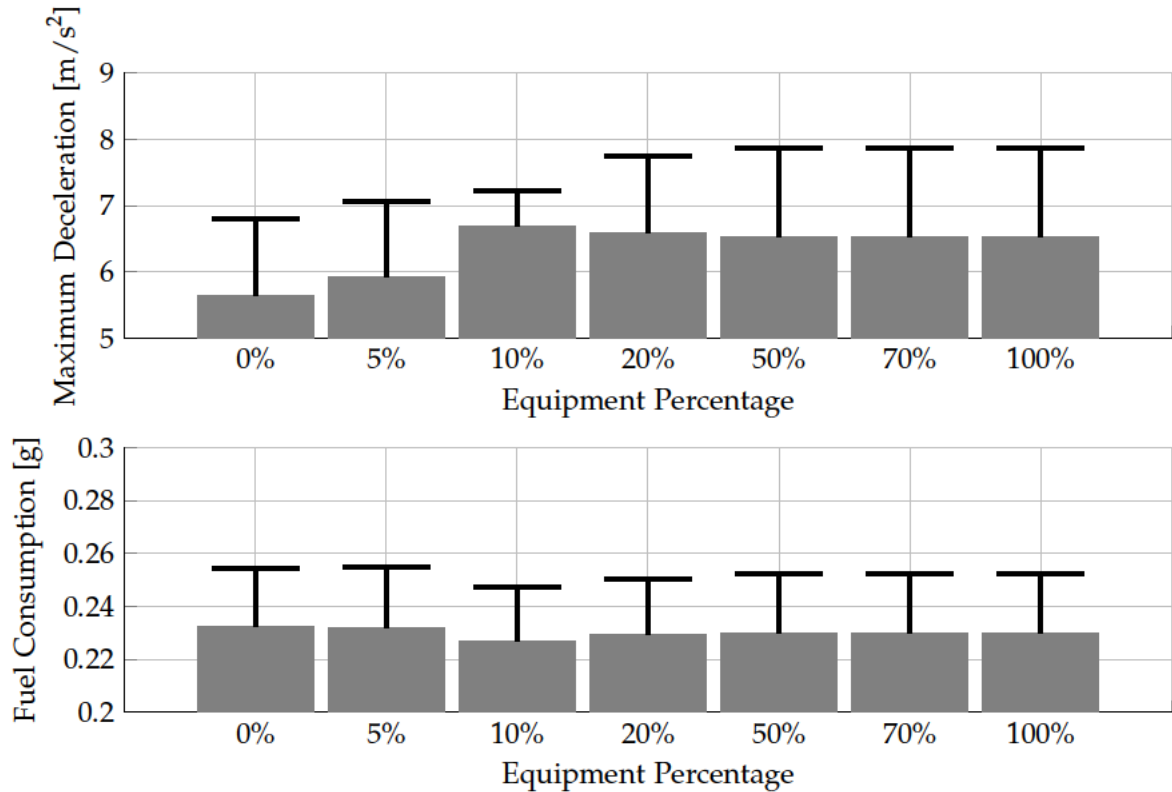
Figure 6.13: Mean values and SD of the maximum deceleration and fuel consumption for different equipment percentages.

6.3 Moving from the static model to the Intelligent Driver Model

For the previously developed model it was concluded that its main weaknesses are the relatively static behavior (the speed curve during deceleration is only determined by the initial speed) and the chosen SIL architecture requiring binary model switching. While the first point limits especially the versatility of the model, the latter one affects largely several safety and efficiency metrics.

As already mentioned the approach of a partially pre-calculated speed development shall be replaced by a "real" CFM. A lesson learned from the previous approach is the presence of a stepwise deceleration of some drivers that can be interpreted as an overreaction to an upcoming obstacle. What follows is a re-interpretation of the scene with potentially several subsequent deceleration maneuvers.

In a first step a different simulation architecture is chosen which provides access to all programming code and therefore allows arbitrary modifications and insights to the current implementation. For this purpose the Open Source simulator SUMO which was also used in chapter 5 for calculating traffic movements in the immersive driving simulator shall serve as the basis. It provides several Car Following Models that are frequently used in the literature such as the Wiedemann model (see [Wie74]), the Krauß model (see [Kra98]), the model by Kerner (see [Ker04]) and finally the IDM by Treiber et al. (see [THH00]). All of these models have also been discussed in chapter 6.1.2. In order to select the model that fits best to the data recorded with real drivers in the driving simulator, a similar scenario was built which every model had to complete. Two versions of the scenario were tested by Tschöpe in [Tsc12]: driving towards a standing vehicle from a distance of 200m with an initial speed of $28\frac{m}{s}$ or $4\frac{m}{s}$.
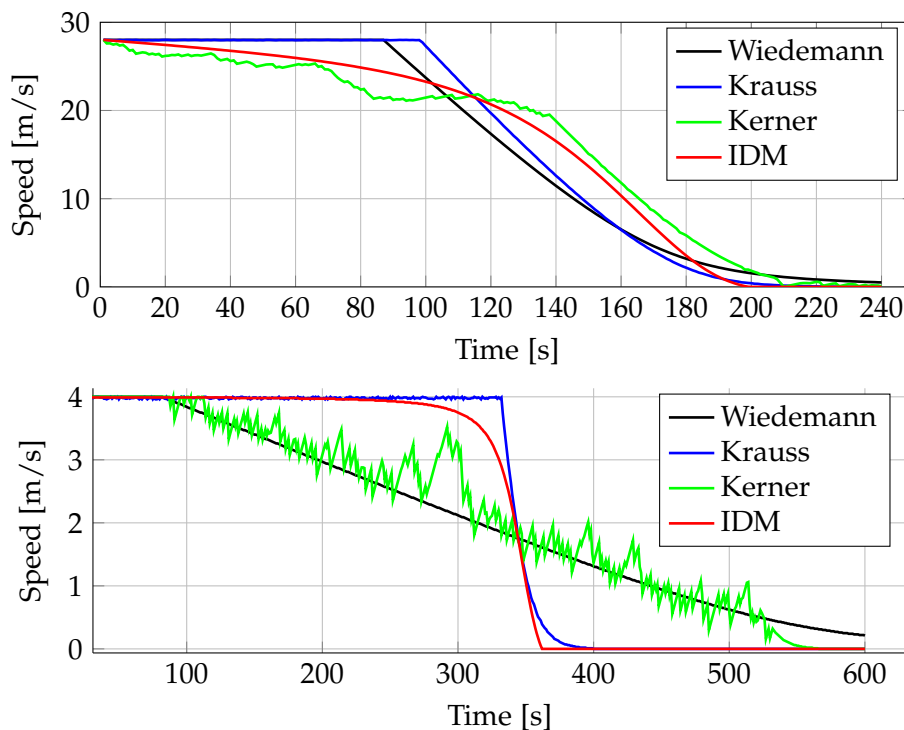
Figure 6.14: Comparison of different Car Following Models approaching a standing vehicle from 200m. Especially for low speeds the models have very different behaviors (see lower plot).

A first conclusion that can be drawn from the plots in Fig. 6.14 is that the Kerner model produces the noisiest speed curve which makes it unusable to derive the desired metrics. The reason for this is the model architecture which is of the CA type that implies a granular speed development. Both models by Wiedemann and Krauß have a sharp corner at the beginning of the deceleration phase which is not observable from the real drivers e.g. in Fig. 6.4. As the remaining model the IDM shows all necessary properties to use it as a basis for further developments. Its capability to extend it to incorporate more details of human behavior has also been shown by its authors in [TK10].

6.3.1 Extension of the Intelligent Driver Model

Up to this point the IDM is designed as a single lane CFM and has proved to produce reliable driving patterns. However most simulation scenarios contain several lanes in the same direction which also implies lane changes of the other vehicles for realistic behavior. In such an event the value of the gap distance to the leading vehicle suddenly jumps to a lower value because the lane changing car becomes the new leader. If the new gap distance is significantly lower than the desired gap, the result would be an unrealistically high deceleration (see [KTH10]). This is an effect of the "worst case heuristic" on which the IDM is based to guarantee a collision free behavior.

6.3.1.1 The Enhanced Intelligent Driver Model

In order to overcome this unwanted behavior a new heuristic was introduced in [KTH10] named the Constant Acceleration Heuristic (CAH). It is based on the experience of real drivers that surrounding leading cars do not change their acceleration within the next few seconds. The heuristic is based on the following assumptions:

- The accelerations of the vehicle under consideration and the leading vehicle will not change in the relevant future

- No safe time headway or minimum distance is required at any moment

- Drivers react without delay

Based on this the acceleration function can be defined as

$$
a_{n,\text{CAH}}(g_n, v_n, v_{n-1}, a_{n-1}) = \begin{cases} \frac{v_n^2 \tilde{a}_{n-1}}{v_{n-1}^2 - 2g_n \tilde{a}_{n-1}} & \text{if } v_{n-1}(v_n - v_{n-1}) \leq -2g_n \tilde{a}_{n-1} \\ \tilde{a}_{n-1} - \frac{(v_n - v_{n-1})^2 \, \Theta(v_n - v_{n-1})}{2g_n} & \text{else} \end{cases}
$$

$$(6.23)$$

$$
\begin{aligned}
\text{with} \quad & \square_n : \text{Index of n-th vehicle} \\
& \square_{n-1} : \text{Index for the preceding vehicle of the n-th vehicle} \\
& \tilde{a}_{n-1} = \min(a_{n-1}, a_n) \quad \text{Effective acceleration} \\
& \Theta : \text{Heaviside step function}
\end{aligned}
$$

In the case of $v_{n-1}(v_n - v_{n-1}) \leq -2g_n \tilde{a}_{n-1}$, the leading vehicle has stopped by the time the minimum gap $g_n = 0$ is reached. The CAH alone would not lead to a complete model in a way the "standard" IDM provides it. Especially in a stationary car following situation where $\Delta v_n = 0$, $a_{n-1} = 0$ can be assumed, the resulting $a_{n,\text{CAH}}$ would be zero for any given gap g_n. Instead a real driver would slowly adapt to his desired gap and consequently decelerate until it is reached. Also the property of minimum time headway would be completely neglected. The solution to this proposed by Kesting is to use the CAH only as an indicator if the standard IDM would lead to unrealistic accelerations. For the resulting Enhanced Intelligent Driver Model (EIDM) the following assumptions formulated in [KTH10] are made:

- The EIDM acceleration is never lower (more negative) than the one of the IDM. This preserves the property of the IDM of being collision free in all situations.

- If the IDM and the CAH produce the same acceleration, the EIDM shall have the same value.

- In case the IDM suggests an extreme deceleration and the value from the CAH is more positive than the comfort deceleration $-b$, the situation is classified to be mildly critical. Then the final EIDM acceleration is a value between both outputs.

- If both accelerations are more negative than $-b$, the situation is classified to be seriously critical. The resulting EIDM acceleration must not be higher than the maximum values from the IDM and the CAH.

- The final EIDM acceleration shall be a continuous and differentiable function of the input accelerations from IDM and CAH.

If the above statements are brought into a mathematical form, the resulting accelerations function of the EIDM can be formulated in Eq. 6.24.

$$
a_{\text{EIDM}} = \begin{cases} a_{\text{IDM}} & \text{if } a_{\text{IDM}} \geq a_{\text{CAH}} \\ (1-c) \cdot a_{\text{IDM}} + c \left[a_{\text{CAH}} + b \cdot \tanh\left(\frac{a_{\text{IDM}} - a_{\text{CAH}}}{b}\right) \right] & \text{else} \end{cases} \tag{6.24}
$$

$$\text{with} \quad c : \text{Coolness factor}, \quad c \in [0; 1]$$

This solves the over reaction of the IDM in case of other vehicles cutting in the gap to the preceding vehicle. The basic design parameters and their meanings stay the same, but the EIDM now also relies on the acceleration of the preceding vehicle through the CAH acceleration. One more design parameter has been introduced for this extension which is the "coolness factor" c. If $c = 0$ is chosen the EIDM is equal to the IDM while a value of $c = 1$ causes the model to be insensitive to low gaps with no velocity difference. Usually a value of $c = 0.99$ yields realistic behavior.

6.3.1.2 Extension with Human Behavior

So far the EIDM acts very similar to an ACC controller and even has been used for such a system (see [KTH10]). Together with the fact that it is by design collision free it cannot be used to gain insights on how an ADAS such as the ISPA system could influence safety metrics or even crash rates. Therefore, this section describes how the ISPA system can be combined with the IDM and also how limited human capabilities like distance estimation and reaction times influence the final behavior.

Similar to the initial static model where the experiment described in [LCR11] served as the data source, the parameters were taken from the same driving simulator experiment. The difference to the previous usage is that sight conditions shall also be taken into account now. The test drivers approached a standing traffic jam from a distance of 1000m while the vegetation only allowed to see this from a maximum distance of 200m. As can be seen in Fig. 6.15, the track shape is defined with the primitives "straight", "circle" and "clothoid". The driving simulator Silab uses these basic shapes for track definition similar to the way

real roads are planned. A specialty is the clothoid (see also [Arc18]) which is a shape used to connect straights and circles in order to allow a gradual change of the steering angle instead of a jump if no clothoids were used. This is of importance because the SUMO simulator needs road network definitions based on nodes and edges. Given the fact that edges can only be linear connections between nodes, shapes like clothoids and circles need to be approximated.
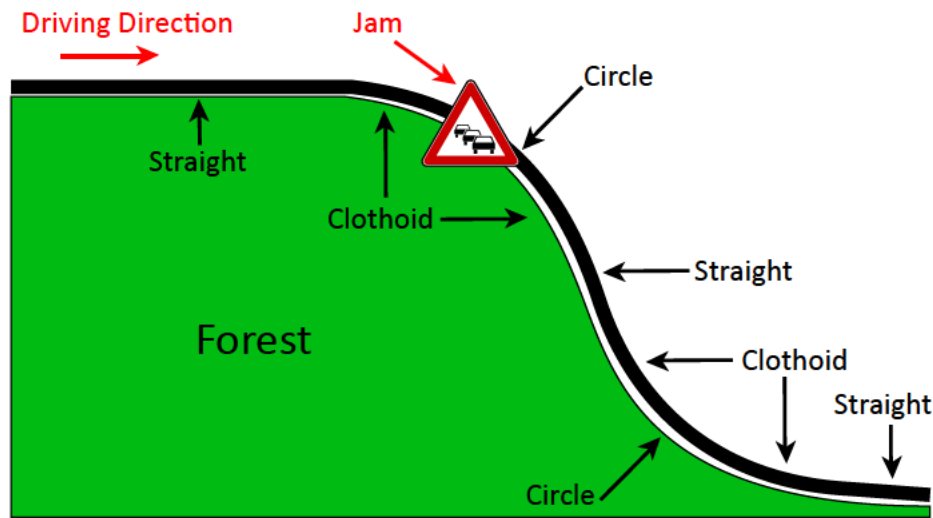
Figure 6.15: Scenario from an ISPA driving simulator experiment, adapted for the SUMO simulator.

The plots in Fig. 6.16 show the cases of an assisted and a baseline driver. For the assisted driver the intervals with ISPA outputs are marked with different colors. We will now investigate more in-depth the different shapes of speed curves exhibited from different drivers.

Baseline Drivers

All drivers in the baseline group could only rely on their visual information to judge the situation. It was observed by Tschöpe in [Tsc12] that three different types of drivers can be distinguished:

- Ideal drivers

- Inattentive drivers

- Cautious drivers

This classification is not fixed for a driver, especially not the type "Inattentive driver". As a result the parameters controlling this behavior shall be determined for every situation the driver encounters. For all types the phases *Visibility* → *Reaction Time* → *Pressure Build-Up Time* → *Braking* apply for their braking maneuvers as depicted in Figures 6.17, 6.18 and 6.19. Depending on the way a driver handles a situation these phases have different length.
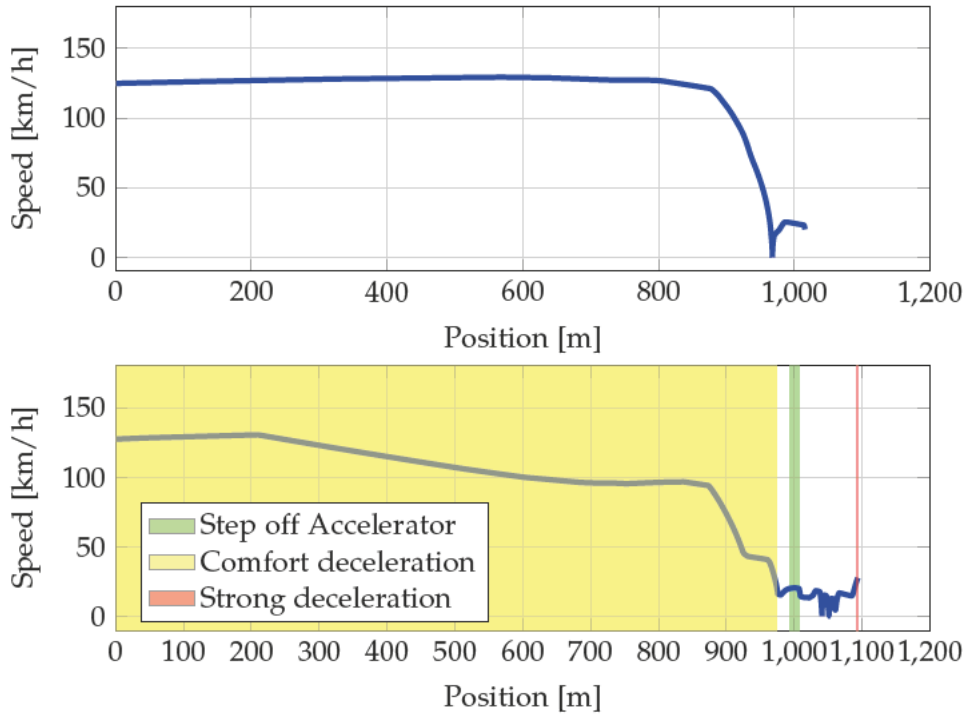
Figure 6.16: Data from the driving simulator experiment without assistance (top) and with ISPA assistance (bottom). The jam was visible 200m before.

After the first impression the reaction time begins during which no actions affecting the vehicle movement take place. Then the intended brake force is gradually applied during the pressure build-up time. Finally the driver brakes until he reaches the target speed.
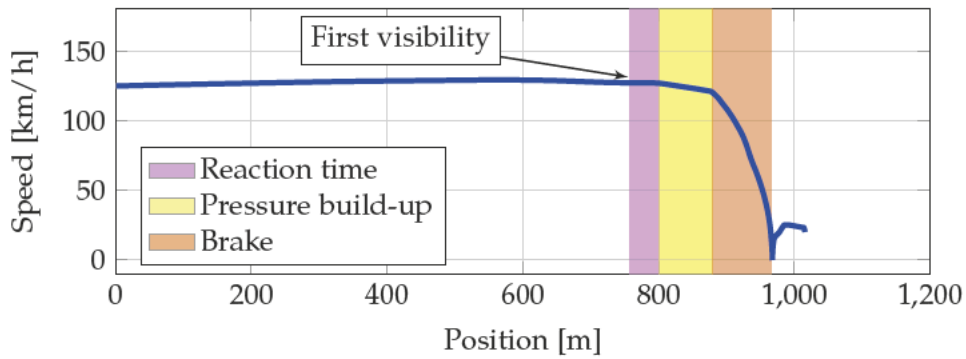
Figure 6.17: Deceleration phases of an ideal driver without ISPA assistance. He decreases speed continuously and stops 33m in front of the jam before he accelerates again to move with the jam.

The "ideal driver" has a short reaction time and estimates the distance to the obstacle precisely. During the deceleration maneuver he does not need to re-estimate the distance

141

or accelerate again causing a strictly monotonically decreasing speed. He stops with a reasonable distance in front of the obstacle, in Fig. 6.17 it is equal to 33m.
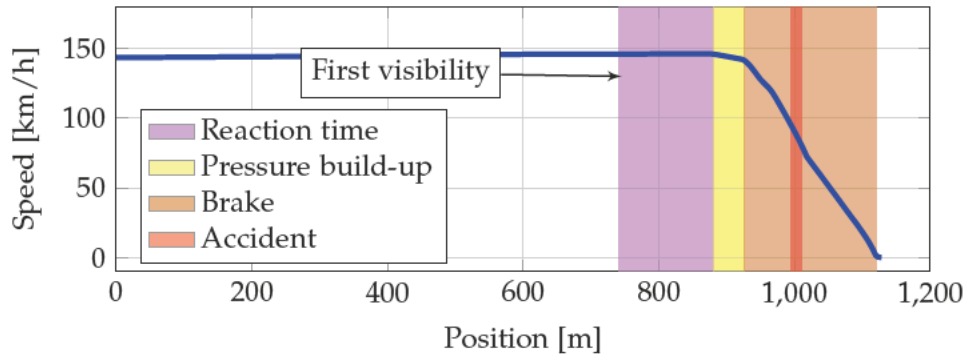
Figure 6.18: Deceleration phases of an inattentive driver without ISPA assistance. The driving simulator allows the ego vehicle to pass through other vehicles, so the deceleration is not interrupted. The event can be recognized by the gap to the leading vehicle.

An "inattentive driver" usually travels too fast for his level of alertness. As a result he reacts too late on an upcoming obstacle (see also the long reaction time in Fig. 6.18) which ultimately leads to a crash. The reason why the speed development continues nearly unaffected is the absence of a physically correct interaction between the ego vehicle and the leading vehicle in the driving simulator. In the gap distance value one can observe that a crash occurred due to jumps caused by a new leading object reference. This behavior of the driving simulator is wanted because it allows to continue the evaluation without larger impairment while the crash can still be detected.
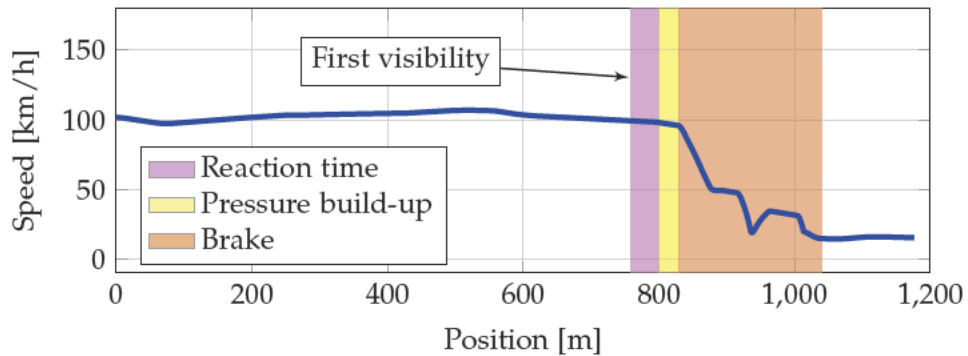
Figure 6.19: Deceleration phases of a cautious driver without ISPA assistance. The plot exhibits a stepwise deceleration and also accelerations while approaching the jam.

For a "cautious driver" it can be observed that the reaction time is comparably low with a short pressure build-up time. Then follows a sharp deceleration which is then interrupted by a re-estimation of the situation with a consecutive resumed deceleration. It may even happen that an acceleration takes place before the driver comes to a final standstill in front of the obstacle (see also Fig. 6.19).

Assisted Drivers

The speed profiles of the drivers that had ISPA assistance do not show such clear properties as the baseline drivers and cannot be categorized in this way therefore. Generally the test persons reacted on the ISPA system with a speed reduction within a reaction time of 1.0 s to 9.5 s. But the way the speed reduction was conducted ranged from simply stepping off the accelerator pedal (coasting) as in Fig. 6.20 to active braking with a stepwise deceleration as seen in Fig. 6.21. The latter drivers even showed acceleration phases which could point to the fact that they did not know precisely enough what deceleration strength is expected by the system. This ultimately led to a more extreme acceleration and deceleration behavior which caused the assistance system to switch between the different possible outputs. As soon as the drivers could see the obstacle, they chose the right deceleration strategy, in this case a strong deceleration.
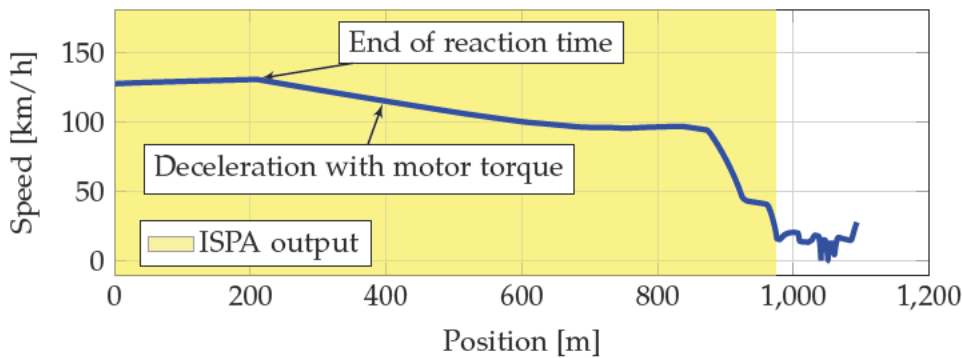
Figure 6.20: Deceleration of an ISPA assisted driver using mainly engine torque. He reacts on the system in the intended way by initially only stepping off the accelerator pedal and finally active braking.

The behavior shown in Fig. 6.21 could possibly diminish after a certain learning phase. If drivers experienced the system behavior several times together with their own observations a learning effect could smooth out their initial overreactions.
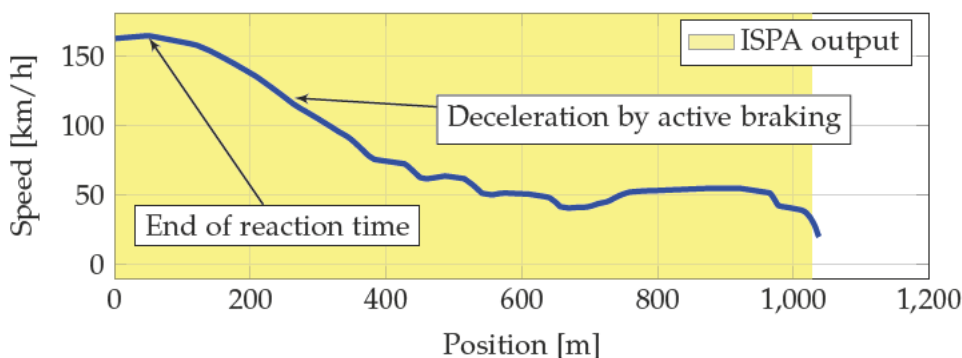
Figure 6.21: Deceleration of an ISPA assisted driver with low confidence in the system behavior. Active braking is used from the beginning causing the need for later acceleration to reach the final position.

6.3.2 Model architecture

It was already mentioned that the traffic simulator SUMO will be used for the following experiments. In order to support the required features for the planned simulation runs several changes have to be made to it. Due to its Open Source licensing scheme all of the source code is accessible which strongly facilitates any modifications.

6.3.2.1 Crash behavior

SUMO supports the implementation of additional CFM variants which can potentially be not collision free, so it also implements two options for the behavior in case of accidents:

- One of the two involved cars is removed from the simulation. A warning is issued.

- No actual collision happens and both vehicles can move through each other unaffectedly. Again a warning is issued.

In a real crash situation the involved cars stay at their current position and become an obstacle which blocks at least the related lane. This behavior has been introduced in such a way that a car stays at its position for 5 minutes after it detected a crash. The event is logged to a file and after this time period the car is removed from the simulation.

6.3.2.2 Limited visibility

The original implementation of SUMO does not implement any facilities for the calculation of driver sight or possible impairments. A way to implement a rudimentary framework for this is the usage of SUMO polygons, an example would be the forest area in Fig. 6.15. These are normally used only for visual representation of vegetation or infrastructure but can also be accessed by a CFM. Consequently the polygons can be used to define the outer shape of sight occluding objects and an individual vehicle unit can test whether there is a line of sight to a preceding car or not. Such a feature is essential if a scenario similar to the above mentioned driving simulator experiment shall be replicated in a traffic simulation.

6.3.2.3 Human reaction time

All built-in Car Following Models in SUMO do not implement any human reaction times. The only time based parameter in the IDM is the desired time gap which must not be misused as a reaction time. In order to adequately model human behavior, one or more reaction times must be implemented such as for the reaction to an external event or the output of an assistance system. From the implementation side certain inputs or reactions are delayed by a certain amount of time. Additionally the value of a certain reaction time shall vary from situation to situation within a given probability distribution.

In this work the reaction time is modeled with a Log-normal distribution ($\mu = 1.3$ s, $\sigma = 0.6$ s, see also [Tao89] and [ZAG06]) during which the driver model leaves its current state unchanged. These parameters for reaction time modeling were obtained during the approach of a traffic light turning yellow which is an event that drivers cannot anticipate exactly. A related idea is proposed by Wagner et al. in [WL03] which they call "action

points". These determine points in time at which the driver changes his behavior, for example the acceleration strategy. Similar to the approach described here the strategy remains untouched between action points.

Besides this "general" reaction time another time delay must be considered related to a reaction on an assistance system output. Analysis of the driving simulator experiment showed that this time lies within a range of 1.01 s and 9.51 s with an average of 2.58 s. For the following simulations the parameters were chosen as $\mu = 4$ s and $\sigma = 2$ s.

Additionally it takes time to build up the desired pressure in the braking system. This is accounted for with another delay of 0.3 s as described in [CSW13] in which the engine brake torque decelerates the vehicle.

6.3.2.4 Driver model without ISPA assistance

This model uses the IDM as a basis and extends it with the above mentioned features. It can be seen as a state machine that manipulates the inputs and parameters of the IDM. Like that the behavior of the previously described driver types of an ideal, inattentive or cautious driver can be resembled with a single model.
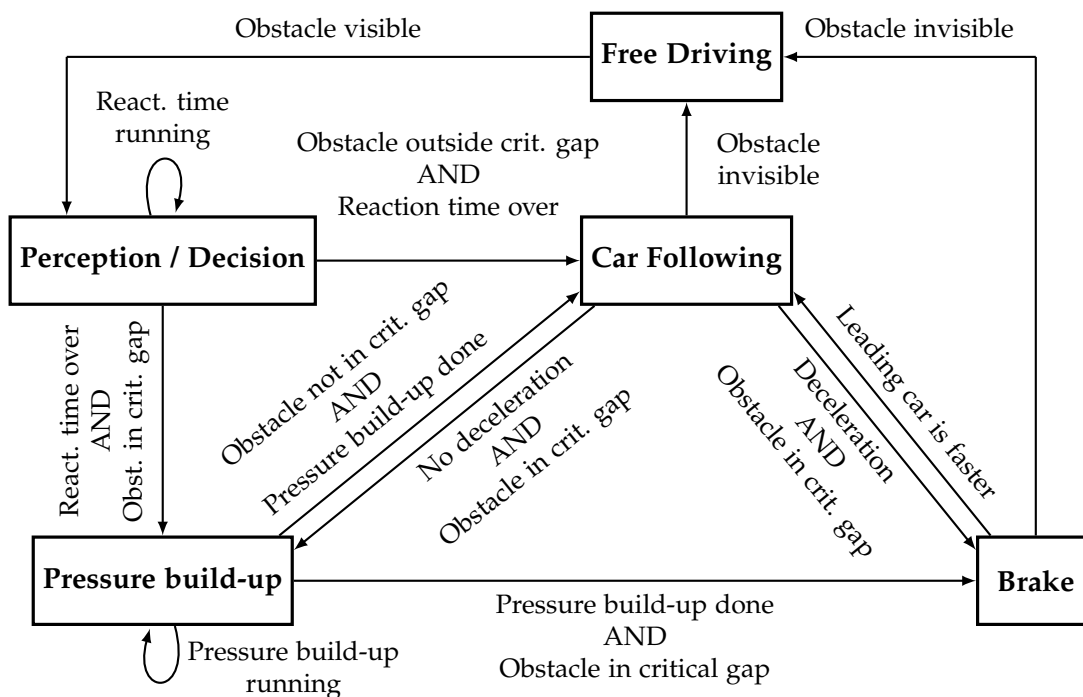
Figure 6.22: State diagram of the IDM with extensions for limited visibility, reaction time and pressure build-up time

As seen in Fig. 6.22 drivers initially travel at their desired speed until an obstacle comes into sight. After that a reaction time modeled the way described above starts running during which the driver takes no action. After that the braking maneuver is initiated which

causes a pressure build-up in the braking system. This process induces another delay of 0.3 s (see section 6.3.2.3) during which the vehicle decelerates with its engine brake torque.

Subsequently the model estimates the final distance to the obstacle within a range of -6 to 114 m. This determines the way the driver decelerates in this situation which refers to the three driver types in Fig. 6.24. Negative distances will result in a crash and relates to an unalert driver while a distance in the range of 0 - 10 m is related to an ideal driver. Larger distances are connected with a cautious driver who performs a stepwise deceleration and possibly even accelerates for a short time. The stepwise approach results in a final stopping distance which is also targeted at the 0 - 10 m range. The negative fraction of the estimation interval (6 m of overall 120 m) results in a crash rate of 5% for every approach. This value is chosen rather high for testing purposes and should be adapted to more realistic numbers.

This approach shares a similar idea as described in [WL03] where the use of so-called "action points" is proposed. These points can be interpreted as times when a driver changes his behavior due to a decision based on a previously chosen acceleration strategy or external stimuli. The latter corresponds to the described re-estimation of the targeted distance due to a local maximum in the perceived TTC value.

A different way of modeling imperfections in perceived distance and speed is described by Treiber et al. in [TKH06]. Different to the method proposed here they apply a continuous additive noise to the actual values. A noteworthy property of their implementation is the application of a stochastic Wiener process instead of white Gaussian noise as proposed by other authors. This provides a better replication of the human estimation error as this error changes slowly over time and not instantly as implied by a δ-correlated white noise.

Based on the German traffic rule of keeping a minimum gap of half the driven speed (50 m at a speed of 100 km/h) the model sets the targeted distance (the critical gap in Fig. 6.22) to the minimum stopping distance if the actual gap is smaller than the critical gap. In case of an unalert or ideal driver, one such distance estimation after the detection of an obstacle is enough. A cautious driver would stop too early if he did not change his behavior during the approach. An analysis done by Tschöpe (see [Tsc12]) of the driving simulator experiments showed that the TTC can serve as an indicator for a re-estimation of the situation if it lies below 6 s. Figure 6.23 shows two possible curves from the driving simulator for both a cautious and an ideal driver.

In the model a new distance estimation is triggered after a local minimum of the TTC value with a subsequent increase of 1 - 4 s. The actual threshold for the increase is determined randomly with a rectangular distribution within that interval. As the actual distance has become smaller during the approach, the new estimation can be made with a lower error leading to an adapted behavior. If the described behavior is turned into program logic, the flow chart in Fig. 6.24 can be obtained for it. The chart can be divided into three columns: the ideal driver in the left, the cautious driver in the middle and the unalert driver in the right column. If the initially determined final distance is below the critical gap of half the speed value in km/h, the desired gap is set to the minimum gap which leads to the ideal behavior. For a negative final distance the column for an unalert driver causing a crash is selected. Finally the middle column shows a decreasing range for the estimation of the final distance which resembles the behavior mentioned above.

The result of this model can be evaluated in Fig. 6.25 which shows both the speed and TTC development of an ideal and a cautious driver. It can be noticed that the model
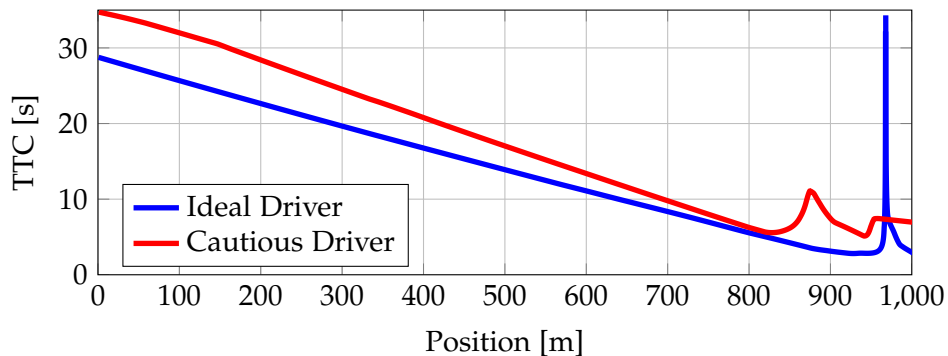
Figure 6.23: TTC values from the driving simulator experiment of an ideal and a cautious driver. The ideal driver has a steadily decreasing TTC while the cautious driver has several local maximums in the curve.

produces comparable TTC values and speed development with the typical shape for both driver types from the driving simulator.

The curves produced by the model can also be compared to the behavior of selected real drivers in the driving simulator. Figure 6.26 shows both speed curves, the chosen parameters for the model are 1s reaction time and a minimum gap of 18m. Similarly the plots in Fig. 6.27 show that also the cautious driver behavior can be met very closely, albeit with a different parameter set. These two examples show that the basic model structure allows for the production of such curves if the parameters are chosen adequately. As mentioned previously for the reaction time, the distance estimation etc. should be implemented with random values based on probabilistic measures if used in a "general purpose" simulation.

6.3.2.5 Driver model with ISPA assistance

To this point the behavior of the unassisted drivers has been modeled with a modified IDM. In order to test the impact of the ISPA system, its output and the driver reaction on it must also be included in the CFM. The first implementation with the static deceleration model implemented a fixed delay for the deceleration after an output of the ISPA system. In the simulator experiments drivers showed a different behavior which included two different reaction times: one for the delay after the first assistance output and one for changes in the output. Here it is assumed that the delay on a change in the output is equal to the general reaction time of a driver. The delay after the first assistance output is higher as the drivers are unalert of a potential event. This is a similar idea to the different reaction times during normal driving depending on the alertness of drivers (see also [ZAG06]). As mentioned before the initial reaction time lied within the interval of 1.01 - 9.51 s with an average of 2.58 s. The second reaction time for a change in assistance output is chosen with $\mu = 1.3$ s and $\sigma = 0.6$ s. Both times are modeled with a log-normal distribution.

The initial goal of a unified model for normal and assisted driving which also avoids model switching has been reached with this implementation. Instead of switching between two very different models (a car following model and a predefined speed curve) the
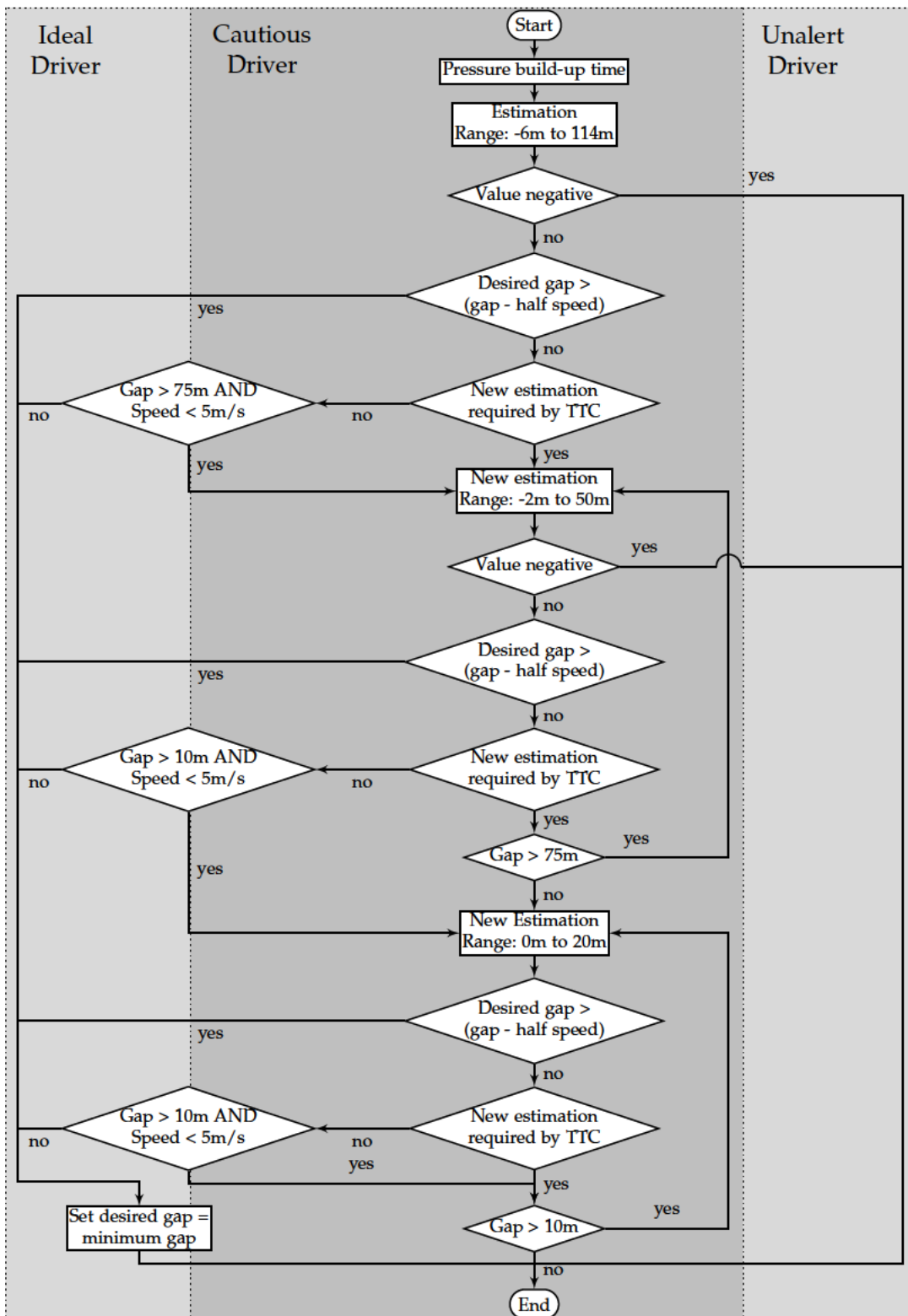
Figure 6.24: Flow chart for the distance estimation of the extended IDM.
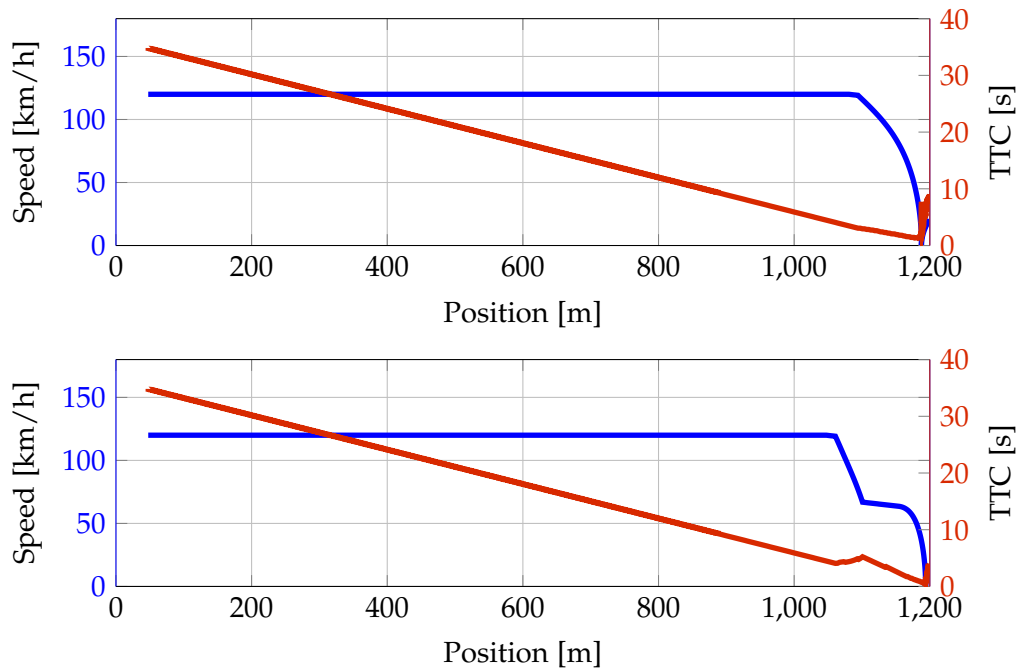
Figure 6.25: TTC values from the modified IDM of an ideal (top) and a cautious (bottom) driver. Both types show the same characteristics (speed and TTC development as the real drivers in the experiment.

proposed model is much closer to the real correlation between the driver and the assistance system. Now the basic car following behavior is equal for the unassisted and the assisted driver with the ISPA system providing earlier information about upcoming obstacles.
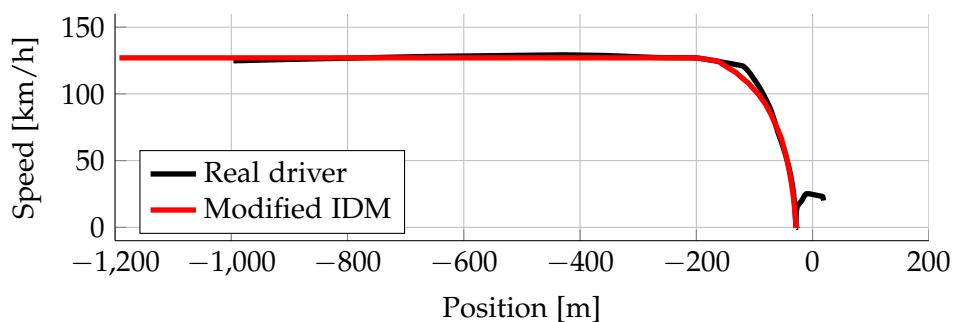
Figure 6.26: Comparison of a selected real driver and the model of an ideal driver with the modified IDM. The chosen model parameters are 1s reaction time, an initial speed of 35,28 m/s and a minimum gap of 18m.
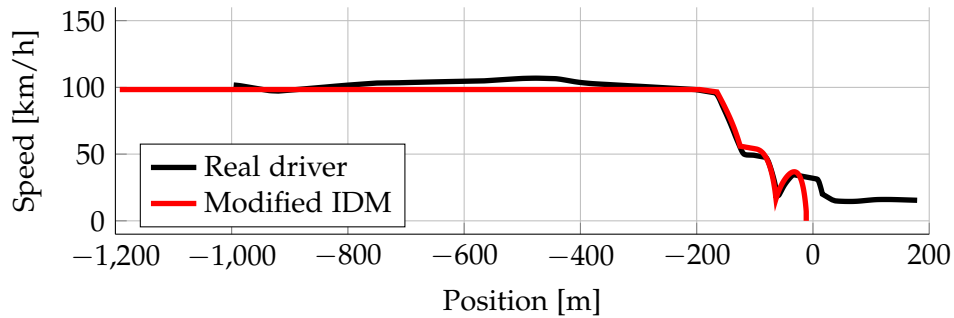
Figure 6.27: Comparison of a selected real driver and the model of a cautious driver with the modified IDM. The stepwise deceleration can be resembled very closely by the model.

6.3.3 Traffic simulation with a single test vehicle

In the next steps the new CFM and its impact on a larger traffic scenario shall be tested. As described previously the traffic simulation SUMO serves as framework for this which allows the conduction of batch simulations. Like that different equipment percentages can be simulated with several simulation runs. Similar to the previous experiments the scenario of approaching a standing traffic jam behind a curve on a highway (see 6.15) is used for these simulations. The parameters in Tab. 6.3 define the car following behavior.

Because several of the parameters are modeled not with fixed values but with random variables based on probability distributions the model produces different behaviors without the need for explicit modeling. This can be observed in Fig. 6.29 where the different driver types cause ideal (blue graph in upper plot), unalert (red graph in upper plot) or cautious behavior (other graphs).

Now it is possible to conduct experiments in batch with one vehicle approaching the traffic jam. For both baseline and assisted driver configurations three simulation sets with 100 simulation runs each are used. This results in overall 300 simulation runs per configuration and still allows an observation of the variations within one configuration.

Parameter	Value
Comfortable deceleration	2.0 m/s^2
Comfortable acceleration	1.4 m/s^2
Maximum deceleration	10.5 m/s^2
Maximum acceleration	6.5 m/s^2
Reaction time / ISPA T_2 (μ)	1.2 s
Std. dev. React. time / ISPA T_2 (σ)	0.6 s
ISPA T_1 (μ)	4.0 s
Std. dev. ISPA T_1 (σ)	2.0 s

Table 6.3: Parameters set of the modified IDM for the batch simulation.
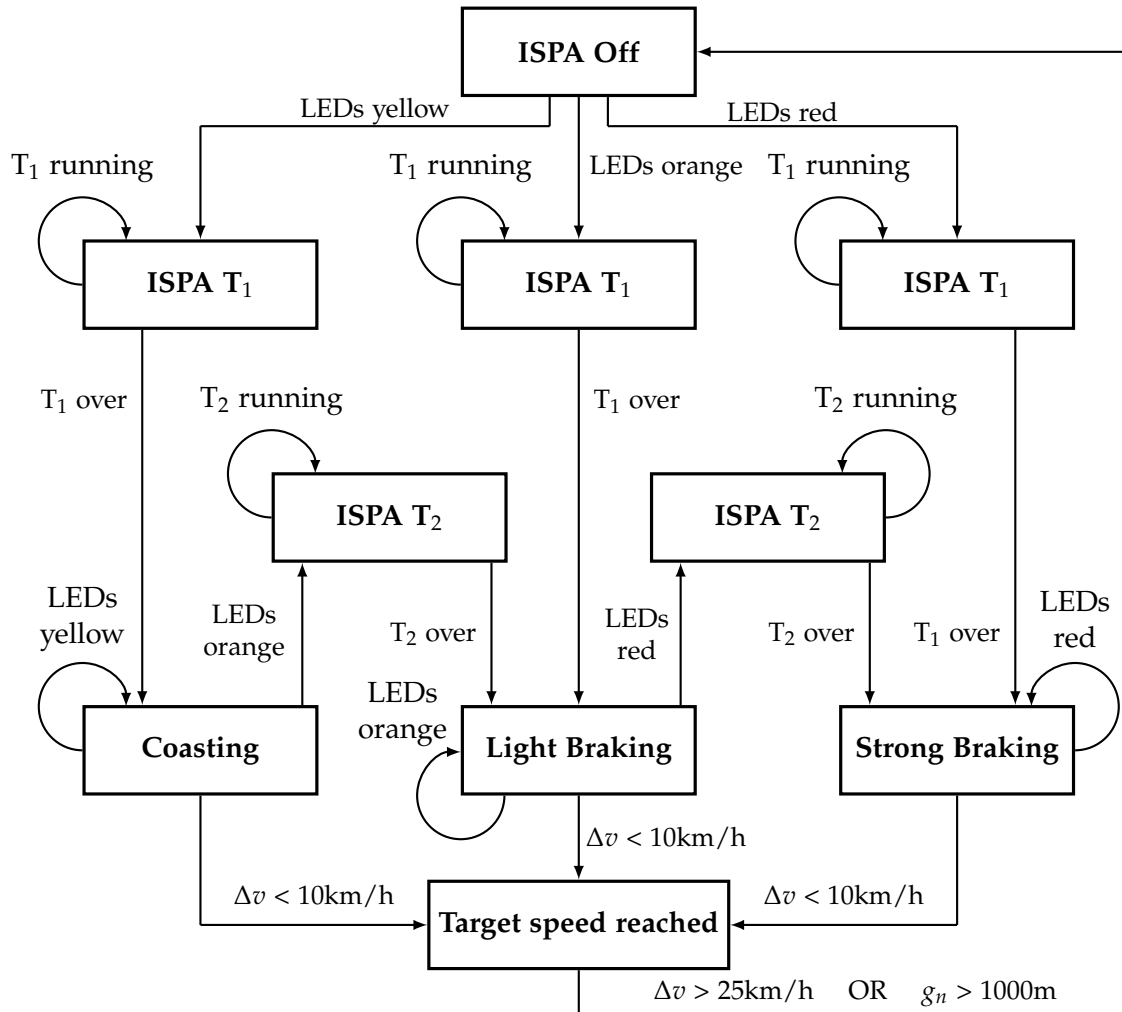
Figure 6.28: State diagram of the driver reactions on ISPA outputs. The different braking states are implemented by a different state machine.

Three metrics are calculated for every simulation set: average minimum TTC, number of crashes and average fuel consumption (based on the HBEFA, see [KH04]).

A first result that can be obtained from Tab. 6.4 is the increased crash rate for the baseline drivers. The most likely reason for this is the earlier beginning of the deceleration phase of the assisted drivers which allows more adaptation to the actual situation. As mentioned before the a-priori crash rate of 5% of all obstacle approaches is chosen rather high but provides a clearer result for an evaluation like this. Also the TTC values of the simulation show a clear safety improvement for the ISPA system. Finally the fuel consumption is also improved in the assisted case as has been shown in the driving simulator experiments. The relative improvement of fuel consumption seems to be high but one must consider that this is only valid for the deceleration phase which is comparably short in relation to the overall travel time. A last result of this experiment are the variations in the derived metrics even for the same model configuration and the same scenario.
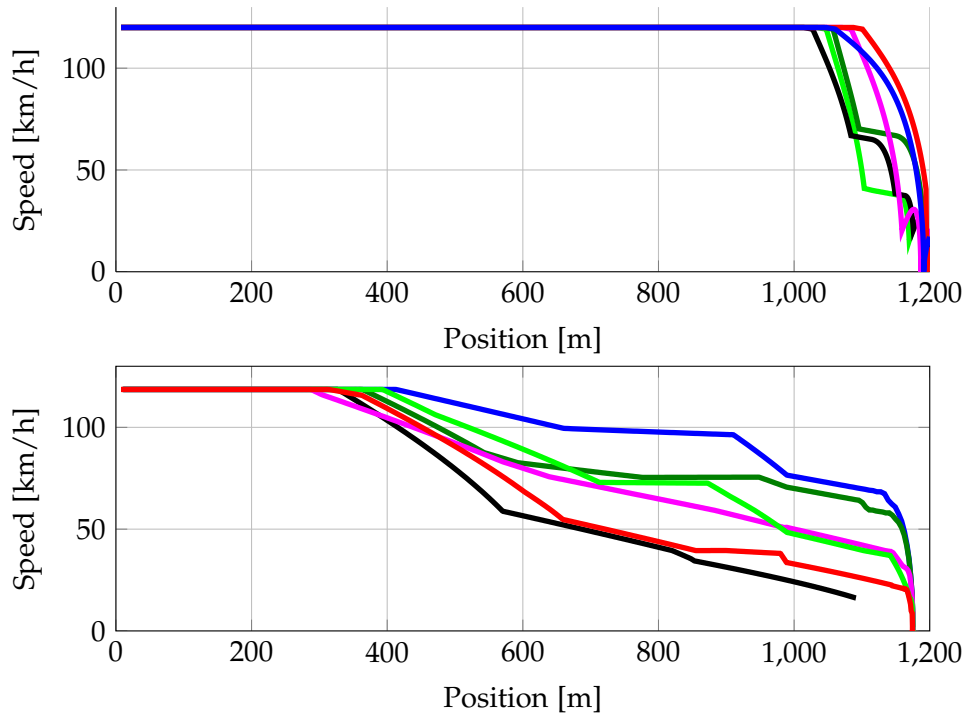
Figure 6.29: Simulation of the highway scenario with random parameter values for the baseline model (top) and assisted model (bottom). Coloring: Ideal driver (blue), unalert driver (red), cautious driver (others).

6.4 A multi lane Car Following Model

The goal introduced in this chapter is to obtain a CFM which resembles the behavior of assisted and baseline drivers close enough to conduct simulations on a larger scale. Ideally it would be possible to draw conclusions about the changes in driver behavior from the differences in the model parameters. One aspect that has not been covered to this point is the fact that human drivers do not only use a single leading vehicle on the same lane but several surrounding vehicles. This is called multi-anticipation or spatial anticipation in

Group	ISPA	Crashes	TTC [s]	Fuel cons. [l/h]
1	yes	1	1.415	1.337
2	yes	0	1.302	1.322
3	yes	0	1.428	1.294
4	no	8	0.967	4.391
5	no	8	0.997	4.374
6	no	7	0.996	4.335

Table 6.4: Configuration and results of the batch simulation runs with the modified IDM.

the literature (see [TKH06], [OH06], [LWS99] and [Che+09]) and is also referred to as the reason for extremely low time headways (down to 0.3s) while maintaining collision free behavior.

As proposed by the publications mentioned before, the ability of human drivers to safely follow leading vehicles at time headways much smaller than their reaction time (factor 2-3, see [TKH06]) seems to be related to the ability to anticipate upcoming fluctuations. As the ISPA system shall improve drivers' anticipation capabilities it is considered a feasible step to incorporate such an extension also to the previously developed CFM.

6.4.1 From a single lane to a multi lane approach

Several approaches have been made to extend an already existing CFM to take not only one leading vehicle into account but several of them. The question of how "important" a certain vehicle is to the driver depending on its relative position is solved very differently by the models in the literature. The following paragraphs give a short survey about some designs and finally describe the idea behind the Behavior Map.

Extension of the Optimal Velocity Model

This model has originally been proposed by Bando et al. in [Ban+95] and has then been adapted by Lenz et al. in [LWS99]. They suggest that a vehicle n reacts on up to m cars ahead out of a total of N cars with an individual weight a_j for each preceding car. These weights are not determined empirically or based on any further assumptions, the only restrictions are the definition of an overall sensitivity a and a decreasing weight for increasing distance:

$$a = \sum_{j=1}^{m} a_j \quad \text{with} \quad a_j/a_1 \leq 1, \quad j = 2, 3, ..., m \tag{6.25}$$

The overall function defining the car following behavior is defined as follows:

$$\ddot{x} = \sum_{j=1}^{m} a_j \left\{ V \left(\frac{x_{n+j} - x_n}{j} \right) - \dot{x}_n \right\} \quad \text{with} \quad n = 1, 2, ..., N \tag{6.26}$$

$$V(x) = \tanh(x - h) + \tanh(h) \quad \text{with} \quad h = const. \tag{6.27}$$

In the case of $m = 1$ the model is equal to the original version. The authors chose the weight factors for $m = 2$ as $a_2/a_1 = 1/2$ and for $m = 3$ as $a_2/a_1 = 1/2$, $a_3/a_1 = 1/4$ respectively. Higher numbers of observed vehicles lead to an increased traffic density and flow while the average speed is decreased. The basic principle can be summarized as a superposition of weighted interactions with each car.

Extension of the Intelligent Driver Model in the literature

The IDM has been extended by its authors in a comparable way as described above (see [TKH06]). They introduced a finite reaction time, limited estimation accuracy for relative

speed and distance with additional noise and finally an extension named the Human Driver Model (HDM). According to Treiber et al. the HDM can be seen as a meta model introducing the mentioned limitations introduced by human cognition. Consequently it is not limited to be applied only to the IDM but could be used with other time continuous models as well. Microscopic CFM that have an equation of the shape

$$\frac{\mathrm{d}v_n}{\mathrm{d}t} = a^{mic}(g_n, v_n, \Delta v_n) \tag{6.28}$$

can be extended with the HDM, where v_n denotes the ego vehicle speed, g_n the gap to the leader and Δv_n the relative velocity resulting in an acceleration a^{mic} of the ego vehicle.

The HDM introduces a finite reaction time T' which represents the time delay that must be applied to all input stimuli of the model. It must be distinguished between T' and T which is actually the safe headway time. In case that T' is not a multiple of the update time interval Δt, Treiber et al. suggest the following interpolation:

$$x(t - T') = \beta \cdot x(t - n - 1) + (1 - \beta) \cdot x(t - n) \tag{6.29}$$

In this case x stands for any input stimulus, n is the number of delayed time steps resulting from the integer result of $n = T'/\Delta t$. The interpolation factor β is determined by $\beta = (T'/\Delta t) - n$. As mentioned before the limited estimation capabilities of drivers for the net distance g and the speed difference Δv are modeled by additive noise produced by a Wiener process (see [Gar09]):

$$g_{est}(t) = g(t) \cdot \exp(V_g w_g(t)) \tag{6.30}$$
$$(\Delta v)_{est} = \Delta v(t) + g(t) r_c w_{\Delta v}(t) \tag{6.31}$$
$$\text{with} \quad V_g = \sigma_g / \langle g \rangle \; : \; \text{Variation coeff.} \quad \text{and} \quad \sigma_g^2 = \langle (g - \langle g \rangle)^2 \rangle \tag{6.32}$$
$$1/r_c : \text{average estimation error for TTC}$$
$$w_s(t), w_{\Delta v}(t) : \text{stochastic variables of independent Wiener processes } w$$
$$\text{with variance 1 and correlation time } \tau$$
$$\frac{\mathrm{d}w}{\mathrm{d}t} = -\frac{w}{\tau} + \sqrt{\frac{2}{\tau}} \cdot \xi(t) \tag{6.33}$$
$$\text{with} \quad \langle \xi \rangle = 0 \,, \quad \langle \xi(t)\xi(t') \rangle = \delta(t - t')$$

For the numerical implementation the authors of [TKH06] chose the following approximation:

$$w(t + \Delta t) = w(t) \cdot e^{-\Delta t/\tau} + \sqrt{\frac{2\Delta t}{\tau}} \cdot \eta(t) \tag{6.34}$$

Here $\eta(t)$ are independent realizations of a random variable with Gaussian distribution, $\mu = 0$ and $\sigma^2 = 1$.

The estimation of the ego velocity was assumed to be perfect because drivers can read the speedometer with sufficient accuracy. The authors also supposed that the estimation error for Δv is proportional to the gap distance and consequently the TTC would have a constant estimation error.

Regarding anticipation Treiber et al. distinguish between temporal and spatial anticipation. For the temporal anticipation they introduce anticipation of the future gap (also found in [Dav03]) as well as the future velocity with a constant-acceleration heuristics. Together with the modifications explained above the following input variables with temporal anticipation for the underlying CFM of a vehicle n can be defined:

$$\frac{\mathrm{d}v_n}{\mathrm{d}t} = a_{mic}(g'_n, v'_n, \Delta v'_n) \tag{6.35}$$

$$\text{with} \quad g'_n(t) = [g_n^{est} - T'\Delta v_n^{est}](t - T') \tag{6.36}$$

$$v'_n(t) = [v_n^{est} + T'a_n](t - T') \tag{6.37}$$

$$\Delta v'_n(t) = \Delta v_n^{est}(t - T') \tag{6.38}$$

The authors state that human drivers have very limited capabilities of judging the acceleration of a different vehicle. Therefore they replaced the constant-acceleration heuristics by a constant-velocity heuristics.

For the spatial anticipation, especially for multiple leading vehicles, they propose to split the acceleration term of the used CFM into a free road term and an interaction term:

$$a_{mic}(g_n, v_n, \Delta v_n = a_n^{free} + a^{int}(g_n, v_n, \Delta v_n) \tag{6.39}$$

Now the multi-anticipation can be implemented for the interaction term by summing the interaction accelerations of the nearest ego vehicle (n) - leader (i) pairs with a number of m pairs (the input stimuli for each pair are determined by Eq. 6.36, 6.37 and 6.38):

$$\frac{\mathrm{d}v_n(t)}{\mathrm{d}t} = a_n^{free} + \sum_{i=n-m}^{n-1} a_{ni}^{int} \tag{6.40}$$

$$\text{with} \quad a_{ni}^{int} = a^{int}(g_{ni}, v_n - v_i) \quad \text{and} \quad g_{ni} = \sum_{j=i-1}^{n} g_j \quad \text{(sum of all net gaps)} \tag{6.41}$$

For simplicity reasons the basic equations already described in Eq. 6.12 and 6.13 shall be repeated here:

$$\dot{v}_n = a_n \left[1 - \left(\frac{v_n}{v_{n,0}} \right)^{\delta} - \left(\frac{g_n^*(v_n, \Delta v_n)}{g_n} \right) \right] \tag{6.42}$$

$$\text{with} \quad \square_n : \text{Index of n-th vehicle}$$

$$\square_{n-1} : \text{Index for the preceding vehicle of the n-th vehicle}$$

$$g_n^*(v_n, \Delta v_n) = g_{n,0} + \max \left(0, v_n T + \frac{v_n \cdot \Delta v_n}{2\sqrt{ab}} \right) \tag{6.43}$$

If the HDM is then applied to the IDM, the equilibrium gap is defined as follows (index n is neglected here for better readability):

$$g_e(v) = \gamma \cdot g^*(v, 0) \left[1 - \left(\frac{v}{v_0} \right)^{\delta} \right]^{-1/2} \tag{6.44}$$

$$\text{with} \qquad \gamma = \sqrt{\sum_{\alpha=1}^{m} \frac{1}{\alpha^2}} \qquad (6.45)$$

The effect is that the new equilibrium distance is γ times higher than the original one. In order to compensate this, the following IDM parameters must be normalized:

$$g_0^{norm} = \frac{g_0}{\gamma} \qquad \text{and} \qquad T^{norm} = \frac{T}{\gamma} \qquad (6.46)$$

By this design the maximum factor γ for an infinite number of anticipation relevant vehicles would be $\pi/\sqrt{6} = 1.283$ which relates to a maximum increase of the equilibrium distance of ca. 28%.

Extension of the Intelligent Driver Model with the Behavior Map

The selected approaches from the literature which extend an existing model to take several leading vehicles into account do this only for the ego lane. A simulation framework that takes adjacent lanes into account (but only slower lanes) is the Aimsun simulator (see also [Bar10]). It calculates the average speed of the adjacent lane and only accelerates to speeds within a certain threshold around the adjacent lane speed. This behavior can be observed frequently in real traffic, a very extreme form of it are traffic jams originating from an accident on the opposite direction lane where no actual obstacle would slow down drivers.

A different example for a situation causing unrealistic behavior of a single lane model would be a highway scenario with several leading cars. If the leading car on the ego lane is for some reason very far away as compared to the others on adjacent lanes, a conventional model would possibly speed up and overtake at high speed. A real driver would not pass through the other leaders at all or only at very low relative speeds.

In cases where a higher level logic combines the CFM with a LCM the speed might be adapted to the average speed on an adjacent lane in case of an upcoming lane change. This has been explained e.g. by Luo et al. in [LB12].

Another justification for the development of a different extension is the fact that all approaches regarding the implementation of multi-anticipation use more or less arbitrary weights for the vehicles taken into account. Either they are treated equally with no relation to the actual distance (see the HDM), or guessed values (see the extension of the Optimal Velocity Model (OVM) above) or a exponentially decreasing weight as proposed by Zhu et al. in [ZJ07]. None of these try to use data from traffic recordings or driving simulator experiments to obtain a realistic weight distribution. Also they do not cover the question how variable driver types could be achieved by systematically altering the weights.

Finally the Behavior Map shall be applicable as a general purpose meta model comparable to the HDM mentioned above. In our case it will be combined with the IDM, but it is not necessarily limited to that.

6.4.2 Development of the Behavior Map

The Behavior Map (BM) is on the one hand inspired by the occupancy grid maps often used in autonomous robots and cars (see [ME85]) and the idea how human drivers could perceive

and segment space around them (see also [Laq+13] and [Gus13]). Different patterns how this segmentation could be done are depicted in Fig. 6.30. The segmentation allows a simple analysis of recorded data and provides a way to condense the data in order to store it for later use in a CFM.

For the first shape of the BM (Fig. 6.30(a)) circles are used to subdivide the area around the ego vehicle. This way the distance to a vehicle would be taken into account, but neither the lateral position nor its lane would be reflected in any way. In the second map shape (Fig. 6.30(b)) the environment is clustered like pie slices. This could be interpreted as the opposite idea of the concentric circles as it only regards relative angular position and not the relative distance. Finally the grid shape depicted in Fig. 6.30(c) shows an approach already known from autonomous vehicles as described in [ME85]. This is also the shape that has been chosen for the following developments with the only but noteworthy difference that the grid is aligned to the road shape. In the case of using a traffic simulation this is a very straight forward implementation as such a simulation usually organizes its data in a structure built of nodes and connecting edges. Consequently this alignment can easily be done by taking the lanes as the rows of the grid (or matrix) and the columns refer to uniform distance intervals along the track. This way the BM inherently has a shape that could mimic human understanding of the traffic scene better than a rigid rectangular grid.

Each cell has the width of the corresponding lane and a length of 7.5 m. In the implementation presented here the BM has 53 columns resulting in a coverage of 400 m ahead of the driver. This corresponds to the distance resulting from a general desired time headway (see [Ayr+01]) and the recommended speed on German highways of 130 km/h. A number of 5 rows correponds to a coverage of two adjacent lanes on each side, so a highway with three lanes can always be monitored completely within the regarded distance independent on the chosen lane. The presented experiments only cover highway scenarios so a fixed size of the cell length causes no problems. However different scenarios like driving in dense city traffic might require different dimensions of the cells and also new measurements for the metrics contained in the map.

(a) Concentric Circles   (b) Pie Slices   (c) Grid
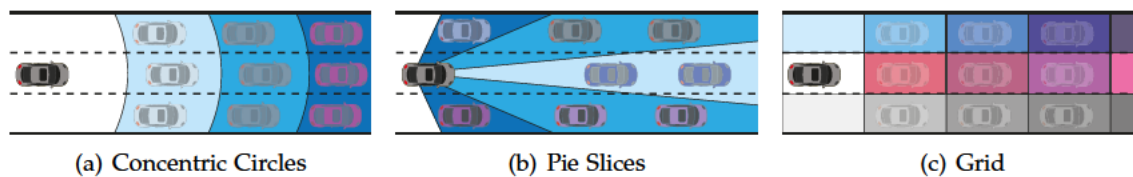
Figure 6.30: Possible patterns for subdividing the area surrounding the driver. Cars within the same color field are merged into one object.

Each cell of the BM stores an arbitrary number of metrics needed for the underlying CFM. Here the metrics are TTC, relative speed, time headway and a weight index "Importance Weight Index (IWI)". It is important that the BM does not only store the IWI values as this would mean that vehicles on an adjacent lane would be treated with the same desired time headway as a vehicle on the ego lane. In contrast a real driver could chose a lower time headway for a neighbor vehicle due to a lower collision probability than for a direct leading vehicle.

Then the BM can be applied by first determining which grid cells are occupied by a vehicle and then calculating the input stimuli for the CFM. By partitioning the area around the ego vehicle with a grid, the movement of a leading vehicle between different grid cells would lead to jumps in the values communicated to the underlying IDM models. This would in turn lead to unsteady movements of the ego car, so it is necessary to determine the exact position of a vehicle within a grid cell to compute a linear interpolation with the neighboring cells. This way a smooth reaction on a vehicle moving over several cells can be achieved.

Together with the previously stored metrics the traffic simulation evaluates the underlying CFM and calculates a speed value for this time step. When this has been done for all grid cells the speed values are summed up weighted by the IWI for each cell. The final speed value is then being communicated to the simulation.

Importance Weight Index

The IWI shall ideally be a representation of how important a vehicle (or cell of the BM) is to the driver. One way to obtain this index could be to ask the drivers, but this is an approach leading to very subjective values and is therefore neglected. Some authors (see [MAP11]) state that drivers use the inverse TTC (1/TTC) as an indicator of the required braking strategy. This could also be interpreted in such a way that the inverse TTC indicates how important it is to react to a certain vehicle. As the TTC depends on the current speed but the BM remains unchanged regardless of the speed (at least in this implementation), it was chosen to use the inverted relative speed ($1 - \Delta v_{norm}$). The idea behind this is also that low relative speeds to a certain vehicle could indicate that it is of special importance to the driver and that he follows the leader's speed profile closely. This assumption is obviously only true in relatively homogenous and dense traffic. In contrast to that a considerably slower car even on the neighbor lane could cause a real driver to slow down and avoid a lane change, in which case the inverted Δv would be very small. So the proper importance indicator or selection process for general use is still to be defined.

For the following experiments the IWI is defined as follows:

$$\text{IWI} = 1 - \frac{|\Delta v| - |\Delta v|_{min}}{|\Delta v|_{max} - |\Delta v|_{min}} \tag{6.47}$$

with

- $|\Delta v|_{min}$: global minimum of all absolute relative speeds in the BM

- $|\Delta v|_{max}$: global maximum absolute relative speeds

- $|\Delta v|$: absolute value of relative speed for this cell

In that way the IWI is normalized to an interval of [0...1] and finally stored in the Behavior Map.

Executing the Behavior Map

When a simulation is started vehicles are instantiated at runtime. Some of the required static parameters like desired speed, maximum acceleration and deceleration etc. can already be defined by the existing SUMO framework. Additionally the desired BM must be selected from three possible choices: from one random driver of the driving simulator experiment, a random linear combination from a certain driver group or a random linear combination of the whole test corpus. Especially the possibility to generate a behavior map from a certain group provides the possibility to create an individual Behavior Map while still controlling the overall behavior characteristics. This way it is possible to obtain an infinite number of (synthesized) parameter sets even for the BM approach.

After the initialization, the actions described in the following paragraphs are executed for every simulation step. One essential step is to fill the so-called "Vehicle Map" which is used to access all vehicles covered by the Behavior Map. This is necessary because SUMO originally does not support the use of several leading vehicles and provides only information about the first leading car on the ego lane. The Vehicle Map with the same dimensions as the Behavior Map stores the following parameters for every contained vehicle:

- Vehicle Index: Individual number to identify every vehicle in the simulation

- Speed: Velocity of the vehicle

- Relative Speed: Differential speed related to the ego vehicle

- Distance: Distance along the track relative to the ego vehicle

- Time Headway: temporal headway to the ego vehicle

- Interpolation: Value in the range [0...1] representing the relative position in a grid cell, used for the interpolation of BM metrics

This way the information provided by the car following API about the direct predecessor is extended to a map of the relevant surrounding vehicles.

Application of the IDM with dynamic Time Headway   As described before the underlying CFM is evaluated for every vehicle in the Vehicle Map. This means that the IDM is executed on a single vehicle with the static parameters from the SUMO API and a THW value obtained from the Behavior Map. The values for relative speed Δv_n and gap distance g_n come from the Vehicle Map while the minimum gap $g_{n,0}$, the desired speed $v_{n,0}$, comfort acceleration a and deceleration b are provided by SUMO.

The output of the IDM is an acceleration value which has to be converted to a speed value by multiplication with the time step length of the simulation. This needs to be done because the car following API expects a speed value rather than an acceleration value. After that several constraints must be applied to the speed output of every car in the Vehicle Map before they can be merged using the IWI values in the BM.

Behavioral constraints   Some constraints need to be formulated due to the nature of the BM. Without such rules it would not be possible for a vehicle to overtake another vehicle on an adjacent lane as this would be treated nearly the same as if it was on the ego lane. This can be solved by comparing the relative speed for the next time step with the relative speed stored in the BM for that position. If the relative speed derived from the underlying IDM is smaller than the value in the BM, the free road term of the IDM is used with a desired speed set to the relative speed from the BM.

As a result the ego vehicle can overtake other cars on lanes to the right because they have positive relative speed values stored in this Behavior Map region.

Another constraint must be introduced for the case that the ego vehicle is being overtaken by vehicle located in a cell of the map with a high headway time. Without further rules the ego vehicle would decelerate strongly even if there is no objective need for it. Again this can be circumvented by analyzing the relative speed. If it is negative (the other vehicle is faster), the old speed value is kept. This is a comparable behavior to the constant-speed or constant-acceleration heuristics found in the EIDM and the HDM.

Deriving a final speed value   At runtime the IWI is determined based on the saved Behavior Map for every vehicle in the Vehicle Map and the obtained list is then sorted by the IWI value. If two entries have the same value, the vehicle which is spatially closer gets the higher rank. Then the values are summed up until the sum reaches 1 or the list ends. In case there are not enough vehicles to reach an IWI sum of 1, the remaining IWI is used with the speed value of the free road term. This also has the effect that drivers approach other vehicles (if the desired speed is higher than the speed choice of the BM) until the factor for the free road term reaches zero.

This way a limited capacity of the driver observing several vehicles can be modeled. The vehicles which contribute to the IWI sum are then used for the final speed calculation. Now a single speed value can be determined by calculating a weighted average of the relevant vehicle speeds with the IWI values used as the weight factors. Finally several external constraints are applied to the final speed value.

External constraints   Several hard constraints for the final speed value must be taken into account like speed limits, maximum acceleration and deceleration and maximum speed of the vehicle. In case one of these constraints is exceeded, the corresponding value is set to the constraint value. Additionally it must be ensured that the speed value is equal or greater than zero because SUMO only allows forward driving or standing vehicles.

6.4.3   Experiments with real drivers

Now that the framework for the BM is set up, the last necessary step is to obtain the contents of it with a driving simulator experiment. In order to obtain these metrics it would theoretically also be possible to analyze real traffic data or to take it from a driving simulator experiment. The latter one probably produces less realistic results but has the advantage that drivers experience exactly the same scenario with or without assistance. If the impact of the ISPA system shall be analyzed also from the contents of the BM, this is

an important prerequisite. Such a constellation is usually not possible in real traffic and therefore a simulator study was chosen to generate the desired data.

6.4.3.1 Driving simulator setup and assistance system

For this experiment the simulator environment developed in Chapter 5 was used to provide the best spatial perception for an experiment involving anticipation. Figure 6.31 shows an outside view of the setup including the CAVE, the cockpit mockup and the ISPA system.

Figure 6.31: View of the driving simulator consisting of a real car cockpit with the ISPA LED system and the CAVE for environment projection

Here the latest version of the ISPA system using RGB-LEDs in combination with an icon in the instrument cluster and a distance bar was chosen. The driver view of it can be seen in Fig. 6.32. The ISPA system is distributed over several functional blocks where the instrument cluster and the LED control software are executed on a dedicated computer. The internal logic runs inside a Virtools Building Block which takes the necessary information from the ego car physics and traffic simulation and only sends the proposed deceleration strategy and the obstacle distance to the HMI functional block.

6.4.3.2 Experiment design

The driving simulator experiment shall serve as the basis for the subsequent development and evaluation of the BM. Additionally it is aimed to deliver data for assisted and baseline drivers in order to derive differences in behavior from the BM contents. Due to the limited time and participant number in the experiment, the tasks must be chosen well in order to create Behavior Maps without too many uncovered areas. This is especially difficult if traffic density is low and the scenarios should not become too complicated to avoid any side effects originating from high mental workload.

Figure 6.32: ISPA output devices: RGB-LED array on top of the dashboard for encoding distance and proposed deceleration strategy, icon graphics in the instrument cluster depicting the obstacle type and the distance

Figure 6.33 shows the configuration of the different tasks that are carried out on the 10 km track. As mentioned before it is desired to cover as much of the BM as possible with the available test drivers. As a consequence they were asked to fulfill certain requirements without changing their car following behavior. In the "Frontal Following Task" drivers had to follow a group of leading vehicles, in any configuration there was a vehicle present on the ego lane. They were also asked to avoid dangerous situations and not to overtake if anyhow possible. The upper part of Fig. 6.33 shows which subtasks had to be accomplished whereas the last subtask included cars which had ISPA assistance. The leading vehicles were programmed with a changing desired velocity in order to force the test persons to react on those speed changes. Otherwise the situation would become very static after the test person settled at his equilibrium distance which could lead to a sparsely covered BM.
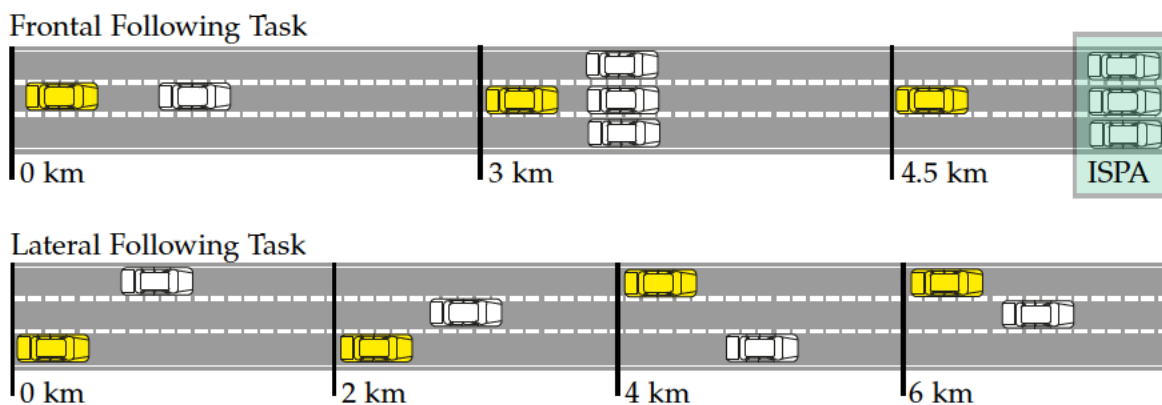
Figure 6.33: Configuration of the track for the Behavior Map driving simulator experiment. Yellow Car: Test person vehicle, white cars: vehicles controlled by SUMO

In the lateral following task (Fig. 6.33 lower part) drivers were instructed to follow a leading car. It drives on a different lane, the respective relative lane positions are depicted in Fig. 6.33. Just like in the task described before they were not allowed to overtake even if this would be their decision in a real world scenario. Again the intention behind this was to obtain a better coverage of the BM. For this task no ISPA assistance was activated as it only uses cars on the same lane which is by definition not the case here.

Finally the test drivers were situated in a free driving task which lasted for the whole 10 km track. The idea is to record driver behavior as naturally as possible and to increase the BM coverage even more.

It is not possible to obtain the desired metrics for the BM from all tasks as already mentioned for the lateral driving task. Table 6.5 shows a matrix of possible metric-task combinations. Especially the IWI and relative speed are only derived from the natural driving task while the desired THW is taken from all tasks. As the distinction between metrics obtained from assisted or baseline drivers shows that two different Behavior Maps are derived from the experiment. The scenario is located on a three lane highway with a

Task	THW	Δv	IWI	THW_{ISPA}	Δv_{ISPA}	IWI_{ISPA}
Frontal Follow	x					
Frontal Follow (ISPA)				x		
Lateral Follow	x			x		
Free Driving	x	x	x			
Free Driving (ISPA)				x	x	x

Table 6.5: Obtainable behavior metrics (Time Headway (THW), relative speed (Δv), importance weight index (IWI)) from varying tasks

very low number of landscape elements like trees, parking lots and some other details. All surrounding traffic is controlled by the modified IDM described in the previous paragraphs either with or without ISPA activated. The tasks have to be accomplished in varying order to keep learning effects low. Still the tasks with assistance are always the last tasks to avoid a potential overload of the drivers due to several unusual circumstances.

The test corpus included 20 persons (16 male, 4 female) with an average age of 26.95 years, all of them held a valid driver license. Overall 100 test drives were accomplished with a recorded distance of ca. 1000 km where data was sampled at a rate of 10 Hz.

6.4.4 Data Analysis

After the driving simulator experiment the obtained data shall be analyzed. All plots containing metrics stored in a BM are arranged in a way so the lanes correspond to the rows and respectively the columns to the road course in front of the ego vehicle. The ego vehicle itself is positioned in the third row of the first column which means that the map moves with the ego vehicle. Even for a relatively large recorded distance the BM could not be covered completely as shows Fig. 6.34. In the first row (starting from top) the first 10 columns and in the second row the first 5 columns have only been covered by very few
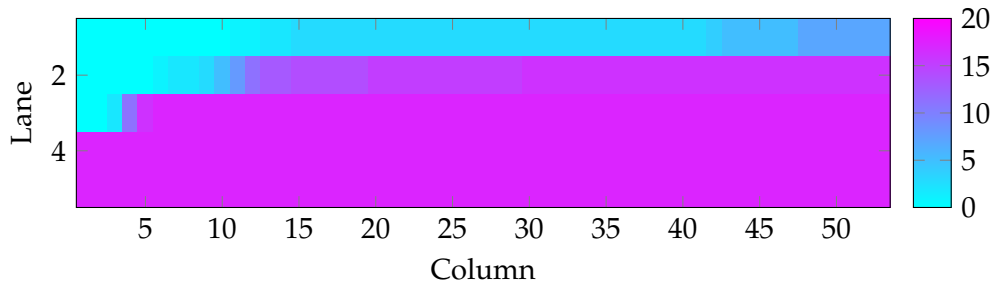
Figure 6.34: Coverage of measurement data (number of vehicle occurrences per grid tile) for the Behavior Map from 20 test persons

vehicles. This is already a first result originating from a behavior enforced by (German) law that overtaking on the right hand side is forbidden. The uncovered area in front of the ego vehicle represents the minimum safety gap all drivers kept. In case of uncovered cells in the map these are filled with the mean value of the 8 surrounding cells to create a fully covered map. To reduce all data points in one cell of a metric, the data of all vehicle occurrences are merged into one value using a Median filter.

Relative Speed The Behavior Map with the relative speed metric in Fig. 6.35 shows relatively uniform values for the second and third lane from column 15 to 53. Here relative speeds in the range of 15 - 20 m/s dominate as well as in most cells of the whole fourth and fifth lane. Especially in the top left corner it is noticeable that relative speeds are chosen very low in a range of 0 - 5 m/s which probably originates from the fact that overtaking on the right hand side is forbidden by German law. Consequently drivers approach vehicles in front or left of them slowly, finally adjust their speed and only overtake after a lane change so the other car is to the right of them. Also this area can be seen as an extended minimum gap that stretches over several lanes.

Importance Weight Index The IWI content of the Behavior Map (Fig. 6.36) has the inverse value distribution than the relative speed map. As described before the IWI is derived from the normalized relative speed values by subtracting them from 1. As a result the value distribution rates areas with high differential speeds as less important than ones with
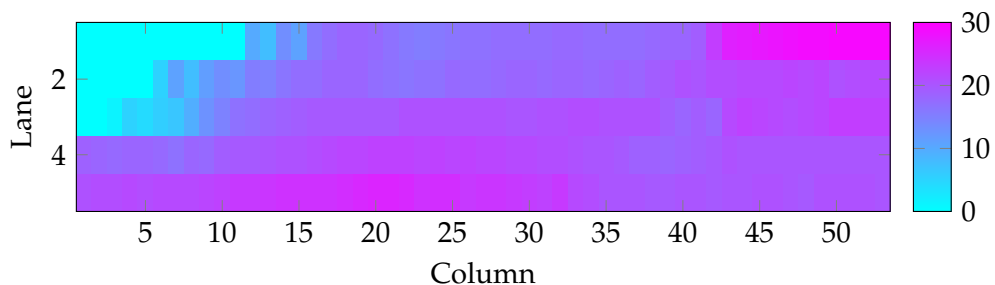
Figure 6.35: Median relative speed in the merged Behavior Map from all 20 test drivers.
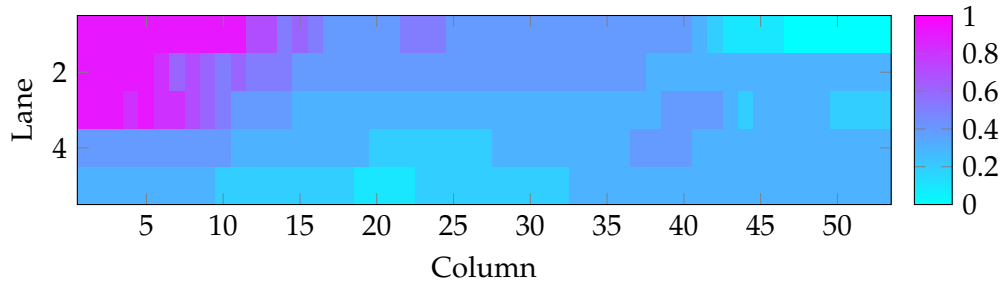
Figure 6.36: Median Importance Weight Index in the merged Behavior Map from all 20 test drivers.

speeds in a close range around the ego speed. In other words drivers tend to adjust their speed to cars in areas with a high IWI value. It is important to note that this index is not intended for "importance" in a general sense but only to the speed choice.

Time Headway   In contrast to the two maps analyzed before the map containing the time headway values does not show this distinct value distribution. Instead the distribution is very similar for all lanes. The main impact on the distribution shape has the equation defining the time headway with $T_{headway} = g/v_{ego}$ where the headway correlates linearly with the gap distance g. Additionally the uniformity must also be attributed to the instructions to the drivers during the experiment. They had to follow one ore more leading vehicles at their desired gap distance without overtaking.

All of those plots show that adjacent lanes do have an impact which should not be neglected. Another insight can be derived from these matrices: the contained values cannot easily be described with simple analytic functions as has been done in other publications mentioned before. Even if this is desired, these functions should be fitted to data obtained from real drivers.

6.4.4.1   Differences In Behavior Maps of Assisted and Unassisted Drivers

The metrics stored in the Behavior Maps of each driver can now be used to investigate the impact of the ISPA system on them. Therefore the maps of all assisted and baseline drivers are merged by writing the median value into the respective BM. Then the difference of
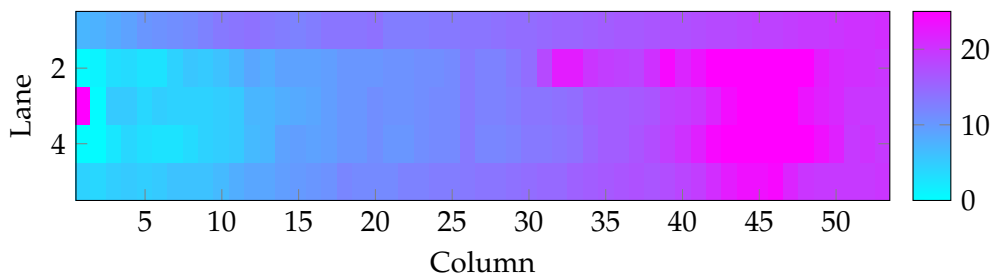
Figure 6.37: Median time headway in the merged Behavior Map from all 20 test drivers.
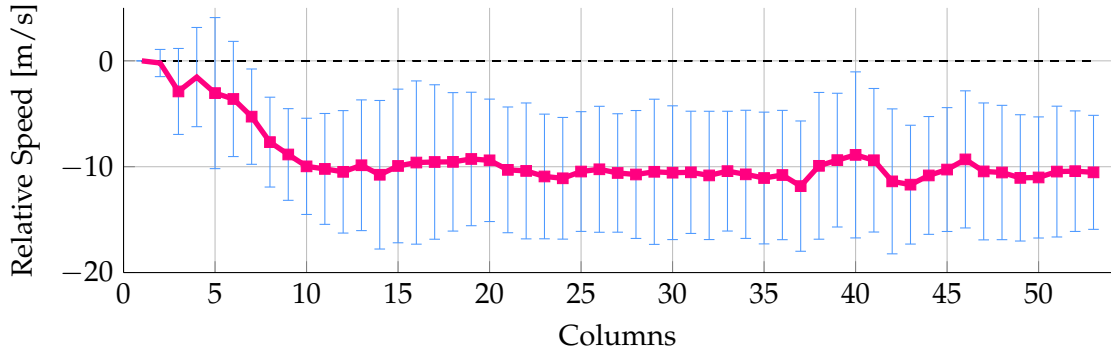
Figure 6.38: Differences between the relative speed contents of the baseline and assisted Behavior Maps on the ego lane. The pink line shows the difference values, pink squares show differences at the 5% significance level, blue whiskers denote the standard deviation.

these maps can be calculated as follows:

$$\Delta B(r, m) = B_{ISPA}(r, m) - B(r, m) \tag{6.48}$$

with r : row relative to the ego vehicle, $r \in [1...53]$

m : metric which is contained in the BM (THW, relative speed and TTC

$B(r, m)$: value in the merged BM without driver assistance

$B_{ISPA}(r, m)$: value in the merged BM with ISPA assistance

$\Delta B(r, m)$: difference between the two BMs for the defined row and metric

In the following sections the metrics "Relative Speed", "Time Headway" and "TTC" are analyzed in the described manner. Additionally it is tested whether the difference is statistically significant for a specifig column. This is done with the Mann-Whitney U Test described in [MW47], consequently a significant difference value is marked with a square in the plots.

Figure 6.38 shows that the assistance has a clear impact on the relative speed choice. While the difference is nearly zero in the first two columns, it gradually increases to ca. -10 m/s at distances greater than 75 m (equal to column 10). The early warning of the system causes the driver to shift his overall speed choice to values which are ca. 10 m/s lower down to a distance of 75 m. In the last distance interval the assisted drivers seem to rely more on their own perception instead of the ISPA suggestions which is supposedly the reason for the difference decrease.

Regarding the time headway (see Fig. 6.39) the difference is not as clear as with the relative speed. An average increase of 1.48s can be calculated, but the figure shows that the effect is not constant over the covered BM area. This is also an effect that has been found in the driving simulator studies before, where assisted drivers tended to keep a lower distance headway while moving with lower relative and absolute speeds. This in turn produces time headways which are very similar to the baseline case. A different picture for the changes can be found in Fig. 6.40 for the TTC distribution in the Behavior Map. The increase in TTC is more constant as it is always significantly higher except for two cases starting from column 13 which equals a distance of 97.5 m. In average drivers exhibited a higher TTC
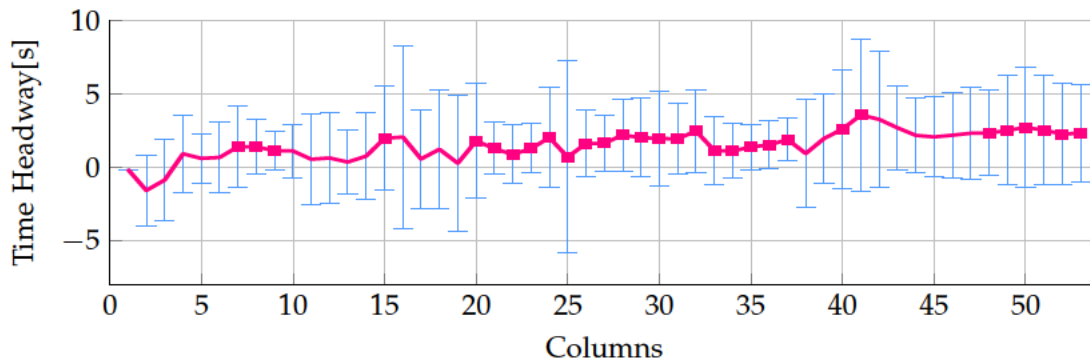
Figure 6.39: Differences between the time headway contents of the baseline and assisted Behavior Maps on the ego lane.

by 2.65 s which gave them more time to react to a certain situation. Similar to the relative speed comparison, the two groups converged with their behavior from the first to the tenth column (equal to 75m distance). Again the explanation could be that the assisted driver fell back to their usual behavior using their own perception which is then comparable to the baseline drivers.

6.4.4.2 Driver Classification

Based on the recorded data and the Behavior Maps it is also possible to classify the test drivers. As mentioned before it would be desireable to combine the Behavior Maps of several drivers to obtain a new driver profile. In order to create a "sensible" new profile a method could be to combine only drivers with comparable behavior patterns. To do this they need to be classified, which is done here with a set of simple static rules. The driver classes are inspired by the classes defined in [RB85].
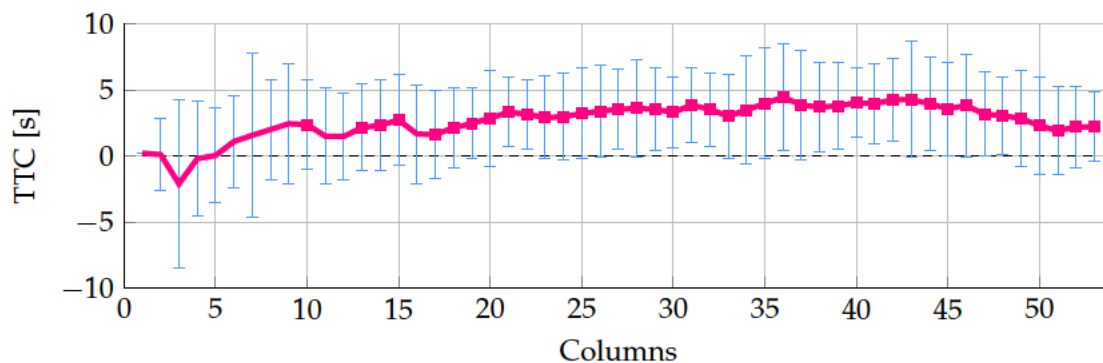
Figure 6.40: Differences between the TTC contents of the baseline and assisted Behavior Maps on the ego lane.
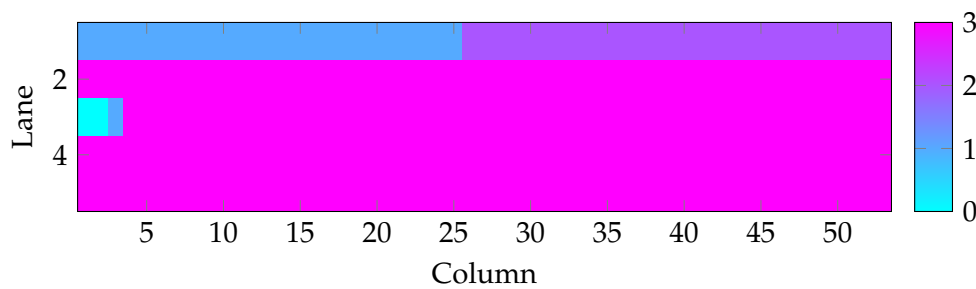
Figure 6.41: Coverage of the combined BM derived from test drivers overtaking on the right lane. Besides a high coverage on the ego lane, both right adjacent lanes and the first left adjacent one, there is even at least one record in every cell of the second adjacent lane on the left.

Prohibited Overtaking Maneuvers In the lateral following task drivers were asked to follow a leading vehicle on a different lane, in some configurations they were driving on lanes further right than the leading vehicle. They were instructed not to overtake which was desired to record realistic behavior. But in this case it is also forbidden by German law to overtake on the right hand side. Still some drivers showed this behavior what also had an effect on their BM and belongs to the category "law abidance" in [RB85].

They can be classified by their comparably small minimum gap (the uncovered area in front of the ego vehicle position). Also these overtaking maneuvers cause a complete coverage of the second adjacent lane on the left. Like that a rule can be formulated that if one of the two lanes on the left is covered in the first column, the driver is a right lane overtaker.

Low Gap Distance According to [RB85] the chosen headway can also be a criterion for driver classification. To derive a threshold below which a driver is classified to have a low gap distance the average time headway is calculated from all drivers. This is only done for the area between the second and tenth column on the third row (the ego lane). The average time headway of all drivers in this region of the BM is 4.23s, so a driver with a lower value in this region is considered to chose low gap distances.

High Relative Overtaking Speed Also the speed choice can be used to distinguish different driver types (see again [RB85] as reference). Especially the relative speed to the surrounding traffic is a valuable indicator for the driving style. Maneuvers where this can be investigated are for example overtaking maneuvers. In the same way as the classification was done relative to a mean of all drivers, the average relative speed between the first and fifth column on the fourth lane (the first adjacent lane on the right) is calculated. If a driver shows a higher relative speed in this area than the average of 18.54m/s, he is classified to choose high relative speeds.

6.4.5 Traffic simulations with vehicle groups

Most microscopic Car Following models do not reflect human behavior in certain situations. Examples for such are passing slower vehicles on adjacent lanes, taking into account several leading vehicles or a re-estimation of the situation while approaching an obstacle. In most applications these situations have no significant impact if the intention is to model larger scenarios where details in the movement of a single vehicle are not of interest.

Here the impact of an assistance system shall be simulated which has mainly an influence on longitudinal movement when approaching an obstacle. In these situations the detailed movements do have an influence on the intended scenarios, so it is essential that a Car Following Model is able to resemble the special behavior properties originating from this assistance. The implementation of the Behavior Map and the extension of the Intelligent Driver Model by Kesting et al. (see [KTH10]) with a reaction time, limited perception accuracy and the optional ISPA system shall be a first step towards those requirements.

The following sections will cover first evaluations about the general feasibility of the new CFM in simple and controlled situations with a single car approaching one or more obstacles. After that several scenarios will be tested with several cars using the modified CFM and with varying percentages of equipped cars. All simulations are conducted with SUMO which also provides the possibility to run it in batch mode for several hundred simulation runs.

In order to define the batch simulations in an efficient way, some parameters are designed as a probability distribution rather than an absolute value which has to be set by an external logic. An example for this is the probability, that a car is equipped with ISPA. If a percentage of equipped cars is desired that cannot be met with an integer number of cars because of a small test group, this can be circumvented by running the simulation several times until the target value is sufficiently met. Each simulated vehicle has the following parameters related to the extensions explained above:

- ISPA: probability whether a driver is assisted

- mixedDriver: boolean switch if the BM is from a distinct driver or a combination

- rightOvertaker: probability that a driver exhibits overtaking on the right

- lowGap: probability for a driver choosing low gap distances

- fastOvertaker: probability that a driver overtakes with high relative speeds

These probability based parameters are generated at the beginning of a simulation while other parameters like the reaction time are defined with a log-normal distribution and are evaluated at runtime for every situation.

The chosen scenario in SUMO is equal to the one used in the driving simulator experiments with a straight three lane highway. All scenarios use Behavior Maps generated from a random combination of all test drivers for a high variability. Statistical significance is tested with a Mann-Whitney U test.

6.4.5.1 Basic Scenarios for Multi Lane Interaction

All scenarios are conducted in a batch mode with 120 runs and six vehicle configurations (defined in Tab. 6.6) which leads to 20 simulation runs per configuration. The track has a standing vehicle on the center lane at the 500 m position, the test vehicle starts at the 0m position with an initial speed of 33 m/s ($\approx$ 120 km/h). Depending on the scenario the ego vehicle is positioned on the center, left (fast) or right (slow) lane. In case the ego

Conf.	ISPA	Max. Speed $[m/s]$	Accel. $[m/s^2]$	Decel. $[m/s^2]$
1	OFF	33	0.6	5.5
2	OFF	36	0.8	6.5
3	OFF	39	1.0	7.5
4	ON	33	0.6	5.5
5	ON	36	0.8	6.5
6	ON	39	1.0	7.5

Table 6.6: Vehicle configurations for the batch simulations using the Behavior Map in simple scenarios.

car approaches a group of cars forming the end of a traffic jam, 30 vehicles are placed homogeneously on all lanes. Here the last row is positioned at the 500 m mark of the track. Lane changes are switched off for a more controlled situation.

Head-on approach to a single vehicle The first scenario to be tested is a single vehicle standing at the 500 m mark. Both the ego and the obstructing vehicle are located on the center lane. The resulting speed plots are shown in Fig. 6.42 for the assisted as well as the baseline case. It is noticeable that the virtual drivers start the deceleration process as soon as the obstructing vehicle is covered by their Behavior Map. The BM covers a distance of 400 m ahead of the ego vehicle, so the obstacle is covered from track the position 100 m which is where the deceleration begins. Both plots show the variations in the deceleration process originating from the underlying CFM with several randomly selected parameter values. Also the stepwise deceleration is still preserved even with the extension of the Behavior Map.

The impact of the ISPA assistance is also preserved in the BM approach which can be identified in the position range [200m; 400m] where speed range is shifted from ca. 20 m/s in the baseline case to a range of 5 - 15 m/s in the assisted case. As with the real drivers

Exp.	ISPA	Dec $[m/s^2]$	Δv [m/s]	Gap [m]	TTC [s]
I	OFF	-1.58	15.36	68.56	12.26
II	ON	-1.33	9.43	106.35	22.79

Table 6.7: Average metrics of the two experiment variants including a single stationary vehicle on the same lane.
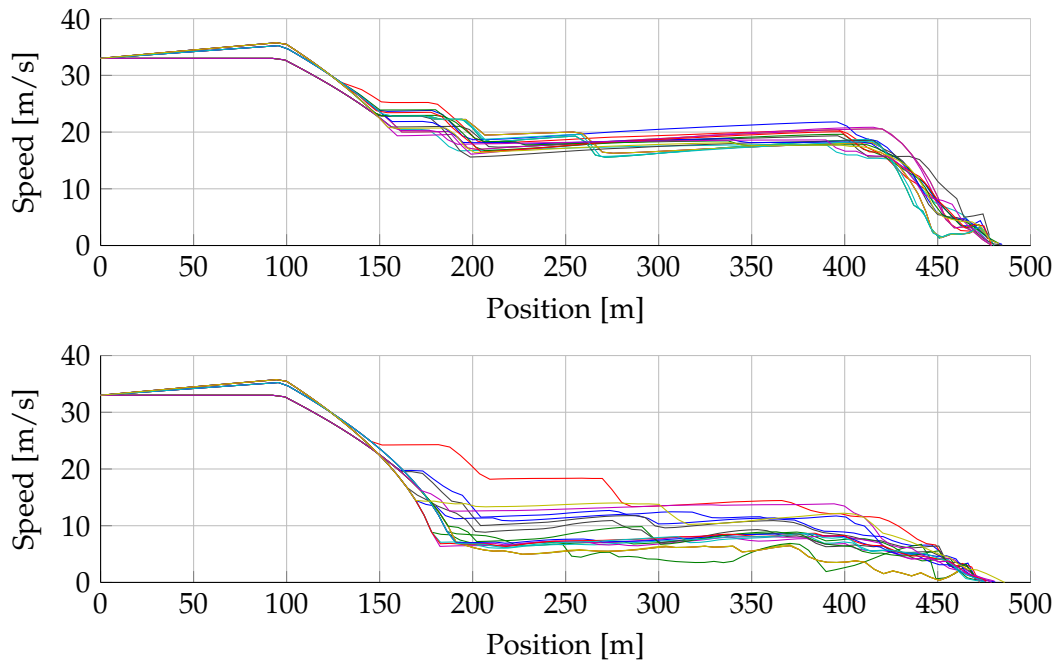
Figure 6.42: Comparison of the assisted (bottom) and baseline (top) speed development when approaching a single car. For simplicity only 20 of 60 runs per plot are shown.

the average maximum deceleration and the relative speed are decreased, while the average gap and the TTC showed higher values (see Tab. 6.7).

Head-on approach to multiple vehicles   The previous experiment showed that the Behavior Map preserves the basic properties of the underlying CFM. In the next experiment the differences between a single lane and a multi lane model shall be investigated. Therefore the obstacle was not a single car at the 500 m position but a group of 30 cars distributed over all lanes representing the end of a traffic jam. In case of a single lane model observing only one leading vehicle the two experiments with one vehicle or a group of vehicles would produce exactly the same results. But as can be derived from Fig. 6.43 and Tab. 6.8 there are clear differences in the plots and the metrics (statistically significant at the 5% level) compared to the previous experiment. In both the assisted and baseline configuration the speed range in the position range 200 - 400 m is lowered, the baseline to range of 10 - 20 m/s and the assisted one to a range of ca. 2 - 10 m/s. The metrics in Tab. 6.8 also show

Exp.	ISPA	Dec [m/s^2]	Δv [m/s]	Gap [m]	TTC [s]
I	OFF	-2.05	15.17	100.98	15.55
II	ON	-1.18	6.87	147.79	38.42

Table 6.8: Average metrics for baseline drivers (Exp. I) and assisted drivers (Exp. II) for multiple stationary vehicles.
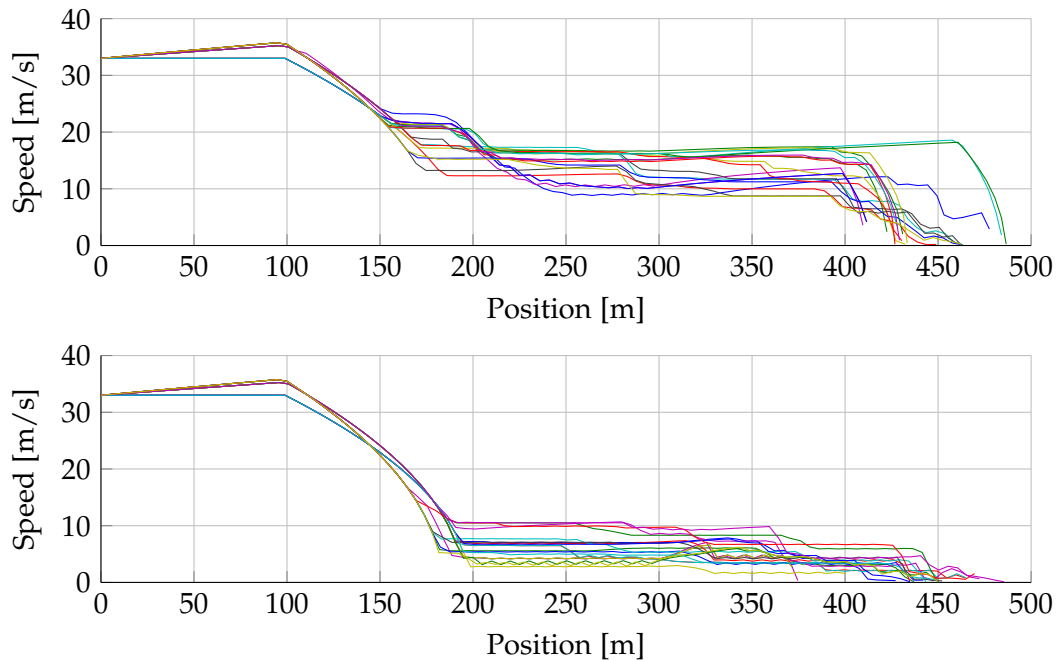
Figure 6.43: Comparison of the assisted (bottom) and baseline (top) speed development when approaching a group of 30 cars. For simplicity only 20 of 60 runs per plot are shown.

the same value shifts between the assisted and baseline configurations as the previous experiment.

Fast lane approach This experiment is the first one where the ego vehicle has no leading vehicle on its own lane but on an adjacent one. All previously reviewed Car Following Models would act as if no obstacle was present and pass by the other vehicle uninfluenced. Only when closely coupled to a Lane Change Model an interaction could be observable in such a way that the LCM would analyze the average speed in the adjacent lane and adjust the desired speed of the CFM accordingly.

Here the interaction is an integral part of the CFM architecture which is also underlined by the plots in Fig. 6.44. For this experiment the obstructing vehicle is set on the center lane while the ego vehicle approaches it from the left (fast) lane. It can be observed in real traffic that drivers reduce their speed when overtaking a slower vehicle even if they are already on a different lane. Such a behavior pattern is also reproduced by the Behavior Map as shown by Fig. 6.44. Here drivers start with a speed of 33 m/s, then slow down to a speed range of ca. 20-30 m/s at the 500 m mark where the other vehicle is positioned and then accelerate again to their desired speeds. Even if the ISPA system does not produce any output as it only observes the ego lane, these drivers showed an overall more defensive driving style which seems to be reflected in the respective Behavior Map. Also the numbers in Tab. 6.9 suggest this interpretation. The table contains no information about time headway or relative speed as this cannot be obtained from this experiment by definition.
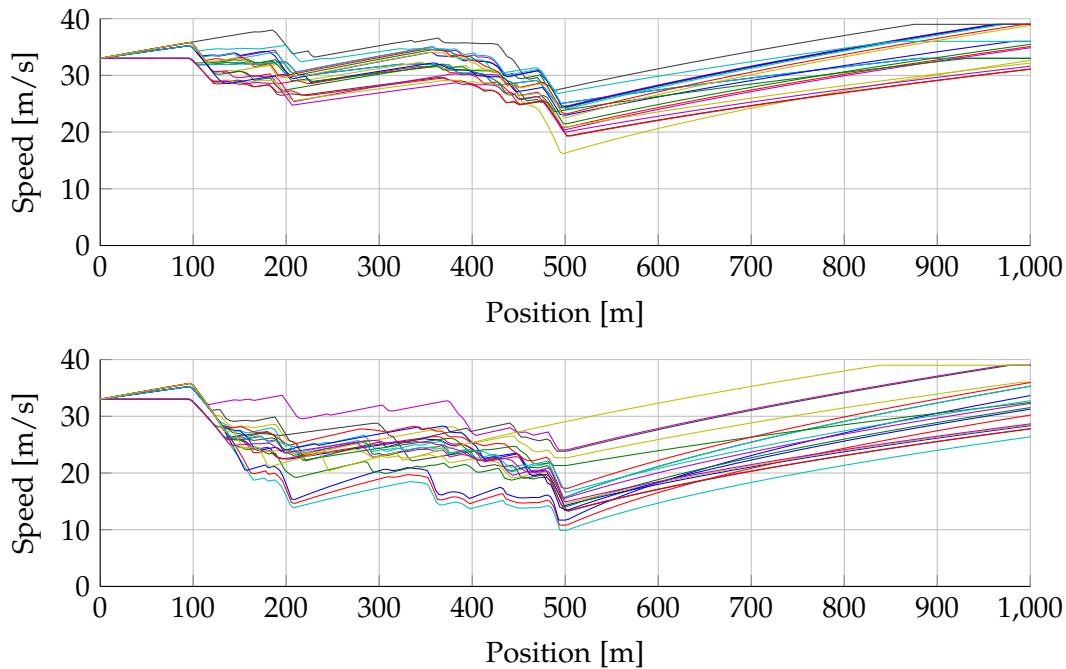
Figure 6.44: Comparison of the assisted (bottom) and baseline (top) speed development when approaching a vehicle on the center lane, the ego car is on the fast lane. For simplicity only 20 of 60 runs per plot are shown.

Slow lane approach   For this experiment the obstructing car was again set on the center lane, but this time the ego car approached it from the right (slow) lane. All other experiment settings were the same. By law it would not be allowed to overtake the standing vehicle on this lane, so the expected behavior would be a deceleration and finally stopping with a certain safety gap. A normal human driver would most likely change lanes twice to the left and overtake in order to keep or approach his desired speed, but as already explained before changing lanes was forbidden for this experiment. Some of the test persons in the driving simulator experiment overtook even if they broke the law by doing so (see also the data analysis for the Behavior Map, Fig. 6.41). They slowed down to speeds below 12 m/s, took over and then accelerated to their desired speed. This is also what can be seen in Fig. 6.45 in the bottom plot, the ISPA assisted drivers showed a comparable behavior but the BM produces higher overtaking speeds in that case. It is remarkable that this behavior is reproduced by the Behavior Maps without explicit modeling but entirely resulting from the

Exp.	ISPA	Min. Speed [m/s]	Avg. Speed [m/s]
I	OFF	22.04	33.83
II	ON	16.10	31.15

Table 6.9: Resulting metrics when overtaking a single stationary vehicle to the right of the ego vehicle.
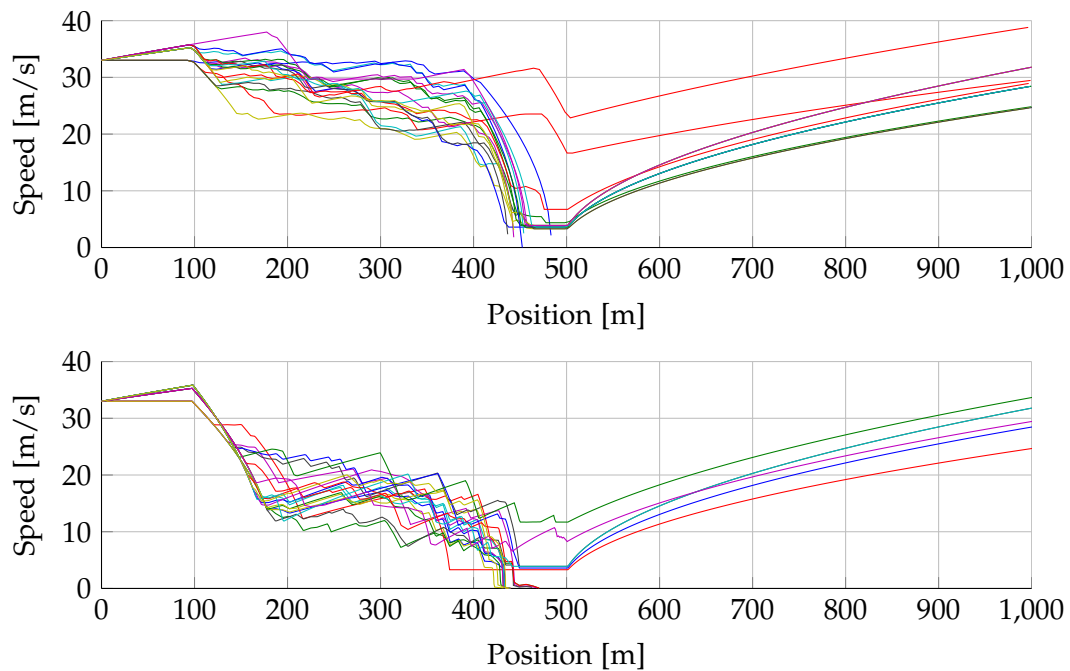
Figure 6.45: Comparison of the assisted (bottom) and baseline (top) speed development when approaching a vehicle on the center lane, ego car is on the slow lane. For simplicity only 20 of 60 runs per plot are shown.

recorded behavior. Also it is worth noting that not all simulated drivers show this behavior but only the ones that have portions of right overtaking real drivers in their Behavior Maps. Again the assisted virtual drivers tend to drive slower even if the assistance produces no output. The explanation are the slower speeds of assisted drivers recorded in the driving simulator.

Summary   At this point it can be stated that the initial intentions behind the development of the Behavior Map have generally been met for the presented situations. The model produces behaviors that are based on the observation of multiple leaders as well as of adjacent lanes. It even showed the same forbidden overtaking maneuvers exhibited by some of the real drivers in the driving simulator. Another effect revealed by the plots and metrics is that assisted drivers generally choose lower speeds which is exposed in scenarios in which the assistance does not work. Consequently the next step would be to evaluate the model in more complex scenarios like driving within a group of vehicles.

6.4.5.2   Complex Scenarios in Dense Traffic

The following experiments shall reveal the effects of the Behavior Map in scenarios with a higher number of vehicles and the effects of the ISPA system in larger groups. Therefore, a group of 12 test vehicles distributed evenly over all three lanes interacts with another group of three vehicles driving side by side to represent the rear end of a traffic jam. In order to

ISPA	v [m/s]	Δv [m/s]	Dec. [m/s^2]	Gap [m]	THW [s]	TTC [s]
0%	**14.66**	**4.33**	**-1.35**	**80.72**	**13.29**	**25.82**
25%	**13.25**	**3.90**	**-1.19**	**85.43**	**14.47**	**28.62**
50%	**11.99**	**3.53**	**-1.12**	**89.69**	**15.68**	**30.81**
75%	**10.88**	**3.21**	**-1.03**	**93.83**	**16.91**	**33.05**
100%	**9.84**	**2.90**	**-0.93**	**97.17**	**17.96**	**35.07**

Table 6.10: Average metrics for a group of 12 cars approaching a traffic jam. Tests were carried out with varying percentages of assisted drivers.

evaluate the impact of the ISPA system in such a setting the percentage of equipped cars is varied between 0%, 25%, 50%, 75% and 100%. This means that for a 25% equipment rate the probability for a car to have the assistance is 25%. Each of these five configurations is evaluated in 300 simulation runs to obtain statistically significant results.

Besides the varying equipment percentages every configuration is tested in three states of a traffic jam: approaching the congestion, moving with stop-and-go traffic and accelerating when the congestion dissolves. Again no lane changes occured due to a suboptimal coupling of the LCM with the CFM which causes the LCM not to initiate a lane change.

Traffic jam approach At the beginning of the simulation the last row of the test vehicles is located at the 0m mark while the three vehicles representing the congestion are at the 1000 m mark. The test group has an initial speed of 27 m/s ($\approx$ 100 km/h) and all use the IDM. Table 6.10 shows the safety metrics which were obtained by averaging over the 300 runs per configuration. For all metrics that require the ego speed as input parameter all time intervals with speeds lower than 1m/s are removed in order to keep the average computation as valid as possible. All values in the table that are significantly different from the same value originating from the next higher assistance percentage are marked in bold numbers. Regarding this experiment this is true for all percentage steps, the test for a statistically significant difference between the metrics was conducted with the Mann-Whitney U Test.

Every increase in equipped vehicles improves the safety metrics. The average speed is reduced in average by 1.21 m/s per step, gap distance with an average increase of 4.11 m per step and time headway with an average improvement of 1.18 s per step. This also matches the expectations for this kind of situation as this is the scenario the ISPA system was developed for. It is also noticeable that the gradual improvement is highest from 0% equipment rate to 25% and then decreases slightly for higher rates.

Moving with a jam In this scenario the test vehicles start with a speed of 0m/s and are positioned directly behind the leading vehicles representing the end of a congestion. The leading vehicles follow a varying desired speed pattern to simulate stop-and-go behavior. Also in this experiment every configuration is simulated 300 times and the same metrics are analyzed, the overview is given in Tab. 6.11. In contrast to the previous scenario not all of the metrics show a statistically significant difference between subsequent percentage

ISPA	v [m/s]	Δv [m/s]	Dec. [m/s^2]	Gap [m]	THW [s]	TTC [s]
0%	**15.77**	**0.56**	**-1.80**	78.78	18.41	**28.67**
25%	15.12	**0.47**	**-1.56**	78.37	**18.12**	**31.64**
50%	14.41	**0.43**	**-1.44**	77.04	17.44	**32.70**
75%	**13.87**	**0.40**	**-1.36**	76.17	**17.07**	**33.60**
100%	13.25	0.36	-1.21	74.38	16.31	34.81

Table 6.11: Average metrics for a group of 12 cars moving with stop-and-go traffic. Tests were carried out with varying percentages of assisted drivers.

steps. If higher percentage differences are compared, e.g. the metrics of the 0% rate with 50% rate, all of them are significantly different again. The ISPA system seems to have a lower impact in this situation which is probably due to the fact that the overall absolute and relative speeds are lower. Also the varying speed patterns in this scenario lower the chance for statistically significant results. It also must be noted that the metrics "Gap" and "Time Headway" show the opposite trend as compared to the previous experiment. The behavior recorded in the BMs seems to lead to the acceptance of lower gap and THW values resulting in more potentially dangerous situations, but this is counterbalanced by lower average speeds and decelerations.

Accelerating after a jam The last investigated scenario is a dissolving congestion in which all cars are able to accelerate to their desired velocities. Again the test group starts at zero speed while there are no obstructing vehicles present as in the previous experiments. That way the cars in the front row of the test group can accelerate freely while the ones behind them interact with them based on their Behavior Maps. Table 6.12 shows the relevant metrics for this experiment, compared to the previous one the metrics "Speed", "Deceleration" and "Time Headway" are omitted as they are not of interest in this constellation. All configurations of the experiment show statistically significant differences of all metrics. This suggests that the ISPA system also has some impact in these situations where the acceleration of a whole group happens in an inhomogeneous manner. The overall impact is positive regarding safety especially through the increased gap and TTC values.

ISPA	Δv [m/s]	Gap [m]	TTC [s]
0%	**-2.87**	**287.97**	**41.50**
25%	**-3.03**	**300.48**	**53.37**
50%	**-3.19**	**316.88**	**68.87**
75%	**-3.30**	**324.18**	**71.11**
100%	**-3.45**	**336.45**	**77.02**

Table 6.12: Average metrics for a group of 12 cars accelerating after a traffic jam. Tests were carried out with varying percentages of assisted drivers.

Summary The experiments with a group of vehicles interacting with each other and in some cases obstructing vehicles show that the overall positive effect of the ISPA assistance persists also in larger scenarios. Increasing equipment rates show a correlating increase in all safety metrics except for the stop-and-go scenario. Here the metrics "Time Headway" and "Gap" exhibit an adverse effect on increasing equipment rate which is in turn counterbalanced by the improvement of the other metrics. In this situation the combination of all effects suggests that the vehicle flow becomes more homogeneous (lower relative speeds and decelerations) while it also becomes more dense (lower gaps and time headways).

As expected the highest impact can be determined for deceleration scenarios which is due to the fact that the system is intended to assist in such situations. The effect is decreased for more complex scenarios like in the stop-and-go experiment because deceleration phases are not as long and distinct and there are more fluctuations in the speed and lane choices.

6.4.6 Discussion

In this section a Car Following Model has been developed which uses a construction called the Behavior Map. This enables the model to react on several vehicles in its vicinity to resemble a more human-like behavior. Additionally it is parametrized with pre-recorded metrics from real drivers to produce a comparable behavior. It uses the well established Intelligent Driver Model as underlying CFM and obtains the weighing factors (IWI) for vehicles that influence the from the behavior of the ego car from real drivers. The experiments using this CFM with the SUMO simulator suggest that the influence of the ISPA system on a group of vehicles retains the effects observed in the driving simulator studies.

Still there are several points in which the model can be improved or generalized that shall be discussed here.

Calculation of the Importance Weight Index Here the IWI was derived from the relative speed of vehicles in a certain Behavior Map cell. The idea behind this was that drivers rely their speed choice on vehicles with high importance to them. A low relative speed could then imply a high importance to the driver and result in a higher weight when summing up all speed choices from the BM. With this approach it is assumed that relative motion of a certain magnitude is equally important for all distances to an obstacle at all speeds which can be questioned.

A calculation of the IWI that also takes the relative distance and absolute speed into account could be based on the Risk Perception as proposed by Kondoh et al. in [Kon+08]. This measure has already been described in chapter 2 (see Fig. 2.6 and Eq. 2.3) where it was shown that it covers both static car following situations as well as dynamic ones with departing or approaching vehicles. If we assume that the Perceived Risk correlates with the importance of a vehicle on the speed choice, this could be an alternative way of calculating the IWI.

Usage of various / dynamic Behavior Maps In this research the Behavior Map content was extracted from a comparably low number of driving situations that were all located on a three lane highway. It is very likely that the results of this map will not produce

reasonable results on a rural road or even in a city scenario. A possible solution could be the introduction of several BM variants that can be switched depending on the current environment. As explained before regarding the calculation of the IWI there could be alternatives that are independent of the ego speed. This could also be applied to the Behavior Map by adjusting its dimensions to the ego speed. One example for the feasibility of such an approach would be the fact that a BM with a coverage of 400 m in front of the ego car is not realistic in a city scenario. This would also overcome the problem of the previous suggestion of switching between Behavior Maps because the transitions must be conducted in a way that causes a continuous parameter change.

Combination with a Lane Change Model It was mentioned several times in this section that the SUMO Lane Change Model did not initiate lane changes in conjunction with the Behavior Map. This was due to the fact that the BM kept distances to the leading vehicle always large enough so there was no reason for the LCM to initiate a maneuver. As this is no realistic behavior and not intended, the coupling between the CFM and the LCM must be improved.

Integration with the modified IDM and ISPA Currently the Behavior Map model uses the standard IDM as the underlying Car Following Model. A next step could be the integration of all previously described models and systems into one unifying model. This could be done by applying the human perception properties (limited distance estimation accuracy, re-estimation of the situation, reaction times, visibility) to the IDM on each vehicle covered by the Behavior Map. Another valuable and already proven extension would be the exchange of the IDM with the Enhanced Intelligent Driver Model proposed by Kesting et al. in [KTH10].

Further an integration of the ISPA system can facilitate additional experiments as this would resemble the real constellation even better. Here the Behavior Map covered a distance of 400 m while the ISPA system warns driver up to 1000 m ahead and even if there is no direct line of sight. In the model this can be especially interesting with the simulation of limited visibility mentioned before. One way to incorporate the system can be to use the modified IDM with the ISPA extension and to take its speed value if the obstacle used by the assistance is outside the Behavior Map. Otherwise the speed choice originating from the ISPA system can either be neglected when the obstacle is inside the BM or added with a lower weight to the overall speed choice.

Calibration of the Behavior Map with real data Finally the BM could be calibrated with data from real traffic flows. This can either be done with a probe vehicle measuring the time headway, TTC etc. from the ego vehicle and if possible with backward facing sensors for the following car as well. There are also several publicly available data sets which are extracted from cameras mounted on high buildings that survey a larger area. With such data sets a very exhaustive calibration can be done, but it is not possible to investigate the impact of an assistance system as it can only provide a baseline. The external conditions would vary too much compared to a driving simulator study to derive any differences in behavior.

7

Discussion and Outlook

The topic "Anticipation Support for Drivers" has been approached from various perspectives that are related to the development of a driver assistance system. All of them were required to answer the following set of questions:

- Which situations are relevant for anticipation support?

- What are the required actions to improve safety, fuel economy and overall traffic performance in these situations?

- When is the optimal time instant for assistance and which information is needed?

- What is the influence on driving style in virtual and real environments?

- Will a stereoscopic driving simulator improve the conditions for anticipation-related experiments?

- Can the different behavior of assisted and unassisted drivers be modeled and applied in larger scenarios?

The following paragraphs will summarize the conclusions to these questions based on the results of the presented experiments.

Relevant Traffic Situations and Driver Actions   Several situations were identified in which a drivers could benefit from an improved anticipation. Those included traffic jams, speed regulations, static obstacles and blocked lanes. All of these examples can basically be located in urban, rural or highway settings which has also been reflected by the proposed situations. One property that all situations have in common is the need for a speed reduction which is either necessary to avoid a collision or dictated by law. Consequently an assistance system must induce a deceleration in time in order to reach a certain target speed even if the driver is not able to recognize the upcoming situation early enough. A speed reduction is in almost all cases beneficial as it reduces the kinetic energy that is involved in a potential collision. This is underlined by the research of Wagenaar et al. (see [WSS90]) who state that the raised speed limit in the US from 55 mph to 65 mph resulted in a 19.2% increase of fatal crashes and a 39.8% increase of serious injuries. Kloeden et al. state in [Klo+97] that each speed increase of 5 km/h above 60 km/h in a 60 km/h speed limit area doubles the probability of being involved in a casualty crash.

In the experiments described in chapter 3 participants had to rate the helpfulness of anticipation support in all situations. The results show that the three most relevant situations are traffic jams, stagnant traffic and construction sites with blocked lanes. Less relevant are the situations with a parking car on the ego lane and a slow leading car on a rural road. These outcomes together with the free answers in the questionnaires indicate that situations that are supported should have the following attributes:

- Assistance only on roads with higher (< 50 km/h) speed limits (highways, rural / urban roads with higher speed limits / more lanes)

- Speed or overtaking regulations should not be supported

- Obstacles with rare occurrence and high crash potential show the highest benefit

Generally it can be summarized that events that occur very frequently should not be supported which is true for most situations in inner cities or urban environments. Here the system would generate an output too often which can lead to annoyance and finally to a system deactivation. Drivers see the greatest benefit in situations that occur at the most a few times per week that have a high potential to result in a crash if no adequate action is taken.

Timing Logic and User Interfaces Now that the relevant situations have been identified the assistance consisting of a Business Logic (BL) and an HMI were designed. The BL was mainly developed by Popiv in [Pop+09] which takes the ego speed, the target speed and the speed development for different deceleration strategies into account. From these input variables it generates a suggestion for the optimal deceleration strategy which can either be coasting (speed reduction through engine drag force), comfortable deceleration (-0.2g) or strong deceleration (-0.4g). Additionally to the proposed deceleration strategy some HMI variants also need information about the type and distance of the obstacle and sometimes the positions of individual surrounding vehicles as well.

On the HMI side several evolutionary steps have been made in an iterative design process as shown in Fig. 7.1. For the initial version a minimalistic icon based system was compared to a system showing a virtual Bird's Eye Perspective with a high level of detail which was developed by Nestler and Duschl (see [Nes+09] and [Dus+10]). The icon based system showed a modified traffic sign representing the upcoming situation and animated accelerator and brake pedals. Especially the animated pedals that suggest the recommended driver action were rejected by evaluation participants as was the modification of the traffic signs. In contrast the Bird's Eye Perspective showed very positive ratings at the cost of a higher cognitive demand and the requirement for more detailed environment data.

The next generation of the Iconic HMI was changed so the original traffic signs were used. Due to the bad reception by users the animated pedals were removed and a distance indicator bar was added that changes colors according to the deceleration strategy: yellow for coasting, orange for comfortable deceleration and red for strong deceleration. This element served as a basis without any further modifications for all later HMI variants. Like that the Iconic HMI is used to provide information about the distance and reason for assistance activation while additional outputs encode the action recommendations. The
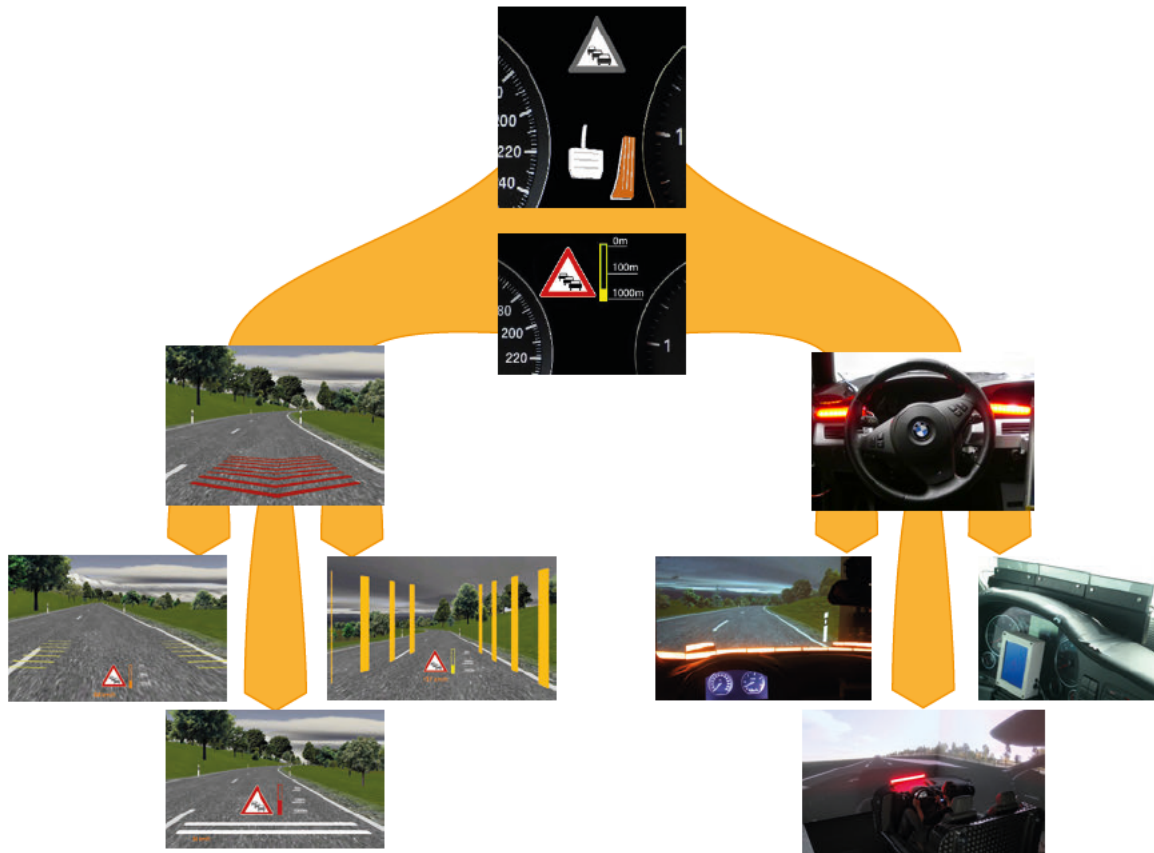
Figure 7.1: Genealogy of the different HMI variants. Originating from the first icon based variants two branches were developed for the Head-Up Display and LED arrays. After a first prototype of each branch three further variants were developed for different purposes.

latter is important to indicate a required speed reduction while the Iconic HMI is needed for acceptance reasons and to build up system trust.

Two branches were developed which both have in common that extremely simple and easy to perceive action recommendations are given. This is either done in the HUD or with various arrangements of LED modules. For the HUD (left branch) it was assumed to have large display areas available in order to generate contact-analogue elements. The basic idea is to display virtual road markings that are similar to their physical counterparts which have been successfully tested by several researchers (Katz in [Kat07], Drakopoulos in [Dra03], Miles et al. in [Mil+05], Manser et al. in [MH06] and Anhäuser in [Anh04]).

The HUD variants in the left branch all require comparably large display areas which will not be available in the near future for end-user applications. As a consequence the systems based on LED modules in the right branch have been developed. The first prototype with light bars mounted on both sides of the steering wheel was only tested in a video experiment. It showed that the light distribution in the modules must be more diffuse and that a more more versatile control of individual LEDs could be beneficial. A new hardware

variant was developed that was used in all systems of the next generation which included the necessary changes.

In Fig. 7.1 the left picture of the second generation LED systems shows the application in the monoscopic, single-screen driving simulator with the two evaluated arrangements. The center image represents the installation in the mockup for the stereoscopic CAVE simulator and finally the setup in a tractor truck on the right side. All variants showed the Iconic HMI in the instrument cluster and the LED modules had the same calibrated color output as the distance bar in the Iconic HMI.

Virtual and Real World Application   First of all it was possible with all presented HMI variants to induce earlier and smoother deceleration than in the baseline case. Still there were differences both regarding the objective measures and the subjective ratings.

The strongest effect of the HUD based HMIs has been evaluated for the rumble strip version of the digital road markings. It combined the contact-analogue graphics with driver seat vibrations that are coupled to the graphical representation. Compared to the baseline condition the average speed during a static traffic jam approach dropped by 22.76 km/h, the maximum deceleration was lowered by 1.98 m/s^2 and drivers started 5.19 s earlier with their speed reduction (all of these effects were statistically significant at the 5% error level). The hit rate of the PDT decreased by ca. 15% and the reaction time for the point acknowledgment increased by ca. 100ms during the deceleration. This shows that the assistance occupies a certain amount of cognitive performance while the unassisted part of the drive showed no difference to the baseline group.

Regarding the subjective ratings the HUD systems "Transversal Bars" and "Rumble Strips" showed equally positive ratings. In contrast the "Vertical Bar" version (right picture in the second generation HUD system branch of Fig. 7.1 was rated to be very disturbing and participants stated that it obstructs a too large area of the FOV.

The LED systems "Static Guiding Point" and "Dynamic Guiding Points" were tested in the monoscopic single-screen driving simulator with the identical scenarios as the HUD variants. Regarding the objective performance the Static Guiding Point showed slightly weaker performance than the dynamic version (25.17 km/h lower average speed and 2.27 m/s^2 lower maximum deceleration during assistance activation) but was accepted much better due to its calmer optical appearance. These results are statistically significant while the 5.5 s earlier beginning of deceleration did not show a statistical significance.

In the real world experiment with the tractor truck it was also possible to influence drivers positively with the LED based anticipation support system. The average speed during assistance activation was lowered by 14.7 km/h and drivers startet to decelerate earlier by 20.5 s than in the unassisted case. Also the maximum deceleration was improved by 1.34 m/s^2. All differences to the baseline group are statistically significant. The different values compared to the driving simulator experiments are caused by the different track layout and the generally lower speed of the truck.

The subjective ratings were overall positive and even better than in the driving simulator experiments. Several reasons can have led to this difference. First of all the participants of the truck experiment were all members of research or development departments who are

probably more open for new assistance systems. Another explanation could be that the system brings higher benefits for truck drivers than for passenger vehicle drivers.

Stereoscopic Driving Simulator for Anticipation Experiments   All experiments in the development phase of the HMI systems were conducted in a monoscopic single-screen driving simulator using the front half of a passenger car as physical mockup. For further experiments related to data acquisition for the behavior modeling process it was decided to develop a driving simulation with improved speed and distance perception than the current one. To achieve this the CAVE at the Chair for Human-Machine-Communication served as the infrastructure. It provides a 180° horizontal FOVwith floor projection, head tracking and stereoscopic presentation capability. The rendering engine Virtools was coupled with the traffic simulator SUMO to provide realistic vehicle behavior. All of the environment content was produced with the procedural modeling tool CityEngine for efficient scene generation. The engine, wind and rolling sounds were produced by a real time sound engine with a sample-based approach.

Correct spatial perception is closely related to anticipation as the latter requires an adequate environment perception to plan future actions. For this reason an experiment was conducted to assess the impact of stereoscopic presentation on speed and distance estimation in an automotive setting. In the experiment drivers had to follow a leading car at 20 m and 70 m and also drive freely without speed gauge at 30 km/h and 50 km/h.

The analysis showed no statistically significant difference between the stereoscopic and monoscopic configuration for all cases of speed and distance estimation. By tendency the interquartile ranges and outliers were lower for the distance estimation task, the others showed practically no difference. When compared to the results of a real world experiment conducted by Evans (see [Eva70]) for speed judgment the results are in a similar range. Only the distance judgment in the simulator shows very poor performance which still should be compared to real world judgments. Another issue could be the lack of known landmarks in the scenario which were intentionally left out to minimize any influence from these cues. Both points could shed more light on this issue for further developments.

Behavior Modeling and Impact on Larger Scenarios   The goal behind the behavior modeling effort was to gain a possibility to evaluate the impact of the proposed anticipatory assistance on larger traffic scenarios. Up to this point it was only possible to have a single test person drive in a driving simulator. This is a reasonable approach for developing and comparing assistance systems during their early development phase. But to assess its impact in a larger context without connecting a large number of driving simulators as proposed by Maag et al. in [Maa+12], the use of a traffic simulator becomes necessary.

Because the anticipatory assistance mainly influences the longitudinal control of the car it was chosen to develop a CFM based on the widely used IDM developed by Kesting et al. in [KTH10]. Analysis of the speed development data from previous driving simulator experiments it was observed that drivers showed a certain reaction time to both the first visibility of an obstacle and the output of the assistance system. Additionally the speed reduction process was not continuous but often happened in a step-wise manner. It was assumed that this is caused by misjudgment of the obstacle distance which is noticed by

drivers if it exceeds a certain value. Then a re-assessment takes place causing a step in the speed curve followed by a new speed reduction maneuver. Both features (several reaction times and step-wise deceleration) have been implemented as extension to the IDM.

The IDM only takes the direct leading vehicle on the ego lane into account which can lead to unrealistic behavior in some situations. Real drivers also include vehicles on adjacent lanes in their decision process both for security and regulatory reasons (right overtaking forbidden etc.). Especially the observation of several leading cars allows them to drive safely with time headways substantially smaller (factor 2-3) than their reaction time (see also Treiber et al. in [TKH06]) which is currently cannot be resembled by most Car Following Models.

In order to address this the IDM was extended to become a multi-anticipative CFM as has previously been done by Treiber et al. in [TKH06], Ossen et al. in [OH06], Lenz et al. in [LWS99] and lately with the IDM by Chen et al. in [Che+09]. The basic approach of all mentioned implementations is to solve the desired CFM for every vehicle in a certain area around the ego vehicle. To obtain a final single acceleration or speed value for the ego car the solutions for every vehicle must be combined. All of the previously mentioned implementations use more or less arbitrary weighting functions when calculating a weighted sum of all solutions.

Because these relatively simple weighting functions (equal weight, linearly or exponentially dependent on distance) probably do not resemble the judgment of real drivers the BM was introduced (see also [Laq+13]). This is a fixed grid moving along with the ego vehicle that stores parameters of the CFM for every grid tile together with an individual weight factor called the IWI.

The contents of the BM were obtained from a driving simulator experiment in the CAVE simulator. As assumed before the weight and parameter value distributions do not follow a symmetrical or simple analytically describable function. Also there are differences between the Behavior Maps of assisted and unassisted drivers which indicates that the altered behavior can be covered by the proposed model. It was also possible to distinguish different driver types that also have been described by Risser et al. in [RB85]. This is a valuable outcome as it provides the possibility to select or mix certain driving styles when defining a scenario for the traffic simulation.

The initial goal was to assess the impact of anticipatory assistance in larger traffic scenarios. This has been done for several situations of which each was repeated 120 times with partly stochastically varying parameter sets. In the first experiments a proof-of-concept was made for the BM with only one test vehicle and different configurations of obstacle vehicles. It showed that the BM behaves in a reasonable way and especially resembles behaviors such as speed reduction when passing a vehicle on a highway and (mostly) obeying the right-overtaking regulation. Such behavior is only the result of the BM without implementing any further fixed rules.

When testing the model in more complex scenarios with 12 cars approaching a static traffic jam it could be shown that an increased penetration rate of assisted vehicles leads to improved safety metrics. In the traffic jam scenario every increase of 25% in penetration rate led to a statistically significant improvement to the respective lower penetration rate. The maximum deceleration could be reduced from 1.35 m/s^2 at 0% penetration to 0.93 m/s^2 at 100% penetration which is a difference of 0.42 m/s^2. This is lower than in the experiments

with real drivers but can be attributed to the lower starting speed of ca. $100km/h$, averaging effects for the statistical analysis and finally the different scenario configuration regarding the approaching vehicles.

Future Development Possibilities   From the HMI side several steps would still have to be made to bring such an assistance system on the road. The variant based on LED modules is probably the most promising one as it can be realized with readily available and economical components. Besides integration in existing cockpit designs it must also be integrated with existing display elements. As already proposed by other authors (see Mahlke et al. in [Mah+07]) a combination with other assistance systems such as Night Vision would make the LEDs a valuable multi-purpose element.

An issue that still needs to be solved to enable a reasonable operation of the system is the current lack of suitable communication based data sources such as C2IC. Some first attempts are already being made on a manufacturer level such as Audi Connect or BMW Connected Drive but these are still not as ubiquitously available as it would be desirable.

Regarding the driver behavior modeling several points could still be improved. The simulations showed that in the SUMO version which was used the integration of the CFM with the Lane Change Model was still not optimal as practically no lane changes occured due to the modified Car Following behavior. Another issue is the calculation of the IWI for the multi-anticipative CFM. This is currently only based on the relative speed resulting in sub-optimal behavior in static following situations. A better and proven alternative for this could be the Perceived Risk as proposed by Kondoh et al in [Kon+08]. Also the usage of currently only a single BM could be improved by recording different Behavior Maps for different situations (urban, rural, highway etc.). Ideally this would be based on real traffic data to produce more meaningful results. Finally the combination of the modified IDM with more human-like behavior with the BM could be a feasible step.

On the driving simulator side a more extensive experiment would be necessary to evaluate the comparability of results related to speed and distance judgment to real life conditions. This could also reveal possibilities for improvement especially regarding distance judgment and the SAS.

List of Figures

List of Tables

List of Acronyms

ACC	Adaptive Cruise Control
ADAS	Advanced Driver Assistance Systems
API	Application Programming Interface
AR	Augmented Reality
BB	Virtools Building Block
BL	Business Logic
BM	Behavior Map
CA	Cellular Automata
CAH	Constant Acceleration Heuristic
CAN	Controller Area Network
C2CC	Car2Car Communication
C2IC	Car2Infrastructure Communication
C2XC	Car2X Communication
CAVE	Cave Automatic Virtual Environment
CFM	Car Following Model
DAB	Digital Audio Broadcast
DCC	Digital Content Creation
DMX	Digital Multiplex
DSP	Digital Signal Processor
DVB	Digital Video Broadcast
ECU	Electronic Control Unit
EIDM	Enhanced Intelligent Driver Model
FCD	Floating Car Data
FFT	Fast Fourier Transformation
FOV	Field Of View
GIS	Geographic Information System
GPS	Global Positioning System
GUI	Graphical User Interface
HDD	Head-Down Display
HDM	Human Driver Model
HMD	Head-Mounted Display
HMI	Human Machine Interface
HUD	Head-Up Display

IDM	Intelligent Driver Model
ILOC	Intersection Location
IPD	Interpupillary Distance
ISPA	Intelligent Support for Prospective Action
ITS	Intelligent Transportation Systems
IWI	Importance Weight Index

JND	Just Noticeable Difference

LCD	Liquid Chrystal Display
LCM	Lane Change Model
LDW	Lane Departure Warning
LED	Light Emitting Diode
LIDAR	Light Detection And Ranging
LRR	Long Range Radar

NiVi	Night Vision

OBD	On Board Diagnosis
OVM	Optimal Velocity Model

PDT	Peripheral Detection Task
PSE	Point of Subjective Equality

RADAR	Radiowave Detection And Ranging
RDS	Radio Data System
RPM	Rotations Per Minute
RSU	Road Side Unit

SA	Situation Awareness
SAS	Simulator Adaptation Syndrome
SD	Standard Deviation
SIL	Software-in-the-loop
SOP	Sense Of Presence
SRR	Short Range Radar
STFT	Short Term Fourier Transformation
SUMO	Simulation of Urban Mobility

TAP	TPEG Automotive Protocol
TCP/IP	Transmission Control Protocol / Internet Protocol
THW	Time Headway
TMC	Traffic Message Channel
TPEG	Transport Protocol Experts Group
TraCI	Traffic Control Interface
TTC	Time To Collision

USB	Universal Serial Bus

VANET	Vehicular Ad-hoc Network
VRPN	Virtual Reality Peripheral Network
VSL	Virtools Scripting Language

WGS84	World Geodetic System 1984

XML   Extensible Markup Language

Bibliography

[ALE03]   Bernard D. Adelstein, Thomas G. Lee, and Stephen R. Ellis. "Head Tracking Latency in Virtual Environments: Psychophysics and a Model". In: *Proceedings of the Human Factors and Ergonomics Society Annual Meeting* 47 (20 2003), pp. 2083–2087.

[Anh04]   Gerhard Anhäuser. *Verkehrssicherheitsgrün. Kolloquium Verkehrssicherheit von Straßen*. Ed. by Universität Karlsruhe. 2004.

[Arc18]   R.C Archibald. "Euler Integrals and Euler's Spiral – Sometimes called Fresnel Integrals and the Clothoide or Cornu's Spiral". In: *American Math Monthly* (25 1918), pp. 276–282. (Visited on 09/23/2013).

[AST00]   T. P. Alkim, H. Schuurman, and C. M. J. Tampere. "Effects of external cruise control and co-operative following on highways: an analysis with the MIXIC traffic simulation model". In: *Intelligent Vehicles Symposium, 2000. IV 2000. Proceedings of the IEEE*. 2000, pp. 474–479.

[Ayr+01]   T. J. Ayres et al. "Preferred time-headway of highway drivers". In: *Proceedings of Intelligent Transportation Systems Conference*. Ed. by IEEE. 2001, pp. 826–829.

[Ban+95]   M. Bando et al. "Dynamical model of traffic congestion and numerical simulation". In: *Phys. Rev. E* 51 (2 1995), pp. 1035–1042.

[Bar10]   Jaume Barcelo, ed. *Fundamentals of Traffic Simulation*. Vol. 145. International Series in Operations Research & Management Science. Springer, 2010.

[Bau+01]   A. Bauer et al. "The relevance of stereopsis for motorists: a pilot study". In: *Graefe's archive for clinical and experimental ophthalmology* 239 (6 2001), pp. 400–406. ISSN: 0721-832X.

[Bau+08]   Günter Bauer et al. "Multi Spectral Pedestrian Detection and Localization". In: *Advanced Microsystems for Automotive Applications*. Ed. by Jürgen Valldorf and Wolfgang Gessner. Berlin and Heidelberg: Springer Berlin Heidelberg, 2008, pp. 21–35.

[BC02]   Karsten Breuer and Frederic Christen. "Development of Driver Assistance Systems by Use of SIL and HIL Techniques in the Traffic Flow Simulation Program PELOPS". In: *Aachener Kolloquium Fahrzeug- und Motorentechnik*. Vol. 11. 11. Aachen, 2002.

[Bec08]   Jörg Becker-Schweitzer. *Gehörgerechte Fahrgeräuschanalyse als Basis für Fahrsimulatoren*. Ed. by Fachhochschule Düsseldorf. 2008. URL: http://www.head-acoustics.de/downloads/de/NVH_User/Usergroupmeeting_2008/Becker-Schweitzer/JBS_1.pdf (visited on 11/04/2013).

[BG03]   Mike Blommer and Jeff Greenberg. "Realistic 3D Sound Simulation in the VIRTTEX Driving Simulator". In: *Driving Simulator Conference North America Proceedings*. (Dearborn, MI, USA). 2003, pp. 1–13.

[Bil91]   Charles E. Billings. *Human-centered aircraft automation: A concept and guidelines*. Ed. by NASA Ames Research Center. 1991.

[Bri96]   Robert Bristow-Johnson. "Wavetable Synthesis 101, A Fundamental Perspective". In: *AES Convention 101*. Ed. by Audio Engineering Society. 1996.

[Brö10]   Markus Bröckerhoff. *PELOPS White Paper*. Aachen, 2010. URL: http://www.fka.de/pdf/pelops_whitepaper-e.pdf (visited on 09/02/2013).

[BS00]   Mark R. Blakemore and Robert J. Snowden. "Textured backgrounds alter perceived speed". In: *Vision Research* 40 (6 2000), pp. 629–638. ISSN: 0042-6989.

[CAR07]   CAR 2 CAR Communication Consortium. *CAR 2 CAR Communication Consortium Manifesto*. Ed. by CAR 2 CAR Communication Consortium. laq. 2007. URL: http://www.car-to-car.org/index.php?id=31 (visited on 01/18/2012).

[Che+09]   Xiqun Chen et al. "Stabilization of traffic flow based on multi-anticipative intelligent driver model". In: *Intelligent Transportation Systems, ITSC '09. 12th International IEEE Conference on*. Ed. by IEEE. 2009, pp. 72–77.

[Cho11]   Fabian Chowanetz. "Supporting Anticipatory Driving with Large-Scale LED Displays". Chair for Human-Machine-Communication. Diploma Thesis. Munich: Technische Universität München, 2011.

[CNM07]   M.J Cook, J.M Noyes, and Y. Masakowski. *Decision Making in Complex Environments*. Ashgate, 2007.

[CSD93]   Carolina Cruz-Neira, Daniel J. Sandin, and Thomas A. DeFanti. "Surround-screen projection-based virtual reality: the design and implementation of the CAVE". In: *Proceedings of the 20th annual conference on Computer graphics and interactive techniques*. SIGGRAPH '93. New York, NY, and USA: ACM, 1993, pp. 135–142. ISBN: 0-89791-601-8.

[CSW13]   Yuan-Lin Chen, Kun-Yuan Shen, and Shun-Chung Wang. "Forward collision warning system considering both time-to-collision and safety braking distance". In: *Industrial Electronics and Applications (ICIEA), 2013 8th IEEE Conference on*. 2013, pp. 972–977.

[Dav03]   L.C Davis. "Modifications of the optimal velocity traffic model to include delay due to driver reaction time". In: *Physica A: Statistical Mechanics and its Applications* 319 (2003), pp. 557–567. ISSN: 0378-4371.

[Den80]   G. G. Denton. "The influence of visual pattern on perceived speed". In: *Perception* 9 (4 1980), pp. 393–402. ISSN: 0301-0066.

[Deu00]   Deutsches Institut für Normung, ed. *Stage lighting control systems - Part 2: Control signals*. Berlin: Beuth Verlag, 2000.

[DH09]   S. Oliver Daum and Heiko Hecht. "Distance estimation in vista space". In: *Attention, Perception, & Psychophysics* 71 (5 2009), pp. 1127–1137. ISSN: 1943-3921.

[DKP01]   Kees van den Doel, Paul G. Kry, and Dinesh K. Pai. "FoleyAutomatic: physically-based sound effects for interactive simulation and animation". In: *Proceedings of the 28th annual conference on Computer graphics and interactive techniques*. SIGGRAPH '01. New York, NY, and USA: ACM, 2001, pp. 537–544. ISBN: 1-58113-374-X.

[DL97]   Paul DiZio and James R. Lackner. "Motion Sickness Side Effects and Aftereffects of Immersive Virtual Environments Created With Helmet-Mounted Visual Displays". In: *RTO HFM Workshop on The Capability of Virtual Reality to Meet Military Requirements*. RTO MP-54. 1997, pp. 11.1–11.4.

[Dra03]   Alex Drakopoulos. *Evaluation of the converging chevron pavement marking pattern at one Wisconsin location*. Ed. by AAA Foundation for Traffic Safety. 2003.

[Dus+10]   M. Duschl et al. "Birdeye Visualization for Assisting Prospective Driving". In: *FISITA 2010 World Automotive Congress*. GTE, 2010.

[EBJ03]   M.R Endsley, B. Bolte, and D.G Jones. *Designing for Situation Awareness: An Approach to User-Centered Design*. Taylor & Francis, 2003.

[EK95]   Mica R. Endsley and Esin O. Kiris. "The Out-of-the-Loop Performance Problem and Level of Control in Automation". In: *Human Factors: The Journal of the Human Factors and Ergonomics Society* 37 (2 1995), pp. 381–394.

[End95]   Mica R. Endsley. "Toward a Theory of Situation Awareness in Dynamic Systems". In: *Human Factors: The Journal of the Human Factors and Ergonomics Society* 37 (1 1995), pp. 32–64.

[ENH86]   K. Eilers, F. Nachreiner, and K. Hänecke. "Entwicklung und Überprüfung einer Skala zur Erfassung subjektiv erlebter Anstrengung". In: *Zeitschrift für Arbeitswissenschaft* (40 1986), pp. 215–224.

[EPR10]   Sergio Escalera, Oriol Pujol, and Petia Radeva. "Traffic sign recognition system with beta - correction". In: *Machine Vision and Applications* 21 (2 2010), pp. 99–111. ISSN: 0932-8092.

[Eva70]   Leonard Evans. "Speed Estimation from a Moving Automobile". In: *Ergonomics* 13 (2 1970), pp. 219–230.

[FCP06]   Angel Felicisimo, Aurora Cuartero, and Maria E. Polo. "Analysis of homogeneity and isotropy of spatial uncertainty by means of GPS kinematic check lines and circular statistics". In: *7th International Symposium on Spatial Accuracy Assessment in Natural Resources and Environmental Sciences*. Ed. by International Spatial Accuracy Research Association. 2006, pp. 85–90.

[FIR13]   FIRELIGHT TECHNOLOGIES PTY LTD. *Corporate Website*. 2013. URL: http://www.fmod.org (visited on 11/08/2013).

[FLI08]   FLIR Systems Inc. *PathFindIR. High Performance Thermal Night Vision System for Every Vehicle*. Ed. by FLIR Systems Inc. 2008. URL: http://www.flir.com/uploadedFiles/PathFindIR_Datasheet.pdf (visited on 01/31/2012).

[Frö07]   Sebastian Fröbisch. *Untersuchung eines hybriden Verkehrsinformationssystems auf der Basis von Car-2-X-Kommunikation. Diploma Thesis*. Ed. by Alexander Schill. 2007.

[Ful84]   Ray Fuller. "A conceptualization of driving behaviour as threat avoidance". In: *Ergonomics* 27 (11 1984), pp. 1139–1155.

[Gam+07]   E. Gambi et al. "A Proposal of Automotive Anticollision Radars Based on Spread Spectrum Techniques". In: *Consumer Electronics, 2007. ICCE 2007. Digest of Technical Papers. International Conference on*. 2007, pp. 1–2.

[Gar09]   C. Gardiner. *Stochastic Methods: A Handbook for the Natural and Social Sciences*. Springer Series in Synergetics. Springer, 2009.

[Gus13]   Claudio Gusmini. "Modeling Group Dynamics in the Context of Anticipative Driver Assistance". Chair for Computer Aided Medical Procedures & Augmented Reality, Chair for Human-Machine-Communication. Master Thesis. Munich: Technische Universität München, 2013.

[Hay72]   J. C. Hayward. "Near-miss determination through use of a scale of danger". In: *Highway Research Record Issue 384*. Ed. by Transportation Research Board Business Office. Iaq. 1972, pp. 24–34.

[HFL08]   D. Hoetzer, D. Freundt, and B. Lucas. *Automotive Radar and Vision Systems – Ready for the Mass Volume Market*. Ed. by Vehicle Dynamics Expo 2008. 2008. URL: http://www.vehicledynamics-expousa.com/08_conf/pdfs/day%202/09.50_hoetzer.pdf (visited on 01/19/2012).

[Hor13]   Berthold K. P. Horn. "Suppressing Traffic Flow Instabilities". In: *Proceedings of the 16th International IEEE Annual Conference on Intelligent Transportation Systems*. Ed. by IEEE. 2013, pp. 13–20.

[Hor90]   A.R.A van der Horst. "A Time-based Analysis of Road User Behaviour in Normal and Critical Encounters". Institute for Perception TNO. Doctoral Thesis. Technische Universiteit Delft, 1990.

[HS93]   Wolf-Heinrich Hucho and Gino Sovran. "Aerodynamics of road vehicles". In: *Annual Review Fluid Mechanics*. Ed. by Annual Reviews Inc. Vol. 25. 1993, pp. 485–537.

[Hub+95]   Roger Hubbold et al. "Design Issues for Virtual Reality Systems". In: *Virtual Environments '95*. Ed. by Martin Göbel. Eurographics. Springer Vienna, 1995, pp. 224–236.

[ISO08]   ISO, ed. *Intelligent transport systems (ITS) - Location referencing for geographic databases - Part 3: Dynamic location references (dynamic profile)*. Version 1. 2008.

[ISO13]   ISO, ed. *Intelligent transport systems - Traffic and travel information messages via traffic message coding - Part 1: Coding protocol for Radio Data System - Traffic Message Channel (RDS-TMC) using ALERT-C*. Version 1. 2013.

[Joh94]   Gunnar Johansson. "Configurations in Event Perception; An Experimental Study by Gunnar Johansson". In: *Resources for ecological psychology*. Lawrence Erlbaum Associates, 1994, pp. 29–122.

[JSF09]   Helmut Jorke, Arnold Simon, and Markus Fritz. "Advanced stereo projection using interference filters". In: *Journal of the Society for Information Display* 17 (5 2009), pp. 407–410. ISSN: 1938-3657.

[Kat07]   Bryan Jeffrey Katz. "Peripheral Transverse Pavement Markings for Speed Control". PhD Thesis. Blacksburg: Virginia Polytechnic Institute and State University, 2007.

[Ker04]   Boris S. Kerner. "Three-phase traffic theory and highway capacity". In: *Physica A: Statistical Mechanics and its Applications* 333 (2004), pp. 379–440. ISSN: 0378-4371.

[KGV11]   Pallavi Kharade, Sanjyot Gindi, and Vinay G. Vaidya. "Generalized Space Frequency Representation Techniques for Enhancement and Detection Under Low Light Conditions". In: *Advanced Microsystems for Automotive Applications 2011*. Ed. by Gereon Meyer and Jürgen Valldorf. VDI-Buch. Springer Berlin Heidelberg, 2011, pp. 99–107.

[KH04]   Mario Keller and Peter de Haan. *Handbook Emission Factors for Road Transport (HBEFA)*. Ed. by Infras. Bern/Heidelberg/Graz/Essen, 2004. URL: http://www.hbefa.net/e/documents/HBEFA12DOKU.pdf (visited on 10/16/2013).

[KHW02]   Daniel Krajzewicz, Georg Hertkorn, and Peter Wagner. "An Example of Microscopic Car Models Validation Using the Open Source Traffic Simulation SUMO". In: *5th International Conference on ITS*. 2002, pp. 23–26.

[KL08]   R. Klette and Z. Liu. *Computer Vision for the Car Industry*. Ed. by CITR The University of Auckland Computer Science Department. 2008. URL: https://researchspace.auckland.ac.nz/handle/2292/2824 (visited on 01/23/2012).

[Klo+97]   C. Kloeden et al. *Travelling Speed and the Risk of Crash Involvement*. Ed. by NHMRC Road Accident Research Unit, The University of Adelaide. 1997.

[Kon+08]   Takayuki Kondoh et al. "Identification of Visual Cues and Quantification of Drivers' Perception of Proximity Risk to the Lead Vehicle in Car-Following Situations". In: *Journal of Mechanical Systems for Transportation and Logistics* 1 (2 2008), pp. 170–180.

[Kra+12]   Daniel Krajzewicz et al. "Recent Development and Applications of SUMO - Simulation of Urban MObility". In: *International Journal On Advances in Systems and Measurements* 5 (3&4 2012), pp. 128–138.

[Kra98]   Stefan Krauß. "Microscopic Modeling of Traffic Flow: Investigation of Collision Free Vehicle Dynamics". Doctoral Thesis. Cologne: University of Cologne, 1998.

[Krü+05]   Hans-Peter Krüger et al. "SILAB - A Task Oriented Driving Simulation". In: *Driving Simulator Conference North America Proceedings*. (Orlando, FL, USA). 2005, pp. 323–331.

[KTH10]   Arne Kesting, Martin Treiber, and Dirk Helbing. "Enhanced intelligent driver model to access the impact of driving strategies on traffic capacity". In: *Philosophical Transactions of the Royal Society A: Mathematical, Physical and Engineering Sciences* 368 (1928 2010), pp. 4585–4605.

[Laq+13]   F. Laquai et al. "A Multi Lane Car Following Model for Cooperative ADAS". In: *Proceedings of the 16th International IEEE Annual Conference on Intelligent Transportation Systems*. Ed. by IEEE. 2013, pp. 1579–1586.

[LB12]   Y. Luo and L. Bölöni. "Modeling the conscious behavior of drivers for multi-lane highway driving". In: *7th International Workshop on Agents in Traffic and Transportation (ATT-2012)*. 2012, pp. 95–103.

[LCR11]   F. Laquai, F. Chowanetz, and G. Rigoll. "A large-scale LED array to support anticipatory driving". In: *Proc. IEEE Systems Men and Cybernetics (SMC 2011)*. 2011, pp. 543–548.

[LDZ13]   F. Laquai, E. Drefers, and Q. Zhou. *Realversuch zur Evaluierung vorausschauender Assistenz*. Ed. by Lehrstuhl für Mensch - Maschine - Kommunikation. 2013.

[Lew73]   P. T. Lewis. "The noise generated by single vehicles in freely flowing traffic". In: *Journal of Sound and Vibration* 30 (2 1973), pp. 191–206. ISSN: 0022-460X.

[Lim+10]   King Hann Lim et al. "UNMC-VIER AutoVision database". In: *Computer Applications and Industrial Electronics (ICCAIE), 2010 International Conference on*. Kuala Lumpur, 2010, pp. 650–654. ISBN: 978-1-4244-9054-7.

[Lin68]   Aristid Lindenmayer. "Mathematical Models for Cellular Interactions in Development". In: *Journal of Theoretical Biology*. Vol. 18. 18. 1968, pp. 300–315.

[LS12]   J. Lüßmann and C. Santa. "Network-wide Evaluation of Cooperative Traffic Systems using Microscopic Traffic Flow Simulation". In: *Simulation News Europe* (Special Issue Simulation of Traffic Systems - Technical Systems 2012).

[LW09]   Philipp Lindner and Gerd Wanielik. "3D LIDAR processing for vehicle safety and environment recognition". In: *IEEE Symposium on Computational Intelligence in Vehicles and Vehicular Systems (CIVVS 2009) proceedings. March 30-April 2, 2009, Sheraton Music City Hotel, Nashville, TN, USA*. [Piscataway and N.J.]: IEEE, 2009, pp. 66–71. ISBN: 1424427703.

[LWS99]   H. Lenz, C.K Wagner, and R. Sollacher. "Multi-anticipative car-following model". In: *The European Physical Journal B*. Vol. 7. Springer-Verlag, 1999, pp. 331–335.

[Maa+12]   Christian Maag et al. "Studying Effects of Advanced Driver Assistance Systems (ADAS) on Individual and Group Level Using Multi-Driver Simulation". In: *Intelligent Transportation Systems Magazine, IEEE*. Vol. 4. 4 vols. 3. 2012, pp. 45–54.

[Mah+07]   Sascha Mahlke et al. "Evaluation of Six Night Vision Enhancement Systems: Qualitative and Quantitative Support for Intelligent Image Processing". In: *Human Factors: The Journal of the Human Factors and Ergonomics Society* 49 (3 2007), pp. 518–531.

[MAP11]   M. Mulder, D.A Abbink, and M.M van Paassen. "Design of a Haptic Gas Pedal for Active Car-Following Support". In: *Intelligent Transportation Systems, IEEE Transactions on* 12 (1 2011), pp. 268–279. ISSN: 1524-9050.

[Maß12]   Christoph Maßmann. "Environment Perception in a Stereoscopic Driving Simulator with External Traffic Generation". Chair for Human-Machine-Communication. Diploma Thesis. Munich: Technische Universität München, 2012.

[MB01]   Michiel M. Minderhoud and Piet H. L. Bovy. "Extended time-to-collision measures for road traffic safety assessment". In: *Accident Analysis & Prevention* 33 (1 2001), pp. 89–97. ISSN: 0001-4575.

[MCK97]   Marieke Martens, Samantha Comte, and Nico Kaptein. *The Effects of Road Design on Speed Behavior: A Literatur Review*. Ed. by European Commision. 1997.

[ME85]   H.P Moravec and A. Elfes. "High resolution maps from wide angle sonar". In: *IEEE International Conference on Robotics and Automation*. Ed. by IEEE. Vol. 2. 1985, pp. 116–121.

[Mey01]   Eric Meyer. "A new look at optical speed bars". In: *ITE Journal* (2001), pp. 44–48.

[MH06]   M.P Manser and P.A Hancock. "The influence of perceptual speed regulation on speed perception, choice, and control: Tunnel wall characteristics and influences". In: *Accident Analysis and Prevention*. Vol. 39. Elsevier, 2006, pp. 69–78.

[Mil+05] Jeffrey D. Miles et al. *Traffic operational impacts of transverse, centerline, and edgeline rumble strips*. Ed. by Texas Department of Transportation. 2005.

[Mil10]   Natasa Milicic. "Sichere und ergonomische Nutzung von Head-Up Displays im Fahrzeug". Chair for Human-Machine-Communication. Doctoral Thesis. Technische Universität München, 2010.

[Min22]   N. Minorsky. "Directional Stability of Automatically Steered Bodies". In: *Journal of the American Society for Naval Engineers* 34 (2 1922), pp. 280–309. ISSN: 1559-3584.

[MIS02]   J. Miura, M. Itoh, and Y. Shirai. "Toward vision-based intelligent navigator: its concept and prototype". In: *Intelligent Transportation Systems, IEEE Transactions on* 3 (2 2002), pp. 136–146. ISSN: 1524-9050.

[mob07]   mobile.info Consortium. *mobile.info Final Report*. Ed. by K&S GmbH Projektmanagement. 2007. URL: http://www.mobile-info.org/prom/mobileinfo.nsf/DocID/D6D289BDF68A0584C125739B00547F9E/%5C$file/Mobile_Info_Schlussbericht.pdf (visited on 03/25/2012).

[Mol04]   Michael A. Mollenhauer. *Simulator Adaptation Syndrome Literature Review*. Ed. by United States Army Tank-Automotive and Armaments Command (TACOM). 2004.

[MQ86]   R. McAulay and T.F Quatieri. "Speech analysis/Synthesis based on a sinusoidal representation". In: *Acoustics, Speech and Signal Processing, IEEE Transactions on* 34 (4 1986), pp. 744–754. ISSN: 0096-3518.

[MW01]   Marieke Martens and Wim van Winsum. "Effects of speech versus tactile driver support messages on driving behavior and workload". In: *17th International Technical Conference on the Enhanced Safety of Vehicles (ESV)*. Ed. by National Highway Traffic Safety Administration. 2001.

[MW47]   H. B. Mann and D. R. Whitney. "On a Test of Whether one of Two Random Variables is Stochastically Larger than the Other". In: *The Annals of Mathematical Statistics*. Vol. 18. 1947, pp. 50–60.

[Nes+09] S. Nestler et al. "Concept for visualizing concealed objects to improve the driver's anticipation". In: *17th World Congress on Ergonomics*. (Beijing, China). 2009.

[Nor02]   Donald A. Norman. *The design of everyday things*. New York: Basic Books, 2002.

[NS92]   K. Nagel and M. Schreckenberg. "A cellular automaton model for freeway traffic". In: *Journal de Physique I* 2 (12 1992), pp. 2221–2229.

[OH06]   S. Ossen and S.P Hoogendoorn. "Multi-anticipation and heterogeneity in car-following empirics and a first exploration of their implications. Empirics and a first exploration of their implications". In: *Intelligent Transportation Systems Conference, ITSC '06.* Ed. by IEEE. 2006, pp. 1615–1620.

[PC11]   V. Punzo and B. Ciuffo. "Integration of Driving and Traffic Simulation: Issues and First Solutions". In: *Intelligent Transportation Systems, IEEE Transactions on* 12 (2 2011), pp. 354–363. ISSN: 1524-9050.

[Pei+09] Pei-Yung Hsiao et al. "A Portable Vision-Based Real-Time Lane Departure Warning System: Day and Night". In: *IEEE Transactions on Vehicular Technology* 58 (4 2009), pp. 2089–2094. ISSN: 0018-9545.

[Pfa01]   Jonathan D. Pfautz. "Sampling artifacts in perspective and stereo displays". In: *Proc. SPIE* 4297 (2001).

[PlaBC]   Plato. *The Republic*. Ed. by The Academy. Athens, 375 B.C.

[PM01]   Yoav I. H. Parish and Pascal Müller. "Procedural modeling of cities". In: *Proceedings of the 28th annual conference on Computer graphics and interactive techniques*. SIGGRAPH '01. New York, NY, and USA: ACM, 2001, pp. 301–308. ISBN: 1-58113-374-X.

[PM03]   J. Piao and M. McDonald. "Low speed car following behaviour from floating vehicle data". In: *Intelligent Vehicles Symposium, 2003. Proceedings. IEEE*. 2003, pp. 462–467.

[Pop+09] D. Popiv et al. "Timing Concept for Assistance of Anticipatory Driving". In: *17th World Congress on Ergonomics*. August. Beijing and China, 2009.

[Pop+10] D. Popiv et al. "Reduction of fuel consumption by early anticipation and assistance of deceleration phases". In: *Proc. of World Automotive Congress Fisita 2010*. 2010.

[Pop12]   Daria Popiv. "Enhancement of driver anticipation and its implications on efficiency and safety". PhD Thesis. München: Technische Universität München, 2012.

[Ran06]   Roman Ranzinger. "Evaluation und Simulation des Verkehrsinformationssystems SOTIS basierend auf selbstgenerierten Karten". Diploma Thesis. Ingolstadt: Fachhochschule Ingolstadt, 2006.

[RAT03]   Hesham Rakha, Kyoungho Ahn, and Antonio Trani. "Comparison of MOBILE5a, MOBILE6, VT-MICRO, and CMEM models for estimating hot-stabilized light-duty gasoline vehicle emissions". In: *Canadian Journal of Civil Engineering* 30 (6 2003), pp. 1010–1021.

[RAT04]   Hesham Rakha, Kyoungho Ahn, and Antonio Trani. "Development of VT-Micro model for estimating hot stabilized light duty vehicle and truck emissions". In: *Transportation Research Part D: Transport and Environment* 9 (1 2004), pp. 49–74. ISSN: 1361-9209.

[Rau+13]   Andreas Rauch et al. "Inter-Vehicle Object Association for Cooperative Perception Systems". In: *Proceedings of the 16th International IEEE Annual Conference on Intelligent Transportation Systems*. Ed. by IEEE. 2013, pp. 893–898.

[RB85]   R. Risser and C. Brandstaetter. *Die Wiener Fahrprobe*. Lebensraum Verkehr. Literas Univ.-Verlag, 1985.

[Rei+98]   G. Reichart et al. "Potentials of BMW Driver Assistance to Improve Fuel Economy". In: *FISITA 1998 World Automotive Congress*. 1998.

[Rei10]   Konrad Reif. *Fahrstabilisierungssysteme und Fahrerassistenzsysteme*. Viehweg + Teubner Verlag, Springer Fachmedien Wiesbaden, 2010.

[Rei95]   R. Reichart. "Mehr aktive Sicherheit durch neue Systeme für Fahrzeug und Straßenverkehr". In: *Mensch Fahrzeug Umwelt*. Iaq. Verlag TUEV Rheinland GmbH, 1995, pp. 199–215. ISBN: 3-925559-80-9.

[RF09]   A. Riener and A. Ferscha. "Effect of Proactive Braking on Traffic Flow and Road Throughput". In: *Distributed Simulation and Real Time Applications, 2009. DS-RT '09. 13th IEEE/ACM International Symposium on*. 2009, pp. 157–164.

[RN05]   R. H. Rasshofer and K. Naab. "77 GHz long range radar systems. Status, ongoing developments and future challenges". In: *Radar Conference, 2005. EURAD 2005. European*. 2005, pp. 161–164.

[RSK08]   Matthias Röckl, Thomas Strang, and Matthias Kranz. "V2V Communications in Automotive Multi-Sensor Multi-Target Tracking". In: *The 68th IEEE Vehicular Technology Conference. VTC 2008-Fall : Calgary : 21-24 September 2008 : connecting the mobile world*. Piscataway and N.J: IEEE, 2008, pp. 1–5. ISBN: 1424417228.

[SB93]   H. Schmidtke and R. Bernotat. *Ergonomie*. Texte zur Arbeitswissenschaft. Hanser, 1993.

[Sch00]   Thomas Schmidt. "Visual Perception Without Awareness: Priming Responses by Color". In: *Neural Correlates of Consciousness*. MIT Press, 2000.

[Sch05]   Mark Schiementz. *Postprocessing architecture for an automotive radar network*. 1st ed. Göttingen: Cuvillier, 2005. XIII, 164 S.

[Sch08]   Benedikt Scheller. "Sample-basierte Simulation von Fahrzeuginnengeräuschen und Untersuchung der Auswirkung derer auf den Aufmerksamkeitsfokus und das Fahrverhalten des Fahrers". Chair for Human-Machine-Communication. Diploma Thesis. Munich: Technische Universität München, 2008.

[sim11]   simTD Consortium. *Communication processes in the Test Field Germany*. 2011. URL: http://www.simtd.de/dyn/mediaout.dhtml/3152c56c443e8d62121o/mime/PDFs_Grafiken/simTD_technology_en_2011/simTD_Technology_EN_2011.pdf (visited on 01/02/2014).

[Som12]   Kerstin Christine Sommer. "Vorausschauendes Fahren - Erfassung, Beschreibung und Bewertung von Antizipationsleistungen im Straßenverkehr". Doctoral Thesis. Regensburg: Universität Regensburg, 2012.

[Son13]   Sonory. *Corporate Website*. 2013. URL: http://www.sonory.org/ (visited on 11/08/2013).

[SS91]   M. Sachsenweger and U. Sachsenweger. "Stereoscopic acuity in ocular pursuit of moving objects. Dynamic stereoscopy and movement parallax: relevance to road safety and occupational medicine". In: *Documenta ophthalmologica* 78 (1-2 1991), pp. 1–133. ISSN: 0012-4486.

[Tao89]   George T. Taoka. "Brake Reaction Times of Unalerted Drivers". In: *ITE Journal*. Ed. by Institute of Transportation Engineers. Vol. 59. Washington D.C., 1989, pp. 19–21.

[Tay+01]   Russell M. Taylor et al. "VRPN: a device-independent, network-transparent VR peripheral system". In: *Proceedings of the ACM symposium on Virtual reality software and technology*. VRST '01. New York, NY, and USA: ACM, 2001, pp. 55–61. ISBN: 1-58113-427-4.

[Tay82]   J. F. Taylor. "Vision and driving". In: *The Practitioner* 226 (1367 1982), pp. 885–889. ISSN: 0032-6518.

[THH00]   M. Treiber, A. Hennecke, and D. Helbing. "Congested traffic states in empirical observations and microscopic simulations". In: *Physical Review E 62* 62 (2000), pp. 1805–1824.

[TK10]   Martin Treiber and Arne Kesting. "Aus Fahrstrategien hergeleitete Fahrzeugfolgemodelle". German. In: *Verkehrsdynamik und -simulation*. Springer-Lehrbuch. Springer Berlin Heidelberg, 2010, pp. 155–172. ISBN: 978-3-642-05227-9.

[TKH06]   Martin Treiber, Arne Kesting, and Dirk Helbing. "Delays, inaccuracies and anticipation in microscopic traffic models". In: *Physica A*. Vol. 360. Elsevier, 2006, pp. 71–88.

[Ton10]   Lin Tong. "Influences of the ISPA Warning System on General Traffic". Chair for Human-Machine-Communication. Diploma Thesis. Munich: Technische Universität München, 2010.

[TS01]   M. Taieb-Maimon and D. Shinar. "Minimum and comfortable driving headways: reality versus perception". In: *Human factors* 43 (1 2001), pp. 159–172. ISSN: 0018-7208.

[Tsc12]   Werner Tschöpe. "A Driver Model for Evaluating Anticipation Supporting Assistance". Chair for Human-Machine-Communication. Diploma Thesis. Munich: Technische Universität München, 2012.

[Tut08]   M. Tutusaus. "Evaluation of automotive commercial Radar for human detection". Department of Radio Science and Engineering. Master Thesis. Helsinki University of Technology, 2008.

[TVK98]   Tero Tolonen, Vesa Välimäki, and Matti Karjalainen. *Evaluation of Modern Sound Synthesis Methods*. Ed. by Helsinki University of Technology. Helsinki, 1998.

[VEH08]   Trent W. Victor, Johan Engström, and Joanne L. Harbluk. "Distraction Assessment Methods Based on Visual Behavior and Event Detection". In: *Driver Distraction*. CRC Press, 2008, pp. 135–165. ISBN: 978-0-8493-7426-5.

[VLM97]   Tony S. Verma, Scott N. Levine, and Teresa H. Y. Meng. "Transient Modeling Synthesis: a flexible analysis/synthesis tool for transient signals". In: *Proceedings of the ICMC*. 1997, pp. 164–167.

[VR92]   K.J Vicente and J. Rasmussen. "Ecological interface design: theoretical foundations". In: *Systems, Man and Cybernetics, IEEE Transactions on* 22 (4 1992), pp. 589–606. ISSN: 0018-9472.

[Wei+09]   Hendrik Weigel et al. "A novel head up display for driver assistance systems". In: *Proceedings of ITS 16th World Congress on Intelligent Transport Systems and Services*. 2009.

[WH92]   C. D. Wickens and J. G. Hollands. "Attention, time-sharing, and workload". In: *Engineering Psychology and Human Performance*. Prentice Hall, 1992, pp. 439–479.

[Wie10]   Christoph Wierer. "Design and Implementation of a Large LED Display System in the Automotive Domain". Chair for Human-Machine-Communication. Diploma Thesis. Munich: Technische Universität München, 2010.

[Wie74]   Rainer Wiedemann. "Simulation des Straßenverkehrsflusses". Institut für Verkehrswesen. Dissertation. Karlsruhe: Universität Karlsruhe, 1974.

[Win+07]   J.C.F. de Winter et al. "Driving simulator fidelity and training effectiveness". In: *European Annual Conference on Human Decision-Making and Manual Control*. 2007.

[Wis+03]   L. Wischoff et al. "SOTIS - a self-organizing traffic information system". In: *Vehicular Technology Conference, 2003. VTC 2003-Spring. The 57th IEEE Semiannual*. Vol. 4. 2003, pp. 2442–2446.

[WL03]   P. Wagner and I. Lubashevsky. "Empirical basis for car-following theory development". In: *arXiv: Condensed Matter / Statistical Mechanics 0311192* (2003), pp. 1–4.

[WLH12]   J.C.F. de Winter, P.M. van Leeuwen, and R. Happee. "Advantages and Disadvantages of Driving Simulators: A Discussion". In: *Proceedings of Measuring Behavior*. Ed. by A.J. Spink et al. Utrecht and The Netherlands, 2012.

[WS98]   Bob G. Witmer and Michael J. Singer. "Measuring Presence in Virtual Environments: A Presence Questionnaire". In: *Presence* 7 (3 1998), pp. 225–240.

[WSS90]   Alexander C. Wagenaar, Frederic M. Streff, and Robert H. Schultz. "Effects of the 65 mph speed limit on injury morbidity and mortality". In: *Accident Analysis & Prevention* 22 (6 1990), pp. 571–585. ISSN: 0001-4575.

[XB06]   Huaying Xu and M. Barth. "An adaptive dissemination mechanism for inter-vehicle communication-based decentralized traffic information systems". In: *Intelligent Transportation Systems Conference, 2006. ITSC '06. IEEE*. 2006, pp. 1207–1213.

[XLF05]   F. Xu, X. Liu, and K. Fujimura. "Pedestrian Detection and Tracking With Night Vision". In: *IEEE Transactions on Intelligent Transportation Systems* 6 (1 2005), pp. 63–71. ISSN: 1524-9050.

[Xu07]   Guochang Xu. *GPS: Theory, Algorithms and Applications*. Springer, 2007.

[ZAG06]   Yizhen Zhang, E.K Antonsson, and K. Grote. "A new threat assessment measure for collision avoidance systems". In: *IEEE Intelligent Transportation Systems Conference*. 2006, pp. 968–975.

[Zan+08]   Yunpeng Zang et al. "Wireless local danger warning using inter-vehicle communications in highway scenarios". In: *Wireless Conference, 2008. EW 2008. 14th European*. 2008, pp. 1–7.

[ZBM06]   Zehang Sun, G. Bebis, and R. Miller. "Monocular precrash vehicle detection: features and classifiers". In: *IEEE Transactions on Image Processing* 15 (7 2006), pp. 2019–2034. ISSN: 1057-7149.

[ZJ07]   Wen-Xing Zhu and Lei Jia. "Analysis of a New Car-following Model with a Consideration of Multi-interaction of Preceding vehicles". In: *Intelligent Transportation Systems Conference, 2007. ITSC 2007. IEEE*. 2007, pp. 320–324.

[Zlo10]   Adrian Zlocki. *Optimization of traffic flow by using running lights*. Ed. by Institut für Kraftfahrzeuge. Aachen, 2010.

Supervised student thesises relevant to this dissertation

[Cho11]   Fabian Chowanetz. "Supporting Anticipatory Driving with Large-Scale LED Displays". Chair for Human-Machine-Communication. Diploma Thesis. Munich: Technische Universität München, 2011.

[Gus13]   Claudio Gusmini. "Modeling Group Dynamics in the Context of Anticipative Driver Assistance". Chair for Computer Aided Medical Procedures & Augmented Reality, Chair for Human-Machine-Communication. Master Thesis. Munich: Technische Universität München, 2013.

[Kir10]   Georgi Kirev. "Foreign Vehicle Simulation for an Immersive Driving Simulator". Chair for Human-Machine-Communication. Bachelor Thesis. Munich: Technische Universität München, 2010.

[Kon10]   Thomas Kontschinsky. "Foreign Traffic Animation in the MMK Driving Simulator". Chair for Human-Machine-Communication. Bachelor Thesis. Munich: Technische Universität München, 2010.

[Maß12]   Christoph Maßmann. "Environment Perception in a Stereoscopic Driving Simulator with External Traffic Generation". Chair for Human-Machine-Communication. Diploma Thesis. Munich: Technische Universität München, 2012.

[Pet12]   Andreas Petermüller. "Generation of Realistic Street Representations for a VR Driving Simulator for an Improved Perception of Speed". Chair for Human-Machine-Communication. Diploma Thesis. Munich: Technische Universität München, 2012.

[Sch08]   Benedikt Scheller. "Sample-basierte Simulation von Fahrzeuginnengeräuschen und Untersuchung der Auswirkung derer auf den Aufmerksamkeitsfokus und das Fahrverhalten des Fahrers". Chair for Human-Machine-Communication. Diploma Thesis. Munich: Technische Universität München, 2008.

[Ton10]   Lin Tong. "Influences of the ISPA Warning System on General Traffic". Chair for Human-Machine-Communication. Diploma Thesis. Munich: Technische Universität München, 2010.

[Tsc12]   Werner Tschöpe. "A Driver Model for Evaluating Anticipation Supporting Assistance". Chair for Human-Machine-Communication. Diploma Thesis. Munich: Technische Universität München, 2012.

[Wie10]   Christoph Wierer. "Design and Implementation of a Large LED Display System in the Automotive Domain". Chair for Human-Machine-Communication. Diploma Thesis. Munich: Technische Universität München, 2010.

[Zob11]   Hans-Peter Zobl. "Contact Analog Displays for Anticipatory Driving". Chair for Human-Machine-Communication. Diploma Thesis. Munich: Technische Universität München, 2011.